

The response of isolated ventricular cardiomyocytes to acute changes in metabolic substrates

Thesis Submitted for the Degree of
Doctor of Philosophy
at the University of Leicester

By

Charlotte Ellen Flavell Poile B.Sc. (Hons) (Leicester)

Department of Cardiovascular Sciences

University of Leicester

2016

Abstract

The response of isolated ventricular cardiomyocytes to acute changes in metabolic substrates

Charlotte Ellen Flavell Poile

During a period of ischaemia, the myocardium switches predominantly from fatty acid metabolism to anaerobic glycolysis in an effort to maintain ATP levels. Increased availability of the metabolic substrates glucose and pyruvate has been found to improve recovery following ischaemia and reperfusion, while the presence of fatty acids upon reperfusion is detrimental. This study used isolated ventricular cardiomyocytes exposed to a simulated ischaemic and reperfusion protocol (metabolic inhibition and re-energisation) to investigate the effects of acute changes in specific metabolic substrates, and concentrations, prior to metabolic inhibition and/or during re-energisation at a cellular level.

Perfusing isolated ventricular cardiomyocytes with an elevated concentration of glucose or fructose prior to metabolic inhibition and during re-energisation reduced a number of markers of ischaemic and re-energisation injury and thus imparted cardioprotection. Elevated glucose also affected electrical activity of the isolated ventricular cardiomyocytes by delaying action potential failure and $\text{SarCK}_{\text{ATP}}$ channel activation. Intracellular magnesium levels were maintained with elevated glucose indicating possible sustained ATP levels, while intracellular calcium levels continued to rise throughout the protocol, suggesting the observed cardioprotection is not linked to reduced calcium overloading. Reducing pyruvate to a physiological concentration (0.5mM) only impacting on the response to metabolic inhibition, whilst elevating pyruvate to a supraphysiological concentration (10mM), only benefited those cardiomyocytes perfused under normoglycaemic conditions. Perfusion with a physiological concentration (0.5mM) of octanoate abrogated the cardioprotection provided by elevated glucose upon re-energisation. Metabolic preconditioning and postconditioning with elevated concentrations of metabolic substrates also improved contractile recovery. These results suggest increased availability of certain metabolic substrates are beneficial to isolated ventricular cardiomyocytes either prior to metabolic inhibition and/or the subsequent re-energisation. These observations may have clinical relevance in patients with acute coronary ischaemia. The precise mechanisms for these effects remain to be determined but are suggested to involve increased ATP availability.

Acknowledgments

Firstly I would like to thank my supervisors Dr Richard Rainbow and Prof. Iain Squire for all their advice and support over the past few years. I'd also like to thank the Department of Cardiovascular Sciences for funding my PhD.

I would like to thank Dr Glenn Rodrigo and Dr Karl Herbert for all of their help and support and Dr Noel Davies, Dr Nina Storey and Prof. John Challiss for the supply of regents and Anthony Oakden and Ken White from BMS.

My biggest thanks goes to my family and friends, especially my mum and dad thank you for all the love and support and the encouragement you have given me. To Allan and Chloe, I couldn't imagine two better people to be stuck in between, thanks for making me laugh. I'm also extremely grateful to all of you for helping me with printing. To my grandparents (John and Connie Flavell, William and Josephine Poile and Bert Poile) thank you for all of your support and for encouraging me, and asking me how it's going even though you might not be entirely sure what I'm on about! To Nathan thanks for being there for me, being on the end of the phone whenever I needed a chat, and for printing all those papers!! All of you have been amazing over the past few years thanks for believing in me, I couldn't have done it without any of you.

Contents

Abstract	I
Acknowledgements	II
List of Contents	IV
List of Tables	X
List of Figures	XI
List of Abbreviations	XVII

List of Contents

CHAPTER ONE INTRODUCTION.....	1
1.1 The Heart	2
1.2 Cardiac Action potential	3
1.2.1 Mechanism of a ventricular action potential	3
1.3 ATP- sensitive inwardly-rectifying potassium channels (K_{ATP}).....	6
1.3.1 Sarcolemmal K_{ATP} channels (Sarck K_{ATP})	6
1.3.2 Mitochondrial K_{ATP} channels (Mito K_{ATP})	7
1.3.3 Pharmacological modulation of Sarck K_{ATP} and Mito K_{ATP} channel activity and cardioprotection	9
1.3.4 Limitations of the pharmacological agents of Sarck K_{ATP} and Mito K_{ATP} channels.....	11
1.4 Excitation-contraction coupling	12
1.4.1 Mechanism behind excitation-contraction coupling.....	12
1.4.2 Calcium regulation in excitation-contraction coupling	14
1.4.3 Ischaemic modulation of excitation contraction coupling.....	15
1.5 Coronary Heart Disease	15
1.6 Ischaemic and Reperfusion injury	16
1.6.1 Ischaemia.....	16
1.6.2 Reperfusion	18
1.7 Monosaccharides	20
1.7.1 Glucose in humans.....	20
1.7.2 Glucose regulation in humans.....	21
1.7.3 Glucose transporters.....	23
1.7.3.1 Sodium dependent glucose transporters (SGLT).....	23
1.7.3.2 GLUT transporters.....	23
1.7.4 Glucose metabolism in the myocardium	27
1.7.4.1 Glycolysis	27
1.7.4.2 Glucose oxidation.....	29
1.7.5 Diabetes and the effects of glucose on the myocardium.....	30
1.7.6 Fructose in humans	33
1.7.7 Fructose transporters	33
1.7.8 Fructose metabolism in the myocardium	33
1.7.9 Fructose effects in the myocardium	33
1.8 Pyruvate	36
1.8.1 Pyruvate in humans	36
1.8.2 Pyruvate Transporters	36
1.8.2.1 Transporters located at the sarcolemmal membrane	36
1.8.2.2 Transporters located at the inner mitochondria membrane	36
1.8.3 Pyruvate metabolism in the myocardium	37
1.9 Fatty acids	38

1.9.1 Fatty acids in humans	38
1.9.2 Regulation of fatty acid availability to the myocardium	38
1.9.3 Fatty acid transporters	39
1.9.3.1 Fatty acid transporters under physiological conditions	39
1.9.3.2 Fatty acid transporters under pathophysiological conditions	39
1.9.4 Fatty acid metabolism in the myocardium	39
1.9.4.1 β -oxidation	40
1.10 Mitochondria	44
1.10.1 Krebs cycle	44
1.10.2 Oxidative Phosphorylation	45
1.10.2.1 Delivery of ATP generated from oxidative phosphorylation to areas of ATP utilisation via phosphotransfer systems	49
1.10.3 Mitochondrial permeability transition pore (mPTP)	49
1.10.3.1 Role of mPTP in cell death	50
1.11 Ischaemic Conditioning	51
1.11.1 Types of ischaemic conditioning	51
1.11.2 Mechanisms of ischaemic conditioning	53
1.11.2.1 Ischaemic preconditioning	53
1.11.2.2 Mechanism behind ischaemic postconditioning and remote IPC	55
1.11.3 Role of metabolism in ischaemic conditioning	56
1.12 Literature views on the role of metabolites in cardioprotection.....	57
1.13 Aims and objectives of the project	59
 CHAPTER TWO Method and Materials.....	 61
2.1 Isolation of adult rat cardiomyocytes	62
2.2 Superfusion and stimulation of cardiomyocytes	63
2.3 Experimental protocols.....	63
2.3.1 Ischaemia/reperfusion injury protocol.....	63
2.3.2 Experimental designs.....	67
2.4 Contractile function measurements	68
2.4.1 Contractile function recordings by Electrical Field Stimulation.....	68
2.4.2 Analysis of contractile function recordings	68
2.5 Electrophysiology	69
2.5.1 Electrophysiology preparation	69
2.5.2 Cell-attached configuration recording.....	70
2.5.2.1 SarCK _{ATP} channel recordings	70
2.5.3 Whole-cell configuration	71
2.5.3.1 Action potential	71
2.5.3.2 SarCK _{ATP} current recordings	71
2.5.4 Analysis of electrophysiology recordings	72

2.6 Fluorescence Imaging	76
2.6.1 Fluorescence imaging preparation	76
2.6.2 Intracellular calcium measurements using Fura- 2-AM	78
2.6.2.1 Analysis of calcium data	78
2.6.3 Intracellular magnesium measurements using Magnesium Green-AM.....	81
2.6.3.1 Analysis of magnesium Green data	81
2.7 Solutions	82
2.7.1 Solutions for isolation of adult rat cardiomyocytes	82
2.7.2 Solutions for Tyrode and Substrate Free Tyrode (SFT)	82
2.7.2.1 Substrate Free Tyrode – Metabolic Inhibition (SFT-MI)	82
2.7.2.2 Osmotically balanced experimental Tyrode solutions	82
2.7.2.3 Solutions used to investigate the effects of pyruvate and fatty acids.....	83
2.7.3 Intracellular pipette solutions for electrophysiology experiments	83
2.8 Materials	83
2.9 Analysis and statistics.....	83
 CHAPTER THREE The role of glycolytic metabolism in isolated cardiomyocytes subjected to metabolic inhibition and re-energisation.....	 88
3.1 Introduction.....	89
3.2 Results.....	90
3.2.1 The effects of acute changes in extracellular glucose on the contractile function of isolated cardiomyocytes during metabolic inhibition and re-energisation	90
3.2.2 The effect of elevated extracellular glucose on cardiac action potential behaviour	97
3.2.3 The effect of elevated extracellular glucose on SarcK _{ATP} channel activity.....	101
3.2.4 The effect of elevated extracellular glucose on intracellular ATP depletion during metabolic inhibition.....	104
3.2.5 The effects of elevated extracellular glucose on intracellular calcium within isolated cardiomyocytes subjected to metabolic inhibition and re-energisation	108
3.2.5.1 Measurements of intracellular calcium as a marker of cell injury.....	108
3.2.5.2 Is the recovery of contractile activity linked to maintained Ca ²⁺ - homeostasis following metabolic inhibition and re-energisation?.....	113
3.2.6 The effects of acute changes in extracellular fructose on the contractile recovery of isolated cardiomyocytes.....	115
3.3 Discussion.....	118
3.3.1 Do acute changes in extracellular glucose prior to metabolic inhibition	

impact on ATP depletion during metabolic inhibition?.....	119
3.3.1.1 Perfusion with elevated glucose delays contractile failure, action potential failure and $\text{SarCK}_{\text{ATP}}$ opening.....	119
3.3.1.2 Elevated glucose prevents ATP depletion but does not prevent a Ca^{2+} overload.....	123
3.3.1.3 The effect of elevated glucose on the development of rigor.....	125
3.3.2 Perfusion with elevated extracellular glucose upon re-energisation prevents ischaemic/re-energisation injury.....	127
3.3.2.1 Can elevated glucose prevent hypercontracture?.....	127
3.3.2.2 Re-energisation with elevated glucose improves ATP production but does not alter Ca^{2+} levels.....	130
3.3.2.3 Perfusion with elevated glucose improves contractile recovery during re-energisation.....	133
3.3.3 The impact of acute hypoglycemic conditions prior to metabolic inhibition and during re-energisation.....	134
3.3.4 The effect of perfusion with elevated fructose during metabolic inhibition and re-energisation.....	135

CHAPTER FOUR The role of oxidative phosphorylation metabolic substrates in isolated cardiomyocytes subjected to metabolic inhibition and re-energisation137

4.1 Introduction.....	138
4.2 Results.....	140
4.2.1 The effects of reducing extracellular pyruvate on isolated cardiomyocytes exposed to metabolic inhibition and re-energisation.....	140
4.2.2 The effects of reduced pyruvate on cardiac action potential behaviour during metabolic inhibition	148
4.2.3 The effects of reduced pyruvate on $\text{SarCK}_{\text{ATP}}$ channel activation during metabolic inhibition	154
4.2.4 The effect of reduced pyruvate on Mg^{2+} -Green fluorescence.....	157
4.2.5 The modifying effect of reduced extracellular pyruvate on intracellular calcium in response to metabolic inhibition and re-energisation in association with acute changes in glucose.....	163
4.2.5.1 Measurements of intracellular calcium as a marker of cell injury.....	163
4.2.5.2. Does reducing pyruvate impact on the recovery of contraction and the corresponding lower resting $[\text{Ca}^{2+}]_i$?.....	168
4.2.6 The effects of acute elevation in extracellular pyruvate on the contractile function of isolated cardiomyocytes.....	170
4.2.7 Fatty acid metabolism prevents the cardioprotection previously	

elicited by elevated extracellular glucose.....	178
4.2.7.1 Replacement of pyruvate for octanoate.....	178
4.2.7.2 The addition of pyruvate on the actions of octanoate.....	187
4.3 Discussion.....	195
4.3.1 Impact of pyruvate during metabolic inhibition.....	196
4.3.1.1 The effect of reducing pyruvate prior to metabolic inhibition.....	196
4.3.1.2 The effect of elevating pyruvate prior to metabolic inhibition.....	199
4.3.2 Pyruvate actions upon re-energisation following acute changes in pyruvate prior to metabolic inhibition and during re-energisation.....	201
4.3.2.1 The effect of reducing pyruvate during re-energisation.....	201
4.3.2.2 The effect of elevating pyruvate during re-energisation.....	202
4.3.3 Detrimental effects of octanoate upon re-energisation following metabolic inhibition.....	203
4.3.3.1 The actions of octanoate prior to metabolic inhibition and during re-energisation.....	203
4.3.3.2 Potential benefits of stimulating glucose oxidation with pyruvate in the presence of octanoate prior to metabolic inhibition and during re-energisation.....	205
CHAPTER FIVE Metabolic pre and post conditioning of isolated cardiomyocytes.....	209
5.1 Introduction.....	210
5.2 Results	211
5.2.1 The effects of preconditioning with elevated glucose on the contractile function of isolated cardiomyocytes.....	211
5.2.2 Preconditioning isolated cardiomyocytes with elevated glucose delays SarcK _{ATP} channel activity during metabolic inhibition.....	216
5.2.3 The effects of preconditioning with elevated fructose on the contractile function of isolated cardiomyocytes	217
5.2.4 The effects of preconditioning with elevated pyruvate on the contractile function of isolated cardiomyocytes	222
5.2.5 Postconditioning with elevated glucose limits re-energisation injury.....	225
5.3 Discussion	229
5.3.1 Are metabolic pre and/or postconditioning relevant?.....	229
5.3.1.1 Metabolic preconditioning imparts cardioprotection.....	230
5.3.1.2 Metabolic postconditioning appears to be cardioprotective.....	235

CHATPER SIX General Discussion.....	237
6. General Discussion.....	238
6.1 The impact of elevating glycolytic substrates at a cellular level.....	238
6.2 Does oxidative phosphorylation impact on the glycolytic effect?.....	241
6.3 Can metabolic pre/postconditioning replicate traditional ischaemic conditioning?.....	242
6.4 Clinical implications.....	244
6.5 Study limitations.....	245
6.5.1 Isolation with 10mM glucose.....	245
6.5.2 Improving the measurement of contractile viability.....	246
6.5.3 Defining SarcK _{ATP} channel activation.....	246
6.5.4 Modification of the Mg ²⁺ -Green experiments.....	247
6.5.5 Limited fatty acid concentration.....	248
6.6 Overall conclusion.....	248
Appendix.....	250
References.....	255
Addenda.....	Back cover

List of Tables

Table 1.1	Class 1 GLUT transporters	25
Table 1.2	Class 3 GLUT transporters	26
Table 1.3	Class 2 GLUT transporters	35
Table 2.1	Standard Tyrode and SFT solutions	84
Table 2.2	The osmotically balanced Tyrode solutions	85
Table 2.3	Tyrode solutions for the varied pyruvate and octanoate experiments	86
Table 2.4	The intracellular pipette solutions	87

List of Figures

Figure 1.1	Ventricular cardiac action potential	5
Figure 1.2	Ventricular SarcK _{ATP} channel structure	8
Figure 1.3	Crossbridge cycling	13
Figure 1.4	Signalling pathways of insulin and glucagon	22
Figure 1.5	GLUT transporter structure	24
Figure 1.6	Glycolysis	28
Figure 1.7	Fatty acid transport into the myocardium	41
Figure 1.8	Activation of long chain fatty acids and transport into the mitochondria	42
Figure 1.9	β -oxidation	43
Figure 1.10	Structure of the mitochondria	46
Figure 1.11	Krebs cycle	47
Figure 1.12	The Electron Transport Chain and ATP synthase	48
Figure 1.13	Mechanism of ischaemic conditioning	54
Figure 2.1	The perfusion chamber	64
Figure 2.2	Contractile function measurements and morphology of cardiomyocytes through metabolic inhibition and re-energisation protocol	65
Figure 2.3	Protocols for contractile function and imaging experiments	66
Figure 2.4	Electrophysiology traces	73
Figure 2.5	Cell-attached traces representing SarcK _{ATP} opening	74
Figure 2.6	Whole-cell trace representing SarcK _{ATP} opening	75
Figure 2.7	Fluorescence imaging set up	77
Figure 2.8	Calcium analysis using Win Fluor 3.6.9	79
Figure 2.9	Contractile recovery using calcium transients	80
Figure 3.1	Metabolic inhibition and re-energisation protocol	94
Figure 3.2	The effects of acute changes in extracellular glucose on the contractile function of isolated cardiomyocytes subjected to metabolic inhibition and re-energisation.	95
Figure 3.3	The effects of acute changes in extracellular glucose on recovery of isolated cardiomyocytes subjected to metabolic inhibition and re-energisation.	96
Figure 3.4	The effects of acute changes in extracellular glucose on the time to action potential failure during metabolic inhibition.	98
Figure 3.5	The effects of acute changes in extracellular glucose on the time to action potential duration to 90% repolarisation (APD ₉₀) and resting membrane potential prior metabolic inhibition.	100
Figure 3.6	The effects of acute changes in extracellular glucose on	102

	SarCK _{ATP} current activation during metabolic inhibition.	
Figure 3.7	The effects of 5mM and 20mM glucose on single channel activity of SarCK _{ATP} during metabolic inhibition recorded using the cell attached configuration.	103
Figure 3.8	The effect of an acute elevation in extracellular glucose on Mg ²⁺ -Green fluorescence in isolated cardiomyocytes exposed to metabolic inhibition and re-energisation.	106
Figure 3.9	The effect of an acute elevation in extracellular glucose on Mg ²⁺ -Green fluorescence in isolated cardiomyocytes exposed to metabolic inhibition and re-energisation.	107
Figure 3.10	The effect of acute changes in extracellular glucose on the intracellular calcium in isolated cardiomyocytes during metabolic inhibition and re-energisation.	109
Figure 3.11	The effect of acute changes in extracellular glucose on the intracellular calcium in isolated cardiomyocytes during metabolic inhibition and re-energisation.	110
Figure 3.12	Capturing of Ca ²⁺ transients during metabolic inhibition and re-energisation to determine recovery.	111
Figure 3.13	The effects of acute changes in extracellular glucose on the recovery of electrically evoked calcium transients following metabolic inhibition and re-energisation.	112
Figure 3.14	The effects of acute changes in extracellular fructose on the contractile function of isolated cardiomyocytes subjected to metabolic inhibition and re-energisation.	116
Figure 3.15	The effects of acute changes in extracellular fructose on recovery of isolated cardiomyocytes subjected to metabolic inhibition and re-energisation.	117
Figure 3.16	The effects of metabolic inhibition.	120
Figure 3.17	The hypothesised mechanisms behind cardioprotection seen when perfusing with elevated glucose, fructose and pyruvate prior to metabolic inhibition.	121
Figure 3.18	Regulation of enzymes involved in both cytosolic and mitochondrial ATP production.	128
Figure 3.19	The effects of re-energisation	129
Figure 3.20	The hypothesised mechanisms behind cardioprotection seen with elevated metabolic substrates during re-energisation.	131
Figure 4.1	The effect of an acute reduction in extracellular pyruvate on the response of isolated cardiomyocytes to metabolic inhibition and re-energisation in response to acute changes in extracellular glucose.	142

Figure 4.2	The effect of a reduction in extracellular pyruvate on the time to contractile failure during metabolic inhibition in response to acute changes in extracellular glucose.	143
Figure 4.3	The effect of a reduction in extracellular pyruvate on the time to rigor contracture during metabolic inhibition in response to acute changes in extracellular glucose.	144
Figure 4.4	The effect of a reduction in extracellular pyruvate on the viability of isolated cardiomyocytes to metabolic inhibition in response to acute changes in extracellular glucose.	145
Figure 4.5	The effect of a reduction in extracellular pyruvate on the recovery of isolated cardiomyocytes to metabolic inhibition and re-energisation in response to acute changes in extracellular glucose.	146
Figure 4.6	The effects of an acute reduction in extracellular pyruvate on the time to action potential failure during metabolic inhibition in response to acute changes in extracellular glucose.	149
Figure 4.7	The effects of an acute reduction in extracellular pyruvate on the time to action potential failure during metabolic inhibition in response to acute changes in extracellular glucose.	150
Figure 4.8	The effects of an acute reduction in extracellular pyruvate on APD ₉₀ prior metabolic inhibition in response to acute changes in extracellular glucose.	152
Figure 4.9	The effects of an acute reduction in extracellular pyruvate on the resting membrane potential prior to metabolic inhibition in response to acute changes in extracellular glucose.	153
Figure 4.10	The effects of an acute reduction in extracellular pyruvate on SarCK _{ATP} current activation during metabolic inhibition in response to acute changes in extracellular glucose.	155
Figure 4.11	The effects of an acute reduction in extracellular pyruvate on SarCK _{ATP} current activation during metabolic inhibition in response to acute changes in extracellular glucose.	156
Figure 4.12	The impact of acute changes in extracellular pyruvate on the fluorescence of Mg ²⁺ -Green in isolated cardiomyocytes during metabolic inhibition and re-energisation in response to acute changes in extracellular glucose.	160
Figure 4.13	The impact of acute changes in extracellular pyruvate on the fluorescence of Mg ²⁺ -Green in isolated cardiomyocytes during metabolic inhibition and re-energisation in response	161

	to acute changes in extracellular glucose.	
Figure 4.14	The impact of acute changes in extracellular pyruvate on the time to the rapid increase in Mg^{2+} -Green fluorescence in isolated cardiomyocytes during metabolic inhibition in response to acute changes in extracellular glucose.	162
Figure 4.15	The impact of acute changes in extracellular pyruvate on intracellular calcium in isolated cardiomyocytes during metabolic inhibition and re-energisation in response to acute changes in extracellular glucose.	164
Figure 4.16	The impact of acute changes in extracellular pyruvate on intracellular calcium in isolated cardiomyocytes during metabolic inhibition and re-energisation in response to acute changes in extracellular glucose.	165
Figure 4.17	The effects of an acute reduction in extracellular pyruvate on the recovery of electrically evoked calcium transients following metabolic inhibition and re-energisation in response to acute changes in extracellular glucose.	166
Figure 4.18	The effects of an acute reduction in extracellular pyruvate on the recovery of electrically evoked calcium transients following metabolic inhibition and re-energisation in response to acute changes in extracellular glucose.	167
Figure 4.19	The effects of an acute elevation in extracellular pyruvate on the contractile function of isolated cardiomyocytes to metabolic inhibition and re-energisation in response to acute changes in extracellular glucose.	172
Figure 4.20	The effects of an acute elevation in extracellular pyruvate on the time to contractile failure during metabolic inhibition in response to acute changes in extracellular glucose.	173
Figure 4.21	The effects of an acute elevation in extracellular pyruvate on the time to rigor contracture during metabolic inhibition in response to acute changes in extracellular glucose.	174
Figure 4.22	The effects of an acute elevation in extracellular pyruvate on the viability of isolated cardiomyocytes to metabolic inhibition and re-energisation in response to acute changes in extracellular glucose.	176
Figure 4.23	The effects of an acute elevation in extracellular pyruvate on the recovery of isolated cardiomyocytes to metabolic inhibition and re-energisation in response to acute changes in extracellular glucose.	177
Figure 4.24	β -oxidation of octanoate	180

Figure 4.25	The effects of replacing pyruvate with octanoate on the contractile function of isolated cardiomyocytes to metabolic inhibition and re-energisation in response to acute changes in extracellular glucose.	181
Figure 4.26	The effects of replacing pyruvate with octanoate and acute changes in extracellular glucose on the time to contractile failure during metabolic inhibition.	182
Figure 4.27	The effect of replacing pyruvate with octanoate and acute changes in extracellular glucose on the time to rigor contracture during metabolic inhibition.	183
Figure 4.28	The effect of replacing pyruvate with octanoate replacement of pyruvate and acute changes in extracellular glucose on the viability of isolated cardiomyocytes during metabolic inhibition and re-energisation.	184
Figure 4.29	The effect of replacing pyruvate with octanoate and acute changes in extracellular glucose on the recovery of isolated cardiomyocytes to metabolic inhibition and re-energisation.	185
Figure 4.30	The impact of the addition of pyruvate on the effects of octanoate on the contractile function of isolated cardiomyocytes to metabolic inhibition and re-energisation in response to acute changes in extracellular glucose.	188
Figure 4.31	The impact of the addition of pyruvate on the effects of octanoate on the time to contractile failure during metabolic inhibition in response to acute changes in extracellular glucose.	189
Figure 4.32	The impact of the addition of pyruvate on the effects of octanoate on the time to rigor contracture during metabolic inhibition in response to acute changes in extracellular glucose.	190
Figure 4.33	The impact of the addition of pyruvate on the effects of octanoate on the viability of isolated cardiomyocytes to metabolic inhibition and re-energisation in response to acute changes in extracellular glucose.	193
Figure 4.34	The impact of the addition of pyruvate on the effects of octanoate on the recovery of isolated cardiomyocytes to metabolic inhibition and re-energisation in response to acute changes in extracellular glucose.	194
Figure 4.35	The hypothesised effects of octanoate and 10mM pyruvate during re-energisation.	208
Figure 5.1	The metabolic contractile function and $\text{SarCK}_{\text{ATP}}$	213

	preconditioning protocols	
Figure 5.2	The effects of metabolic preconditioning with elevated glucose on the response of isolated cardiomyocytes to metabolic inhibition and re-energisation.	214
Figure 5.3	The effects of metabolic preconditioning with elevated glucose on the recovery of isolated cardiomyocytes subjected to metabolic inhibition and re-energisation.	215
Figure 5.4	The effects of metabolic preconditioning with elevated glucose on $\text{SarCK}_{\text{ATP}}$ current activation during metabolic inhibition.	219
Figure 5.5	The effects of metabolic preconditioning with elevated fructose on the response of isolated cardiomyocytes to metabolic inhibition and re-energisation.	220
Figure 5.6	The effects of metabolic preconditioning with elevated fructose on the recovery of isolated cardiomyocytes subjected to metabolic inhibition and re-energisation.	221
Figure 5.7	The effects of metabolic preconditioning with elevated pyruvate on the response of isolated cardiomyocytes to metabolic inhibition and re-energisation.	223
Figure 5.8	The effects of metabolic preconditioning with elevated pyruvate on the recovery of isolated cardiomyocytes subjected to metabolic inhibition and re-energisation.	224
Figure 5.9	The metabolic postconditioning protocols	226
Figure 5.10	The effects of metabolic postconditioning with elevated glucose on the response and recovery of isolated cardiomyocytes subjected to metabolic inhibition and re-energisation.	228

List of Abbreviations

ACC	Acetyl-coenzyme A carboxylase
ACT	Carnitine/acylcarnitine translocase
ADP	Adenosine disphosphate
AGEs	Advance Glycation end products
AM	Acetoxymethyl-ester
AMI	Acute myocardial infarction
AMP	Adenosine monophosphate
AMPK	AMP-activated protein kinase
APD	Action potential duration
ATP	Adenosine triphosphate
AV	Atrioventricular
BSA	Bovine serum albumin
Ca ²⁺	Calcium
CaCl ₂	Calcium chloride
CAD	Coronary artery disease
CD36	Fatty acid translocase
CHD	Coronary heart disease
CICR	Calcium induced calcium release
Cl ⁻	Chloride
CN ⁻	Cyanide
CoA	Coenzyme A
CPT 1	Carnitine palmitoyltransferase 1
CPT 2	Carnitine palmitoyltransferase 2
Cr	Creatine
Cyt C	Cytochrome C
DADs	Delayed afterdepolarisations
DAG	Diacylglycerol
DCA	Dichloroacetate
DM	Diabetes Mellitus
DMSO	Dimethyl sulfoxide
DNP	Dinitrophenol
EADs	Early delayed afterdepolarisations
ECC	Excitation contraction coupling
EDTA	Ethylenediaminetetraacetic acid
EFS	Electrical field stimulation
EGFR	Epidermal growth factor receptor
EGTA	Ethylene glycol-bis(2-aminoethylether)-N,N,N',N'-tetraacetic acid
E _K	Equilibrium potential for potassium
E _{Na}	Equilibrium potential for sodium
ER	Endoplasmic reticulum
ERK1/2	Extracellular signal regulated kinase 1/2
ETC	Electron transport chain
FABP _{pm}	Fatty acid binding protein
FAD ⁺	Flavin adenine dinucleotide (reduced form)
FADH ₂	Flavin adenine dinucleotide (oxidised form)

FAT	Fatty acid translocase
FATP	Fatty acid transporter protein
FBP	Fructose 1-6-bisphosphate
FFA	Free fatty acid
F6P	Fructose-6-phosphate
G6P	Glucose-6-phosphate
GAPDH	Glyceraldehyde 3-phosphate dehydrogenase
GDP	Guanosine diphosphate
GLUT	Glucose transporter
GMP	Guanosine monophosphate
GSH	Glutathione
GSK	Glycogen synthetase kinase
GSK-3 β	Glycogen synthetase kinase-3 β
GTP	Guanosine triphosphate
Hepes	4-(2-Hydroxyethyl)piperazine-1-ethanesulfonic acid
H-FABP	Fatty acid binding protein
H ₂ O ₂	Hydrogen Peroxide
HSLs	Hormone sensitive lipases
IAA	Iodoacetic acid
I _{k1}	Inwardly rectifying potassium channel
I _{Kr}	Rapid delayed rectifier potassium current
I _{Ks}	Slow delayed rectifier potassium current
IP ₃	Inositol 1,4,5-trisphosphate
IP ₃ R	IP ₃ receptor
IPC	Ischaemic preconditioning
IPostcon	Ischaemic postconditioning
I/R	Ischaemia/ reperfusion injury
IRS-1	Insulin receptor subunit-1
I _{to}	Transient outward potassium current
K ⁺	Potassium
KCl	Potassium Chloride
Kir	Inwardly-rectifying potassium channel
KOH	Potassium hydroxide
LDH	Lactate dehydrogenase
LPLs	Lipoprotein lipases
MAPs	Mitogen-activated protein kinase
MCD	Malonyl CoA decarboxylase
MCT	Monocarboxylate transporter
Mg ²⁺	Magnesium
MgCl ₂	Magnesium chloride
Mg ²⁺ - Green	Magnesium Green
MI	Metabolic inhibition
MIA	5-(N-methyl-N-isobutyl)amiloride
MitoK _{ATP}	Mitochondrial ATP-sensitive inwardly-rectifying potassium channel
mnSOD	Superoxide dismutase
MPC	Mitochondrial Pyruvate carrier
mPTP	Mitochondrial permeability transition pores

Na ⁺	Sodium ion
NaCl	Sodium chloride
NaCN	Sodium Cyanide
NAD ⁺	Nicotinamide adenine dinucleotide (reduced form)
NADH	Nicotinamide adenine dinucleotide (oxidised form)
NaHCO ₃	Sodium bicarbonate co-transporter
Na ⁺ /K ⁺ ATPase	Sodium/potassium ATPase
NaOH	Sodium Hydroxide
Na pyruvate	Sodium pyruvate
NCX	Sodium calcium exchanger
NHE	Sodium hydrogen exchanger
NO	Nitric Oxide
O ₂	Oxygen
O ₂ ⁻	Superoxide
PCI	Percutaneous coronary intervention
PCr	Phosphocreatine
PDH	Pyruvate dehydrogenase
PDHK	Pyruvate dehydrogenase kinase
PDHP	Pyruvate dehydrogenase phosphatase
PFK-1	Phosphofructokinase-1
PGC-1	Peroxisome proliferator-activated receptor-γ coactivator-1
Pi	Inorganic phosphate
PIP ₂	Phosphatidylinositol 4,5-bisphosphate
PI3-K	Phosphatidyl inositol 3-kinases
PI3-K-AKT	Phosphatidyl inositol 3-kinase-protein kinase B
PKA	Protein kinase A
PKB	Protein kinase B
PKC	Protein kinase C
PKC-ε	Protein kinase C-epsilon
PKG	Protein kinase G
PLB	Phospholamban
PLC	Phospholipase C
RER	Rough endoplasmic reticulum
RISK	Reperfusion injury survival kinases
RMP	Resting membrane potential
ROS	Reactive oxygen species
RPP	Rate pressure product
RYR	Ryanodine receptor
SAN	Sino-atrial node
SarCK _{ATP}	Sarcolemmal ATP-sensitive inwardly-rectifying potassium channel
SEM	Standard error of the mean
SERCA	Sarcoplasmic/endoplasmic reticulum calcium-ATPase
SFT	Substrate free tyrode
SFT-MI	Substrate free tyrode-metabolic inhibition
SGLT	Sodium glucose dependent transporter
SNS	Sympathetic nervous system
SR	Sarcoplasmic reticulum

STZ	Streptozotocin
SUR	Sulphonylurea receptor
TAGs	Triacylglycerols
TMD	Transmembrane spanning domain
TMRE	Tetramethyl rhodamine ethyl ester
TMRM	Tetramethyl rhodamine methyl ester
TnC	Troponin C
TnI	Troponin I
TTX	Tetrodotoxin
VDAC	Voltage activated anion channel
VDKC	Voltage dependent potassium channel
VGCC	Voltage gated calcium channel
VGSC	Voltage gated sodium channel
VLDLs	Very low density lipoproteins
$[Ca^{2+}]_i$	Intracellular Calcium concentration
$[Na^+]_i$	Intracellular Sodium concentration
$[pH]_i$	Intracellular pH
ΔG_{ATP}	Free energy of ATP hydrolysis
2DOG	2 Deoxy-D-glucose
5-HD	5-hydroxydecanoic acid
α -HCN	Alpha-cyano-4-hydroxycinnamate

CHAPTER ONE
INTRODUCTION

1. Introduction

1.1 The Heart

The heart is a muscle comprised of four chambers, each having a specific role for maintaining function. The middle layer of the heart wall is known as the myocardium, which is a striated cardiac muscle composed mostly of cardiomyocytes. These are binuclear, contain multiple mitochondria and have a sarcolemmal membrane with invaginations of t-tubules running along it to aid excitation contraction coupling (ECC).

Contraction of the cardiac muscle is initiated by depolarisation of the cardiomyocytes, which in itself is triggered by the spread of an electrical signal (action potential) across the heart originating in the sino-atrial node (SAN). Prolonged depolarisation of the cardiomyocyte sarcolemmal membrane results in an increase in intracellular calcium ($[Ca^{2+}]_i$), stimulating ECC, aiding coupling of electrical activity to contraction.

Contraction is maintained by the availability of adenosine triphosphate (ATP), which is produced via the metabolism of a variety of metabolic substrates including glucose and fatty acids. The myocardium is able to turnover its ATP pool every 10 seconds under normal physiological conditions (Lopaschuk *et al.*, 2010), therefore maintained ATP production is important.

The production of ATP requires oxygen (O_2). At rest the heart consumes 8-10ml O_2 /minute per 100g of tissue, which is sufficient to meet the O_2 demands for metabolism, however during ischaemia the O_2 supply to the heart decreases. As a result the myocardium predominantly metabolises glucose anaerobically, but is unable to produce sufficient amounts of ATP, therefore ischaemic injury can occur.

At rest under normal physiological conditions the human heart contracts between 60-100 times per minute. The number of contractions per minute (heart rate) can be modulated by both the parasympathetic and sympathetic nervous systems.

Parasympathetic stimulation reduces heart rate (negative chronotropy), while sympathetic stimulation can increase both heart rate (positive chronotropy) and force of contraction (positive inotropy) (Levick, 2010). Depolarisation of the action potential

is counterbalanced by a subsequent repolarisation to allow relaxation to occur; together these stages produce the cardiac action potential.

1.2 Cardiac Action potential

Under normal physiological conditions, the human cardiac action potential has a duration of 280-340ms, however under pathophysiological conditions this duration can vary. For example acute ischaemia shortens duration, whilst prolongation is seen with chronic heart diseases such as cardiac hypertrophy and heart failure.

1.2.1 Mechanism of a ventricular action potential

The action potential of human ventricular cardiomyocytes consists of 5 phases (0-4) as indicated in Figure 1.1. Phase 4 represents the resting membrane potential (RMP) that exists prior to the activation of a cardiac action potential during diastole and is predominantly maintained by an efflux of potassium (K^+) ions through the inwardly rectifying potassium channels (Kir2.1/2.2) (I_{K1}) (Grant, 2009). The Nernst equation ($E_{ion} = (RT/zF) \ln ([ion]_o/[ion]_i)$) (Bers, 2001) predicts the K^+ equilibrium potential (E_K) to be -89mV (when the concentration of K^+ is 5mM outside and 140mM inside). However, the actual RMP for cardiomyocytes is more positive than E_K (-80 to -70mV), due to the sarcolemmal membrane having a relative permeability to other ions (e.g. sodium (Na^+) or chloride (Cl^-)). Therefore the overall RMP is contributed to by the sarcolemmal membrane's relative permeability to all ions. The Goldman-Hodgkin-Katz equation (Bers, 2001), as illustrated below, can be used to predict the actual RMP.

The Goldman-Hodgkin-Katz equation

$$V_m = RT/F \ln (p_K [K^+]_o + p_{Na} [Na^+]_o + p_{Cl} [Cl^-]_i) / (p_K [K^+]_i + p_{Na} [Na^+]_i + p_{Cl} [Cl^-]_o)$$

(Abbreviations: R= Gas constant = $8.314 \text{ J K}^{-1} \text{ mol}^{-1}$, T= absolute temperature in Kelvins ($0^\circ\text{C} = 273\text{K}$), Z = ionic valency, F = Faraday's constant = 96500 C mol^{-1} , V_m = membrane potential, $p_{K,Na,Cl}$ = membrane permeability for K^+ , Na^+ or Cl^- , $[ion]_o$ = concentration of that particular ion in the extracellular fluid and $[ion]_i$ = concentration of that particular ion in the intracellular fluid).

Initiation of the cardiac action potential occurs via depolarisation of the SAN (primary pacemaker cells), through the atrial myocardium to the atrioventricular (AV) node and onwards to the ventricles via highly specialised, rapidly conducting pathways of the His-Purkinje system. Depolarisation then propagates through the individual cardiomyocytes within the myocardium via gap junctions (Severs *et al.*, 2008; Boyett, 2009). Depolarisation stimulates the cardiomyocyte membrane potential to reach a threshold of around -55mV causing activation of the voltage-gated sodium channels (VGSC) $\text{Na}_v1.5$, resulting in a rapid depolarisation (upstroke) of the action potential (Phase 0) (Grant, 2009). At the end of phase 0 a brief overshoot occurs, due to increased conductance of $\text{Na}_v1.5$, this drives the membrane potential towards the equilibrium potential for sodium ($E_{\text{Na}} = +70\text{mV}$). On approaching E_{Na} , the VGSC inactivation gate closes rapidly and the overshoot is halted (Grant, 2009; Nerbonne & Kass, 2005). This is followed by a brief repolarisation (Phase 1) due to the inactivation of the VGSC and activation of the transient outward K^+ current (I_{to}) (Tamargo *et al.*, 2004).

Phase 1 is followed by a plateau (Phase 2) which last for 100-200ms and is maintained at around +20mV. The plateau arises from activation of L-type calcium channels ($\text{Ca}_v1.2$) passing an influx of calcium (Ca^{2+}) ions (Grant, 2009), which is balanced by an efflux of K^+ ions through the voltage dependent delayed rectifier potassium channels (VDKC), the rapid delayed rectifier potassium channel ($\text{Kv}11.1$) and the slow delayed rectifier potassium channel ($\text{Kv}7.1$), which pass the currents I_{Kr} and I_{Ks} respectively (Tamargo *et al.*, 2004). These VDKC are activated during the latter stages of the plateau due to their slow activation compared to the L-type Ca^{2+} channels (Levick, 2010) and play an important role in preventing arrhythmias by maintaining the refractory period (Levick, 2010; Tamargo *et al.*, 2004).

Repolarisation (Phase 3) occurs due to time-dependent inactivation of the L-type Ca^{2+} channels ($\text{Ca}_v1.2$) (Levick, 2010) and an increased conductance of the VDKCs. This allows a more dominant efflux of K^+ ions, which repolarises the RMP back towards E_{K} (Tamargo *et al.*, 2004). The voltage dependence of the VDKCs prevents E_{K} being reached, however the RMP is maintained close to E_{K} via activation of the I_{K1} current during repolarisation, until depolarisation occurs again (Grant, 2009).

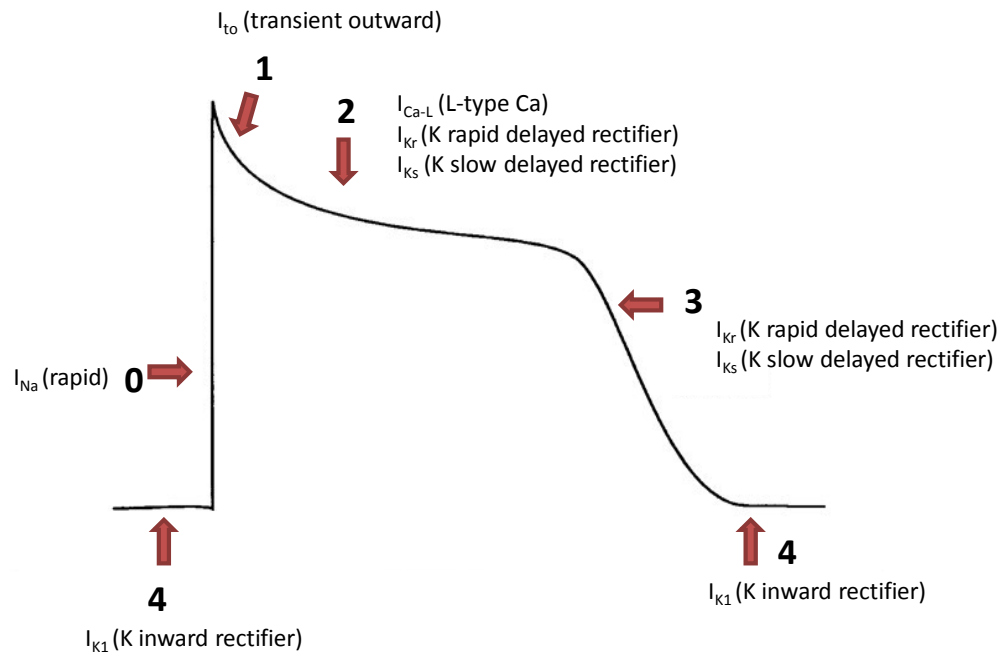


Figure 1.1 Ventricular cardiac action potential

A representation of a ventricular cardiac action potential and the ionic currents which contribute to each phase, 0 = rapid depolarisation (upstroke), 1=brief repolarisation, 2= plateau, 3= repolarisation and 4 = resting membrane potential. Diagram adapted from Nerbonne & Kass, 2005.

1.3 ATP- sensitive inwardly-rectifying potassium channels (K_{ATP})

K_{ATP} channels are a class of potassium channel that exist in a hetero-octomeric configuration comprised of an inwardly-rectifying potassium channel (Kir6.1 or Kir6.2), which is co-expressed with a member of the ATP-binding cassette (ABC) family of proteins, the sulphonylurea receptor (SUR1 or 2A/2B) (Peart & Gross, 2002; Elrod *et al.*, 2008). The exact configuration depends on the location of the K_{ATP} channel which can include cardiomyocytes, vascular smooth muscle, skeletal muscle and pancreatic β cells. Cardiac Sarcolemmal K_{ATP} (Sarc K_{ATP}) channels were first identified in isolated guinea pig ventricular myocytes by Noma in 1983 (Noma, 1983). Since this discovery other K_{ATP} channels have been postulated in cardiomyocytes, including the mitochondrial K_{ATP} (Mito K_{ATP}) channels. K_{ATP} channels are modulated by numerous pharmacological agents and by the metabolic state of the cell; a decrease in the [ATP]/[ADP] ratio stimulates opening, while a high [ATP]/[ADP] ratio inhibits opening. These channels are believed to be involved in cardioprotection (discussed further in section 1.11.2) and can be either pro or anti-arrhythmic.

1.3.1 Sarcolemmal K_{ATP} channels (Sarc K_{ATP})

Sarc K_{ATP} channels are located in the sarcolemmal membrane of cardiomyocytes. Atrial Sarc K_{ATP} channels are composed of Kir6.2/SUR1 subunits, while ventricular Sarc K_{ATP} channels are believed to have a Kir6.2/SUR2A subunit configuration as shown in Figure 1.2.

Sarc K_{ATP} channels are regulated by intracellular ATP concentrations. Increased application of ATP (0.2 to 2mM) decreases the open probability of Sarc K_{ATP} channels (Elrod *et al.*, 2008; Kakei *et al.*, 1985), which range in their sensitivity to ATP with the average IC_{50} being 37 μ M (Findlay & Faivre, 1991). The sensitivity of Sarc K_{ATP} channels to ATP is modulated by ADP, GDP and Mg^{2+} , all of which have stimulatory effects on the channel. In inside-out patch configurations, the presence of 200 μ M ADP, 50 μ M GDP and 1mM free Mg^{2+} increases the K_i for ATP to 100 μ M (Nichols & Lederer, 1990a). However, in isolated ferret hearts, subjected to simulated ischaemia by metabolic inhibition, Sarc K_{ATP} channels open when intracellular ATP remains within the mM range (Elliott *et al.*, 1989), suggesting ATP levels need not reduce significantly before

Sarck_{ATP} channels open. This agrees with findings that opening a small proportion (1%) of Sarck_{ATP} channels (due to the high density of Sarck_{ATP} channels in the sarcolemmal membrane of cardiomyocytes and their large conductance of 70pS) or an increase in open probability, significantly hyperpolarises the cardiomyocyte membrane potential and shortens action potential duration (APD) by up to 50% (Noma, 1983; Nichols & Lederer, 1990a; Weiss & Lamp, 1987). The close proximity to the Sarck_{ATP} channels of several glycolytic enzymes including glyceraldehyde-3-phosphate (GADPH), aldolase, triose phosphate isomerase, phosphoglycerate kinase and pyruvate kinase (Dhar-Chowdhury *et al.*, 2005; Jovanovic *et al.*, 2005; Hong *et al.*, 2011) further suggests these channels will open even when ATP levels are maintained locally. As during ischaemia, anaerobic glycolytic metabolism continues to produce ATP, but Sarck_{ATP} channels still open.

Opening of Sarck_{ATP} channels shortens the APD, which limits Ca²⁺ influx via the L-type Ca²⁺ channels, preventing Ca²⁺ overload and negative inotropism (Stowe, 1999). The reduction in Ca²⁺ overload is attributed not only to inhibition of the L-type Ca²⁺ channel, but is also speculated to be due to a reduction in the reverse-mode activity of the NCX, which controls Ca²⁺ homeostasis during reoxygenation (Baczko *et al.*, 2004). Shortening the APD means arrhythmias are less likely to occur. However opening Sarck_{ATP} channels can result in accumulation of extracellular K⁺; especially during the late phase of an acute myocardial infarction (AMI), causing depolarisation of the membrane potential and potentially stimulate arrhythmias (Baczko *et al.*, 2004).

1.3.2 Mitochondrial K_{ATP} channels (MitoK_{ATP})

The existence of MitoK_{ATP} channels in the inner mitochondrial membrane was first demonstrated by Inoue, by patch clamping mitoplasts prepared from rat liver mitochondria (Inoue *et al.*, 1991). Since then reconstituted MitoK_{ATP} channels from rat liver, bovine heart and isolated mitochondria, have illustrated similar properties to Sarck_{ATP} including a K⁺ current, which can be regulated by similar pharmacological agents as the Sarck_{ATP} channel current including diazoxide, pinacidil, (mg)ATP and glibenclamide, while possessing a distinct profile (Paucek *et al.*, 1992; Garlid *et al.*, 1996).

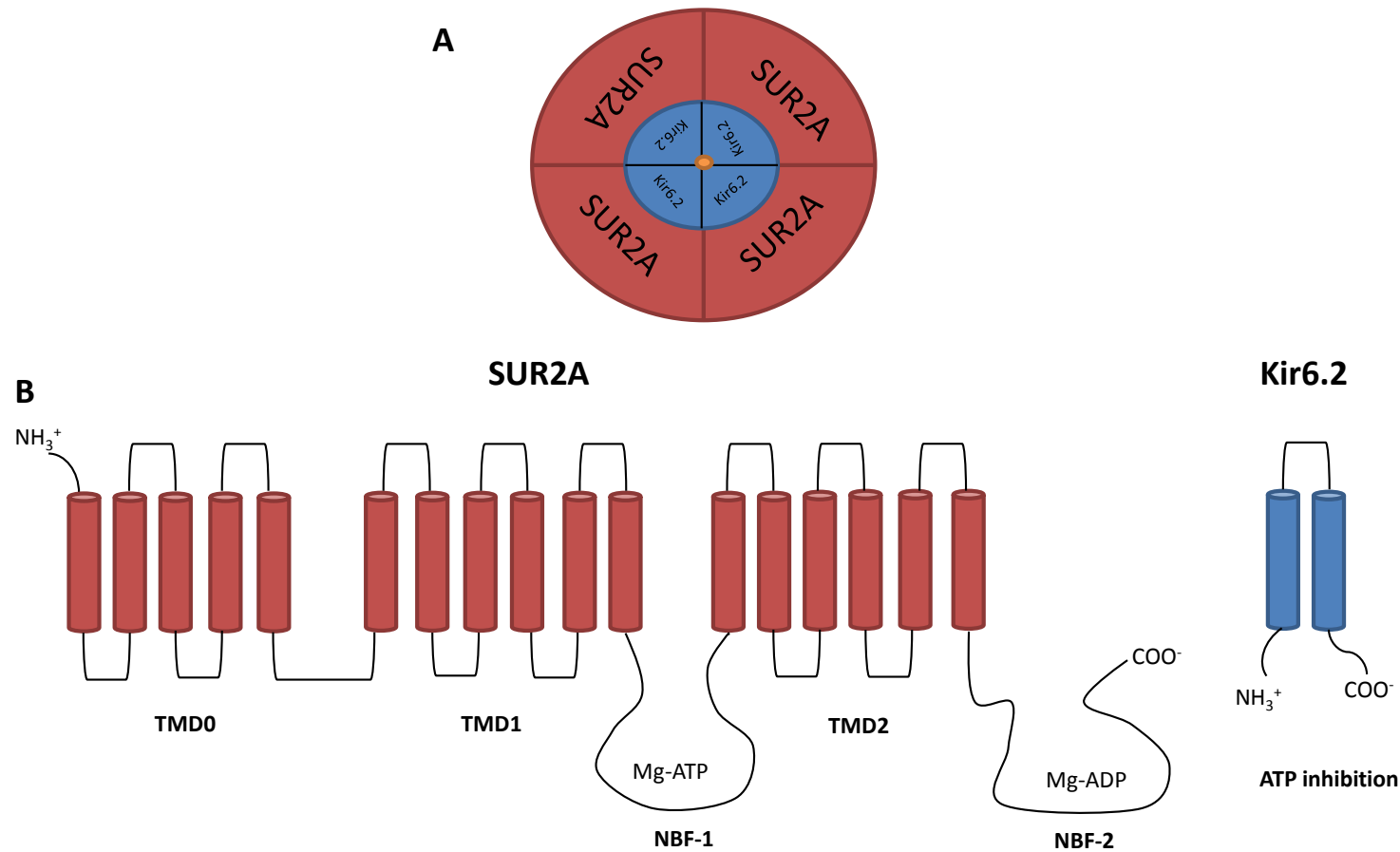


Figure 1.2 Ventricular SarcK_{ATP} channel structure

(A) The hetero-octameric structure of SarcK_{ATP} with 4 Kir6.2 subunits combining with 4 SUR2A sulfonylurea subunits. (B) Membrane topology of SarcK_{ATP} structure. The SUR subunit is believed to have three transmembrane spanning domains (TMD) and two nucleotide binding sites (NBS), the first of these (NBF-1) is located between TMD1 and 2. The second NBS (NBF-2) is located on the intracellular carboxy terminal end of TMD3. The amino terminus is located on the extracellular side. The Kir subunit has two transmembrane spanning domains with both the N and C termini located intracellularly. Diagram adapted from Seino, 1999.

As genetic studies on MitoK_{ATP} null mice are currently unavailable, agonists and antagonists known to activate SarcK_{ATP} channels have been used to pharmacologically profile MitoK_{ATP}. Opening of MitoK_{ATP} channels has been hypothesised to lead to oxidation of mitochondrial flavoproteins causing a change in fluorescence. Measuring the fluorescence of flavoproteins has been used as an indication of MitoK_{ATP} activity (Liu *et al.*, 1998). Experiments on native cardiac channels expressed in human embryonic kidney 293 cells and rabbit ventricular cardiomyocytes, revealed the agonists diazoxide and pinacidil (100µM) both induced reversible oxidation of flavoproteins, which was not altered by the antagonist HMR 1098 (30µM/10 µM) or by the agonist P-1075 (30µM /100µM) but was blocked or attenuated by the antagonist sodium 5-hydroxydecanoate (5-HD) at 500µM and 200µM respectively (Sato *et al.*, 2000; Liu *et al.*, 2001). These findings suggest pinacidil activates both K_{ATP} channel isoforms but HMR 1098 and P-1075 selectively inhibits/ activates SarcK_{ATP} respectively rather than MitoK_{ATP}. After simulated ischaemia, diazoxide (50 or 100µM) significantly improved cell recovery, this was abolished by 5-HD (100µM) and the antagonist glibenclamide (1µM) but not HMR 1098 or P-1075 suggesting the cardioprotection elicited is MitoK_{ATP} based rather than SarcK_{ATP} (Sato *et al.*, 2000; Liu *et al.*, 2001). These experiments lead to the assumption that the configuration of MitoK_{ATP} is Kir6.1/SUR1 (Liu *et al.*, 2001). This was backed up by experiments that transfected Kir6.1/SUR1 and Kir6.2/SUR2A into tsA201 cells and found HMR 1098 only inhibited the Kir6.2/SUR2A current (Manning Fox *et al.*, 2002). While ventricular cells from Kir6.2 K/O mice still displayed diazoxide induced reversible flavoprotein oxidation, suggesting MitoK_{ATP} function is preserved therefore Kir6.2 is believed to not be involved in MitoK_{ATP} (Suzuki *et al.*, 2002).

1.3.3 Pharmacological modulation of SarcK_{ATP} and MitoK_{ATP} channel activity and cardioprotection.

SarcK_{ATP} and MitoK_{ATP} channels are both modulated by numerous pharmacological agonists including; pinacidil, P-1075 and diazoxide (believed to be MitoK_{ATP} specific) and antagonists; the sulphonylurea agents glibenclamide, HMR 1098 (which is more potent for the cardiac specific SUR2A isoform) and 5-HD (MitoK_{ATP} specific) (Gross & Auchampach, 1992; Manning Fox *et al.*, 2002; Sato *et al.*, 2000).

Diazoxide activation of the cardiac specific Kir6.2/SUR2A SarcK_{ATP} channel has been shown to be cardioprotective, however this activation is only achieved by the presence of high levels of ADP/Mg²⁺ which are associated with ischaemia (D'hahan *et al.*, 1999).

Pre-treating isolated guinea pigs hearts with pinacidil before no flow ischaemia has been found to reduce ADP₉₀ leading to reduced ischaemia and reperfusion injury, while glibenclamide enhances damage (Cole *et al.*, 1991). Meanwhile pinacidil stimulation of SarcK_{ATP} opening during reoxygenation, hyperpolarises the membrane potential, reducing the percentage of cardiomyocytes entering hypercontracture, possibly by reducing Ca²⁺ during reoxygenation. The antagonist HMR 1098 has the opposite affect (Baczko *et al.*, 2004).

During reoxygenation, HMR 1098 (10μM) has been found to abolish the protection afforded by pre-treatment with PMA (activator of PKC) but not during chemically induced hypoxia (CIH) (Light *et al.*, 2001), suggesting SarcK_{ATP} channels are involved during reoxygenation. During the same study application of 5-HD during CIH attenuated the protection afforded by pre-treatment with PMA, which usually prevents the Ca²⁺ increase during CIH, but had no effect on the PMA induced protection during reoxygenation (Light *et al.*, 2001). This suggests MitoK_{ATP} channels are involved during ischaemia through Ca²⁺ loading effects. Together these results indicated inhibition of different K_{ATP} channels at different stages of cell injury may be more detrimental than the other and that activity of MitoK_{ATP} is important during ischaemia.

Pharmacological agents have also been used to determine the effects of opening MitoK_{ATP} channels. During normoxia it has been suggested opening MitoK_{ATP} leads to an influx of K⁺ ions into the mitochondrial matrix causing swelling of the mitochondria; depolarisation of the mitochondrial membrane potential and dissipation of the inner mitochondrial membrane potential, which accelerates respiration and leads to reduced ATP synthesis (Liu *et al.*, 1998; Suzuki *et al.*, 2002; Costa *et al.*, 2006; Holmuhamedov *et al.*, 1998), increased oxidation of mitochondrial matrix flavoproteins and suppressed ROS production (Kopustinskiene *et al.*, 2010). However, opening of MitoK_{ATP} channels during ischaemic conditions, results in a maintained

mitochondria matrix volume, accompanied by a reduction in the outer mitochondrial membrane permeability to ADP and ATP (Costa *et al.*, 2006). This reduces ATP hydrolysis and maintains ATP/ADP levels. These findings suggest opening MitoK_{ATP} during ischaemia may protect the myocardium from ischaemia injury, whereas opening during normoxic conditions can be detrimental.

The cardioprotection effects associated with MitoK_{ATP} opening includes, increased ROS production and prevention of mitochondrial Ca²⁺ overload, due to depolarisation of the mitochondrial membrane potential reducing Ca²⁺ uptake into the mitochondria via the Ca²⁺ uniporter (Liu *et al.*, 1998; Costa *et al.*, 2006). These effects can result in inhibition of the formation of mPTP and as a result can prevent necrosis and apoptosis.

1.3.4 Limitations of the pharmacological agents of SarcK_{ATP} and MitoK_{ATP} channels

Many of the pharmacological agents mentioned in the previous section have other effects which do not relate to SarcK_{ATP} and MitoK_{ATP} channels. For example diazoxide has been shown to have no effect on flavoprotein fluorescence or mitochondrial membrane potential, but can interfere with the activity of the electron transport chain (ETC) by inhibiting succinate oxidation and succinate dehydrogenase activity (complex 2 of the ETC) (Hanley *et al.*, 2002). Meanwhile pinacidil can inhibit NADH oxidation (complex 1 of the ETC) (Hanley *et al.*, 2002). In addition 5-HD can be a substrate for acyl-CoA synthetase, thus overcoming the inhibition of the ETC that diazoxide and pinacidil can cause (Hanley *et al.*, 2002). These findings suggest rather than affecting MitoK_{ATP} channels, diazoxide, pinacidil and 5-HD have metabolic effects within cardiomyocytes and that opening of these channels may result in inhibition of ATP synthesis. Therefore it is possible these compounds have both metabolic and MitoK_{ATP} channel activity effects, within cardiomyocytes.

Furthermore many of the sulphonylurea pharmacological inhibitors of SarcK_{ATP} such as glibenclamide (which is not selective and therefore cannot distinguish between SarcK_{ATP} and MitoK_{ATP} channels), glimepiride and HMR1098, have been demonstrated to be ineffective during metabolic inhibition due to increased intracellular ADP relieving the block these inhibitors cause (Ripoll *et al.*, 1993; Findlay, 1993; Lawrence *et al.*, 2002; Rainbow *et al.*, 2005). Therefore these agents may not be suitable for

effectively deducing activity of SarcK_{ATP} channels under conditions of metabolic inhibition.

1.4 Excitation-contraction coupling

Excitation-contraction coupling (ECC) is the mechanism by which individual cardiomyocytes couple electrical activity to contraction, by coupling Ca²⁺ to contraction and utilising ATP as energy. ECC results in the formation of crossbridges, which are regulated by the [Ca²⁺]_i level, and in turn can be altered by pathophysiological conditions.

1.4.1 Mechanism behind excitation-contraction coupling

The arrival of an action potential which travels down the t-tubule invaginations of the sarcolemmal membrane, triggers depolarisation, opening the L-type Ca²⁺ channels, leading to an influx of Ca²⁺ ions, raising the local [Ca²⁺]_i. L-type Ca²⁺ channels are positioned in close proximity to ryanodine receptors (RyR2) located on terminal feet like projections on the sarcoplasmic reticulum (SR). The increase in local Ca²⁺ causes Ca²⁺ to bind to the RyR2 opening them, allowing Ca²⁺ release from the SR, this process is calcium induced calcium release (CICR) (Bers, 2002). Ca²⁺ entry through the L-type Ca²⁺ channel is the dominant Ca²⁺ current to stimulate CICR (Bers, 2002; Sipido *et al.*, 1998). However the T-type Ca²⁺ current and the reverse mode activity of the sodium-calcium exchanger (NCX) are also believed to have minor roles in CICR in ventricular myocytes (Sipido *et al.*, 1998; Leblanc & Hume, 1990; Levesque *et al.*, 1994; Levi *et al.*, 1994). CICR raises the [Ca²⁺]_i enabling crossbridge cycling to occur, while ATP is involved in cross-bridge detachment as illustrated in Figure 1.3. Contraction ceases allowing for relaxation when [Ca²⁺]_i reduces as this enables troponin C to move back to its original position, so the actin binding site is no longer exposed to myosin thus ending contraction. The [Ca²⁺]_i levels are reduced either via re-uptake of Ca²⁺ into the SR via the sarcoplasmic/endoplasmic reticulum calcium ATPase (SERCA-2A); by uptake into the mitochondria via Ca²⁺ uniports, or by removal at the sarcolemmal membrane via the NCX and Ca²⁺ ATPase (Bers, 2002).

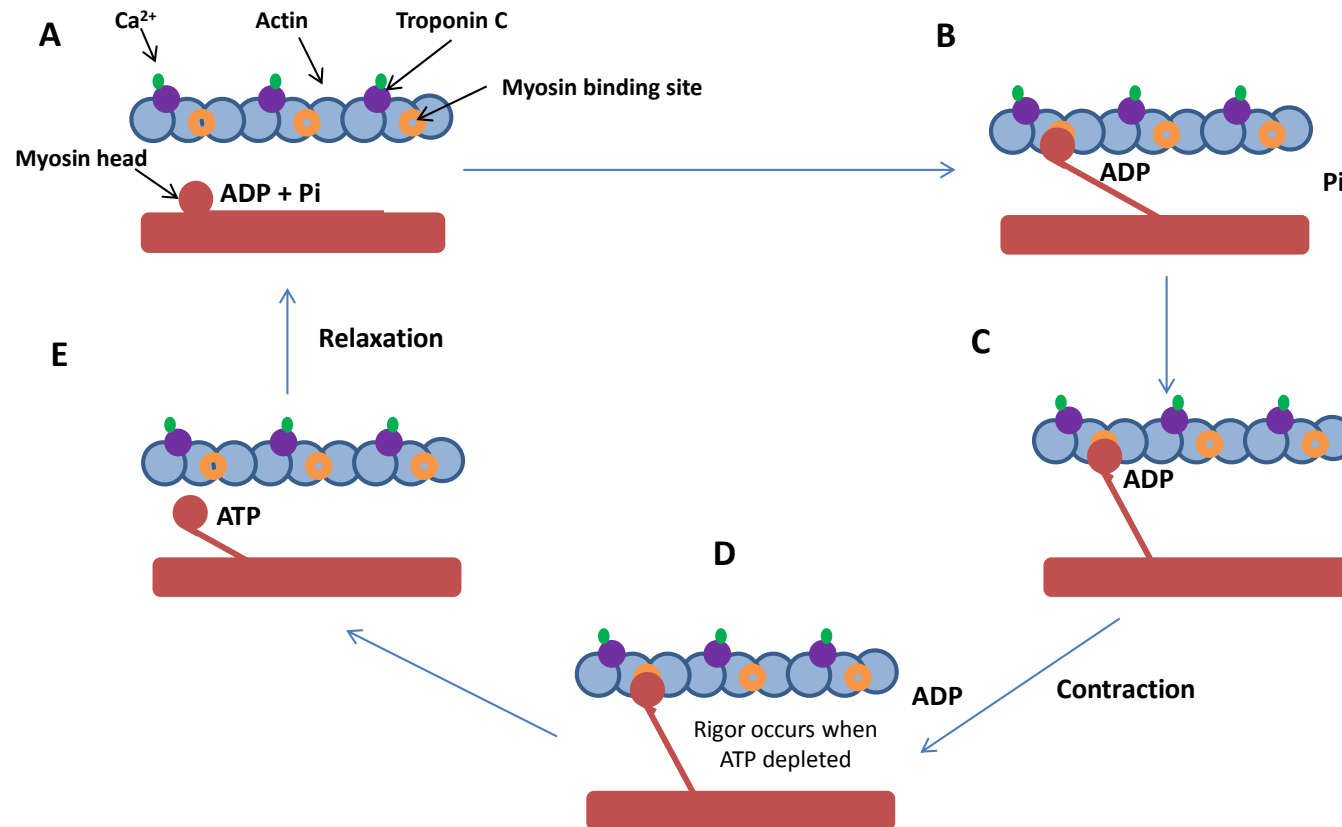


Figure 1.3 Crossbridge cycling

(A) Calcium binds to Troponin C on the thin filament, causing a conformational change which allows tropomyosin to move, this exposes myosin binding sites on the actin thin filament. (B) The myosin head (located on the thick filament) binds to the myosin binding site, forming a crossbridge. Pi is released enhancing binding of the myosin head to actin. (C) The myosin head flexes causing a power stroke which releases ADP (D) this shortens the sarcomere causing contraction. (E) A new ATP molecule binds to the myosin head, this renders myosin unable to bind to the myosin binding site. Reactivation of the myosin head occurs when ATP is hydrolysed, as this allows the myosin head to move back into its original conformation. Diagram adapted from Longmore, 1968.

1.4.2 Calcium regulation in excitation-contraction coupling

The SR acts as a Ca^{2+} store within cardiomyocytes, with Ca^{2+} being sequestered into the SR via SERCA. SERCA is regulated by phospholamban (PLB) which in its unphosphorylated state inhibits SERCA activity; this inhibition is relieved by phosphorylation via protein kinase A (PKA) (Bers, 2002). Under physiological conditions, sympathetic stimulation increases SERCA activity resulting in greater Ca^{2+} uptake into the SR. This can increase contraction strength (+ve inotropism) and the rate of relaxation (+ve lusitropism). Thapsigargin also inhibits SERCA and results in a slower decline in the electrically evoked Ca^{2+} uptake. The concentration of thapsigargin required for the half maximal reduction of the uptake rate ($K_{1/2}$) for both rabbit and rat has been determined and used to estimate that in rabbit cardiomyocytes SERCA pump density is $7.7\mu\text{mol/kg wet wt}$, compared to $54.6\mu\text{mol/kg wet wt}$ in rats cardiomyocytes (Hove-Madsen & Bers, 1993), this finding is in keeping with the understanding that rats have a higher reliance on SERCA than rabbits (Bers, 2002).

The close proximity of the L-type Ca^{2+} channels to the RYRs allows for a microscopic domain to be created, which allows a rapid response of adjacent RYRs to the local influx of Ca^{2+} via the L-type Ca^{2+} channels (Cannell & Kong, 2012). These local release events are visualised as Ca^{2+} sparks (Cheng *et al.*, 1993). Termination of Ca^{2+} release from RYRs can occur via many mechanisms including; competition of the $\text{Ca}^{2+}/\text{Mg}^{2+}$ binding sites on the SR (cytoplasmic/luminal sites) at times of elevated Mg^{2+} , and a coupling gating mechanism where the state of one RYR cluster will impact on the state of adjacent RYRs. A decrease in the SR Ca^{2+} content also reduces Ca^{2+} release by the RYR and the Ca^{2+} binding protein calsequestrin (located on the luminal side RYR) can also impact on the activity of the RYR (Cannell & Kong, 2012). Recovery of RYRs from inactivation can take milliseconds-seconds (Bers, 2002), and can prevent inappropriate Ca^{2+} release from the SR, which may prevent Ca^{2+} oscillations.

The SR also contains Inositol 3 triphosphate (IP_3) receptors (Perez *et al.*, 1997; Lipp *et al.*, 2000). However with low abundance of IP_3 receptors compared to RYR2 receptors and the action potential not stimulating IP_3 release, these receptors are not significantly involved with CICR during normal ECC. They are thought to play a role in

the regulation of gene expression and are most abundantly located in the nuclear envelope of cardiomyocytes.

1.4.3 Ischaemic modulation of excitation contraction coupling

During ischaemia ECC activity is modulated by a reduction in Ca^{2+} entry due to shortening of the plateau phase of the action potential. Shortening of the APD occurs due to increased activity of the $\text{SarcK}_{\text{ATP}}$ channels (Lederer *et al.*, 1989). This reduces L-Type Ca^{2+} Channel activity and as a result $[\text{Ca}^{2+}]_i$ reduces (Allen & Orchard, 1987; Lederer *et al.*, 1989). Acidosis and increased inorganic phosphate (P_i) levels which occur during ischaemia also affect contraction; by decreasing the ability of Ca^{2+} to bind to troponin C, and by reducing the Ca^{2+} sensitivity of the contractile machinery respectively (Katz, 1973; Kentish, 1986). During ischaemia ATP is also depleted, resulting in the contractile machinery entering the state of rigor. As there are no new ATP molecules available to dislodge the myosin head from the actin binding site, the contractile machinery remains locked together in a shortened configuration. Upon reperfusion of the ischaemic tissue ATP production recommences, this can result in hypercontracture (further shortening of the sarcomere) due to contractile machinery being re-established in an uncontrolled manner in combination with elevated Ca^{2+} levels. The elevated Ca^{2+} levels can also lead to spontaneous Ca^{2+} release from the SR, triggering Ca^{2+} oscillations, resulting in activation of the NCX, causing delayed after depolarisations (DADs) which can lead to arrhythmias (Piper *et al.*, 2004). These types of arrhythmias also occur under pathophysiological conditions other than ischaemia, i.e. hypertrophy or heart failure.

1.5 Coronary Heart Disease

Coronary Heart Disease (CHD) occurs when arteries harden and fatty deposits (atheroma) develop to form atherosclerotic plaques (accumulation of cholesterol, triglycerides and calcium) within the walls of the coronary arteries (Zaman *et al.*, 2000), which narrows the arteries, reducing blood flow. Partial blockage of the artery can cause angina pectoris which can be pre-emptive of a myocardial infarction. If the plaque ruptures, blood clotting is stimulated by exposure to sub-endothelial tissues of platelets and clotting factors, leading to thrombus formation. A large thrombus can

completely occlude the coronary artery, preventing blood flow to a region of the myocardium, resulting in that region becoming ischaemic. Limited blood flow to the myocardium over a significant time period can result in myocardial infarction (cardiomyocyte death by necrosis and apoptosis) (Verma *et al.*, 2002), the severity and duration of ischaemia determines the proportion of myocardial tissue which becomes infarcted. Restoration of blood flow through the blocked artery is known as reperfusion; however, reperfusion can stimulate cell death itself, known as reperfusion injury (Verma *et al.*, 2002). Myocardial ischaemia for a substantial time can also result in structural changes (cardiac remodelling) occurring within the myocardium i.e. fibrosis. Fibrosis occurs when dead cardiomyocytes are replaced by fibroblasts. Fibrosis can lead to other CHD related conditions such as heart failure and cardiac hypertrophy, which can affect the electrical activity of the heart, leaving it more susceptible to arrhythmias (Swynghedauw, 1999; Nguyen *et al.*, 2014). Prior to cardiac remodelling, ischaemia can also leave the heart susceptible to arrhythmias due to biochemical changes. The British Heart Foundation and the NHS estimate that CHD is the UK's biggest killer and was responsible for over 80,000 deaths in 2010; of these 68% occurred in the over 75's population with the highest incidence occurring in males (Townsend *et al.*, 2012). Although the incidence of CHD related deaths has declined over the past 50 years, the morbidity rates of CHD related occurrences such as myocardial infarction, still stands at >103,000 per year (Townsend *et al.*, 2012) and is of considerable expense to the NHS. Diabetes is a common comorbidity of CHD as it can contribute to endothelial dysfunction; hypertension, atherosclerosis, inflammation and thrombus formation (Creager *et al.*, 2003). Diabetes can also increase the risk of an individual suffering from the no-flow phenomenon following re-vascularisation (Iwakura *et al.*, 2001).

1.6 Ischaemic and Reperfusion injury

1.6.1 Ischaemia

Ischaemia as a result of inadequate blood flow brought about by coronary artery stenosis or occlusion results in impaired contractility, as a consequence of altered mechanisms within the cardiomyocytes. During ischaemia ATP levels become depleted

due to a lack of O₂ inhibiting oxidative phosphorylation. In an effort to maintain ATP levels required to support the energy demands of cardiomyocytes, creatine kinase and adenylate kinase work to buffer ATP levels at sites of ATP utilisation (see section 1.10.2.1) but these are only short term stores (Depre & Taegtmeyer, 2000; Nichols & Lederer, 1990b). There is also an increase in activity of the anaerobic glycolytic pathway. However stimulation of this pathway (at normoglycaemic glucose concentrations) does not produce enough ATP to maintain long term crucial activity of the ATP-dependent ion pumps/transporters such as SERCA, the sodium-potassium ATPase (Na⁺/K⁺ ATPase) and Ca²⁺ ATPase (at sarcolemmal membrane) located within the cardiomyocytes.

Increased activity of the anaerobic glycolytic pathway also results in increased conversion of pyruvate to lactate via lactate dehydrogenase (LDH); this increases lactic acid formation resulting in intracellular acidosis, which eventually inhibits glycolysis. In an effort to reduce the acidosis, activity of the sodium/hydrogen exchanger (NHE) is increased; however this causes a rise in intracellular sodium ([Na⁺]_i). The rise in Na⁺ during ischaemia has also been attributed to activity of the persistent Na⁺ channels (Xiao & Allen, 1999). However as the rise in [Na⁺]_i observed during ischaemia can be delayed by inhibiting the NHE with 5-(*N*-methyl-*N*-isobutyl)amiloride (MIA) (Murphy *et al.*, 1991), it is suggested both the persistent Na⁺ channel and NHE contribute to the rise in [Na⁺]_i occurring during ischaemia. In addition to the increased activity of the NHE and the persistent Na⁺ channels; inhibition of Na/K⁺ ATPase due to depletion of ATP also contributes to the [Na⁺]_i level, as inhibition of this pump means Na⁺ ions are no longer extruded from the cytosol (Buja, 2005). The increased [Na⁺]_i concentration and depolarisation of the membrane potential drives NCX to work in reverse mode, therefore Na⁺ rather than Ca²⁺ is extruded from the cardiomyocytes in a ratio of 3Na⁺:1Ca²⁺ (Inserte *et al.*, 2002). Reverse mode activity of NCX in combination with a lack of Ca²⁺ removal from the cytosol due to inhibited SERCA and PMCA, results in accumulation of Ca²⁺ within the cytosol of cardiomyocytes. The rise in [Ca²⁺]_i can be inhibited by the postponement of activity of NHE with MIA, as a result contractile function is improved (Murphy *et al.*, 1991). Increased sympathetic activity during ischaemia (due to decreased cardiac output and arterial pressure) can also contribute

to the increased Ca^{2+} levels and can stimulate early delayed afterdepolarisations (EADs), DADs, necrotic and apoptotic cell death.

1.6.2 Reperfusion

To limit ischaemic damage, rapid reperfusion of the ischaemic tissue following an AMI is essential. Currently the most effective and rapid method for this is revascularisation via either thrombolytic treatment (thrombolytic drugs) or percutaneous coronary intervention (PCI). Reperfusion taking place greater than 3 hours after the onset of ischaemia, can result in the reversible cellular injury sustained during ischaemia becoming irreversible this is known as reperfusion injury (Buja, 2005).

Reperfusion involves the ischaemic tissue being resupplied with oxygenated blood and metabolic substrates. This re-energises the mitochondria and repolarises the mitochondrial membrane; as a result ATP production via oxidative phosphorylation recommences. This restores activity of the ATP-dependent pumps/transporters. Increased ATP production enables the Na^+/K^+ ATPase to reduce the $[\text{Na}^+]_i$ level acquired during ischaemia (Van Emous *et al.*, 1998; Van Emous *et al.*, 2001). This stimulates the NHE to remove protons, reducing the acidosis and enabling contraction to recommence, however activation of the NHE during reperfusion can cause a rapid rise in $[\text{Na}^+]_i$. Inhibition of the NHE during reperfusion can limit reperfusion injury, possibly by inhibiting the rise in Na^+ , thus reducing activity of the NCX which is found to be further activated during reperfusion leading to Ca^{2+} overload (Xiao & Allen, 1999; Murphy *et al.*, 1991; Karmazyn, 1988; Tani & Neely, 1989; Tani, 1990; Van Echteld *et al.*, 1991). The Ca^{2+} overload occurring during reperfusion can be attenuated by reperfusion with a Ca^{2+} free tyrode; inclusion of a NCX inhibitor KB-R7943, or by inhibiting the sarcolemmal and mitochondrial Ca^{2+} channels with verapamil and ruthenium red respectively. These inhibitory mechanisms can increase the percentage of cardiomyocytes recovering Ca^{2+} homeostasis and contractile function, but does not prevent hypercontracture (Inserte *et al.*, 2002; Figueredo *et al.*, 1991; Benzi & Lerch, 1992; Massoudy *et al.*, 1995; Rodrigo & Standen, 2005).

Reperfusion also leads to reactivation of SERCA allowing excess $[\text{Ca}^{2+}]_i$ to be sequestered into the SR, this can trigger Ca^{2+} oscillations, which is also contributed to

by Ca^{2+} influx via the reverse mode activity of the NCX. Once the oscillations begin, the NCX works to remove the Ca^{2+} released by the SR, this can induce DADs (Piper *et al.*, 2004; Schafer *et al.*, 2001). Ca^{2+} oscillations together with the cytosolic Ca^{2+} overload, in combination with recommenced ATP production, results in cardiomyocytes being subjected to maximal activation of the contractile machinery resulting in hypercontracture, which is a characteristic of reperfusion injury (Rodrigo & Standen, 2005; Vander Heide *et al.*, 1986; Bowers *et al.*, 1993; Piper *et al.*, 2004).

Hypercontracture is preceded by a rapid rise in $[\text{Ca}^{2+}]_i$ and occurs when ATP rises by 100-200 μm . In isolated cardiomyocytes hypercontracture is characterised by irreversible morphological changes, including sarcolemmal blebbing, cell shortening and loss of the characteristic rod-shaped morphology (Baczko *et al.*, 2004; Rodrigo & Standen, 2005; Bowers *et al.*, 1993). Reperfusion injury in the myocardium following an AMI is characterised by the appearance of contraction band necrosis (hypercontracted sarcomeres and sarcolemmal membrane rupturing), loss of ionic homeostasis and the release of intracellular cardiac proteins and enzymes (troponin I, LDH and creatine kinase) (Piper *et al.*, 2004; Laclau *et al.*, 2001).

Increased $[\text{Ca}^{2+}]_i$ levels during reperfusion can also activate Ca^{2+} dependent nucleases, proteases and phospholipases leading to cell damage (Murphy *et al.*, 1991; Tani, 1990; Halestrap *et al.*, 2004). During reperfusion Ca^{2+} up-take into the mitochondria is driven by the increased cytosolic Ca^{2+} level, this can increase free oxygen radical production (oxidative stress) (Halestrap *et al.*, 2004; Bowers *et al.*, 1993).

During reperfusion, intracellular pH is restored due to re-established activity of the NHE, HCO_3 influx and the removal of lactate and CO_2 (Vandenberg *et al.*, 1993). Maintaining an acidic intracellular pH (pH 6.8 and 6.4) during reperfusion (even for the first 5 minutes) or prolonging acidosis by inhibiting NHE with HOE-694 has been found to be protective and prevent hypercontracture (Ladilov *et al.*, 1995). This may be due to inhibited NHE preventing H^+ extrusion from the cytosol (Ladilov *et al.*, 1995), therefore reverse mode activity of the NCX would be inhibited, resulting in an attenuated Ca^{2+} influx. Prevention in hypercontracture could also result from cytosolic acidosis desensitising tropomyosin C to Ca^{2+} (Fabiato & Fabiato, 1978).

During ischaemia, mPTP opening is inhibited by acidic conditions. Restoration of pH during reperfusion, in combination with other events arising in the first few minutes of reperfusion, such as mitochondrial repolarisation; oxidative stress, free radical production, and increased cytosolic Ca^{2+} driving mitochondrial Ca^{2+} accumulation, can stimulate mPTP to open (Halestrap, 1991; Griffiths & Halestrap, 1995; Di Lisa *et al.*, 2001; Halestrap *et al.*, 2004; Crompton *et al.*, 1987; Crompton & Costi, 1988; Korge *et al.*, 2001). Opening mPTP can stimulate cell death via apoptosis and/or necrosis (described in section 1.10.3), with the majority of cell death arising during reperfusion being apoptotic.

The presence of either Cyclosporin A (CsA) or Sanglifehrin A (SfA) (both inhibitors of mPTP) during reperfusion can protect against ischaemic/reperfusion injury in both isolated cardiomyocytes and whole heart studies. The protection observed includes reduced infarct size in intact hearts and a higher proportion of cardiomyocytes recovering Ca^{2+} and contractile function (Griffiths & Halestrap, 1993; Hausenloy *et al.*, 2003; Rodrigo & Standen, 2005). Administration of SfA for only the first 15 minutes has been found to be protective, indicating again that the first few minutes of reperfusion are critical and offer a window for protection (Hausenloy *et al.*, 2003).

1.7 Monosaccharides

Monosaccharides (e.g. glucose, fructose and galactose) are the simplest form of sugar. The majority of human monosaccharide intake comes from the diet; either directly or from the breakdown of disaccharides (e.g. sucrose). In this section two monosaccharides glucose and fructose will be discussed further, as under both normal and pathophysiological conditions cardiomyocytes metabolise these monosaccharides via glycolytic metabolism to generate ATP. Generation of ATP is essential in maintaining intracellular ionic homeostasis in order to limit ischaemic injury.

1.7.1 Glucose in humans

The human body has the capacity to release glucose either from glycogen stores via glycogenolysis, or synthesize glucose from other metabolites (i.e. pyruvate or amino acids) via gluconeogenesis, when blood glucose concentrations are too low. When

glucose is in plentiful supply several organs (e.g. liver and myocardium) and the skeletal muscle convert glucose into glycogen via glycogenesis. The main site of glucose metabolism is the liver, which has a metabolic pathway similar to the myocardium. However rather than the first enzyme being glucose hexokinase it is a glucokinase which has a lower affinity for glucose (Van Schaftingen, 1994). Once metabolised glucose can generate ATP or can act as pre-cursors for other metabolic components such as amino acids, ketones and fatty acids.

1.7.2 Glucose regulation in humans

The normal blood glucose range in a non-diabetic is 3.5-5.5mM; post-prandial blood glucose (2 hours after a meal) levels increase to 5.6-7.8mM, while after a 24 hour fast the blood glucose level decreases to 3.3-4.4mM. In order to regulate blood glucose levels, two hormones, insulin and glucagon are secreted by the pancreas. The peptide hormone insulin is released when blood glucose levels are elevated. Insulin is synthesised in the pancreatic β -cells of the islets of Langerhans. Glucose is transported into the β -cells via GLUT-2 and metabolised, which raises intracellular ATP levels. This results in the closure of K_{ATP} channels located on the β -cell plasma membrane, which depolarises the membrane, causing activation of voltage-gated calcium channels (VGCC) and an influx of Ca^{2+} into the β -cell. This stimulates exocytosis of the insulin secretory vesicles, which concludes in the release of insulin into the bloodstream (Koster *et al.*, 2005).

Once released, insulin binds to the insulin receptors, which belong to the family of Tyrosine Kinase receptors (Backer *et al.*, 1992). The actions of insulin are to stimulate the uptake of glucose in order to lower the blood glucose concentration, as illustrated in Figure 1.4A. Termination of the insulin signal occurs via internalisation of the insulin receptor to the Golgi apparatus (Hedo & Simpson, 1984), or by dephosphorylation of the tyrosine residues on the insulin receptor β -subunit (Solow *et al.*, 1999).

The pancreatic α -cells synthesises and secrete a second regulatory peptide hormone glucagon, which is stimulated to be released when blood glucose levels reach <4mM. Once released glucagon binds to glucagon receptors and works to promote glucose release (Jiang & Zhang, 2003) as illustrated in Figure 1.4B.

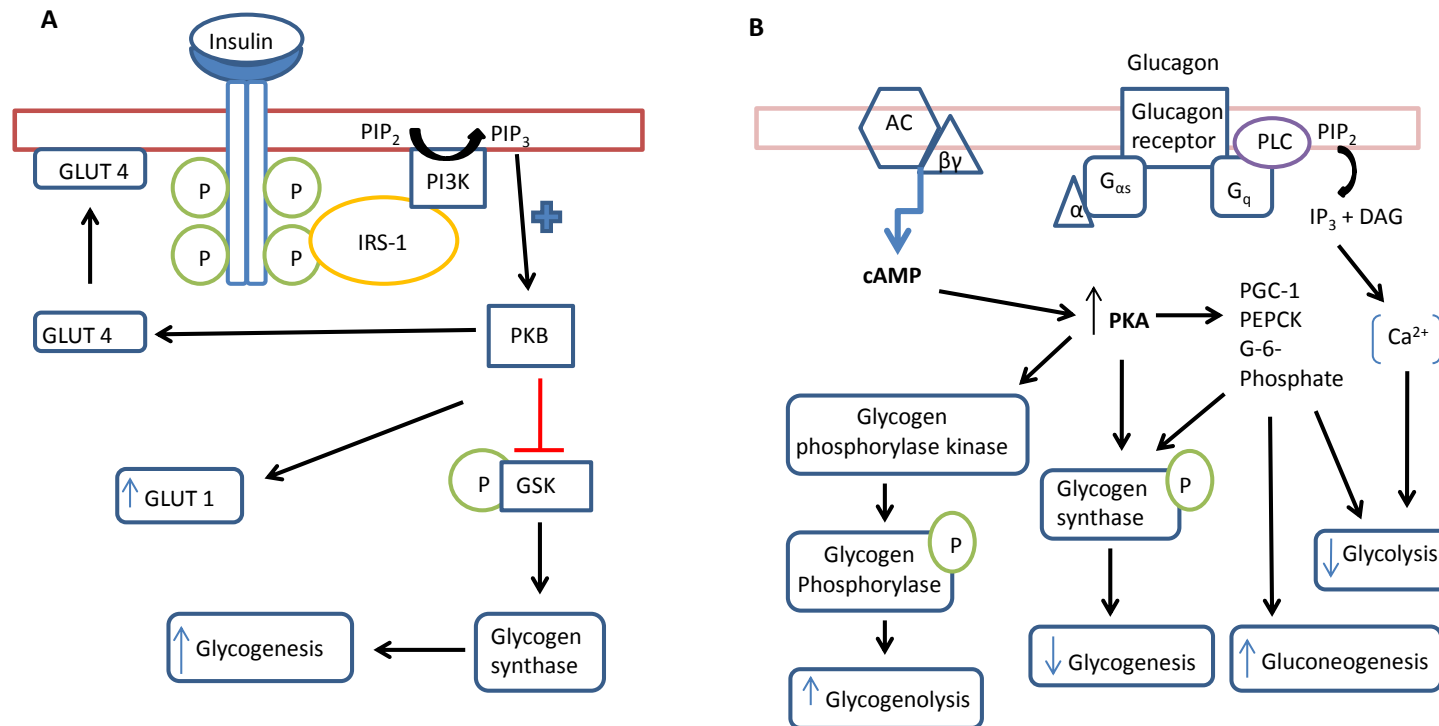


Figure 1.4 Signalling pathways of insulin and glucagon

- (A) Insulin binding to the extracellular domain of the α -subunits on the insulin receptor, induces a conformational change, resulting in autophosphorylation (phosphorylation of the dimeric partner's tyrosine residues) on the c-terminus of the β -subunits of the receptor and subsequently the insulin receptor subunit (IRS-1). IRS-1 can then bind SH2 containing domains, such as phosphatidylinositol 3-kinase (PI3K), which has downstream effects of indirectly activating protein kinase B (PKB), which has numerous effects including inhibiting glycogen synthase kinase (GSK). Inhibition of GSK promotes glycogenesis, stimulating translocation of GLUT 4 to the plasma membrane and increasing the expression of GLUT 1. Diagram depicted from work by Cross *et al.*, 1995; Cong *et al.*, 1997; Hill *et al.*, 1999; Tanti *et al.*, 1997.
- (B) Glucagon binding stimulates two signalling pathways $G_{\alpha s}$ and $G_{\alpha q}$ both of which stimulate increased glucose release, via stimulating gluconeogenesis and glycogenolysis and inhibiting glycogenesis and glycolysis. Peroxisome proliferator-activated receptor- γ coactivator-1 (PGC-1), phosphoenolpyruvate carboxykinase (PEPCK), glucose-6-phosphate (G-6-Phosphate). Diagram adapted from Jiang & Zhang, 2003.

1.7.3 Glucose transporters

1.7.3.1 Sodium-dependent glucose transporters (SGLT)

Sodium-dependent glucose transporters (SGLT) are located predominantly in the small intestine and kidneys. SGLTs use the electrochemical potential difference generated by the Na^+/K^+ ATPase to co-transport glucose and Na^+ into cells down their electrochemical/concentration gradients (Wright *et al.*, 1997). Six isoforms of SGLTs exist (SGLT 1-SGLT 6); of these SGLT 1 is located predominantly at the sarcolemmal membrane of cardiomyocytes (Banerjee *et al.*, 2009). The expression of SGLT 1 was found to be decreased in studies on STZ diabetic mice (mice which have been given Streptozotocin to destroy their pancreatic β -cells, in order to induce type 1 diabetes), while increased expression was observed in type 2 diabetes (thought to be due to chronic hyperinsulinaemia) and ischaemia (mice leptin-deficient ob/ob model and human cardiac tissue) (Banerjee *et al.*, 2009).

1.7.3.2 GLUT transporters

The facilitative glucose transporters (GLUTs), use facilitated diffusion to transport glucose down the glucose concentration gradient into cells, therefore no energy is required. The mechanism behind facilitative diffusion involves glucose binding to a specific site located on the transporter. This induces a conformational change, allowing the glucose molecule to be transported across the plasma membrane (Uldry & Thorens, 2004). Metabolism of glucose in cardiomyocytes is rapid; therefore the change in the intracellular glucose concentration is negligible, which creates a stable concentration gradient allowing facilitative diffusion (Klip & Paquet, 1990).

The GLUT family consists of three classes (distribution of expression are summarised in Tables 1.1, 1.2 and 1.3), all of which have a similar morphology (Figure 1.5). Class 1 GLUT transporters (Table 1.1) includes the most well studied and most highly conserved of the glucose transporters GLUT-1; first cloned from human erythrocytes in 1985 (Mueckler *et al.*, 1985).

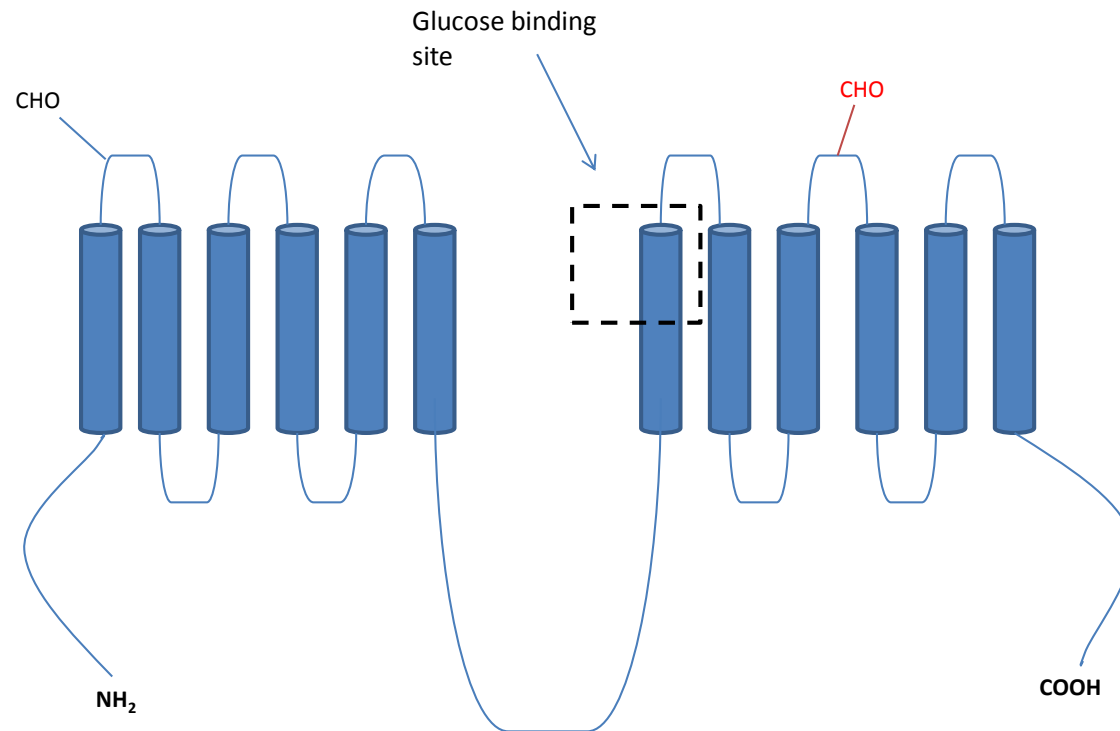


Figure 1.5 GLUT transporter structure

All GLUTs have the same morphology of 12 α helices transmembrane spanning domains, with both the amino (NH₂) and carboxy (COOH) terminal located on the cytoplasmic side. Class 1 and 2 GLUTs have an N-linked oligosaccharide located on the first loop, between transmembrane domains 1 and 2 (indicated by CHO in black). In class 3 GLUTs the N-linked oligosaccharide is located on the 9th loop between transmembrane domains 9 and 10 (indicated by the red CHO). The cytoplasmic loop between transmembrane domains 6 and 7 is extremely long. The extracellular binding site for glucose is on transmembrane 7. Diagram based on findings by Joost *et al.*, 2002; Uldry & Thorens, 2004; Wood & Trayhurn, 2003; Rogers *et al.*, 2002; Doege *et al.*, 2000; Doege *et al.*, 2001b.

Table 1.1 Class 1 GLUT transporters

Class	Isoform	Examples of species located in	Example of organ/tissue	Additional Information	Effects of disease on expression
1	GLUT 1	Fetal and adult mammalian tissue (human, rat, mouse, pig and rabbits)	Brain; erythrocytes, adipose tissue, muscle, liver and heart (ubiquitously distributed).		Decreased expression due to type 1 diabetes. Diabetic cardiomyopathy and heart failure cause an increase in expression.
	GLUT 2	Human, rats and mice (high abundance in fetal tissue)	Liver; kidney, pancreatic beta cells, intestine and hepatocytes	Also transport fructose but due to high Km of 17mM for glucose is classed as a class 1 GLUT transporter	
	GLUT 3	Human, rat and mice	Brain; nervous system (mice only) and placenta		
	GLUT 4	Human and rat	Heart; skeletal muscle, liver, adipose tissue and brain	Insulin, hyperglycaemia or exercise stimulate translocation to the sarcolemmal membrane from GLUT-4 storage vesicles.	Type 2 diabetes causes loss of translocation. Diabetic cardiomyopathy and heart failure cause a decrease in expression. Failing heart and aortic stenosis causes an increase in expression in combination with a decrease in the fatty acid transporters (FAT/CD36).

Those in red are present in the myocardium. Information collected from: Joost *et al.*, 2002; Uldry & Thorens, 2004; Wood & Trayhurn, 2003; Fukumoto *et al.*, 1988; Kayano *et al.*, 1988; Thorens & Mueckler, 2010; Mueckler, 1994; Aerni-Flessner *et al.*, 2012; Kalra & Roy, 2011; Phay *et al.*, 2000; Steinbusch *et al.*, 2011; Duehlmeier *et al.*, 2007; Klip & Paquet, 1990; Wheeler & Chien, 2012; Heather *et al.*, 2006; Heather *et al.*, 2011.

Table 1.2 Class 3 GLUT transporters

Class	Isoforms	Examples of species located in	Examples of organs/tissues	Effects of disease on expression
3	GLUT 6	Humans, rats and mouse	Spleen; leucocytes, brain and adipose tissue	
	GLUT 8	Human, mouse and Rat	Testis; brain and blastocyst	Diabetic cardiomyopathy and heart failure cause a decrease in expression.
	GLUT 10	Human and mice	Skeletal muscle; heart, liver, pancreases, brain, lung, placenta and kidney	
	GLUT 12	Mouse and Rat	Heart; small intestine, liver, prostate and skeletal muscle	Diabetic cardiomyopathy and heart failure cause a decrease in expression.
	GLUT 13 (HMIT)	Human, Rat and Mouse	Brain, glial cell and neurons	

Those in red are present in the myocardium. Information collected from: Joost *et al.*, 2002; Uldry & Thorens, 2004; Wood & Trayhurn, 2003; Fukumoto *et al.*, 1988; Kayano *et al.*, 1988; Thorens & Mueckler, 2010; Mueckler, 1994; Aerni-Flessner *et al.*, 2012; Kalra & Roy, 2011; Phay *et al.*, 2000.

The predominant location of GLUT- 1 in cardiomyocytes is the sarcolemmal membrane, where their main role is to maintain basal glucose levels at rest. GLUT-1 is known to co-exist with another class 1 GLUT transporter (GLUT-4) in insulin sensitive tissues such as the myocardium and skeletal muscle (Klip & Paquet, 1990). GLUT-4 was discovered by James *et al* (1988), who identified GLUT-4 as an insulin regulated GLUT located in the myocardium, skeletal muscle and adipose tissue (James *et al.*, 1988).

Class 2 of the GLUTs are widely regarded as fructose transporters even though some have the ability to also transport glucose, these will be discussed in the fructose transporters section (section 1.7.7).

Class 3 GLUTs (see Table 1.2); all solely transport glucose, this class contains GLUT-13 also referred to as the H⁺-coupled myo-inositol transporter (HMIT), which is located predominately in the brain (Uldry *et al.*, 2001). The brain uses glucose as its main source of energy therefore having a unique transporter located here is beneficial and is a key example of tissue-specific GLUT distribution.

In a number of clinical conditions differences in GLUT expression are exhibited, which depend on blood glucose levels and whether there has been a shift in favour of glucose metabolism as a result of a lack of O₂ availability, examples of disease states which gives rise to changes in levels of GLUT expression are given in Tables 1.1 and 1.2.

1.7.4 Glucose metabolism in the myocardium

1.7.4.1 Glycolysis

The myocardium generates 5% of its ATP from glycolysis (substrate level phosphorylation), which occurs within the cytosol of cardiomyocytes, and is the anaerobic stage of glucose metabolism, therefore it can continue during periods of ischaemia. The stages of glycolysis are summarised in Figure 1.6. Glycolysis is regulated at 4 separate enzyme stages; hexokinase, phosphofructokinase-1 (PFK-1), GAPDH and pyruvate kinase.

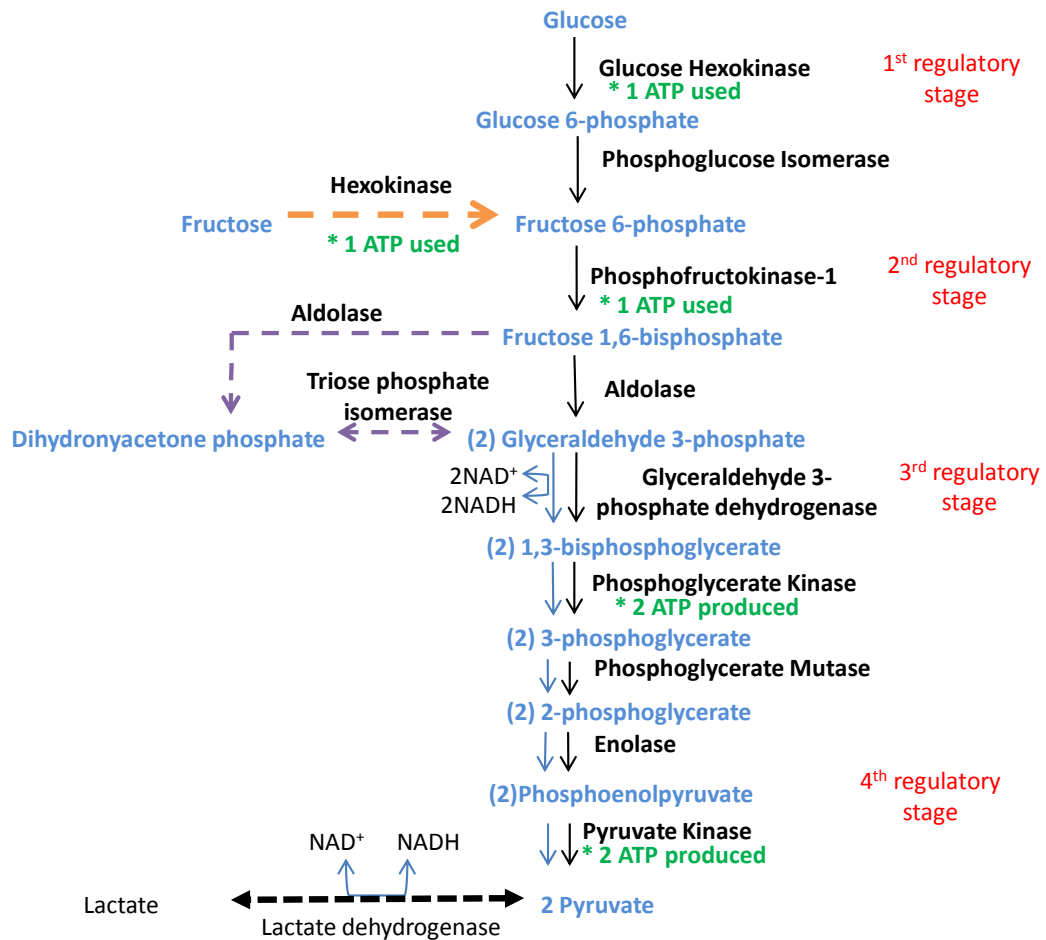


Figure 1.6 Glycolysis

Glucose enters glycolysis and is firstly phosphorylated by glucose hexokinase to glucose 6-phosphate. This process uses 1 molecule of ATP. Glucose 6-phosphate is then converted into fructose 6-phosphate by phosphoglucose isomerase. It is below this enzyme where fructose directly feeds into glycolysis and is phosphorylated by fructose hexokinase into fructose-6-phosphate. Fructose 6-phosphate is phosphorylated by phosphofructokinase-1 into fructose 1,6-bisphosphate, which is split by Aldolase into two 3 carbon fragments by glyceraldehyde 3-phosphate and dihydroxyacetone phosphate (this process consumes another ATP molecule). Dihydroxyacetone can be isomerised to glyceraldehyde 3-phosphate, by triose phosphate isomerase. The two glyceraldehyde 3-phosphate molecules then feed down into the later stages of glycolysis and give rise to two of each molecules along the way (indicated by (2)), as a result glycolysis concludes in the formation of two pyruvate molecules. The later stages of glycolysis yields 4 ATP molecules, meaning overall glycolysis yields 2 ATP molecules.

The overall net reaction for glycolysis is:

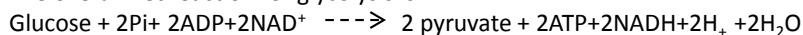


Diagram adapted from Berg *et al.*, 2007, Salway, 2004.

Hexokinase is inhibited by its product glucose 6-phosphate (England & Randle, 1967; Regen *et al.*, 1964) and is the enzyme which commits glucose to be metabolised within the tissue it has been taken up in, as once phosphorylated into glucose 6-phosphate it cannot be transported back out by the GLUTs. The actions of PFK-1 are irreversible and unique to glycolysis and commits glucose-6-phosphate to glycolysis, as unless converted into fructose 6-phosphate, glucose 6-phosphate can be used as a precursor for the synthesis of other metabolites (e.g. glycogen) (Stanley *et al.*, 2005; Berg *et al.*, 2007; Salway, 2004). PFK-1 is inhibited by high levels of ATP or by its product fructose 1,6-bisphosphate. Citrate; phosphocitrate, and a decrease in pH also renders the enzyme inactive. Activation occurs when the ATP/AMP ratio is low (i.e. during ischaemia) (Regen *et al.*, 1964; Stanley *et al.*, 2005; Pogson & Randle, 1966; Oguchi *et al.*, 1973). GADPH is activated by low NADH/NAD⁺ ratios (i.e. during ischaemia), ATP and phosphocreatine (Stanley *et al.*, 2005; Oguchi *et al.*, 1973). The final enzyme pyruvate kinase is also inhibited by ATP, which inhibits the production of pyruvate possibly in an effort to limit lactate production within the cardiomyocytes.

Glycolysis contributes to the energy status of cardiomyocytes by generating a net yield of two ATP molecules per glucose. Glycolysis also generates 2 NADH⁺ + H⁺ molecules, which can be oxidised at complex 1 of the ETC (Berg *et al.*, 2007; Salway, 2004). However NADH⁺ + H⁺ cannot freely diffuse across the mitochondrial membranes; in order to enter the mitochondria, the malate/aspartate shuttle is utilised (Salway, 2004).

During ischaemia due to the lack of available O₂, cardiomyocytes convert pyruvate into lactate via lactate dehydrogenase (LDH), which reduces NADH⁺ + H⁺ to regenerate NAD⁺, which is then utilised by GADPH allowing glycolysis to continue (Salway, 2004).

1.7.4.2 Glucose oxidation

Glucose oxidation (oxidative phosphorylation) is the aerobic stage of glucose metabolism (Kalra & Roy, 2011). Under normal physiological conditions pyruvate that has either been created as the end-product of glycolysis, or been directly taken up by cardiomyocytes, is transported into the mitochondria, where it is oxidised by pyruvate dehydrogenase (PDH) into acetyl-CoA (see section 1.8.3) (Stanley *et al.*, 2005), which

enters the Krebs cycle and leads to generation of ATP by the ETC (see sections 1.10.1 and 1.10.2). Glucose oxidation contributes 10-40% of acetyl-CoA required by the myocardium to generate 95% of its ATP via oxidative phosphorylation (Stanley *et al.*, 2005). Overall complete glucose metabolism (glycolysis and glucose oxidation) yields around 31 ATP molecules per glucose molecule; the ATP generated drives all energy requiring processes within the myocardium.

1.7.5 Diabetes and the effects of glucose on the myocardium

Diabetes Mellitus (DM) is a metabolic disease, characterised by a chronically raised blood glucose concentration due to the lack, or ineffective action, of insulin. Type 1 diabetes is an autoimmune disease in which T lymphocytes attack and destroy the pancreatic islets of Langerhan (Crowley, 2007). Type 2 diabetes involves insulin sensitive tissue(s) (such as the liver, muscle and adipose) becoming insulin resistant (Crowley, 2007).

Detection of diabetes occurs when an individual presents with symptoms of glycosuria; polyuria and/or polydipsia and is confirmed via blood glucose readings. Multiple fasting blood glucose concentrations > 7mmol/L indicates diabetes; and a single recording of >10mmol/L is confirmation of a diabetic state. The degree of long-term control or otherwise, of diabetes can be assessed by measurement of glycosylated haemoglobin (HbA1c), normally around 6% (Crowley, 2007). Poorly controlled diabetes and acute hyperglycaemia can lead to critical conditions such as diabetic ketoacidosis. Long term poor glycaemic control is associated with adverse outcomes such as diabetic nephropathy and retinopathy.

Hypoglycaemia (blood glucose <4mmol/L) can occur as a result of treatment of diabetes (excessive insulin or oral glucose-lowering medication dosage) or hyperinsulinemia.

The effects of glucose on the myocardium vary depending on physiological and pathophysiological conditions and whether the myocardium has been ischaemically preconditioned. Hyperglycaemia alone or associated with diabetes is associated with increased mortality following an AMI (Kosiborod *et al.*, 2005; Goyal *et al.*, 2006; Squire

et al., 2009). Hyperglycaemia (related to diabetes) can lead to numerous complications including development of diabetic cardiomyopathy, which is characterised by impairment of myocardial function (Ren & Ceylan-Isik, 2004) due to alterations in its structure (i.e. fibrosis, left ventricular hypertrophy) and vascular function (i.e. microvascular dysfunction). In diabetic cardiomyopathy both systolic and diastolic dysfunction can occur resulting in an inability of the myocardium to pump and eject blood effectively with each contraction (Hayat *et al.*, 2004).

Hyperglycaemia stimulates increased productions of AGEs by increasing flux through the polyol and hexosamine pathways (Brownlee, 2005). Increased AGEs production is associated with increased ROS production, due to increased $\text{NADH} + \text{H}^+/\text{FADH}_2$ production (caused by increased pyruvate metabolism in the mitochondria) (Brownlee, 2005). Increased $\text{NADH} + \text{H}^+/\text{FADH}_2$ production causes electrons to build up at coenzyme Q at complex 3 in the ETC. Coenzyme Q then donates one electron at a time to O_2 creating a reactive oxygen species (ROS) superoxide (Brownlee, 2005), which can go on to form hydrogen peroxide (H_2O_2). However the diabetic heart can over express an isoform of superoxide dismutase (mnSOD), which neutralises H_2O_2 into O_2 and water (Brownlee, 2005) suggesting the effects of ROS on the diabetic heart may not be that detrimental.

Fatty acid supply to the myocardium also increases with hyperglycaemia; stimulating increased β -oxidation. As a result PDH is inhibited allowing glycolytic intermediates to build up within the cytosol and stimulate apoptosis (Hayat *et al.*, 2004).

Sudden cardiac death which can occur in healthy type 1 diabetics has been linked to prolongation of the Q-T interval, which disrupts repolarisation of the cardiac action potential and increases $[\text{Ca}^{2+}]_i$ (Gordin *et al.*, 2008). Prolongation of the Q-T interval has been suggested to be associated with a reduction in hERG channel function (possibly due to increased ROS production), which can occur either with hypoglycaemia or hyperglycaemia (Zhang *et al.*, 2003). During or following coronary artery occlusion, insulin induced hypoglycaemia can cause an increase in the ST interval at the anterior surface of the areas supplied by the occluded coronary artery, due to increased myocardial necrosis (Libby *et al.*, 1975). Studies on STZ-treated rats

have also revealed decreased expression of the K⁺ channels (Kv 2.1, Kv 4.2 and Kv 4.3) associated with repolarisation, which could contribute to the arrhythmias associated with the diabetic heart (Qin *et al.*, 2001). A hyperglycaemic glucose concentration of 10mM has also been found to inhibit the VGKC (Kv) channel currents in isolated rat mesenteric artery smooth muscle cells (Rainbow *et al.*, 2006).

Hyperglycaemia (not related to diabetes) has been shown to increase myocardial infarct size (evident by infarct size seen in a canine model undergoing coronary artery occlusion) (Kersten *et al.*, 1998; Kersten *et al.*, 2000) in normal protocol settings and in those exposed to ischaemic preconditioning (IPC). Abolition of the protection usually conveyed by IPC has been attributed to impaired MitoK_{ATP} activity (see section 1.11.2). This is due to canine models which have either been induced with diabetes via STZ treatment or been made hyperglycaemic via intravenous dextrose, showing no attenuation of reduction in infarct size following IPC when the MitoK_{ATP} agonist diazoxide has been administered (Kersten *et al.*, 2001). However hyperglycaemia has also been shown to increase translocation of GLUT-4 to the sarcolemmal membrane (in the presence/absence of ischaemia). Ramasay *et al* (2001) demonstrated that increased translocation of GLUT-4 occurred in isolated rat myocardia subjected to low-flow ischaemia and could be associated with the protection observed (identified by a reduction in creatine kinase release and improved left ventricular function during reperfusion) (Ramasamy *et al.*, 2001). Increased GLUT-4 at the sarcolemmal membrane may aid an increase in glycolysis which occurs during ischaemia. Enhanced glycolytic flux during ischaemia has been shown to increase glycolytic ATP production and as a result reduce ischaemia damage and improve recovery (identified via LDH and creatine kinase levels, an absence of ventricular arrhythmias and the recovery of left ventricular pressure). As with the Ramasay group these results were obtained from isolated animal myocardia (Bricknell & Opie, 1978; Owen *et al.*, 1990; Vanoverschelde *et al.*, 1994; Wang *et al.*, 2005, Malfitano *et al.*, 2010). These latter observations suggest improving metabolism (or the availability of metabolic substrates) in the ischaemic heart is likely to be important and will be investigated within this study.

1.7.6 Fructose in humans

Fructose is an isomer of glucose and is naturally found in fruit. Its commercial use as a sweetener has increased in recent years and is associated with being a significant risk factor in the development of insulin resistance, hyperinsulinemia and hypertension (Park *et al.*, 1992; Mellor *et al.*, 2010). Fructose is absorbed into the blood stream, however the plasma concentration of fructose is relatively low (8-20 μ M) compared to plasma glucose concentrations (Mellor *et al.*, 2011). Fructose is absorbed from the gastrointestinal tract either directly or by the degradation of sucrose into fructose by sucrase (Salway, 2004). Once absorbed the main site of metabolism is the liver, which is initiated by fructokinase and is so rapid that uncontrolled production of lactate and pyruvate can occur (Mellor *et al.*, 2011). However the myocardium is known to use fructose as a metabolic fuel.

1.7.7 Fructose transporters

There are 4 isoforms of fructose transporters GLUT-5, 7, 9 and 11 (Doege *et al.*, 2001; Wu *et al.*, 2002) (Table 1.3). The presence of GLUT-5 in the myocardium was identified in studies investigating the effects of fructose on the myocardium (Mellor *et al.*, 2011, Mellor *et al.*, 2012).

1.7.8 Fructose metabolism in the myocardium

Fructose enters cardiomyocytes and is quickly phosphorylated into fructose-6 phosphate by fructose hexokinase. Fructose 6-phosphate then enters glycolysis at the rate limiting step of PFK-1 (as indicated on Figure 1.6) (Mellor *et al.*, 2010). Entry at PFK-1 means fructose by-passes another rate limiting step glucose hexokinase; this can lead to rapid accumulation of glycolytic intermediates and cause detrimental effects within the myocardium.

1.7.9 Fructose effects in myocardium

The effects of fructose on the myocardium have been investigated using rodents fed a high fructose (60-70%) diet or in humans after administration of fructose orally or intravenously. In mice a high fructose diet (60%) has been shown to induce an increase

in the generation of myocardial superoxide (primarily in the ventricles) with no increase observed in the vascular tissue (Mellor *et al.*, 2010). The increased superoxide levels were stimulated by upregulation of the enzyme NADPH oxidase. This rise in superoxide levels was not counterbalanced by an increase in antioxidant levels, leaving the myocardium susceptible to oxidative stress and damage (Mellor *et al.*, 2010). These studies showed no signs of fructose induced hypertrophy or hypertension as previously showed by Delbosc *et al* (2005), who showed that a high fructose (60%) intake in rat also lead to increased superoxide formation in both the ventricles and aorta by day 7, and also stimulated cardiac hypertrophy after 1 week and hypertension by day 21 (Delbosc *et al.*, 2005).

Park *et al* (1992) showed rats fed a 70% fructose diet developed an increase in the plasma triacylglycerol concentration (hypertriglyceridemia) (Park *et al.*, 1992), which concurs with findings that administration of oral fructose in humans increased serum level of triacylglycerols (Cook, 1971). Hypertriglyceridemia can stimulate detrimental effects in the myocardium such as lipotoxicity (Park *et al.*, 1992) and atherosclerosis. Additionally administration of oral fructose to humans has been found to stimulate increases in blood lactate concentrations compared to those given glucose (Cook, 1971), which could relate to the fact that fructose is more rapidly metabolised. An increase in blood lactate decreases $[pH]_i$ which can interfere with myocardial contractility. Contraction of the myocardium could also be affected by fructose having effects on SERCA, as Mellor *et al* (2012) also observed mice fed a high fructose (60%) diet showed a delayed time for Ca^{2+} removal from the cytosol (due to decreased SERCA2a expression and phosphorylation of PLB). Decreases in systolic and diastolic Ca^{2+} levels were also observed (Mellor *et al.*, 2012), which in the short term may be protective as ROS levels can be elevated. Other protective effects of fructose during I/R injury have also been investigated using rats fed a 66% fructose diet for either 3 days or 4 weeks. Myocardial tissue from these rats showed decreased infarct size compared to control (no high fructose diet), implying cardioprotection (Jordan *et al.*, 2003).

Table 1.3 Class 2 GLUT transporters

Class	Isoforms	Examples of species located in	Examples of organs/tissue	Additional information
2	GLUT 5	Rabbit, cattle, pigs, horse, predominantly humans	Small intestine; testis, kidney, brain, skeletal muscle, liver, testis and sperm	Can transport glucose at low levels in addition to fructose. Insulin increases the abundance and functional activity of GLUT-5 in skeletal muscle.
	GLUT 7	Rat	Liver (located at ER)	
	GLUT 9 (2 splice variants 9a and 9b shorter NH ₂ termini)	Human and Mouse	Liver (9a only), placenta and kidney	Believed to transport urate rather than glucose or fructose
	GLUT 11 (3 splice variants which differ in amion (NH ₂) termini lenght:11a has 7 amino acids,11b has 14 amino acids, and 11C has 10 amino acids)	Human and rat	Heart; skeletal muscle, liver (not 11a), brain, lung, trachea, kidney and small intestine	Can transport glucose at low levels but this is inhibited by 5mM fructose, which is believed to show GLUT-11 is primarily a fructose transporter

The GLUT highlighted in red is present in the myocardium. Information collected form: Kayano,T. 1990; Joost,H.G. 2002; Uldry & Thorens, 2004; Mueckler,M. 1994; Aerni-Flessner,L. 2012; Kalra,B.S. 2011; Phay,J.E. 2000; Doege *et al.*, 2000, Doege *et al.*, 2001; Burant *et al.*, 1992; Wood & Trayhurn, 2003; Douard & Ferraris, 2008; Doblado & Moley,2009, Thorens & Mueckler, 2010.

1.8 Pyruvate

1.8.1 Pyruvate in humans

Pyruvate is a monocarboxylate, with multiple functions within cardiomyocytes including being a key metabolic substrate for ATP generation, acting as a potent antioxidant against ROS and being a precursor for glucose (via gluconeogenesis), fatty acids and amino acids. Like glucose, the physiological concentration of circulating pyruvate varies throughout the day depending on physical activity and food consumption.

1.8.2 Pyruvate Transporters

1.8.2.1 Transporters located at the sarcolemmal membrane

Monocarboxylate transporters (MCT) act as a symporter and directly transport monocarboxylates in a proton-linked facilitated diffusion manner across the sarcolemmal membrane of cardiomyocytes. The concentration gradients of the respective monocarboxylates being transported, and the pH gradient, drive the direction of the facilitated movement (Halestrap & Price, 1999). MCTs export lactic acid, formed during periods of ischaemia, into the bloodstream (Wang *et al.*, 1993). Fourteen MCT isoforms have been identified in humans (MCT1-14), of these fourteen, 8 isoforms have been identified in the human myocardium, two of which, MCT 1 and 4 are known to transport pyruvate (Halestrap, 2012). In rats 4 isoforms (MCT 1- 4) have been detected, with MCT 1 having been identified in the rat myocardium (Halestrap & Price, 1999; Halestrap, 2012). The structure of MCT's is believed to differ between isoforms with MCT 1,2,3,7, and 8 having 12 α -helical TMD, while MCT 4, 5, 6, and 9 has between 10-12 α -helical TMD (Halestrap & Price, 1999; Poole *et al.*, 1996).

1.8.2.2 Transporters located at the inner mitochondria membrane

The outer mitochondrial membrane is permeable to small solutes, so pyruvate can simply diffuse across, however a transporter is needed at the inner mitochondrial membrane. Mitochondrial pyruvate carrier (MPC) has been identified at the inner mitochondrial membrane and is inhibited by alpha-cyano-4-hydroxycinnamate (α -

HCN) (Halestrap & Denton, 1974). MPC is believed to be composed of 6 TMD (Thomas & Halestrap, 1981). Recently Herzig *et al* (2012) identified that the mammalian MPC is composed of two components MCP1 and MCP2 (Herzig *et al.*, 2012).

1.8.3 Pyruvate metabolism in myocardium

Pyruvate is either metabolised in the cytosol of cardiomyocytes into lactate or enters the mitochondria and feeds into the Krebs cycle, where it is either irreversibly decarboxylated into acetyl-CoA ($+ \text{CO}_2 + \text{NADH} + \text{H}^+$) via PDH or is carboxylated into oxaloacetate ($+ \text{ADP} + \text{P}_i$) by Pyruvate carboxylase (Kerbey *et al.*, 1976; Linn *et al.*, 1969; Utter & Keech, 1963). Carboxylation of pyruvate occurs in a biotin dependent manner, which utilises 1 ATP molecule per pyruvate (St Maurice *et al.*, 2007) and is essential in replenishing the amount of oxaloacetate available to the Krebs cycle; when amino acid synthesis is taking place.

Decarboxylation occurs via PDH, which is a multi-enzyme complex consisting of three enzymes E1-E3, which can be allosterically inhibited by high acetyl-CoA, NADH and ATP concentrations (Kerbey *et al.*, 1976; Linn *et al.*, 1969). The activity of PDH is also regulated by Pyruvate dehydrogenase kinase (PDHK) and Pyruvate dehydrogenase phosphatase (PDHP). PDHK inactivates PDH by phosphorylating serine residues on E1 (Kerbey *et al.*, 1979; Sugden *et al.*, 1979). This phosphorylation can be removed by PDHP, which is activated by Ca^{2+} and Mg^{2+} (Linn *et al.*, 1969; McCormack *et al.*, 1990). PDHK is also inhibited by ADP, NAD^+ and pyruvate (Kerbey *et al.*, 1976). Inhibition of PDHK increases activity of PDH, thus metabolism of pyruvate increases. This causes negative feedback as increased concentrations of acetyl-CoA, NADH and ATP will occur, resulting in inhibition of PDH. During ischaemia Kobayashi *et al* (1983) found PDH activity remained despite increases in NADH and acetyl-CoA. The continued activation was postulated to occur due to low ATP levels and high ADP levels inhibiting PDHK. However PDH activity was inhibited during reperfusion possibly due to re-establishment of ATP (Kobayashi & Neely, 1983).

1.9 Fatty acids

1.9.1 Fatty acids in humans

Fats absorbed through diet can be stored in the adipose tissue, liver and myocardium (in small amounts) in the form of triacylglycerols (TAGs) (Lopaschuk *et al.*, 2010). TAGs release fatty acids, which can then be used as a source of energy. The normal physiological blood fatty acid concentration is 0.2-0.6mM, this concentration can vary depending on age or the underlying pathophysiology (Lopaschuk *et al.*, 2010). Fatty acids are classified into two groups; saturated (no double bonds) or unsaturated (1⁺ double bonds/triple bonds). Fatty acids also vary in chain length; short chain fatty acids (<6 carbons); medium-chain fatty acids (6-12 carbons), long chain fatty acids (13-21 carbons) and very long chain fatty acids (>22 carbons). Essential fatty acids are the most common fatty acid absorbed through diet as the body is unable to synthesize large quantities.

1.9.2 Regulation of fatty acid availability to the myocardium

TAGs are broken down via the action of lipases in a process known as lipolysis, to release free fatty acid (FFA) molecules and either a glycerol or a monoglycerol depending on where lipolysis takes place. The FFA available to the myocardium derived from TAGs present in three forms; either they are released from circulating chylomicrons and/or very low-density lipoproteins (VLDL) via lipolysis via lipoprotein lipases (LPLs), which line the luminal surface of endothelium cells and are found in the capillaries of the myocardium (O'Brien *et al.*, 1994; Blanchette-Mackie *et al.*, 1989; Vannier & Ailhaud, 1989) or they present as FFA bound to the protein serum albumin, following their release from the adipose tissue via actions of hormone sensitive lipases (HSLs). The released FFA are taken up into the cardiomyocytes and undergo oxidation via β -oxidation (Lopaschuk *et al.*, 2010; Augustus *et al.*, 2003).

1.9.3 Fatty acid transporters

1.9.3.1 Fatty acid transporters under physiological conditions

Transport of FFA into the cytosol of cardiomyocytes is mediated by fatty acid binding proteins (FABP_{pm} and H-FABP), fatty acid translocase (FAT/CD36) or fatty acid transporter proteins (FATP), as summarised in Figure 1.7. One particular FATP, FATP6 has been shown to be specific to the myocardium and co-localise with CD36 at the sarcolemmal membrane (Gimeno *et al.*, 2003). The use of a specific inhibitor (Sulfo-N-Succinimydyl-oleate) and gene knockout studies of CD36; have shown FAT/CD36 to be the principal transporter for FFA uptake into cardiomyocytes, and be responsible for between 50-70% of the uptake (Luiken *et al.*, 1997; Luiken *et al.*, 1999; Habets *et al.*, 2007). Other knockout mice studies have revealed an absence of H-FABP also leads to decreased FFA uptake (Binas *et al.*, 1999; Schaap *et al.*, 1999); which coincides with work by Goresky *et al.* (1994), who observed in isolated rat hearts FABP_{pm} is required for the transition of FFA from the capillary across the endothelia membrane (Goresky *et al.*, 1994).

1.9.3.2 Fatty acid transporters under pathophysiological conditions

Under pathophysiological conditions, changes occur in fatty acid transporters, to allow the myocardium to adapt in an effort to maintain substrate availability. In diabetic animals increases in cytoplasmic FABP, and FAT/CD36 at the endothelium and sarcolemmal membrane have been detected (Greenwalt *et al.*, 1995; Veerkamp *et al.*, 1996; Pelsers *et al.*, 1999). Insulin resistant animals show relocation of FAT/CD36 to the sarcolemmal, while GLUT 4 is internalised (Steinbusch *et al.*, 2011). However in hypertrophic hearts decreases in cytoplasmic FABP content has been observed, correlating with a decrease in fatty acid metabolism (Vork *et al.*, 1992). The failing rat heart also down regulates expression of FAT/CD36, in combination with an increase in expression of GLUTs (Heather *et al.*, 2011).

1.9.4 Fatty acid metabolism in the myocardium

Inside the cytosol of cardiomyocytes, fatty acids are initially “activated” for β -oxidation by acyl-CoA synthetases which converts fatty acids into fatty acid acyl-CoA, this

process uses 2 ATP molecules. Figure 1.8 shows activation of long chain fatty acids (the preferred fatty acids to the myocardium) in the cytosol and the following movement through the mitochondria to the mitochondrial matrix by carnitine palmitoyltransferase 1 (CPT1), carnitine palmitoyltransferase 2 (CPT2) and the carnitine/acylcarnitine translocase (ACT) (Lopaschuk *et al.*, 2010). Both CPT1 and CPT2 are inhibited by malonyl CoA (McGarry *et al.*, 1978; Murthy & Pande, 1987) which is synthesised by acetyl CoA carboxylase (ACC). Malonyl CoA inhibition of CPT1 decreases with advancing age; as ACC produces less malonyl CoA, as the myocardium switches metabolic preference from lactate and glycolytic substrates (during fetal stages), to fatty acids (with adult myocardium) (Lopaschuk *et al.*, 1994). The activity of malonyl CoA is therefore regulated by the activity of ACC (Saddik *et al.*, 1993) and by its degradation by malonyl CoA decarboxylase (McGarry & Foster, 1980).

Unlike long chain fatty acids, short chain and medium chain fatty acids do not undergo “activation” in the cytosol and therefore do not require CPT1/2 or ACT, instead they freely diffuse across the mitochondrial membranes, into the mitochondrial matrix, where either medium or short chain acyl-CoA synthetases “activate” these fatty acids (Haddock *et al.*, 1970). All fatty acid acyl-CoAs then undergo β -oxidation.

1.9.4.1 β -oxidation

The process of β -oxidation is summarised in Figure 1.9. The four enzymes involved in β -oxidation exist in numerous isoforms that show specificity for the various fatty acid chain lengths (Houten & Wanders, 2010). All four are sensitive to feedback inhibition via by-products of the cycle as indicated on Figure 1.9.

In total each β -oxidation cycle generates 1 NADH + H^+ ; 1 FADH₂ and 1 acetyl-CoA molecule (except the last cycle which generates 2) (Berg *et al.*, 2007). Acetyl-CoA passes into the Krebs cycle as described in section 1.10.2; while NADH + H^+ and FADH₂ are reoxidised by the ETC generating 2.5 ATP per NADH + H^+ and 1.5 ATP per FADH₂ molecule.

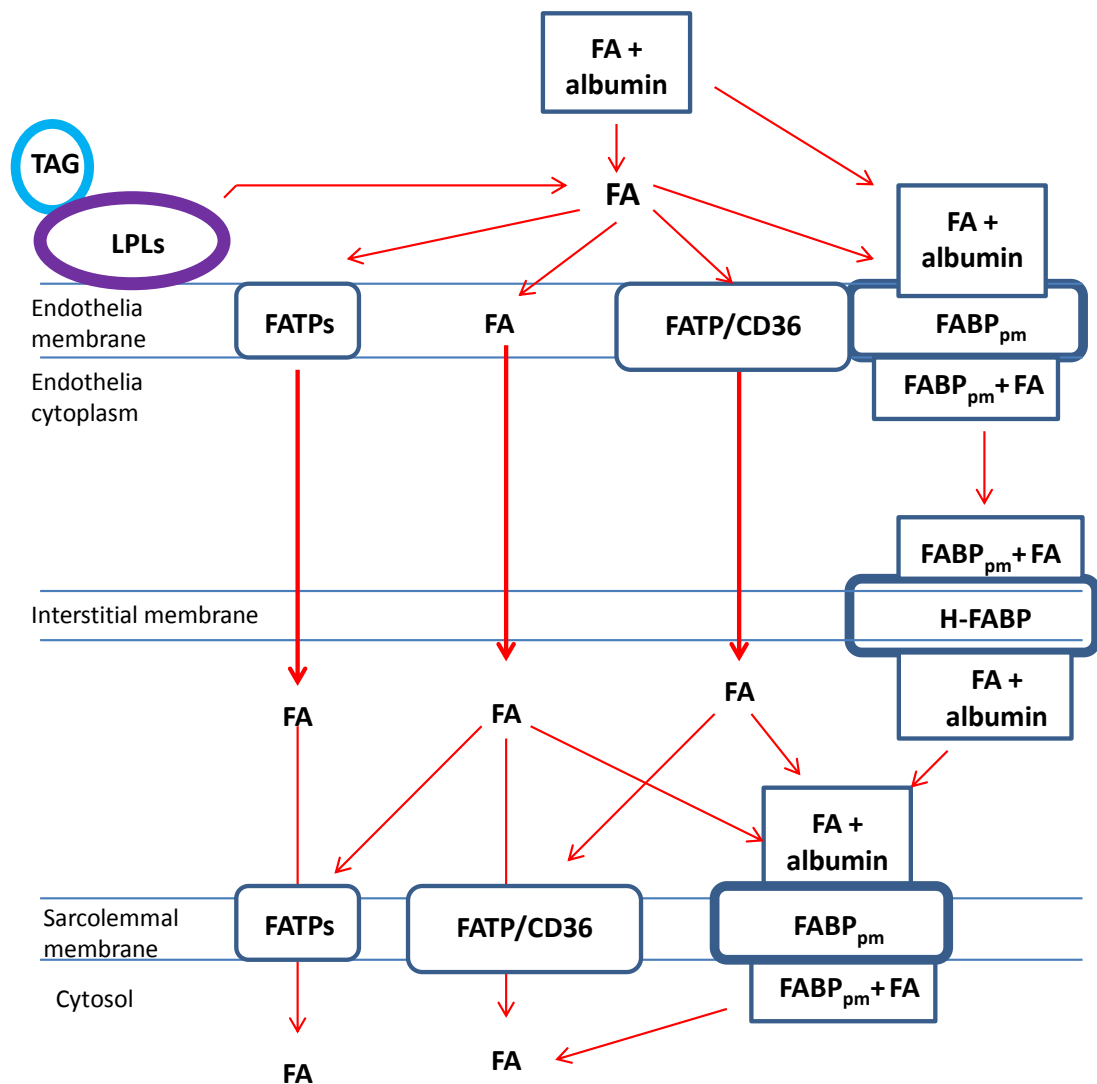


Figure 1.7 Fatty acid transport into the myocardium

Circulating FFA released from albumin can either passively diffuse across the endothelia membrane, endothelia cytoplasm and the interstitial membrane and then be released into the interstitial space, or they bind to a FABP_{pm} and passively diffuse across endothelia cytoplasm, and then bind to a H-FABP and are transported across the interstitial membrane and are released into interstitial space. While FFA incorporated into TAGs are firstly released by LPLs (produced by the myocardium). Once released the FFA binds to FABP_{pm}, FAT/CD36 or FATPs located in the endothelia membrane and are transported to the sarcolemmal membrane, where on arrival FFA (are released from albumin if bound) and once again bind to FABP_{pm} and H-FABP, FAT/CD36, or FATP and are trafficked across the sarcolemmal membrane and released into the cytosol of cardiomyocytes, where metabolism can take place. Diagram adapted from Van der Vusse *et al.*, 1992; Schaap *et al.*, 1998.

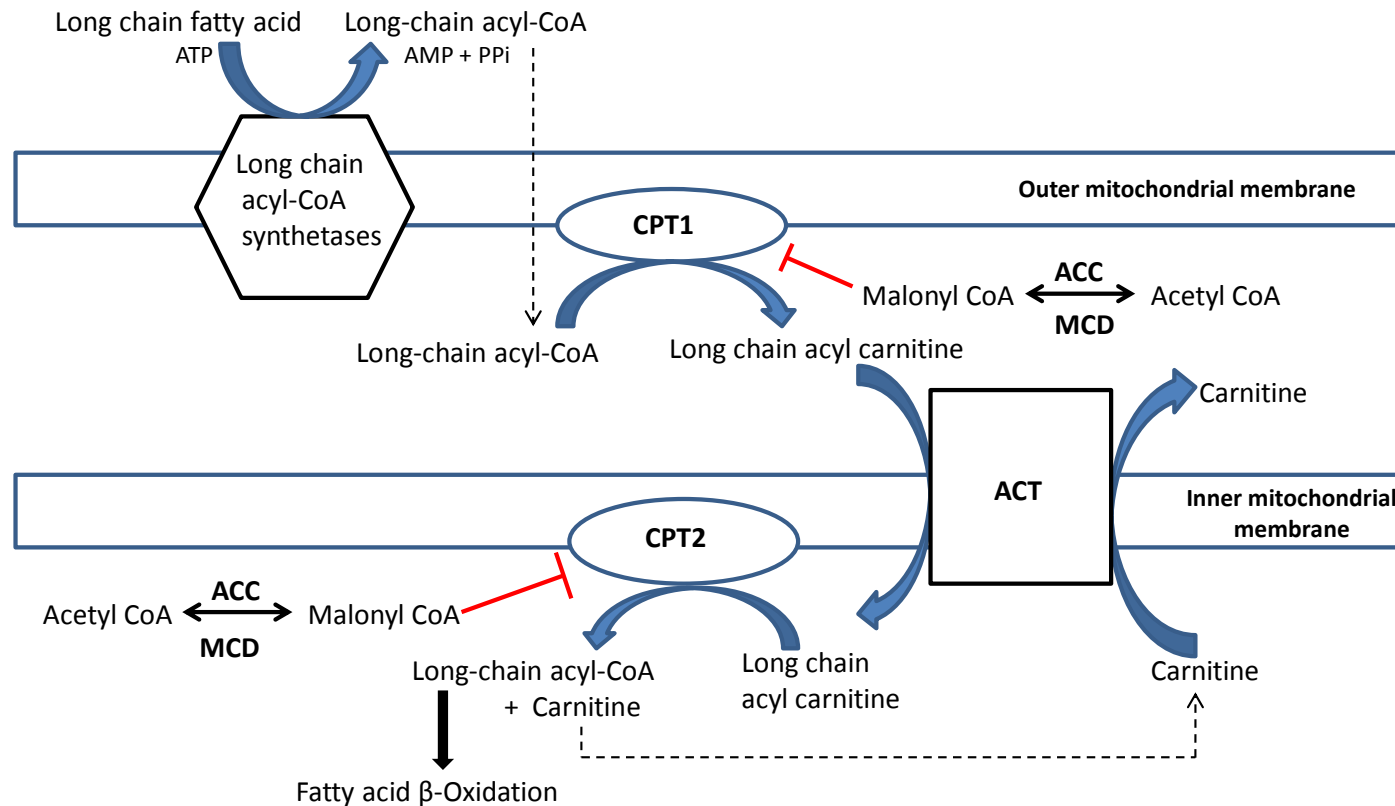


Figure 1.8 Activation of long chain fatty acids and transport into the mitochondria

Long chain fatty acids are activated by long chain acyl-CoA synthetases into long chain acyl-CoA, and pass into the mitochondrial intermembrane space. Carnitine palmitoyltransferase 1 (CPT1) located on the outer mitochondrial membrane, then catalyses the conjugation of carnitine to long chain acyl-CoA to form long chain acyl carnitine. This is then transported across the inner mitochondrial membrane by the carnitine/acylcarnitine translocase (ACT). Once inside the mitochondrial matrix, carnitine palmitoyltransferase (CPT2) located on the inner mitochondrial membrane, catalyses the reformation of long chain acyl-CoA and carnitine. Carnitine is transported back across the mitochondria membranes by ACT and reused with another acyl-CoA molecule, while long-chain acyl-CoA enters fatty acid β-oxidation. CPT1 and CPT2 are both inhibited by malonyl CoA which is synthesised from acetyl CoA by acetyl CoA carboxylase (ACC) and degraded by malonyl CoA decarboxylase (MCD). Diagram adapted from Lopaschuk *et al.*, 2010.

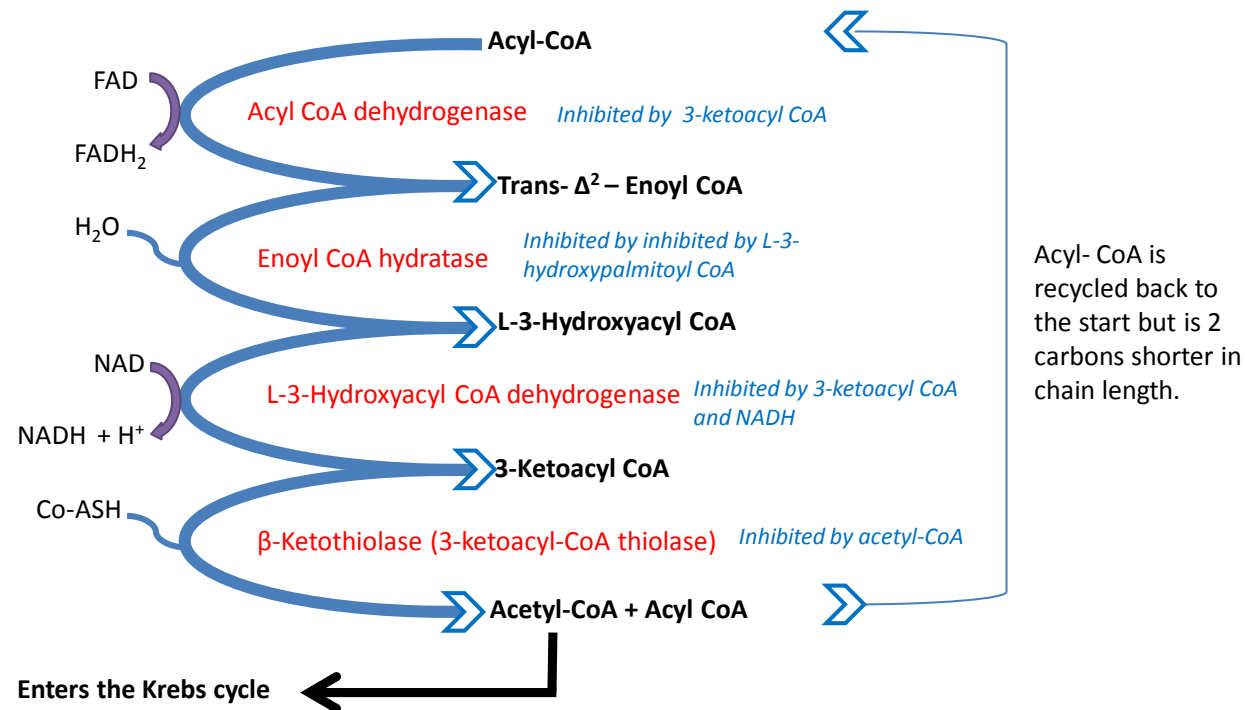


Figure 1.9 β -oxidation

Acyl-CoA enters β -oxidation and is dehydrogenated into Trans- Δ^2 -Enoyl CoA by acyl-CoA dehydrogenase, this process yields one FADH₂ molecule. Trans- Δ^2 -Enoyl CoA is then hydrated into the L isoform of hydroxyacyl CoA (L-3-hydroxyacyl coA) via the addition of H₂O, this process is catalysed by Enoyl CoA hydratase. The third stage is another dehydrogenation catalysed by L-3-Hydroxyacyl CoA dehydrogenase, here 3-ketoacyl CoA and a NADH + H⁺ are generated. The final stage is the cleavage of 3-ketoacyl CoA into acetyl-CoA and acyl-CoA by β -ketothiolase. Acyl-CoA is then recycled back to the start and the process is repeated until a molecule of 4 carbons in length (C₄) is left (longer chain fatty acids will have more β -oxidation cycles than shorter chain fatty acids). This C₄ molecule in the final cycle is cleaved into two acetyl-CoA molecules rather than just one. The acetyl-CoAs produced feed into the Krebs cycle to undergo further metabolism. Inhibition of each enzyme by a by-product is indicated on the diagram. Inhibition of the last enzyme leads to accumulation of other intermediates of oxidation thus inhibition of other the enzymes. Diagram adapted from Berg *et al.*, 2007, Salway, 2004 and annotated based on work by Olowe & Schulz, 1980, Fong & Schulz, 1977, Schifferdecker & Schulz, 1974.

Each acetyl-CoA produced via β -oxidation that feeds into the Krebs cycle can generate 10 ATP molecules, therefore fatty acid chain length determines how much ATP is produced, for example complete metabolism of octanoate generates 50 ATP molecules, whereas metabolism of palmitate (C_{16}) yields 106 ATP molecules. The large quantities of ATP produced by fatty acid metabolism, means under normal physiological conditions the myocardium generates 60-90% of the ATP required for contraction from fatty acids. Following an AMI (or in uncontrolled diabetes), fatty acid metabolism increases (Lopaschuk *et al.*, 2010; Januszewicz *et al.*, 1971; Paulson & Crass, 1982) leading to increased production of citrate and acetyl-CoA (via the Krebs cycle), which can inhibit glucose metabolism via inhibition of PFK-1 and PDH respectively (Pogson & Randle, 1966; Kerbey *et al.*, 1976; Randle *et al.*, 1964).

1.10 Mitochondria

Cardiomyocytes contain large amounts of mitochondria to enable the generation of sufficient amounts of ATP required for cellular function. The structure of the mitochondria is shown in Figure 1.10.

1.10.1 Krebs cycle

The Krebs cycle is the point at which the glycolytic and β -oxidation pathways converge during aerobic conditions, with both pathways providing acetyl-CoA for the Krebs cycle. The Krebs cycle involves a series of 8 consecutive reactions, as shown in Figure 1.11, one cycle of Krebs yields 1CoA-SH, 3NADH+ H^+ , 1FADH₂, 1GTP and 2CO₂. If the acetyl-CoA used in the initial step is generated from pyruvate then an additional NADH + H^+ and CO₂ are generated (Kerbey *et al.*, 1976). During aerobic conditions the GTP formed can phosphorylate ADP to ATP, catalysed by nucleotide diphosphate kinase. This is an example of substrate-level phosphorylation (Berg *et al.*, 2007).

Nucleotide levels within the mitochondria are a major regulator of Krebs activity, with many of the enzymes being inhibited by high ATP/ADP and NADH/NAD⁺ ratios (Kohn *et al.*, 1979). The first product of the Krebs cycle citrate, can accumulate due to inhibition of isocitrate dehydrogenase (Kohn *et al.*, 1979), this leads to inhibition of PFK-1 kinase in glycolysis (and thus inhibits glycolysis) (Pogson & Randle, 1966). During anaerobic

conditions (ischaemia) the Krebs cycle cannot function (due to the lack of available O_2 and build up of intermediates e.g. NADH) therefore anaerobic glycolysis becomes essential to cardiomyocytes.

1.10.2 Oxidative Phosphorylation

Oxidative phosphorylation is the combined effects of the ETC and ATP Synthase to generate ATP, which is summarised in Figure 1.12. NADH + H^+ and $FADH_2$ generated via glycolysis, fatty acid β -oxidation and the Krebs cycle act as reducing agents, which donate electrons at complex 1 and 2 respectively. Donation of electrons oxidises these agents back to their original state of NAD^+ and FAD^+ , which are then recycled back to the Krebs cycle. The ATP generated is free to diffuse into the cytosol of the cell, or is transported to specific location by specific shuttle mechanisms as described in 1.10.2.1

During the flow of electrons through the ETC, a small amount of the ROS superoxide (O_2^-) may be produced, as a result of the donation of one electron at a time to O_2 from both complex 1 and 3 (Camello-Almaraz *et al.*, 2006). Ischaemia (and hyperglycaemia) can stimulate the generation of the ROS' O_2^- and hydrogen peroxide (H_2O_2) (Vanden Hoek *et al.*, 1997), due to increased NADH + H^+ / $FADH_2$ levels, causing a build up of electrons at coenzyme Q at complex 3. Coenzyme Q then donates one electron at a time to O_2 creating O_2^- (Brownlee, 2005, Camello-Almaraz *et al.*, 2006). The blockage of electron donation at complex 3 can also stimulate electrons to leak out to form superoxide at complex 1 (Camello-Almaraz *et al.*, 2006). Reperfusion can lead to the further generation of H_2O_2 and hydroxyl radical ($\cdot OH$) formation (Vanden Hoek *et al.*, 1997). In addition Superoxide (O_2^-) can be converted by superoxide dismutase (SOD) into H_2O_2 , which can then be reduced to H_2O by glutathione peroxide (GSH) (Figure 1.10) (Camello-Almaraz *et al.*, 2006). During ischaemia disruption of oxidative phosphorylation halts ATP synthesis and stimulates ATP synthase to work in reverse (as an ATPase) to hydrolyse ATP into ADP + Pi (Jennings *et al.*, 1991), thus further reducing the ATP available to the cell.

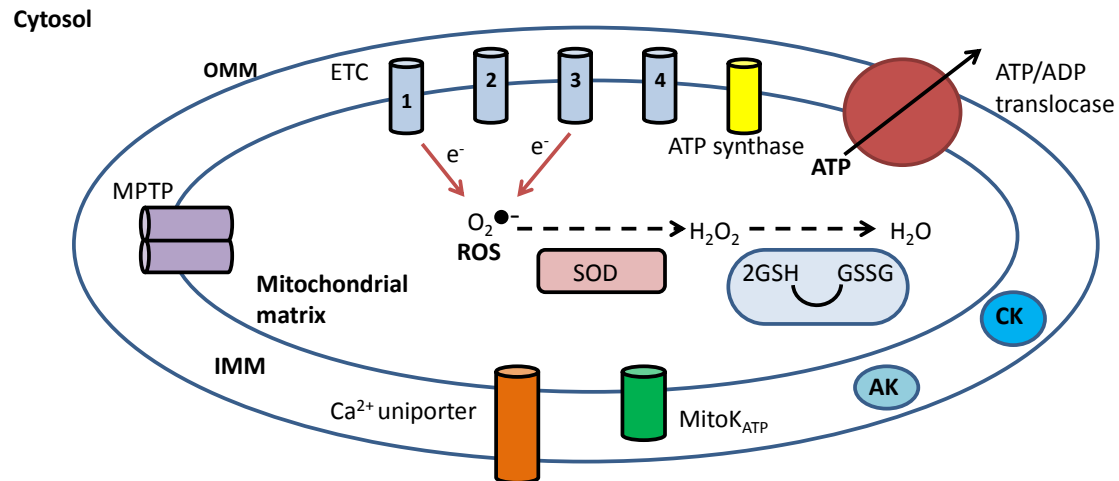


Figure 1.10 Structure of the mitochondria

The mitochondria consists of an inner (IMM) and outer membrane (OMM) encasing a mitochondrial matrix, within the mitochondria are various components which aid numerous functions including ATP synthesis via the electron transport chain (ETC) and ATP synthase. The translocation of ATP from the mitochondrial matrix to the cytosol via ATP/ADP translocase. Spanning the two mitochondrial membranes are the mitochondrial permeability transition pore (mPTP), the Ca^{2+} -uniporter, the mitochondrial K_{ATP} channel. Within the mitochondrial matrix reactive oxygen species (ROS) can be generated for example superoxide ($O_2^{\bullet -}$), these can be scavenged by the ROS-scavengers, superoxide dismutase (SOD) into hydrogen peroxide (H_2O_2) and then by glutathione (GSH) into water (H_2O) and oxidised glutathione (GSSG). Within the interstitial space are creatine kinase (CK) and adenylate kinase (AK), which transfer high energy phosphate to areas of ATP utilisation within the cytosol.

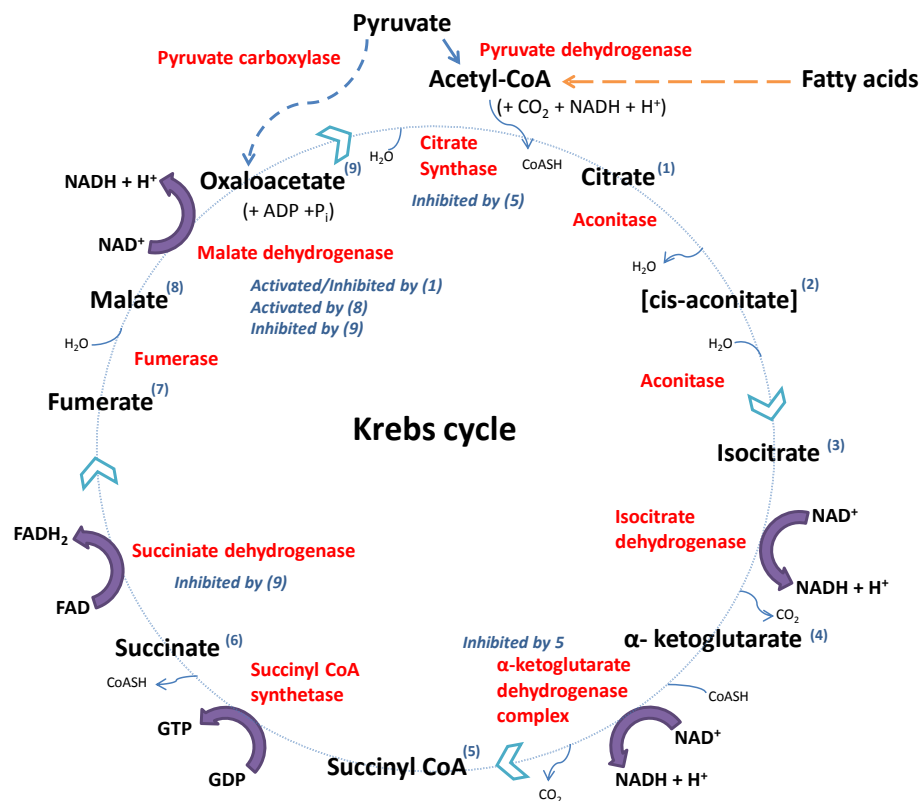


Figure 1.11 Krebs cycle

The initial step in the Krebs cycle is the condensing of oxaloacetate⁽⁹⁾ with Acetyl-coA (supplied via pyruvate or fatty acid metabolism) to produce citrate⁽¹⁾, via citrate synthase. Citrate⁽¹⁾ then undergoes two reactions which results in isocitrate⁽³⁾ being formed, each reaction is catalysed by Aconitase. Isocitrate⁽³⁾ is then dehydrogenase by isocitrate dehydrogenase. This reaction yields α -ketoglutarate⁽⁴⁾, which then undergoes dehydrogenation via the combined efforts of the α -ketoglutarate dehydrogenase complex and CoA-SH to form succinyl coA⁽⁵⁾. Succinyl coA⁽⁵⁾ is then converted into succinate⁽⁶⁾ by succinyl coA synthetase. The final stages of the Krebs cycle involve succinate dehydrogenase catalysing the conversion of succinate⁽⁶⁾ into fumarate⁽⁷⁾. Fumarate⁽⁷⁾ is then converted into malate⁽⁸⁾ via a hydration catalysed by fumarase. Malate⁽⁸⁾ is then converted back into oxaloacetate⁽⁹⁾ by malate dehydrogenase. The regulation of some of the enzymes by certain by-products of the reactions is illustrated on the diagram underneath the enzyme name in *italics* with a number illustrating which by product it is regulated by. Diagram is adapted from Berg *et al.*, 2007 Salway, 2004 and annotated based on work by LaNoue *et al.*, 1972, Smith *et al.*, 1974, Smith & Williamson, 1971, Shepherd & Garland, 1969, Kohn *et al.*, 1979, Mullinax *et al.*, 1982 and Gelpi *et al.*, 1992.

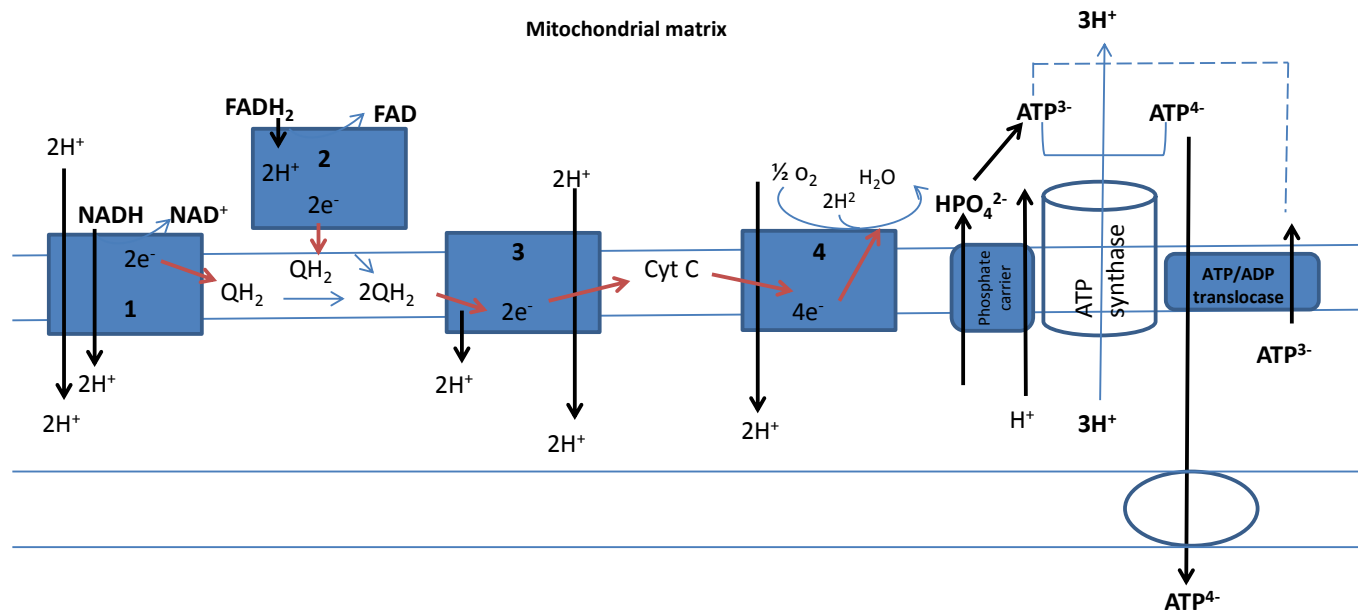


Figure 1.12 The Electron Transport Chain and ATP synthase

The electron transport chain (ETC) consists of 4 inner membrane bound complexes (complexes 1-4). The reducing agents NADH and FADH₂ donate electrons (e⁻) at complex 1 and complex 2 respectively. The electrons donated at each complex are transferred along the ETC via Coenzyme Q (QH₂) and cytochrome C (Cyt C) to the final electron acceptor oxygen, which combines with H⁺ and uses the electrons to become reduced to H₂O. The transfer and passage of electrons along the ETC generates an electrochemical potential across the mitochondrial membrane, which pumps H⁺ from the mitochondrial matrix into the interstitial space. The H⁺ then converge onto the ATP synthase (complex 5 of the ETC), which pumps H⁺ back into the mitochondrial matrix down their electrochemical gradient. This generates energy allowing the synthesis of ATP from ADP + Pi also by ATP synthase. The synthesised ATP is transported from the matrix into the interstitial space by ATP/ADP translocase in exchange for the import of ADP. The Pi required for the synthesis of ATP enters the matrix via the phosphate carrier. Transportation of ATP across the outer membrane occurs via a porin channel (voltage-dependent anion channels). Diagram modified from Berg *et al.*, 2007, Salway, 2004, Huttemann *et al.*, 2008, Knox & Tsong, 1984.

1.10.2.1 Delivery of ATP generated from oxidative phosphorylation to areas of ATP utilisation via phosphotransfer systems.

A key ATP phosphotransfer system in cardiomyocytes is the phosphocreatine pathway, which transports high energy phosphates to areas of ATP utilisation. This occurs via mitochondrial creatine kinase using ATP to convert creatine into phosphocreatine (PCr), which then transfers through the cytosol to the areas of ATP utilisation, such as the contractile proteins or membrane bound ATPases. Cytosolic creatine kinase then converts PCr back into creatine (which is transferred back to the mitochondria to be reused) and ATP, which is utilised by ATPases at the specific areas (Rauch *et al.*, 1994). Adenylate kinase is another phosphotransfer system, which maintains ATP levels by reversibly converting two ADP molecules into ATP and AMP. This system operates in the mitochondria, cytosol and at the membrane (Dzeja *et al.*, 1998). However these systems only produce short term energy reserves and soon diminish during ischaemia (Depre & Taegtmeyer, 2000).

1.10.3 Mitochondrial permeability transition pore (mPTP)

The mPTP is a large conductance channel located in the inner mitochondrial membrane. Although its exact structure remains unclear it is believed to include a voltage-dependent anion channel (VDAC), however knockout studies of the VDAC genes suggest this channel is not required for mPTP function, an adenine nucleotide translocator, a cyclophilin D residue and a phosphate carrier (Hausenloy & Yellon, 2003; Garrido *et al.*, 2006). Once open mPTP allows solutes of up to 1500Da to enter the usually impermeable inner membrane (Hausenloy & Yellon, 2003), causing swelling of the mitochondria, rupturing the mitochondrial membrane, leading to the release of cytochrome C (Cyt C) and other pro-apoptotic factors (such as endonucleases, BAX, Smacs and IAPs) which induce apoptotic cell death (see section 1.10.3.1) (Hausenloy & Yellon, 2003).

The mPTP channels are suggested to remain closed during ischaemia due to acidic conditions inside the cells (Qian *et al.*, 1997; Halestrap, 1991) and actually open during reperfusion due to high Ca^{2+} in the mitochondrial matrix, an increased P_i load, ATP

depletion, oxidative stress and correction of pH (Qian *et al.*, 1997; Griffiths & Halestrap, 1995; Di Lisa *et al.*, 2001).

1.10.3.1 Role of mPTP in cell death

Prolonged opening of mPTP is proposed to cause collapse of the mitochondrial membrane potential, disrupting the electrochemical gradient used by ATP synthase to generate ATP, which uncouples the mitochondrial oxidative phosphorylation. This combined with ROS generation, DNA damage and Ca^{2+} overload, leads to necrosis (Hausenloy & Yellon, 2003). However it has been suggested mPTP may also open in shorter bursts at the onset of oxidative stress, to try and counteract some of these deleterious effects and prevent ATP depletion (Huser & Blatter, 1999).

Apoptosis stimulated cell death occurs when Cyt C is released through the open mPTP into the cytosol; where it activates the pro-apoptotic factor APAF-1 to generate an apoptosome, which then activates pro-caspase 9 into Caspase 9. Caspase 9 goes onto activate a cascade of other caspases (caspase 3 and caspase 7) and stimulates apoptosis (programmed cell death) (Acehan *et al.*, 2002).

Activated caspase 3 can re-enter the mitochondria through the pro-apoptotic proteins BAX/BAK pores and cleave complex 1 of ETC; this impairs electron flow and further disrupts the mitochondrial membrane potential, leading to further ROS generation (Depre & Taegtmeyer, 2000; Garrido *et al.*, 2006; Ricci *et al.*, 2004). During opening of mPTP antioxidants generated within the mitochondria are lost, thus neutralisation of the formed ROS is unachievable.

The close proximity of the mitochondria to the SR leads to a positive feedback loop associated with opening of mPTP during reperfusion. Opening mPTP increasing $[\text{Ca}^{2+}]_i$, this can impact on the SR by causing SR Ca^{2+} oscillations. This can induce hypercontracture leading to cell death and also induce permeabilisation of other intact mitochondria membranes, which in turn stimulates opening of mPTP within these mitochondrial membranes and can generate further SR Ca^{2+} oscillations (Garcia-Dorado *et al.*, 2012).

1.11 Ischaemic Conditioning

1.11.1 Types of ischaemic conditioning

Ischaemic preconditioning (IPC) was first described by Murry *et al* (1986), who identified that if they subjected a canine myocardium to brief (5 minute) non-lethal periods of ischaemia, interspersed by brief (5 minute) periods of reperfusion prior to a sustained ischaemia period (40 minutes), the myocardium was protected against ischaemia/reperfusion injury evident by a significant reduction in infarct size (Murry *et al.*, 1986). Murry *et al* (1986) hypothesised that preconditioning slows ATP depletion, via increased anaerobic glycolysis, reducing the energy demands required during ischaemia or by increasing the net availability of high-energy phosphates (Murry *et al.*, 1986). Murry *et al* (1986) also proposed that individuals who experience multiple episodes of angina pectoris before an AMI may be preconditioning their hearts and thus altering the time course of cell death after the onset of a sustained coronary occlusion (Murry *et al.*, 1986). The protection imparted by IPC has been observed by various other end points including delayed ATP depletion, a reduction in O₂ consumption, decreased LDH and creatine kinase release and cardiomyocytes being able to retain their intracellular structure (Murry *et al.*, 1986; Kuzuya *et al.*, 1993; Bolli *et al.*, 2007; Laclau *et al.*, 2001; Kitakaze, 2010).

IPC appears to have two windows; an early or classical window, which is established from the point of stimulus and last for 1-4 hours, and a second or delayed window of protection, which returns 12-72hrs hours after the IPC stimulus and last for 48-72 hours (Kuzuya *et al.*, 1993; Bolli *et al.*, 2007; Marber *et al.*, 1993). The second window of IPC still protects against cell death and preserves post-ischaemic left ventricular function (Bolli *et al.*, 2007).

Ischaemic conditioning also exists in numerous others forms including; ischaemic postconditioning (IPostcon), remote preconditioning (Remote PC) and pharmacological conditioning. All conditioning types have been found to confer protection on the myocardium in a variety of species including rats, rabbits, canines and humans.

IPostcon was demonstrated by administering 3 repetitive cycles of reperfusion (30 seconds) interspersed with periods of ischaemia (30 seconds) after a main ischaemic event (occlusion of the left anterior descending artery for 60 minutes), but before the onset of prolonged reperfusion (3 hours). This postconditioning stimulus attenuated cellular damage caused by ischaemia-reperfusion injury (Zhao *et al.*, 2003). The protective effects of IPostcon include reduced infarct size, maintained endothelial function, reduction in apoptosis and fewer reperfusion arrhythmias (Zhao *et al.*, 2003; Galagudza *et al.*, 2004; Halkos *et al.*, 2004; Kin *et al.*, 2004; Sun *et al.*, 2005; Kloner *et al.*, 2006; Wang *et al.*, 2006). IPostcon also attenuates superoxide anion generation in the area at risk after 3hr of reperfusion (Kin *et al.*, 2004; Sun *et al.*, 2005), resulting in low levels of superoxide anions, which can act as a signal for endogenous protection.

Remote PC involves applying a brief period of an ischaemia and reperfusion conditioning pulse to a region of the body (i.e. a limb) (Oxman *et al.*, 1997; Kharbanda *et al.*, 2002; Cheung *et al.*, 2006) or an organ (i.e. kidney or small intestine) (Gho *et al.*, 1996; Pell *et al.*, 1998) which is remote from the organ that is protected. Remote PC has been achieved in humans via inflation of an automated cuff to 200mm Hg on the right upper arm, in three 5 minute cycles interspersed with 5 minutes of reperfusion (cuff deflated). This generates a signal in the remote ischaemic tissue, which stimulates a blood born agent or reflex neural pathway to confer a distal protection to other tissues including the myocardium against a sustained period of ischaemia (Hausenloy & Yellon, 2008). Remote PC reduces infarct size, preoperative troponin T-release over 24-72hr after surgery and reperfusion arrhythmias (Oxman *et al.*, 1997; Cheung *et al.*, 2006; Kharbanda *et al.*, 2006).

Application of certain pharmacological agents before (pre) or after (post) a sustained ischaemic event in a laboratory or clinical setting, have been shown to be cardioprotective. Agents include adenosine, bradykinin, opioids agonist, muscarinic agonists, angiotensin and endothelin (Granfeldt *et al.*, 2009). These agents are thought to activate similar signalling pathways to those of IPC, IPostcon and Remote PC.

1.11.2 Mechanisms of ischaemic conditioning

1.11.2.1 Ischaemic preconditioning

The mechanisms behind early and late IPC are illustrated in Figure 1.13. One of the main stimuli of ischaemia conditioning is the generation of numerous endogenous receptor tyrosine kinase and G-protein coupled receptors (GPCR) ligands including adenosine; bradykinin, opioids, angiotensin, catecholamine and acetylcholine (Hausenloy & Yellon, 2008; Peart & Headrick, 2009; Yang *et al.*, 2010). As illustrated in Figure 1.13, binding of these ligands to GPCRS and or receptor kinase receptors such as EGR, activate multiple intracellular cardioprotective signalling pathways, including those involving the reperfusion injury survival kinases (RISK) (Peart & Headrick, 2009; Yang *et al.*, 2010; Hausenloy *et al.*, 2005; Hausenloy & Yellon, 2006). The first window of IPC is instant, while late IPC involves genetic modulation of channel receptor, proteins and enzymes (Yang *et al.*, 2010; Hausenloy & Yellon, 2010).

One of the main signalling pathways activated in IPC involves PKC. The known involvement of PKC in IPC has been enhanced by findings that PKC activators mimic IPC, while PKC inhibitors abolish the cardioprotection usually elicited by IPC and remote PC. Deleting cardiac PKC- ϵ in mice also prevents IPC from decreasing infarct sizes (Ytrehus *et al.*, 1994; Inagaki *et al.*, 2005; Weinbrenner *et al.*, 2002). Once activated PKC- ϵ and PKG stimulate opening of MitoK_{ATP} channels (Grover & Garlid, 2000; Nakano *et al.*, 2000). Opening MitoK_{ATP} can reduce Ca²⁺ overload through depolarisation of the mitochondrial membrane potential, reducing the driving force for Ca²⁺ uptake, resulting in a decreased mitochondrial Ca²⁺ accumulation (Holmuhamedov *et al.*, 1998; Wang *et al.*, 2001) which usually triggers mPTP formation and opening, therefore this is inhibited. Involvement of MitoK_{ATP} in inhibiting mPTP is supported by the finding that application of the putative MitoK_{ATP} opener diazoxide causes inhibition of mPTP (Kowaltowski *et al.*, 2001; Hausenloy *et al.*, 2009). These main signalling pathways ultimately lead to inhibition of mPTP which reduces necrosis, apoptosis and infarct size (Murry *et al.*, 1986; Hausenloy *et al.*, 2009).

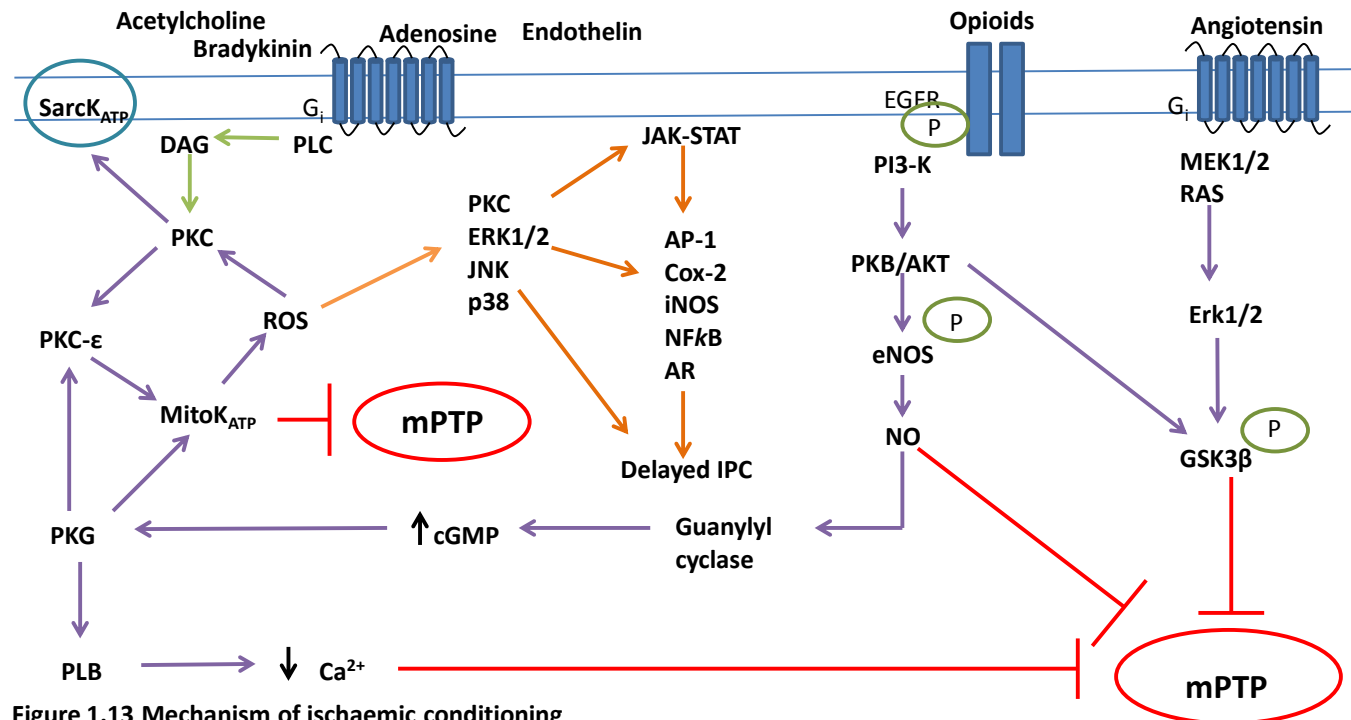


Figure 1.13 Mechanism of ischaemic conditioning

Ischaemic conditioning involves binding of ligands to GPCRs (predominantly G_i) and/or a receptor tyrosine kinase such as the epidermal growth factor receptor (EGFR). This stimulates the phosphatidylinositol 3-kinase–Protein Kinase B (PI3-K-AKT) pathway, the extracellular signal regulated kinase 1/2 (ERK1/2) pathway (via MAPK MEK1/2 or RAS) and PKC (via phospholipase C (PLC) stimulating production of diacylglycerol (DAG)). These pathways regulate downstream components including glycogen synthetase kinase 3β (GSK-3β), protein kinase C-ε (PKC-ε) and endothelial nitric oxide (eNOS). Which go on to activate or stimulate the production of the following; protein kinase G (PKG), the SarcK_{ATP} and Mitok_{ATP} channels, guanylyl cyclase, nitric oxide (NO), phospholamban (PLB), cyclic GMP, ROS and the reperfusion injury survival kinases (RISK). All of these pathways result in inhibition of the mitochondrial permeability transition pore (mPTP), indicated by the red arrows. Pathways highlighted by purple arrows give rise to early IPC and IPostcon. The PI3-K-AKT pathway can activate the delayed IPC window of protection on its own or by activating the JAK-STAT pathway (Orange pathway from ROS). The PI3-K-AKT and the ERK 1/2 pathways have also been suggested to stimulate remote PC. Diagram adapted from Peart & Headrick, 2009, Hausenloy & Yellon, 2006.

The released ROS has its own cardioprotective roles as illustrated in Figure 1.13 such as triggering activation of RISK (p38-MAPK) and JAK/STAT or by inhibiting mPTP (Bolli *et al.*, 2007; Hausenloy & Yellon, 2008; Granfeldt *et al.*, 2009; Hausenloy *et al.*, 2005; Vanden Hoek *et al.*, 1998). Free radical scavengers abolish protection imparted by IPC suggesting ROS is involved (Granfeldt *et al.*, 2009). Mitochondrial release of ROS also has anti-apoptotic effects such as inhibiting caspase activity (Erhardt *et al.*, 1999) and activating PKB (AKT) via phosphorylation by phosphatidylinositol-3-kinase (PI-3 kinase). Activated PKB (AKT) phosphorylates the pro-apoptotic protein BAD and the proteolytic activity of caspase 9 inhibiting the caspase pathway therefore preventing apoptosis (Cardone *et al.*, 1998; Kennedy *et al.*, 1999).

The involvement of SarcK_{ATP} and MitoK_{ATP} in IPC is widely reported but remains controversial (Pell *et al.*, 1998; Yang *et al.*, 2010; Cleveland *et al.*, 1997; Yang *et al.*, 2004), as animals deficient in SarcK_{ATP} or with the Kir6.2 subunit deleted show no IPC protection (Gumina *et al.*, 2003; Suzuki *et al.*, 2002). In addition administration of K_{ATP} antagonists (glibenclamide, 5-HD and HMR-1098) has been shown to abolish the protective effects previously elected by IPC and remote IPC (Sato *et al.*, 2000; Suzuki *et al.*, 2002; Auchampach *et al.*, 1992; Dickson *et al.*, 2002). However glibenclamide and HMR-1098 have also both been found to not affect the protection imparted by IPC (Suzuki *et al.*, 2002; Thornton *et al.*, 1993). This suggest SarcK_{ATP} is not involved in IPC but this may be due to a difference in species or possibly the MitoK_{ATP} channel is the predominantly K_{ATP} channel involved in IPC.

1.11.2.2 Mechanism behind ischaemic postconditioning and remote IPC

The mechanisms behind IPostcon and remote PC are relatively similar to IPC as illustrated in Figure 1.13. IPostcon is believed to involve activation of PKC, ERK1/2 and PI3-K pathways (Peart & Headrick, 2009; Hausenloy & Yellon, 2006). Remote PC involves a neural or humoral pathway generating the endogenous GPCR ligands, which activate mechanism illustrated in Figure 1.13 (Hausenloy & Yellon, 2008), or it could be due to production of a systemic anti-inflammatory phenotype that protects the distant organ against subsequent ischaemia/reperfusion (Granfeldt *et al.*, 2009).

1.11.3 Role of metabolism in ischaemic conditioning

IPC and IPostcon both stimulate a significant increase in glucose uptake, this is attributed to the ischaemic period of IPC and IPostcon stimulating GLUT-4 translocation, resulting in an acute increased expression of GLUT-4 at the sarcolemmal membrane (Tong *et al.*, 2000; Nishino *et al.*, 2004; Correa *et al.*, 2008; Ji *et al.*, 2013). This increase in GLUT-4 expression has been shown to last for 24 hours in IPC (Nishino *et al.*, 2004), but decreases during prolonged reperfusion in IPostcon hearts (Correa *et al.*, 2008). Possible mechanisms for ischaemic conditioning inducing GLUT-4 translocation include stimulation by PKC- ϵ activated AMPK, which can be attenuated by Chelerythrine (PKC inhibitor) (Nishino *et al.*, 2004) or stimulation by p38 MAPK. As increased glucose uptake, observed (via increased 2-deoxyglucose-6-phosphate production) during IPC was significantly reduced in the presence of a p38 MAPK inhibitor SB202190, p38 MAPK could be involved in stimulated increased Glut-4 transport during IPC (Tong *et al.*, 2000). The involvement of PI3-K is not as clear, as inhibition of PI3-K with Wortmannin did not reduce the increased glucose uptake observed during IPC thus suggesting PI3-K is not involved (Tong *et al.*, 2000). However another group showed pre-treatment with Wortmannin prior to IPC did prevent the increased glucose uptake via GLUT-4 translocation (Ji *et al.*, 2013), suggesting PI3-K is involved in translocation of GLUT-4. The difference in PI3-K involvement could relate to when Wortmannin was applied.

As a result of increased glucose uptake, the rate of anaerobic glycolysis significantly increases leading to improved ATP, Ca^{2+} and PCr levels and higher levels of lactate during reperfusion which correlates with changes in exogenous glucose uptake. This suggests that for IPC hearts during ischaemia and reperfusion, anaerobic glycolysis is maintained (Janier *et al.*, 1994; Yabe *et al.*, 1997, Fralix *et al.*, 1992, de Jonge & de Jong, 1999; Correa *et al.*, 2008). However during the first few minutes of reperfusion lower lactate levels have been observed in ischaemic conditioned hearts, suggesting increased lactate efflux upon initial reperfusion, which could prevent the detrimental effects associated with lactate such as acidosis (Yabe *et al.*, 1997; Correa *et al.*, 2008). The idea of maintained glycolysis during reperfusion of ischaemic conditioned hearts is confirmed by the finding that applying iodoacetic acid (IAA) during reperfusion

following IPostcon attenuates the observed higher ATP level and reduced recovery even in the presence of pyruvate (Correa *et al.*, 2008).

Pyruvate increases the threshold for IPC, with IPC only being achieved (as observed by improved LVDP recovery and reduced LDH release by the end of the prolonged reperfusion) in pyruvate perfused hearts, when the ischaemic pre-treatment period was increased from 5 minute intervals to 7 minute (an increase in time by 40%). This suggests to achieve IPC with pyruvate there has to be an increase in the severity of the ischaemia damage, as pyruvate can have its own protective effects (Sargent *et al.*, 1994). Reperfusion with pyruvate following IPC for 4 x 5 minutes has also been found to result in no cardioprotection, due to pyruvate inhibiting glycolysis (Fralix *et al.*, 1992).

Ischaemic conditioning is also believed to improve the rate of glycolytic flux, as a result the levels of Glucose-6-Phosphate (G6P) and Fructose-6-Phosphate (F6P) at the end of reperfusion are significantly lower. This suggests IPC prevents inhibition of the glycolytic pathway which can occur during reperfusion, this results in an increase in glycolytic flux through the rate limiting 3rd enzyme in glycolysis PFK-1. Increased flux through PFK-1 in IPC hearts is represented by an improvement in the ratio of $[FBP]/[G6P]+[F6P]$ which is a marker of glycolytic flux rate through PFK-1 (Yabe *et al.*, 1997).

1.12 Literature views on the role of metabolites in cardioprotection

In addition to the suggestions outlined in section 1.11.3 that the cardioprotection observed with IPC and IPostcon may have an element based around metabolites and their metabolism, many studies have also investigated the cardioprotection linked to metabolites following a ischaemic/reperfusion injury protocol.

A number of whole heart studies have demonstrated that perfusion with high glucose (>10mM) in the presence or absence of insulin, prior to the induction of ischaemia (induced by low-flow) and during reperfusion protects against ischaemia/reperfusion injury. This was indicated by various end points including; a delay in the development of ischaemic contracture, higher glycolytic ATP production during ischaemia, reduced

LDH and creatine kinase release and improved functional recovery (Bricknell & Opie, 1978; Vanoverschelde *et al.*, 1994; Wang *et al.*, 2005; Owen *et al.*, 1990). Global ischaemia in whole heart studies, has also shown that high glucose (16mM) present before and after the period of ischaemia improved recovery of function, compared to those perfused with non-glycolytic substrates (either 5mM pyruvate or 5mM acetate) in combination with iodacetate (to inhibit glycolysis) throughout the reperfusion period (Jeremy *et al.*, 1993). These works suggest increased glycolysis prior to and during ischaemia is essential in decreasing ischaemic injury, and that glycolysis is required during reperfusion to improve recovery of contractile function.

Metabolites related to oxidative phosphorylation have also been shown to impact on ischaemic/reperfusion injury in whole heart studies. Perfusion of isolated mice hearts with 10mM pyruvate with or without glucose (15mM) as a co-substrate, prior to global no-flow ischaemia, has been found to prolong the time to ischaemic contracture and improved post-ischaemic functional recovery (Flood *et al.*, 2003). Whereas perfusion with palmitate (a long chain fatty acid), at different stages of an ischaemic/reperfusion injury protocol have been shown to be detrimental compared to those where glucose was also perfused in part or in combination with, for part of the protocol (Johnston & Lewandowski, 1991, Bricknell & Opie, 1978). These studies suggest metabolites which feed directly into the Krebs cycle can have opposing affects on recovery, suggesting metabolism in the mitochondria impacts heavily on cardioprotection.

Whole heart studies have also shown the effects of elevating glucose, either prior to ischaemia or solely upon reperfusion. Perfusion with elevated glucose prior to ischaemia, show protection in terms of prevented or delayed rigor (Owen *et al.*, 1990; Kingsley *et al.*, 1991), but as these studies did not continue through to reperfusion, the benefits of elevating glucose solely prior to ischaemia on contractile recovery cannot be established. Studies investigating perfusion with elevated glucose solely during reperfusion are conflicting, a study by Vanoverschelde *et al* (1994), demonstrated that elevating glucose (10mM) and insulin (140mU/L) solely during reperfusion did not improve contractile recovery (Vanoverschelde *et al.*, 1994). However inhibition of glycolysis with iodacetate throughout reperfusion has been shown to prevent recovery of function, this is in contrast to where application of iodoacetate only in the latter

stages of reperfusion had no effect on contractile recovery (Jeremy *et al.*, 1993; Jeremy *et al.*, 1992). These conflicting data suggest that elevated glucose may be detrimental or beneficial at the time of reperfusion and that glycolysis is required during the early stages of reperfusion in order to achieve contractile recovery.

Due to these studies focusing on the whole heart, little is known about the impact these metabolites have at a cellular level, and whether the same level of cardioprotection can be achieved in isolated cardiomyocytes. Therefore work in this thesis will aim to identify the impact a variety of metabolic substrates have on isolated cardiomyocytes throughout an ischaemic/reperfusion injury protocol. Additionally as previous studies have also not investigated the effect upon reperfusion of only elevating glucose prior to ischaemia and as the effects on reperfusion are conflicting, it would be interesting to observe what effects increased availability of certain metabolites either acutely prior to one sustained period of ischemia or during different stages of reperfusion, would have on isolated cardiomyocytes following a complete ischaemia/reperfusion protocol. These studies would provide an insight as to whether a type of “metabolic conditioning” can provide similar cardioprotective effects as traditional preconditioning protocols.

1.13 Aims and objectives of the project

The overall aim of this project was to investigate the response of isolated ventricular cardiomyocytes to acute changes in metabolic substrates, while being subjected to a simulated ischaemia/reperfusion injury protocol. Due to differences in activity of many of the metabolic pathways prior to, during and after ischaemia, and with previous studies identifying the impact on the whole heart, several metabolic substrates were chosen to be investigated; as a result the following hypotheses were established:

- The first stage of glucose metabolism (glycolysis) can continue during periods of ischaemia; therefore it was hypothesised that an increased availability of glycolytic metabolic substrates would be beneficial.
- Due to oxidative phosphorylation predominating in the period prior to and during reperfusion but being inhibited during ischaemia, it was hypothesised

that alterations in oxidative phosphorylation metabolic substrates concentrations, would impact on the contractile response.

- Ischaemic conditioning is believed to have an element based around metabolism and as previous whole heart studies have shown a potential role for metabolites, it was hypothesised there may be a role for metabolites either prior to (preconditioning) or after (postconditioning) ischaemia as a type of metabolic conditioning.

These aims and hypotheses will be investigated by the following objectives:

- To identify the effects of increased availability of glycolytic metabolic substrate concentrations; glucose and fructose were perfused at various concentrations.
- To investigate the effects of oxidative phosphorylation metabolic substrates; the pyruvate concentration was altered to either a physiological or supraphysiological concentration. In addition, separate experiments investigating the addition of a medium chain fatty acid were carried out.
- The effects of the acute changes in metabolic substrates were assessed by observing contractile function, and by using electrophysiology to identify any changes in cardiac action potentials and activation of the $\text{SarcK}_{\text{ATP}}$ channels during metabolic inhibition. Additionally the effects on Ca^{2+} regulation and energy use, were investigated using fluorescence imaging to observe changes in $[\text{Ca}^{2+}]_{\text{i}}$ and Mg^{2+} concentrations.
- Based on investigations outlined above; hypotheses on which metabolic substrates and their time of application were generated and experiments were designed to investigate the effects of metabolic conditioning.

CHAPTER 2

Methods and materials

2. Methods and materials

2.1 Isolation of adult rat cardiomyocytes

Adult male Wistar rats (weighing 200-400g) were humanely killed using a schedule 1 procedure (stunning followed by cervical dislocation) in accordance with Home Office Regulations and guidelines (Animals Scientific Procedures Act 1986, 2012 amendment). The heart was rapidly excised and placed in cold nominally calcium-free Tyrode solution (Zero Ca^{2+} Tyrode, see 2.7.1 for solutions). The heart was cannulated via the aorta and perfused for 6 minutes; at a constant flow rate of 8ml/min with Zero Ca^{2+} Tyrode, at $37 \pm 2^\circ\text{C}$ (bubbled with 100% O_2), in a retrograde fashion using Langendorff apparatus.

The perfusate was then switched to the enzyme solution outlined in section 2.7.1 for 5-8 minutes. The first minute of enzyme perfusate was discarded, after this it was recycled until the heart was digested. Upon appearance of individual rod-shaped cardiomyocytes in the perfusate, the solution was switched to 2mM Ca^{2+} Tyrode solution (2 Ca^{2+} Tyrode, see 2.7.1 for solutions), for 1-3 minutes. The atria were discarded and the heart cut along three axis and placed into a conical flask (containing 2 Ca^{2+} Tyrode), which was then placed into a water bath at $37 \pm 2^\circ\text{C}$ and gently agitated for 3-5 minutes to further release individual ventricular rod-shaped cardiomyocytes. The 2 Ca^{2+} Tyrode solution was transferred to a new conical flask at regular intervals, and more 2 Ca^{2+} Tyrode applied to the remains of the heart in the original flask. This process was repeated until a number of fractions were collected.

Each fraction was individually sieved to remove any undigested tissue and the filtered cell suspension poured into test tubes, and left to settle for 10-15 minutes. The supernatant was then removed and cardiomyocytes re-suspended in fresh 2 Ca^{2+} Tyrode and left to settle for a further 10 minutes. The supernatant was once again removed; and isolated cardiomyocytes transferred to 75mm petri-dishes in 2 Ca^{2+} Tyrode. Cardiomyocytes were maintained in 2 Ca^{2+} Tyrode at room temperature until use.

2.2 Superfusion and stimulation of cardiomyocytes

Isolated cardiomyocytes were left to adhere for 10 minutes in 1 ml of Tyrode solution on a glass coverslip; attached to a Dagan Heatwave perfusion chamber (see Figure 2.1) mounted on either a Nikon Diaphot 300 inverted microscope (contractile function); an inverted Nikon eclipse Ti U microscope (electrophysiology), or an inverted Nikon eclipse TE 200 microscope (fluorescence imaging). Superfusion was then started and maintained at 5ml/min using a Gilson Minipuls Evolution Peristaltic pump. A Dagan Heatwave temperature controller (HW-30) maintained the temperature at $32 \pm 2^\circ\text{C}$. Initially cardiomyocytes were perfused for 3 minutes to remove dead or unsettled cardiomyocytes. Cardiomyocytes were stimulated to contract at 1Hz by electrical field stimulation (EFS) with a pulse width of 3ms, via platinum electrodes running parallel along the bottom of the glass coverslip, using a Digitimer Stimulator DS9A (contractile function) or a Farnell stimulator (Fura-2 fluorescence imaging).

2.3 Experimental protocols

2.3.1 Ischaemia/reperfusion injury protocol

Inducing ischaemia in isolated cardiomyocytes is difficult, however this can be achieved by pelleting cardiomyocytes and replacing the supernatant with an oil layer (Vander Heide *et al.*, 1990). This technique does not permit measurements of contractile function, therefore the technique of chemically inducing ischaemia in isolated cardiomyocytes was chosen for this study, as it enables the contractile function of the isolated cardiomyocytes to be monitored throughout the simulated ischaemia and reperfusion protocol.

Ischaemia was simulated chemically in cardiomyocytes with iodoacetic acid (IAA) and sodium cyanide (NaCN), which inhibit glycolysis (at GAPDH) and oxidative phosphorylation (at cytochrome c oxidase at complex 4 of the ETC) respectively. IAA (1mM) and NaCN (2mM) were added to substrate free Tyrode (SFT) solution, creating a metabolic inhibition (MI) solution (SFT-MI) (see section 2.7.2.1). Cardiomyocytes were reperfed with Tyrode solution containing glucose and pyruvate, which re-

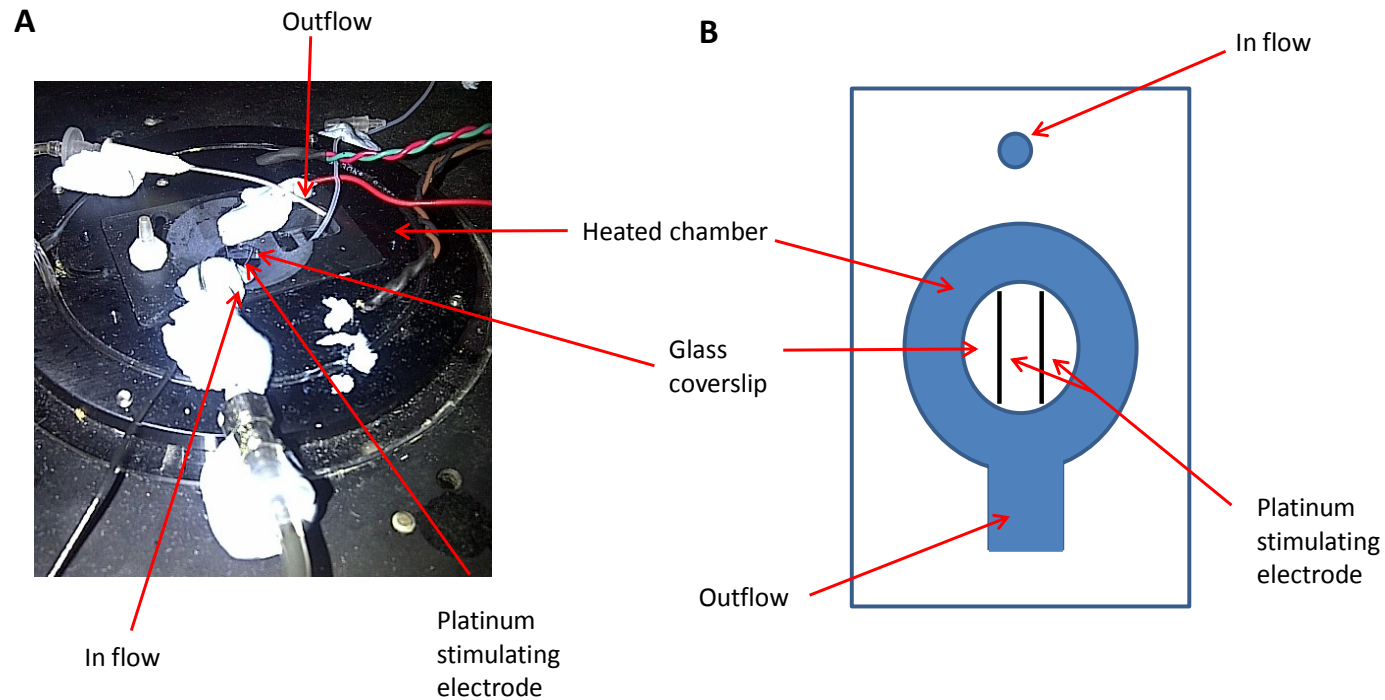


Figure 2.1 The perfusion chamber

(A) A picture of a perfusion chamber that would be used in contractile function and imaging experiments. (B) Top view of the perfusion chamber, solution enters the perfusion chamber through the inflow pre-heated and exits via the outflow. Platinum stimulating electrodes run parallel to each other across the bottom of the glass coverslip. No electrodes were in the perfusion chamber used in electrophysiology experiments.

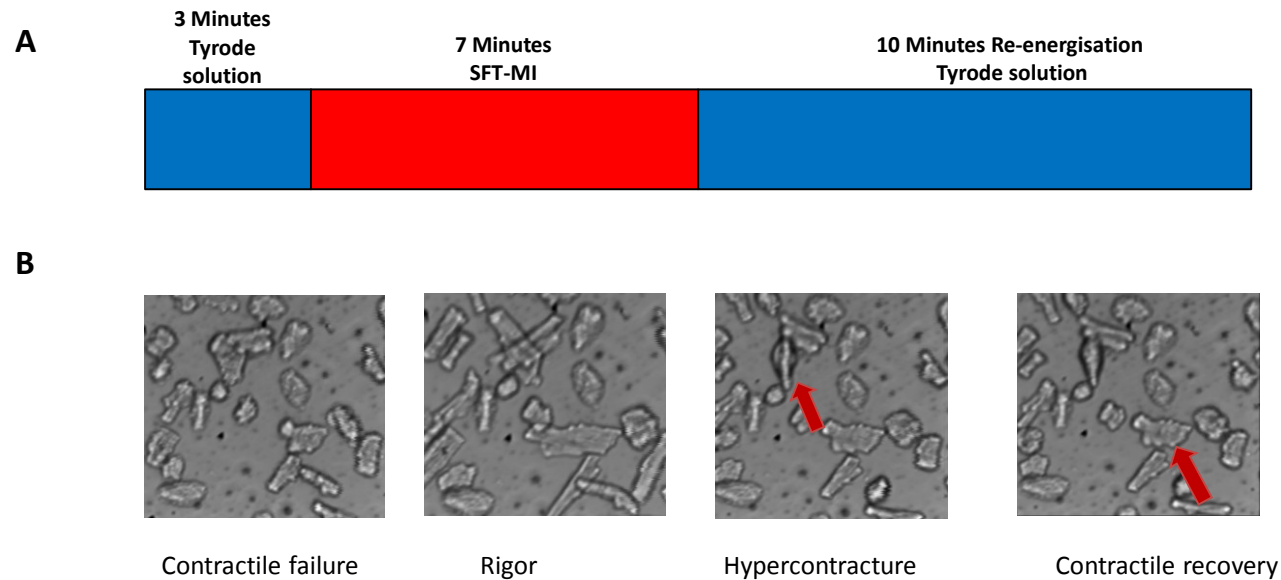


Figure 2.2 Contractile function measurements and morphology of cardiomyocytes through metabolic inhibition and re-energisation protocol

- (A) The control metabolic inhibition and re-energisation protocol (MI/R protocol).
- (B) Images from the DVD (attached to the thesis) showing the morphology of cardiomyocytes through an example MI/R injury control protocol. At the beginning of the MI/R protocol, the cardiomyocytes in the Tyrode solution (5mM glucose/5mM pyruvate) appear rod shaped. During SFT-MI cardiomyocytes first lose contractile activity and then enter the structural state of rigor and can be seen to shorten, due to ATP depletion at the contractile proteins. During re-energisation cardiomyocytes can enter hypercontracture and can be seen to shorten further with a decrease in the length to width ratio, due to ATP repletion/mitochondrial re-energisation coupled to an overload of calcium. When this occurs membranes are often seen to bleb and rupture, an example of this is indicated by the red arrow within the 3rd image. At the end of re-energisation, a range of cell types are visible, with the proportion of rod-shaped, rigor and hypercontracted cardiomyocytes varying dependent on the degree of MI/R injury. In addition some of the cardiomyocytes that have retaining more of their rod shaped structure, contract in time with the electrical field stimulation. The red arrow in the 4th image indicates a cardiomyocyte which had regained contraction by the end of the MI/R protocol.

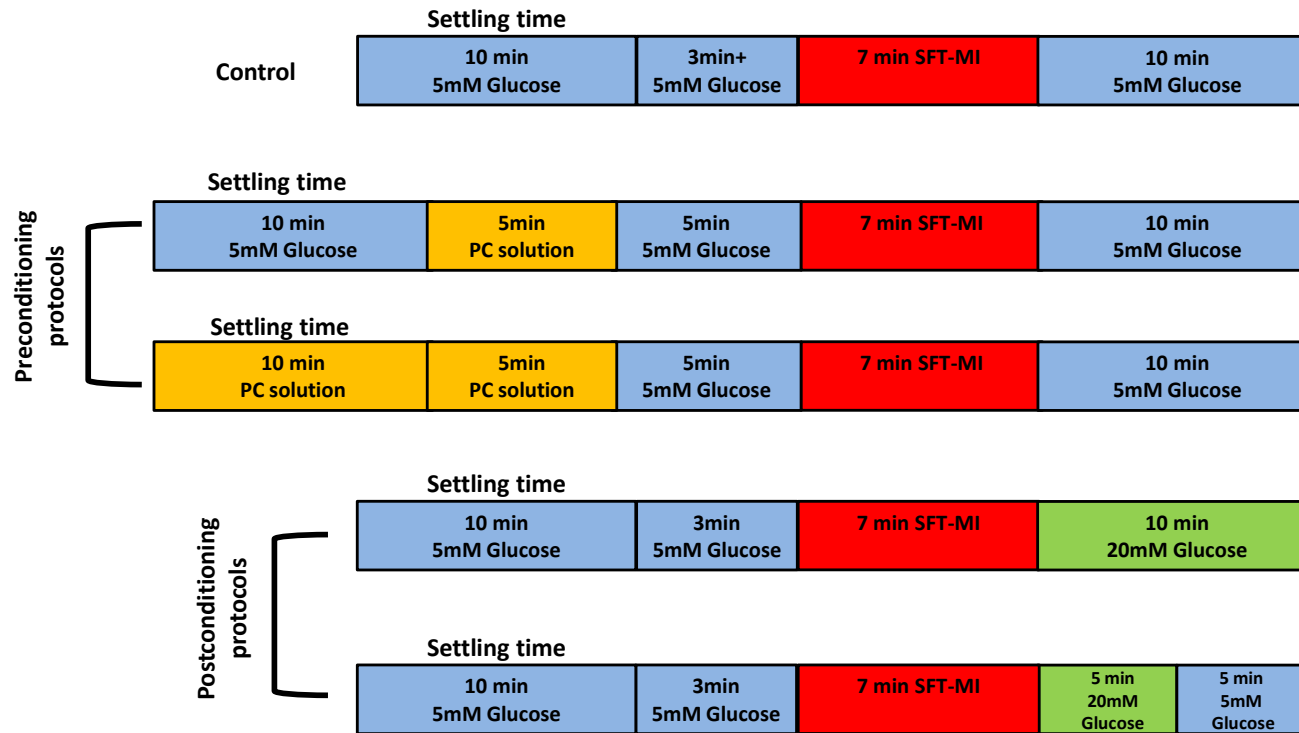


Figure 2.3 Protocols for contractile function and imaging experiments

The perfusion protocols for contractile function and imaging experiments used within this study. Cardiomyocytes were subjected to the control protocol or the protocols involving preconditioning (PC) or postconditioning with varying metabolic substrates.

energises the mitochondria. Throughout the thesis simulated ischaemia and reperfusion will be referred to as metabolic inhibition and re-energisation.

The control experimental protocol involved superfusion of Tyrode solution for 3 minutes followed by 7 minutes of SFT-MI, followed by 10 minutes of re-energisation with Tyrode solution (and an example of a control protocol is attached with the thesis as a DVD and stills from this example are represented in Figure 2.2B). This protocol was used as a screening method, to determine whether the cells had been “cardioprotected” during the isolation procedure, and strict exclusion criteria was implemented where cells that showed a greater recovery than 35% or less than 20% were not used. The exact metabolic composition of the Tyrode solution used in each experimental condition is described for each experiment in the result sections. The control experimental protocol outlined above was modified to include pre- and post-conditioning protocols as shown in Figure 2.3 and for the electrophysiology experiments (no re-energisation occurred). Following each protocol different end-points were used to determine the effect of metabolic inhibition and re-energisation (as discussed in each section).

2.3.2 Experimental design

In this study, contractile function (section 2.4), electrophysiology (section 2.5) and fluorescence imaging (section 2.6) experimental procedures were used to investigate the effects of acute changes in metabolic substrates on isolated ventricular cardiomyocytes prior to metabolic inhibition and/or during re-energisation at a cellular level.

The most appropriate way of carrying out the experiments outlined in this study would have been to have control experiments, followed by all experimental conditions tested on cells isolated from the same animal. This would then be repeated over a number of animals. Given the duration of the experimental protocol, and limitations on the duration of cell viability each day, this was not a feasible approach. The experimental protocol for contractile function experiments was therefore designed so that on each day a control experiment as outlined in section 2.3.1 was carried out, and used to ensure cell usability. Following the control a minimum of 3 experimental conditions

were tested for each heart preparation. In each data set a minimum of 3 hearts were used.

For each electrophysiology protocol and the fluorescence imaging experiments a control experiment with a 5mM glucose/5mM pyruvate Tyrode solution was carried out first each day and verified, this was in addition to a control contractile function experiment to ensure cell usability. Following the appropriate control and assurance of cell viability, a minimum of 3 experimental conditions were tested for each heart preparation for the electrophysiology and the fluorescence imaging experiments. In each data set a minimum of 3 hearts were used.

2.4 Contractile function measurements

2.4.1 Contractile function recordings by Electrical Field Stimulation

Contractile function experiments were set up as described in sections 2.2/2.3. The contractile function protocols can be seen in Figure 2.3. Following isolation, cardiomyocytes samples were exposed to different Tyrode solutions (see results sections for exact Tyrode solution used). For each sample, once contracting, one field of view (containing >15 cardiomyocytes) was selected at random for analysis, on a TV screen, using a JVC CCD (charged couple device) microscope camera. The field of view obtained from each sample was recorded onto DVD for later analysis.

2.4.2 Analysis of contractile function recordings

The contractile function experiments were stored as video recordings on DVD and analysed later off-line using Windows Media Player; only cardiomyocytes contracting at the beginning of the experiment, in response to the EFS were included in the analysis. Several end-points indicative of cellular injury during the metabolic inhibition and on re-energisation were determined: time to contractile failure (indicated by the failure to contract in response to EFS); time to rigor (indicated by the complete progressive shortening of the cell length by $\geq 60\%$), percentage of 'non-hypercontracted' cardiomyocytes, this included those that either recovered from hypercontracture or did not hypercontract (hypercontracture was observed as a decrease in the length to width ratio) and percentage of cardiomyocytes that regain

contraction in time with EFS by the end of the protocol. The data was analysed so that the 3 minutes (or 10 minutes in the preconditioning protocols) of superfusion of Tyrode before SFT-MI were subtracted from each time point, therefore data is presented as from the start of SFT-MI. Analysis was then carried out in a contractile function analysis template spreadsheet (Microsoft Excel 2010) and GraphPad Prism 6.

2.5 Electrophysiology

Two electrophysiology patch clamp configurations whole-cell and cell-attached, were used in this study. The whole-cell configuration was used to investigate both SarK_{ATP} channel activity and action potentials in isolated cardiomyocytes, during metabolic inhibition, following perfusion with different metabolic substrates. In addition to the macroscopic whole-cell current, the cell-attached configuration was used to measure the activity of a small number of SarK_{ATP} channels during metabolic inhibition. These recordings allowed for a definitive identification of the metabolic inhibition-induced current as the K_{ATP} channel complex by virtue of the channel conductance. Such confirmation of the identity of the current was not possible in the whole cell configuration due to a number of the pharmacological inhibitors of SarK_{ATP} channels (e.g. glibenclamide) being ineffective during metabolic inhibition (Ripoll *et al.*, 1993; Findlay, 1993; Lawrence *et al.*, 2002; Rainbow *et al.*, 2005).

2.5.1 Electrophysiology preparation

Electrodes were made from filamented thick walled borosilicate glass, using a two stage Narishige (PC-10) vertical electrode puller. The internal filament of the glass gave the electrodes a strong capillary action, which enabled the electrodes to be filled with the required intracellular pipette solution, so that the pipette solution was always in contact with both the solution in the perfusion chamber and the Ag/AgCl wire. Electrodes were filled prior to use and then mounted into an electrode holder attached to an Axopatch 200B headstage. Experiments set up as described in sections 2.2. Perfusion of Tyrode solution was maintained at a constant flow rate of 5ml/min (via a Gilson Minipuls Evolution Peristaltic pump) at $32 \pm 2^\circ\text{C}$ (via a heat wave HW-30 temperature controller). An individual cardiomyocyte was located with the aid of the attached Motic images USB camera and Motic images plus 2.0ML (MIplus 07) imaging

software. A Siskiyou micromanipulator was used to position the electrode at the surface of the cardiomyocyte. The electrode resistances were typically between 3-6 M Ω when filled with the pipette filling solutions (see section 2.7.3). The electrode tip was slowly lowered down onto the surface of the cardiomyocyte using the micromanipulator. An Axopatch 200B then amplified the signal recorded while filtering it at 2 kHz. The analogue signal was then digitised using a Digidata 1440, which sampled the data at 10 kHz and then stored it on the PC for later analysis.

2.5.2 Cell-attached configuration recording

Once the electrode was touching the cardiomyocyte (indicated by an increase in pipette resistance, see Figure 2.4), suction was applied using a syringe (connected via tubing to the headstage) to achieve a Gigaohm (G Ω) seal. The holding potential was changed from 0mV to -65mV to help improve the seal (see Figure 2.4). The cardiomyocyte was now held in the cell-attached configuration. All experiments recorded in the cell-attached configuration had electrodes filled with the cell-attached intracellular pipette solution (see section 2.7.3).

2.5.2.1 SarCK_{ATP} channel recordings

Once a leak current ≤ -20 pA was achieved a gap-free recording protocol was used, with the command 0 channel changed to +40mV. Assuming that the isolated cardiomyocytes had a RMP of -70mV, holding at +40mV means that the patch of membrane would be held around -110mV. The SarCK_{ATP} channels containing the Kir6.2 subunit, have a single channel conductance of between 70 – 80pS, and so, the single channel current at this potential (-110mV) would be between 9 - 10pA. This current can then be used to identify opening of these channels. Once a stable relatively noise free current trace was achieved; perfusion was switched to SFT-MI and the single channel current recorded for later analysis. Traces were analysed by looking for bursts of activity which fitted the criteria of being >10 pA (which would be the current acquired when holding the patch at around -110mV) and ≥ 500 ms, as this duration would exclude any spontaneous burst of activity that can occur which have not been induced by metabolic inhibition (Brennan *et al.*, 2015). Figure 2.5 is an example of a current trace before and during SarCK_{ATP} channel opening.

2.5.3 Whole-cell configuration

An individual cardiomyocyte was only deemed acceptable for conversion into the whole-cell configuration, from the cell-attached configuration once a G Ω seal had been achieved, and the resulting traces remained stable after the holding potential had been changed from 0mV to -65mV. The whole-cell configuration was attained by applying further suction to the pipette following formation of a G Ω seal with a minimal leak current (\leq 30pA). An increase in the capacitance transients (see Figure 2.4D-E), which resulted from the charging and discharging of the entire sarcolemmal membrane was observed when the whole-cell configuration had been achieved. For the SarcK_{ATP} current recordings only, these increases in capacitance transients were adjusted using the whole-cell compensation on the Axopatch amplifier (whole-cell capacity compensation circuits). The membrane capacitance was measured by pClamp 10.3. Series resistance was not measured or compensated for in this study, as these experiments only involved clamping the cardiomyocytes at a constant holding potential of 0mV. Following adjustment a trace illustrated in Figure 2.4F had to be observed in order for the trace to be deemed recordable from. In all whole-cell experiments electrodes were filled with whole-cell intracellular pipette solutions (see section 2.7.3).

2.5.3.1 Action potential

Action potentials were recorded once in the whole-cell configuration, the amplifier mode was switched from voltage clamp (V-clamp) to current clamp (I clamp-normal). An action potential trigger protocol was applied and the individual cardiomyocyte was stimulated at a rate of 1 Hz via the electrode, with a 5ms depolarising pulse set to 130% of that required to trigger an action potential. Time to action potential failure, action potential duration to 90% repolarisation (APD₉₀) and resting membrane potential of each cardiomyocyte recorded was analysed later using pClamp 10.3.

2.5.3.2 SarcK_{ATP} current recordings

SarcK_{ATP} currents were recorded using the whole-cell configuration, with the cardiomyocyte voltage clamped at a holding potential of 0mV, which inactivates the

voltage gated ion channel. Holding at this potential also means that upon activation of the $\text{SarcK}_{\text{ATP}}$ channels, a larger outward K^+ current would be observed, as 0mV is 80mV away from E_{K} . The whole-cell capacitance, a measure of the cell size, was measured by pClamp 10.3 and the returned value was noted, on average this was $62.0 \pm 1.6\text{pF}$. The recorded currents would later be normalised to their given cell capacitance value (pA/pF) to allow for variation in cell size. As these experiments were held at a steady-state voltage of 0mV, series resistance compensation was not necessary. In addition, the time at which $\text{SarcK}_{\text{ATP}}$ activation was measured, the current amplitudes were still small, therefore any voltage drop due to series resistance should be minimal. Tyrode solution was perfused for a few minutes once recording began then switched to SFT-MI. An increase in the outward current observed during the period of metabolic inhibition (SFT-MI) indicated $\text{SarcK}_{\text{ATP}}$ channel opening. The steady-state outward current measured prior to SFT-MI, which is composed of any outward K^+ current and the leak current was on average $259.6 \pm 10.6\text{pA}$. Therefore traces were analysed to identify the time at which the outward current had increased by 20pA during SFT-MI, as an increase in current by this amount would be detectable against the steady-state outward current measured prior to SFT-MI. The time at which the outward current had increased by 20pA was recorded as the time $\text{SarcK}_{\text{ATP}}$ channels opened, as indicated in Figure 2.6.

2.5.4 Analysis of electrophysiology recordings

All electrophysiology experiments were analysed in pClamp 10.3. All recordings were analysed from the time SFT-MI solution reached the perfusion chamber.

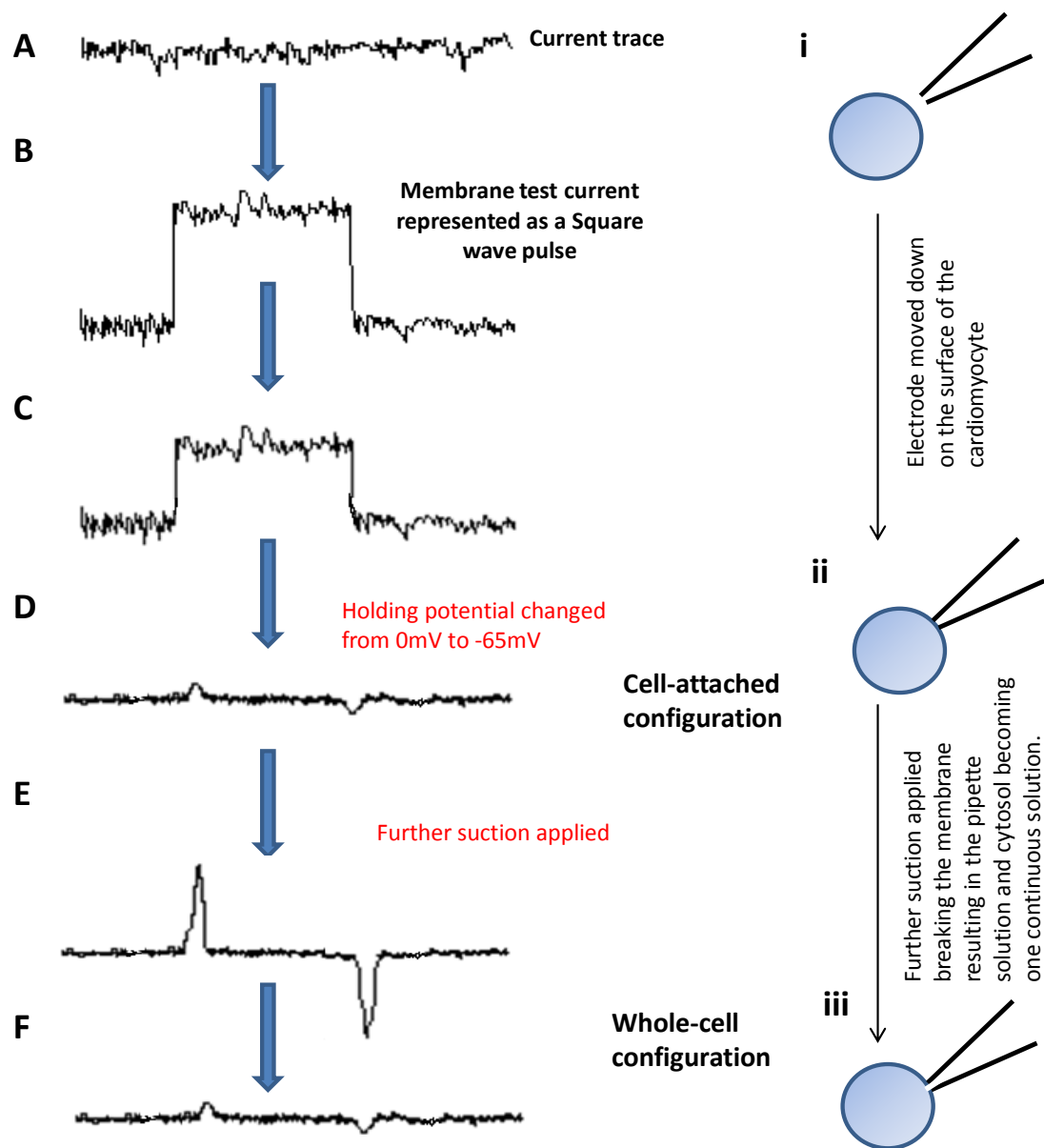


Figure 2.4 Electrophysiology traces

(A) Current trace that appears once the electrode enters the bath (i). Holding potential at 0mV. (B) Membrane test current that appears as the electrode tip gets closer to the membrane, as seen the electrode current decreases in size as the electrode resistance increases (B to C). (D) Suction then applied to the membrane via a syringe to achieve a Gigaohm ($G\Omega$) seal and the holding potential changed from 0mV to -65mV (to aid $G\Omega$ seal development) resulting in capacitance transients. This gives the cell-attached configuration. (E) Further suction is applied to the electrode (iii), this causes an increase in capacitance transients which are adjusted by the whole-cell parameters circuits on the amplifier, resulting in (F), the whole-cell configuration used for recording.

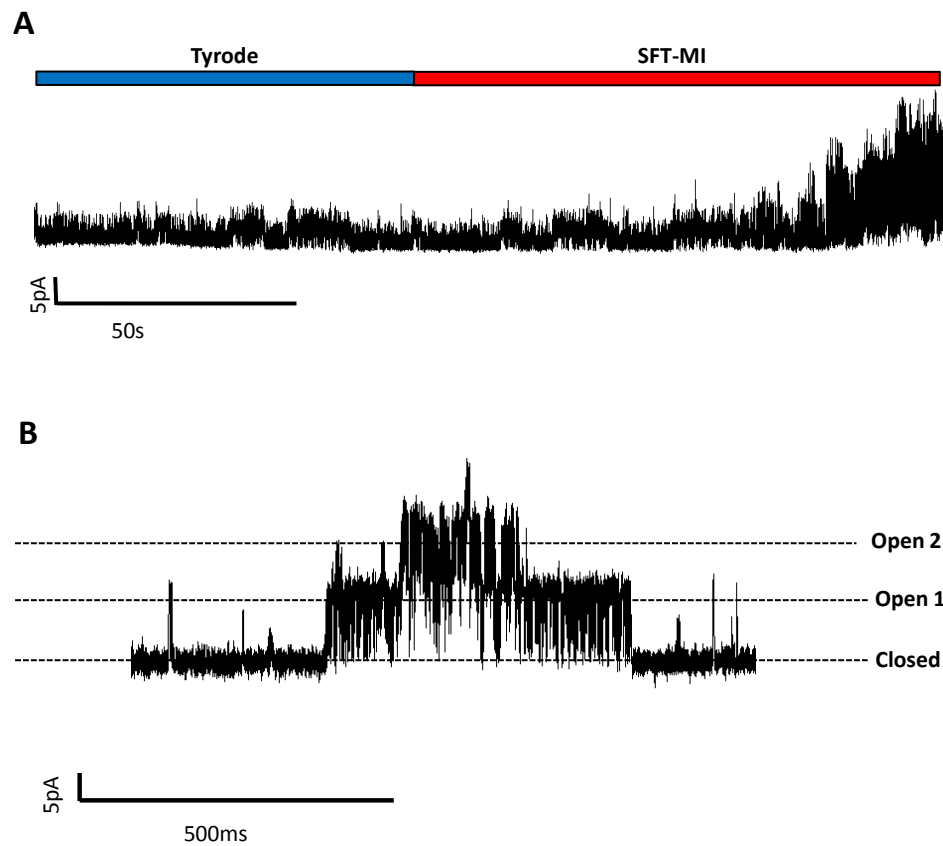


Figure 2.5 Cell-attached traces representing SarcK_{ATP} opening

(**A**) A representation of a full SarcK_{ATP} trace recorded in the cell-attached configuration. (**B**) A region of the trace in (A) representing an example of SarcK_{ATP} opening at ≥ 500 ms with a current >10 pA, as indicated by the outward current (upward reflections). This channel opening involves 2 channels as represented by the 2 stage opening.

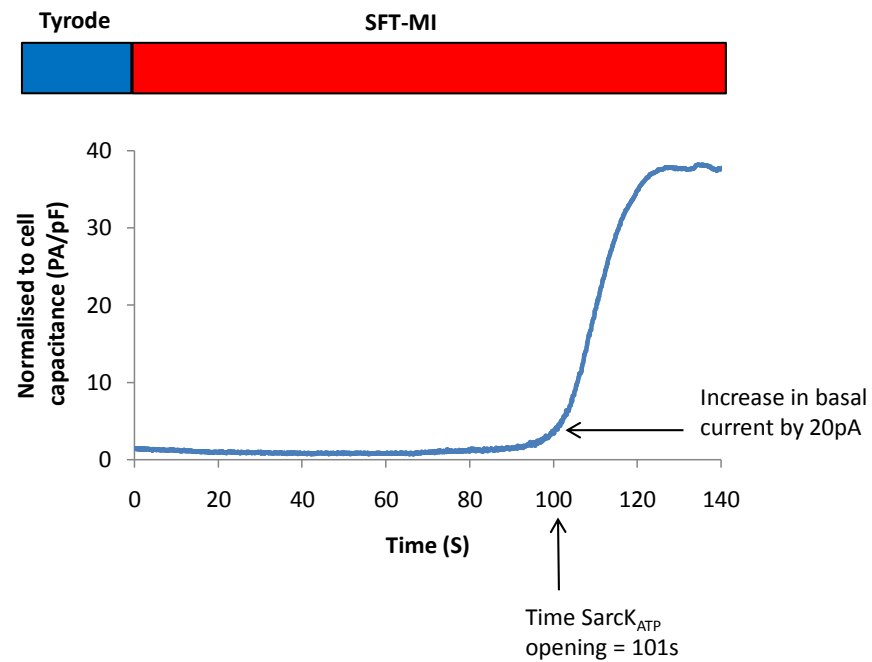


Figure 2.6 Whole-cell trace representing $\text{SarcK}_{\text{ATP}}$ opening

A representative trace of a whole-cell $\text{SarcK}_{\text{ATP}}$ recording in 5mM glucose normalised to cell capacitance (pA/pF). Opening of $\text{SarcK}_{\text{ATP}}$ was identified by an increase in outward current during SFT-MI and specifically by an increase in basal current by 20pA, as indicated on the graph. The protocol above the trace represents the analysis starting from the point SFT-MI entered the perfusion chamber.

2.6 Fluorescence Imaging

Two molecular acetoxymethyl ester (AM) probes; Fura-2-AM and Magnesium Green AM, were used in this study to investigate changes in intracellular calcium and magnesium (as a surrogate marker of intracellular ATP) respectively.

2.6.1 Fluorescence imaging preparation

Each fluorescent indicator was stored as a 1mM stock in Dimethyl Sulfoxide (DMSO) at -20°C. 1 ml of cardiomyocyte suspension (cardiomyocytes and Tyrode solution) was incubated with 4µl of the fluorescent indicator (either Fura-2-AM or Magnesium Green-AM) to give a final concentration of 4µM of AM-indicator. Both indicators are in an acetoxymethyl (AM) ester form (Fura-2-AM and Magnesium Green-AM). AM allows the dye to cross the cardiomyocyte sarcolemmal membrane, once inside esterases cleave off the AM ester group leaving behind either free Fura-2 or free Magnesium Green (Mg^{2+} -Green). The suspension was gently agitated on a rocking platform for 10 minutes wrapped in foil to prevent photo bleaching of the indicator. The contents of the eppendorf then transferred to a glass coverslip; and the experiments set up as described in sections 2.2/2.3. Fields of view were selected using a X 20 objective and measured using a video imaging system (PTI). A deltarax high speed random access monochromator (controlled by EasyRatioPro software) was used to excite the fluorophore at specific wavelengths (see 2.6.2 and 2.6.3) appropriate for the indicator, via a fibre optic cable attached to the microscope. Fluorescence images of the cardiomyocytes within the field of view were captured using a Roper Cascade camera (CCD camera) (see Figure 2.7). Changes in fluorescence for each experiment were recorded using EasyRatioPro software (PTI).

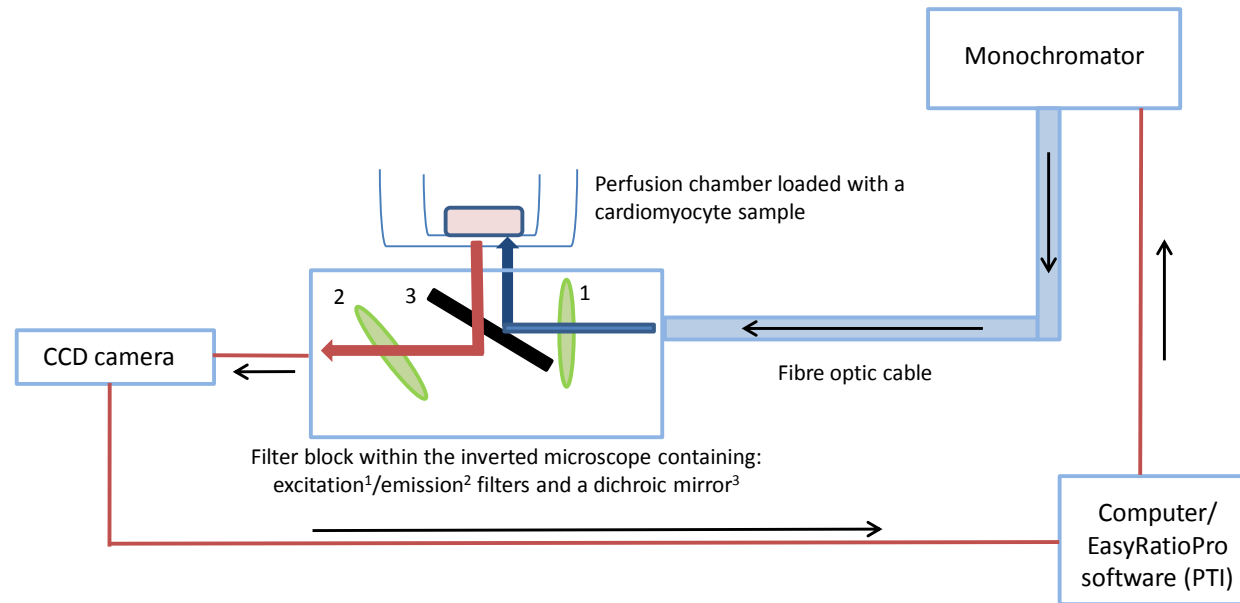


Figure 2.7 Fluorescence imaging set up

A monochromator (controlled by the computer) excites cardiomyocytes loaded with the fluorescent indicator (either Fura-2 or Mg^{2+} -green) via a fibre optic cable attached to the microscope. Within the microscope is a filter block, which contains a series of excitation and emission filters and a dichroic mirror. The correct filters for each fluorescent indicator, regulate the wavelengths allowed to pass through the cardiomyocytes in the field of view and the dichroic mirror allow specific excitation light (blue arrow) and emission light (red arrow) through, depending on the wavelength selected. The emitted light (emissions) from the cardiomyocytes in the field of view are then captured by a CCD camera, which passes the signal back to the EasyRatioPro software (PTI). Red lines indicate electrical connections and blue line indicate light pathways.

2.6.2 Intracellular calcium measurements using Fura- 2-AM

Fura-2 is a ratiometric, cell-permeable calcium chelating fluorescent indicator. This dual excitation indicator fluoresces on excitation at 340nm when bound to Ca^{2+} and at 380nm when Ca^{2+} is unbound. Once excited, irrespective of the excitation wavelength, Fura-2 emits light that can be collected at $>520\text{nm}$. The intensity of emitted light at 520nm can then be expressed as a ratio of the excitation light (340:380nm). Therefore as $[\text{Ca}^{2+}]_i$ increases the emitted fluorescence from Fura-2 in response to 340nm increases but shows a decreased response to 380nm, resulting in an increased 340:380nm ratio. Cardiomyocytes loaded with Fura-2 were alternately excited at wavelengths of 340nm and 380nm at a rate of 16 ratio images per second. Exposing the cardiomyocytes to these wavelengths meant every 3 seconds a ratio of 340:380nm was acquired for the majority of the protocol. However at the beginning and end of the each experiment fast recordings (no gaps in exposure time) were selected to capture calcium transients. Throughout the metabolic inhibition and re-energisation protocol, the cardiomyocytes were stimulated to contract via EFS, this allowed changes in intracellular calcium ($[\text{Ca}^{2+}]_i$) to occur. The Fura-2 ratio could then be used to determine the changes in $[\text{Ca}^{2+}]_i$ throughout the metabolic inhibition and re-energisation protocol.

2.6.2.1 Analysis of calcium data

Tif files for the calcium imaging data were downloaded from the EasyRatioPro software and transferred to Win Fluor 3.6.9 (University of Strathclyde, Dr. John Dempster), in which regions of interest (ROI) were drawn around cardiomyocytes. The resulting 340nm and 380nm signals were transferred to Microsoft Excel (2010) and 340:380nm ratios calculated. Time courses from changes in the Fura-2 ratio were created (see Figure 2.8), cardiomyocytes not displaying Ca^{2+} transients in synchrony with EFS at the start of the recording were excluded from the analysis. Three time points of interest were investigated; 180s (basal); 600s (end of MI), and 1200s (end of re-energisation), 10 data points before each of these times were averaged to give a mean Fura-2 ratio during diastole for that time point. Therefore changes in $[\text{Ca}^{2+}]_i$ throughout the metabolic inhibition and re-energisation protocol could be observed.

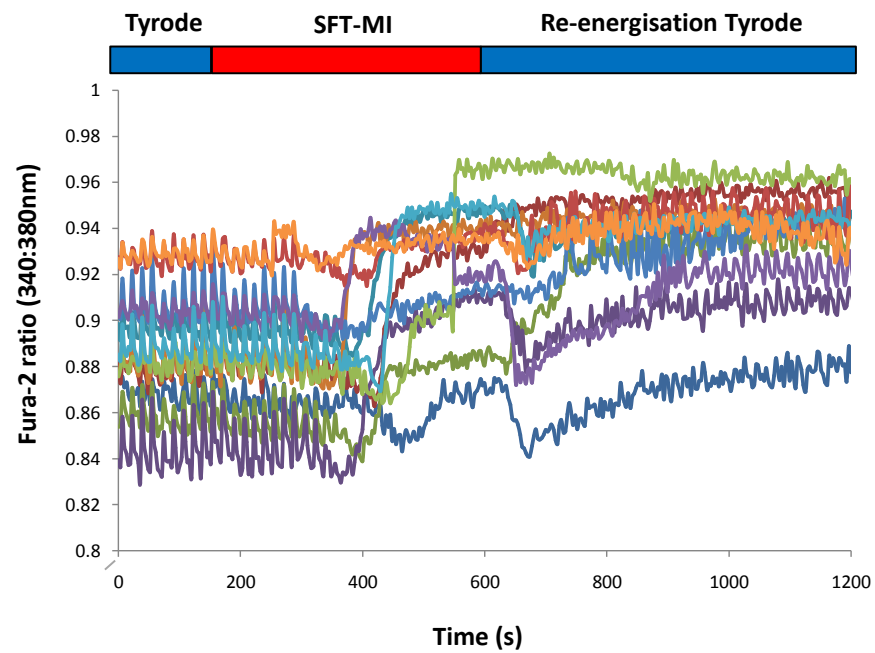


Figure 2.8 Calcium analysis using Win Fluor 3.6.9

Trace recordings of the Fura-2 ratio from cardiomyocytes perfused with 5mM glucose. Alternately exciting at 340nm and 380nm allowed for a Fura-2 ratio (340:380nm) to be obtained throughout the metabolic inhibition and re-energisation protocol.

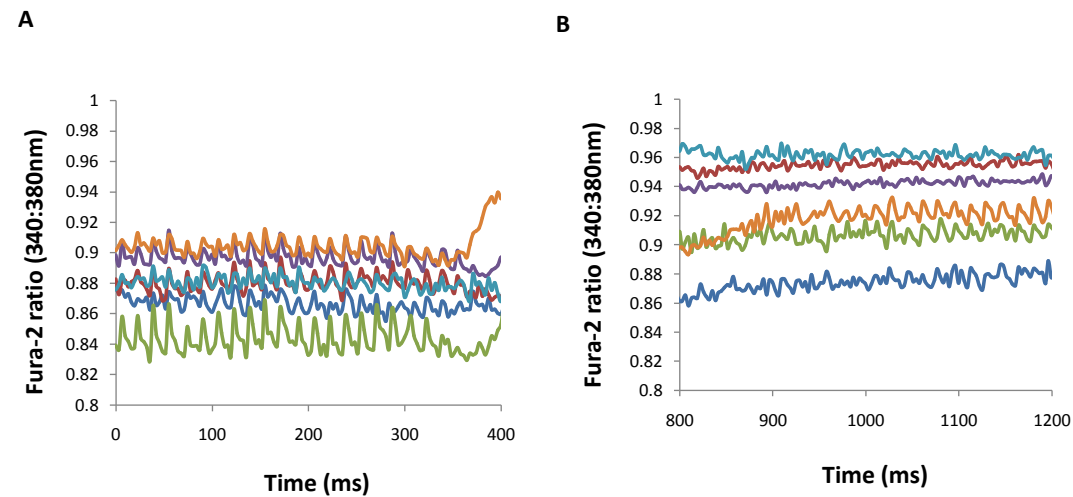


Figure 2.9 Contractile recovery using calcium transients

- (A) Example of six traces at the start of the MI/R protocol, taken from the previous time course shown in Figure 2.8. All six were contracting in time to EFS as indicated by the calcium transients. The individual calcium transients were captured by decreasing the exposure time from 3 to 0 seconds and increasing the sampling rate.
- (B) Example of calcium traces from the same 6 cardiomyocytes as in (A) taken towards the end of re-energisation, to assess if calcium transients had recovered in time with EFS at 1Hz or not, or if asynchronous calcium transients had developed. Those cardiomyocytes exhibiting a lower Fura-2 ratio can be seen to have recovered synchronous calcium transients (blue, green and orange traces). While those cardiomyocytes with a higher Fura-2 ratio exhibited an absence of calcium transients (red and purple traces) or asynchronous calcium transients (blue trace).

Analysis of the fast recordings taken prior to 180s and 1200s enabled the presence or absence of Ca^{2+} transients to be observed. The diastolic Fura-2 ratios during the Ca^{2+} transients were also analysed. Cardiomyocytes ability to regain contractile function was observed by looking at the fast transients recorded at the beginning and end of each experiment see Figure 2.9 and results.

2.6.3 Intracellular magnesium measurements using Magnesium Green-AM

Magnesium Green (Mg^{2+} -Green) was excited at a wavelength of 480nm. Cardiomyocytes were exposed to this wavelength of light every 3 seconds, throughout the metabolic inhibition and re-energisation protocol. The wavelength of light emitted by Mg^{2+} -Green was measured at 520nm. Increases in fluorescence emission intensity occur with increases in free magnesium concentrations. The majority of intracellular magnesium is bound to ATP molecules within cardiomyocytes, when ATP is hydrolysed magnesium is free within the cytosol and can bind to the indicator, leading to the increase in fluorescence emission intensity (Leyssens *et al.*, 1996). Therefore when ATP levels are high, magnesium binds to ATP rather than the indicator. This indicator can then be used to give a qualitative indication for changes in ATP levels within the cardiomyocytes during the experiment.

2.6.3.1 Analysis of Magnesium Green data

Mg^{2+} -Green image files were exported from the EasyRatioPro software into Microsoft excel (2010). Data was normalised to the Basal Fluorescence (F_0) determined at the start of each experiment and plotted as the ratio F/F_0 . Two time points were selected: 600s (end of MI) and 1200s (end of reperfusion). Each was then normalised to the fluorescence intensity recorded at the end of the stabilization phase following superfusion with Tyrode solution for 180s (F_0). A representative time course for each experiment was produced. This allowed for changes in intracellular magnesium (as a surrogate of ATP) to be observed throughout the metabolic inhibition and re-energisation protocol. These changes were used as a marker for the change in ATP, as ATP depletion is expected during metabolic inhibition, while ATP replenishment is known to occur during re-energisation.

2.7 Solutions

2.7.1 Solutions for isolation of adult rat cardiomyocytes

Nominally calcium-free Tyrode solution (Zero Ca²⁺ Tyrode) (mM): NaCl 135, KCl 5, NaH₂PO₄ 0.33, Na Pyruvate 5, Glucose 10, Hepes 10, and MgCl₂ 1.

2mM Calcium Tyrode solution (2Ca²⁺ Tyrode) (mM): NaCl 135, KCl 5, NaH₂PO₄ 0.33, Na Pyruvate 5, Glucose 10, Hepes 10, MgCl₂ 1 and CaCl₂ 2.

Both solutions were titrated to pH7.4 with NaOH.

Enzyme solution: 20mg Protease (type XIV from *Streptomyces griseus*), 30mg Collagenase (type I from *Clostridium histolyticum*) and 50mg Bovine Serum Albumin (BSA) (prepared from factor V albumin) dissolved in 30ml of Zero Ca²⁺ Tyrode solution.

2.7.2 Solutions for Tyrode and Substrate Free Tyrode (SFT)

Table 2.1 shows the standard composition of the Tyrode and SFT solutions used. Tyrode solution with 5mM glucose was used as the control for all experiments. For specific metabolic substrate (i.e. glucose/fructose/pyruvate) concentrations and combinations used see results.

2.7.2.1 Substrate Free Tyrode – Metabolic Inhibition (SFT-MI)

SFT-MI used in all experiments was made by adding the metabolic inhibitors IAA (1mM) and NaCN (2mM) to SFT.

2.7.2.2 Osmotically balanced experimental Tyrode solutions

Table 2.2 A, B and C illustrates the concentrations of glucose and fructose used in experimental solutions, when investigating the effects of acute changes in these on isolated cardiomyocytes. All glucose and fructose solutions (except the glucose concentrations of 20, 30 and 40mM and the fructose preconditioning solutions) were osmotically balanced with mannitol. The preconditioning fructose contractile function solution, although not balanced with mannitol had a total sugar concentration of 20mM. Therefore all experimental solutions had a total sugar concentration, which

was balanced in SFT with the same concentration of sucrose. Tyrode solution containing 5mM pyruvate (Table 2.1A) with 5mM glucose/15mM Mannitol (Table 2.2A) was used as the control solution in many experiments.

2.7.2.3 Solutions used to investigate the effects of pyruvate and fatty acids

Table 2.3 shows the experimental solutions where either the sodium pyruvate (Na Pyruvate) and/or the fatty acid sodium octanoate (Na Octanoate) concentrations were varied. Changes in Na Pyruvate and Na Octanoate were compensated by altering the NaCl concentration in order to maintain the Na concentration.

2.7.3 Intracellular pipette solutions for electrophysiology experiments

Table 2.4A, B and C shows the intracellular pipette solutions used for whole-cell recordings of action potentials and voltage clamp recordings of whole-cell $\text{SarCK}_{\text{ATP}}$ currents, and cell-attached recordings of single $\text{SarCK}_{\text{ATP}}$ channel.

2.8 Materials

Laboratory reagents were obtained from Sigma-Aldrich and Fisher Scientific UK LTD. The fluorescent indicators Fura-2-AM (catalog number F-1221) and Magnesium Green-AM (catalog number M-3735) were obtained from Invitrogen (Life technologies).

2.9 Analysis and statistics

All data was analysed using Microsoft excel (2010) and GraphPad Prism 6. Data is presented as mean \pm SEM. Data in chapter 4 has been normalised to control data to allow comparison between data sets which were not recorded on the same day. Statistical significance was analysed using unpaired T-test (for two groups) or one-way ANOVA with Fisher's post-hoc test (for multiple comparisons versus control). Repeated measures were selected where appropriate. A P-value of $P < 0.05$ was classed as statistically significant. Contractile function and fluorescence imaging data are represented as N= number of hearts, number of fields of view, number of cardiomyocytes. Electrophysiology data are represented as N= number of hearts, number of cardiomyocytes/experiments.

A

Tyrode	
Reagent	mM
NaCl	135
KCl	5
NaH ₂ PO ₄	0.33
Na Pyruvate	5
Hepes	10
CaCl ₂	2
MgCl ₂	1

B

SFT	
Reagent	mM
NaCl	140
KCl	5
NaH ₂ PO ₄	0.33
Hepes	10
CaCl ₂	2
MgCl ₂	1
Sucrose	20*

Table 2.1 Standard Tyrode and SFT solutions

(A) The composition of the standard 5mM pyruvate Tyrode solution.

(B) The composition of the SFT solution used in most experiments.

*The sucrose concentration in SFT changed depending on the total sugar concentration used in the experimental solutions see section 2.8.2.2/ Table 2.4A, B and C.

All solutions were pH to 7.4 with NaOH.

A

Variable Glucose solutions		SFT solution
Glucose (mM)	Mannitol (mM)	Sucrose (mM)
0	20	20
2	18	20
5	15	20
10	10	20
15	5	20
20	0	20
30	0	30
40	0	40

B

Variable Fructose solutions		SFT solution
Fructose (mM)	Mannitol (mM)	Sucrose (mM)
5	15	20
20	0	20

C

Fructose preconditioning Tyrode solution		SFT solution
Fructose (mM)	Glucose (mM)	Sucrose (mM)
15	5	20

Table 2.2 The osmotically balanced Tyrode solutions

- (A) The variable glucose concentrations used and the corresponding mannitol concentrations. The total sugar concentration for each glucose/mannitol set was matched by sucrose in the SFT.
- (B) The variable fructose concentrations used and corresponding mannitol concentrations. The total sugar concentration for each fructose/mannitol set was matched by sucrose in the SFT.
- (C) The fructose preconditioning Tyrode solution and its corresponding SFT sucrose concentrations.

	0.5mM Pyruvate	10mM Pyruvate	Fatty acid (0.5mM) + 0mM Pyruvate	Fatty acid (0.5mM) + 5mM Pyruvate
Reagent	mM	mM	mM	mM
NaCl	139.5	130	139.5	134.5
KCl	5	5	5	5
NaH ₂ PO ₄	0.33	0.33	0.33	0.33
Na Pyruvate	0.5	10	0	5
Na Octanoate	-	-	0.5	0.5
Hepes	10	10	10	10
CaCl ₂	2	2	2	2
MgCl ₂	1	1	1	1

Table 2.3 Tyrode solutions for the varied pyruvate and octanoate experiments.

The composition of the Tyrode solutions used in the varying pyruvate and octanoate experiments. All solutions were pH to 7.4 with NaOH.

A

Whole-cell solution for action potentials recordings	
Reagent	(mM)
KOH	30
KCl	110
EGTA	5
Hepes	10
ATP(Mg)	1
ADP(Na)	0.1
GTP	0.1
CaCl ₂ (20nM free)	0.61
MgCl ₂	1

B

Whole-cell solution for SarcK _{ATP} recordings	
Reagent	(mM)
KOH	30
KCl	110
EGTA	10
Hepes	10
ATP(Mg)	1
ADP(Na)	0.1
GTP	0.1
MgCl ₂	1

C

Cell-attached solution for SarcK _{ATP} recordings	
Reagent	(mM)
KCl	140
Hepes	10
CaCl ₂	1
MgCl ₂	0.5

Table 2.4 The intracellular pipette solutions

- (A) The composition of the intracellular pipette solution used in the whole-cell action potential electrophysiology experiments.
- (B) The composition of the intracellular pipette solution used in the whole-cell SarcK_{ATP} electrophysiology experiments.
- (C) The composition of the intracellular pipette solution used in the cell-attached SarcK_{ATP} electrophysiology experiments.
- All were pH to 7.2 with KOH.

CHAPTER 3

The role of glycolytic metabolism in isolated cardiomyocytes subjected to metabolic inhibition and re-energisation

3. The role of glycolytic metabolism in isolated cardiomyocytes subjected to metabolic inhibition and re-energisation

3.1 Introduction

As described in the introduction, under normal physiological conditions, the myocardium generates 95% of its ATP from oxidative phosphorylation, with fatty acid metabolism contributing 60-90% of the acetyl-CoA required for this and the remaining 10-40% coming from oxidation of pyruvate (which has been formed by glycolysis and lactate oxidation) (Stanley *et al.*, 2005). The remaining 5% of ATP generated for the myocardium comes from substrate level phosphorylation (i.e. glycolysis and GTP formation). However the myocardium can shift its reliance on substrates depending on availability and metabolic demand (Heather & Clarke, 2011). For example during ischaemic conditions, the myocardium switches solely to anaerobic glycolytic metabolism in an effort to maintain ATP synthesis (Kalra & Roy, 2011), however this yields lower quantities of ATP (2 ATP molecules per glucose or fructose molecule).

Anaerobic glycolytic metabolism during times of ischaemia has been postulated to be important to the myocardium, with numerous studies (as described in section 1.12) showing glucose to be cardioprotective when administered prior to, during and after a period of ischaemia (Bricknell & Opie, 1978; Vanoverschelde *et al.*, 1994; Wang *et al.*, 2005; Owen *et al.*, 1990; Jeremy *et al.*, 1993). However it should be noted, that the blood glucose concentration of an individual presenting with an AMI, and in particular persistent hyperglycaemia during an AMI, have strong associations with an adverse prognosis in a clinical setting (Squire *et al.*, 2009; Kosiborod *et al.*, 2008).

As these previous studies were carried out in the whole heart, the aim of this study was to investigate whether the same cardioprotection could be achieved in isolated cardiomyocytes and therefore what impact glycolytic substrates have at cellular level, and as a result the possible cellular mechanisms involved. Therefore the effects on isolated ventricle cardiomyocytes of elevating glycolytic metabolic substrates prior to simulated ischaemia and during reperfusion were investigated. This was achieved using a well-established method of metabolic inhibition to simulate ischaemia, whilst

reperfusion was simulated by re-energisation of the mitochondria. This was achieved by the removal of metabolic inhibitors and the re-supply of the metabolic substrates pyruvate and glucose, as described in the methods (Eisner *et al.*, 1989; Lawrence *et al.*, 2001; Rainbow *et al.*, 2004; Rodrigo & Samani, 2008). The technique of chemically inducing ischaemia in isolated cardiomyocytes was chosen for this study, as unlike ischaemic pelleting of isolated cardiomyocytes (Vander Heide *et al.*, 1990) it facilitates measurements of contractile function (i.e. electrical induced contractions, ischaemic contracture and reperfusion induced hypercontracture) throughout the simulated ischaemia and re-energisation protocol. This method also allows for $[Ca^{2+}]_i$ to be measured and ATP levels within living cells to be monitored by fluorescence microscopy. In addition electrophysiological techniques can be used to investigate specific ion channels associated with metabolic status (i.e. $SarCK_{ATP}$), that can act as markers of cell injury and oxidative stress and therefore provide an insight into cellular damage.

As the mean blood glucose of rats has been calculated to be 5.2mM (from a range of 2.8-7.5mM) (Johnson-Delaney, 2008), 5mM glucose has been used throughout this experimental set as the control glucose concentration (normoglycaemic conditions). Throughout the thesis glucose concentrations below 5mM have been described as hypoglycaemic, while glycolytic metabolic substrate concentrations above 5mM have been described as elevated extracellular glucose/fructose and in the case of glucose act as a surrogate for acute hyperglycaemia.

The results in this chapter will demonstrate the cardioprotective actions of elevated concentrations of glycolytic metabolic substrates, to isolated cardiomyocytes prior to metabolic inhibition and during re-energisation.

3.2 Results

3.2.1 The effects of acute changes in extracellular glucose on the contractile function of isolated cardiomyocytes during metabolic inhibition and re-energisation

To determine the effects of acute changes in extracellular glucose on contractile function during metabolic inhibition and on re-energisation, isolated cardiomyocytes

were incubated for 10 minutes in Tyrode containing the experimental glucose concentration (2-40mM) and 5mM pyruvate (the primary available metabolic substrate able to generate ATP via oxidative phosphorylation). Cardiomyocytes were then stimulated to contract at 1Hz by EFS, and perfused with Tyrode containing glucose (2-40mM) and 5mM pyruvate for 3 minutes. To simulate ischaemia cardiomyocytes were then perfused with SFT-MI for 7 minutes and to simulate reperfusion, cardiomyocytes were re-energised by perfusion with Tyrode containing glucose (2-40mM) and 5mM pyruvate for 10 minutes (protocol is outlined in Figure 3.1). The time to contractile failure and rigor contracture from the onset of metabolic inhibition were measured as markers of ischaemic injury. As markers of protection against re-energisation injury, the percentage of cardiomyocytes in a non-hypercontracted state (i.e. those that had relaxed from hypercontracture or not entered hypercontracture) and the percentage regaining contractile function (in response to EFS) after 10 minutes of re-energisation, were measured. To ensure the effects were due to changes in glycolytic metabolism rather than an effect of osmolarity, all Tyrode solutions $\leq 15\text{mM}$ were osmotically balanced with mannitol, so that the final total sugar concentration in all Tyrode solutions (2-20mM) was 20mM. Tyrode solutions of 30mM and 40mM were not osmotically balanced with mannitol, however osmolarity between all Tyrode and SFT solutions in all data sets were osmotically balanced with sucrose (see section 2.7.2.2).

During SFT-MI isolated cardiomyocytes lose the ability to contract in time with EFS (contractile failure). After the cardiomyocytes develop contractile failure, they develop a sustained rigor-like contracture, indicated by a progressive shortening of the cell length by $\geq 60\%$. Following the metabolic inhibition period, cardiomyocytes were re-energised by the removal of the metabolic inhibition and the re-supply of the metabolic substrates (glucose and pyruvate), which re-energises the mitochondria leading to repolarisation of the mitochondria and re-establishes ATP production (Rodrigo & Standen, 2005). This can stimulate hypercontracture, with some cardiomyocytes undergoing irreversible contracture and others relaxing; of those that relax some cardiomyocytes can recover contractile activity in response to EFS. As an indicator of cardioprotection occurring during re-energisation, the percentage of

cardiomyocytes within a single field-of-view (>15 cardiomyocytes), that relaxed from hypercontracted and the percentage of cardiomyocytes that recovered contractile activity in response to EFS was determined.

Initially the effects of acute changes in extracellular glucose (2-30mM) prior to metabolic inhibition and during re-energisation were investigated. Figure 3.2A shows the time dependent effects of metabolic inhibition on contractile function in response to SFT-MI and the partial recovery of contractile function upon 10 minutes of re-energisation.

Acute increases in extracellular glucose from the normoglycaemic concentration (5mM glucose) to hyperglycaemic concentrations (10-30mM glucose), resulted in a graded increase in the time to contractile failure (Figure 3.2B), from $147.0 \pm 7.1s$ (5mM glucose) to $150.7 \pm 12.7s$ (10mM glucose, $P=0.77$), $158.6 \pm 4.0s$ (15mM glucose, $P=0.35$), $175.6 \pm 10.6s$ (20mM glucose, $P<0.05$) and $172.9 \pm 4.8s$ (30mM glucose, $P<0.05$). Acute hypoglycaemic conditions (2mM glucose) did not affect time to contractile failure compared to normoglycaemic conditions ($135.9 \pm 9.4s$, $P=0.37$).

Acute increases in extracellular glucose from the normoglycaemic concentration (5mM glucose), up to 20mM glucose, resulted in a concentration-dependent increase in the time to rigor (Figure 3.2C) from $247.9 \pm 15.3s$ (5mM glucose) to $271.9 \pm 14.9s$ (10mM glucose, $P=0.15$), $299.3 \pm 15.2s$ (15mM glucose, $P<0.01$) and $322.1 \pm 16.3s$ (20mM glucose, $P<0.0001$). The acute hyperglycaemic condition of 30mM glucose had no effect on the time to rigor compared to normoglycaemic conditions ($253.3 \pm 11.6s$, $P=0.74$). Acute hypoglycaemic conditions also had no effect on the time to rigor contracture compared to normoglycaemic conditions ($232.2 \pm 16.4s$, $P=0.34$).

During 10 minutes of re-energisation, acute increases in extracellular glucose from the normoglycaemic concentration (5mM glucose) up to 20mM glucose, resulted in a graded increase in the percentage of cardiomyocytes 'non-hypercontracted' (Figure 3.3A) from $78.2 \pm 4.3\%$ (5mM glucose), to $79.2 \pm 5.5\%$ (10mM glucose, $P=0.86$), $89.8 \pm 2.4\%$ (15mM glucose, $P=0.057$) and $94.4 \pm 2.4\%$ (20mM glucose, $P<0.01$). The acute hyperglycaemic conditions of 30mM glucose had no effect on the percentage of cardiomyocytes 'non-hypercontracted' compared to normoglycaemic conditions (78.6

$\pm 4.7\%$, $P=0.94$). Acute hypoglycaemic conditions did not affect the percentage of cardiomyocytes 'non-hypercontracted' compared to normoglycaemic conditions ($68.2 \pm 4.5\%$, $P=0.10$).

During re-energisation, acute hyperglycaemic conditions increased the percentage of cardiomyocytes regaining contractile function in response to EFS (Figure 3.3B) and this was glucose concentration dependent. Contractile function increased from $29.5 \pm 2.4\%$ (5mM glucose) to $45.1 \pm 0.9\%$ (10mM glucose, $P<0.01$), $54.9 \pm 1.6\%$ (15mM glucose, $P<0.001$), $58.4 \pm 4.1\%$ (20mM glucose, $P<0.0001$) and $63.5 \pm 6.5\%$ (30mM glucose, $P<0.0001$). Acute hypoglycaemic conditions did not affect contractile recovery compared to normoglycaemic conditions ($26.8 \pm 3\%$, $P=0.61$).

An experimental data set of 40mM glucose was carried out as the contractile recovery in Figure 3.3B had not reached a plateau. This concentration was found to be particularly damaging to the cardiomyocytes, as a high percentage appeared to have already entered hypercontracture prior to the start of the metabolic inhibition and re-energisation protocol. As a result of this cardiotoxicity further experiments were only carried out up to a maximum glucose concentration of 30mM.

Taken together, these data suggest that isolated cardiomyocytes subjected to acute hyperglycaemic conditions are able to maintain contractile function for longer during metabolic inhibition. In addition, in this model elevated glucose confers a degree of cardioprotection as demonstrated by the improvement in 'non-hypercontracted' cardiomyocytes and the increased contractile recovery.

Settling time



Figure 3.1 Metabolic inhibition and re-energisation protocol

Cardiomyocytes were initially settled for 10 minutes in Tyrode solution containing either glucose (0-40mM) or fructose (5 or 20mM) with 5mM pyruvate. Cardiomyocytes were then stimulated to contract at 1Hz by electrical field stimulation (EFS), while being perfused with Tyrode solution containing either glucose (0-40mM) or fructose (5 or 20mM) with 5mM pyruvate for 3 minutes. Metabolic inhibition was then induced by perfusing with substrate free-Tyrode containing iodoacetic acid (1mM) and sodium cyanide (2mM) (SFT-MI) for 7 minutes, followed by 10 minutes of re-energisation with Tyrode solution containing either glucose (0-40mM) or fructose (5 or 20mM) and 5mM pyruvate.

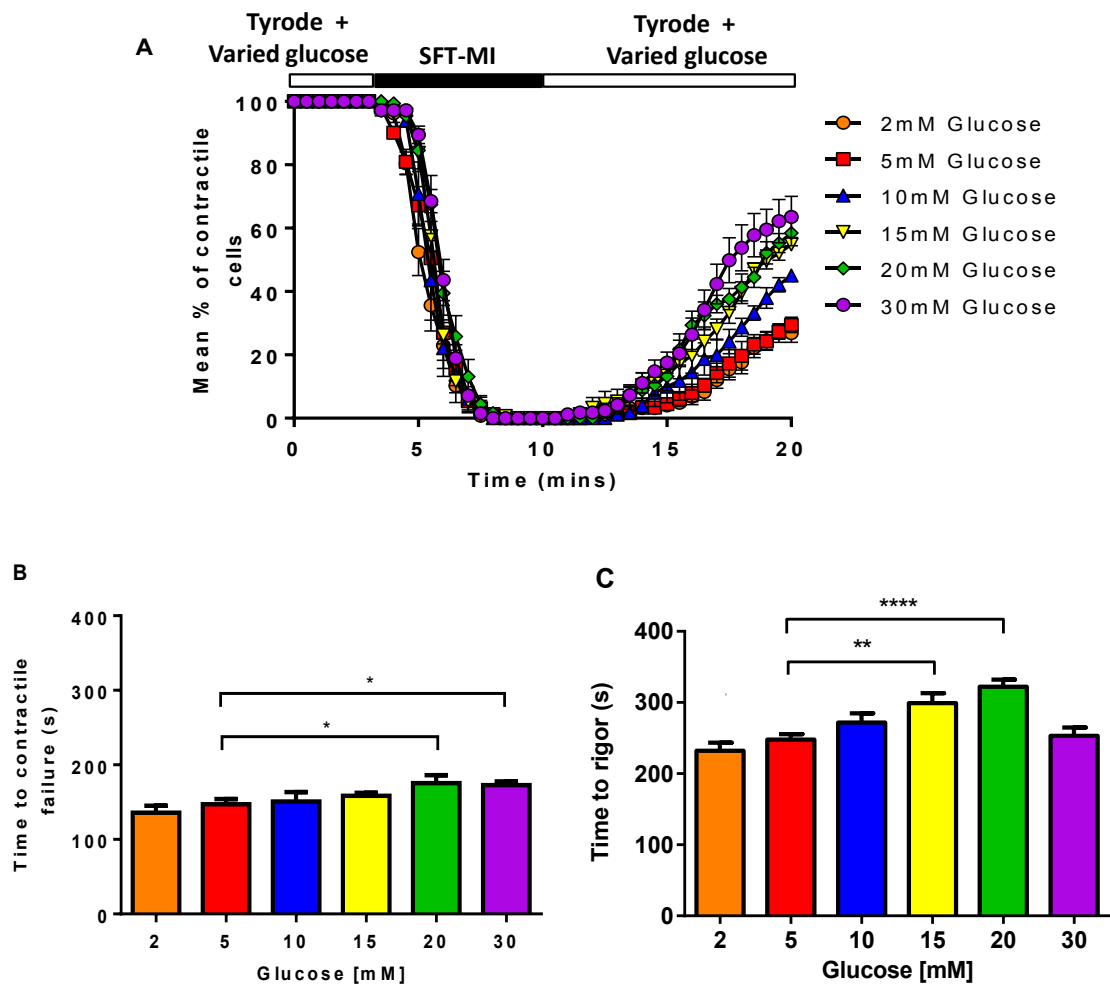


Figure 3.2 The effects of acute changes in extracellular glucose on the contractile function of isolated cardiomyocytes subjected to metabolic inhibition and re-energisation.

(A) Time course showing the percentage of cardiomyocytes contracting in response to EFS, during perfusion with SFT-MI and re-energisation. Prior to SFT-MI and during the 10 minutes of re-energisation cardiomyocytes were superfused with Tyrode solution containing glucose (2, 5, 10, 15, 20 or 30mM) with 5mM pyruvate.

(B) Time to contractile failure from the onset of metabolic inhibition for cardiomyocytes superfused with 2-30mM glucose and 5mM pyruvate.

(C) Time to rigor contracture from the onset of metabolic inhibition for cardiomyocytes superfused with 2-30mM glucose and 5mM pyruvate.

Data presented as mean \pm s.e.m. Data for 2mM glucose (orange bar, N=3 hearts, 6 fields of view, 158 cardiomyocytes), 5mM glucose (red bar, N=4, 6, 122), 10mM glucose (blue bar, N=4, 6, 116), 15mM glucose (yellow bar, N=4, 6, 142), 20mM glucose (green bar, N=5, 6, 153) and 30mM glucose (purple bar, N=3, 6, 178). *P<0.05, **P<0.01, ****P<0.0001 (one-way ANOVA with Fisher's post-hoc test).

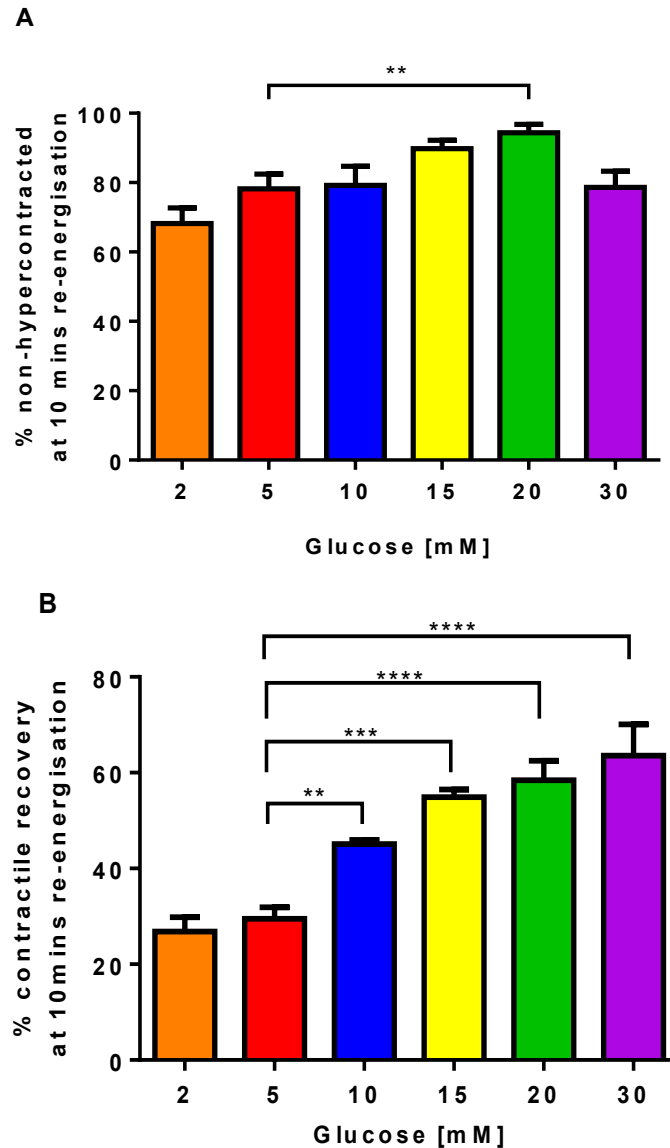


Figure 3.3 The effects of acute changes in extracellular glucose on recovery of isolated cardiomyocytes subjected to metabolic inhibition and re-energisatation.

(A) The percentage of ‘non-hypercontracted’ cardiomyocytes by the end of 10 minutes of re-energisatation for cardiomyocytes superfused with 2-30mM glucose and 5mM pyruvate.

(B) The percentage of cardiomyocytes regaining contractile function in response to EFS, by the end of 10 minutes of re-energisatation for cardiomyocytes superfused with 2-30mM glucose and 5mM pyruvate.

Data presented as mean \pm s.e.m. Data for 2mM glucose (orange bar, N=3 hearts, 6 fields of view, 158 cardiomyocytes), 5mM glucose (red bar, N=4, 6, 122), 10mM glucose (blue bar, N=4, 6, 116), 15mM glucose (yellow bar, N=4, 6, 142), 20mM glucose (green bar, N=5, 6, 153) and 30mM glucose (purple bar, N=3, 6, 178). **P<0.01, ***P<0.001, ****P<0.0001 (one-way ANOVA with Fisher’s post-hoc test).

3.2.2 The effect of elevated extracellular glucose on cardiac action potential behaviour

During metabolic inhibition, intracellular ATP depletes within isolated cardiomyocytes, this causes failure of electrical activity (action potential), which results in contractile failure. As acute increases in extracellular glucose concentrations caused a delay in contractile failure during metabolic inhibition, it was hypothesised this would be reflected in the time to action potential failure during metabolic inhibition. To investigate this, action potentials from isolated cardiomyocytes were recorded (using the whole-cell patch-clamp technique), in which the glucose concentration was acutely changed (2-30mM). Action potentials were stimulated at a rate of 1 Hz until a steady-state was reached and recorded continuously for 3-6 minutes prior to perfusion with SFT-MI solution and until the action potential failed.

Figure 3.4A shows action potentials recorded before and during perfusion with SFT-MI, selected to illustrate the changes that occur during metabolic inhibition, which concluded in complete failure of the stimulus to trigger an action potential in the cardiomyocyte.

Increasing extracellular glucose from the normoglycaemic concentration (5mM glucose) to hyperglycaemic glucose concentrations (10-30mM glucose), resulted in a graded increase in the time to action potential failure (Figure 3.4B) from $145.3 \pm 5.0s$ (5mM glucose) to $154.7 \pm 10.4s$ (10mM glucose, $P=0.36$), $164.1 \pm 7.3s$ (15mM glucose, $P=0.07$), $177.9 \pm 10.2s$ (20mM glucose, $P<0.01$) and $184.1 \pm 8.2s$ (30mM glucose, $P<0.001$). Acute hypoglycaemic conditions (2mM glucose) did not affect the time to action potential failure compared to normoglycaemic conditions ($128.4 \pm 7.7s$, $P=0.10$).

A comparison between the times to action potential failure and contractile failure shows a close correlation (Figure 3.4B), confirming that the time to contractile failure was likely to reflect loss of electrical activity. This was expected as contractile failure is thought to result from failure of the action potential due to opening of the $\text{SarcK}_{\text{ATP}}$ channels.

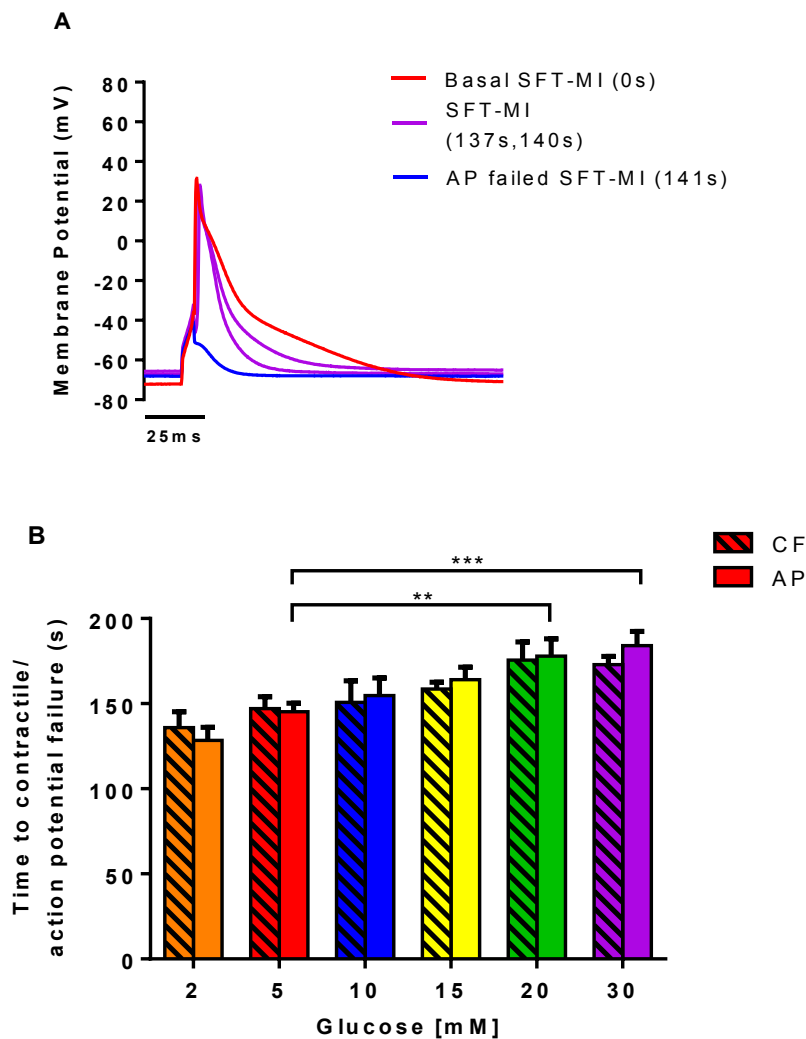


Figure 3.4 The effects of acute changes in extracellular glucose on the time to action potential failure during metabolic inhibition.

(A) Example traces of an action potential pre-incubated in 5mM glucose prior to metabolic inhibition, showing shortening and eventual failure of the action potential during metabolic inhibition.

(B) Time to action potential failure for cardiomyocytes superfused with 2-30mM glucose prior to metabolic inhibition, compared with time to contractile failure.

Data presented as mean \pm s.e.m. For (B) contractile failure (CF) data as described in from 3.2B. For action potential (AP) data, 2mM glucose (orange bar, N=7 hearts, 7 experiments/cardiomyocytes), 5mM glucose (red bar, N=5, 7), 10mM glucose (blue bar, N=6, 7), 15mM glucose (yellow bar, N= 4, 7), 20mM glucose (green bar, N=5, 7) and 30mM glucose (purple bar, N=3, 7). **P<0.01 and ***P<0.001 (one-way ANOVA with Fisher's post-hoc test).

Action potential duration to 90% repolarisation (APD₉₀) was also measured from these cardiomyocytes. The APD₉₀ was measured from 20 consecutive action potentials, once a steady-state had been reached and prior to SFT-MI. Acutely increasing extracellular glucose to hyperglycaemic concentrations (10-30mM glucose) had no effect on APD₉₀ (Figure 3.5A), compared to normoglycaemic conditions with 81.3 ± 8.3 ms (5mM glucose), versus 96.1 ± 12.2 ms (10mM glucose, $P=0.30$), 78.3 ± 8.6 ms (15mM glucose, $P=0.83$), 91.4 ± 14.4 ms (20mM glucose, $P=0.48$) and 65.7 ± 5.9 ms (30mM glucose, $P=0.28$). Acute hypoglycaemic conditions also did not affect the APD₉₀ compared to normoglycaemic conditions (93.0 ± 14.0 ms, $P=0.42$).

The resting membrane potential (RMP) was also measured from these 20 consecutive action potentials prior to SFT-MI for each glucose concentration. Acute increases in extracellular glucose from the normoglycaemic concentration (5mM glucose) to hyperglycaemic concentrations (10-30mM glucose), had no effect on the RMP (Figure 3.5B) with -69.1 ± 1.4 mV (5mM glucose), versus -68.0 ± 0.9 mV (10mM glucose, $P=0.60$), -68.0 ± 1.7 mV (15mM glucose, $P=0.59$), -69.3 ± 1.4 mV (20mM glucose, $P=0.92$) and -67.9 ± 1.1 mV (30mM glucose, $P=0.53$). Acute hypoglycaemic conditions significantly hyperpolarised the RMP compared to normoglycaemic conditions (-73.7 ± 1.4 ms, $P<0.05$).

These data suggest that acute exposure to elevated extracellular glucose delays the time to action potential failure in a concentration-dependent fashion, which corresponds to the previous findings of delayed contractile failure with elevated extracellular glucose (section 3.2.1). These data also suggest acute increases in extracellular glucose do not affect APD₉₀ or RMP, while acute hypoglycaemic conditions hyperpolarises the RMP.

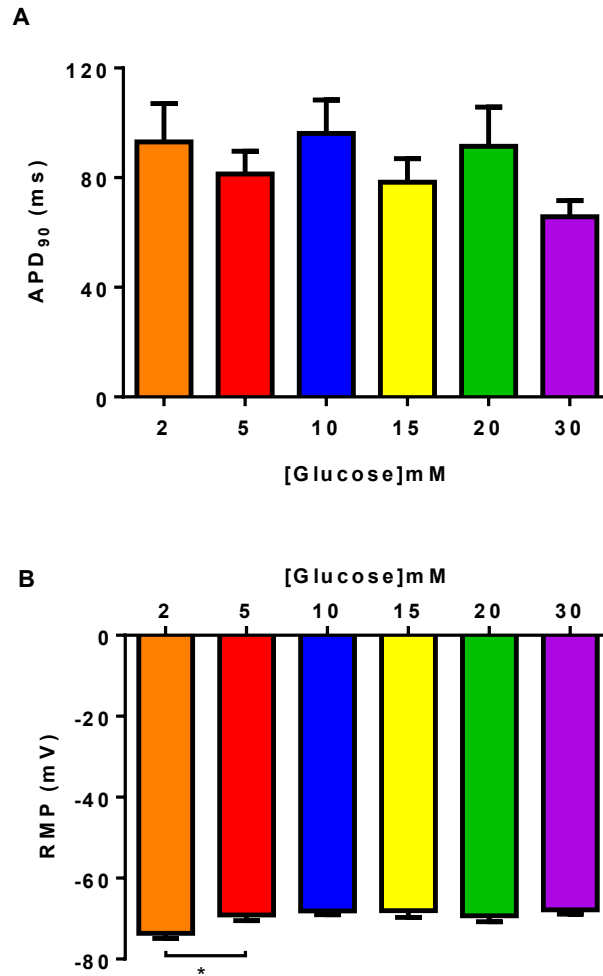


Figure 3.5 The effects of acute changes in extracellular glucose on the time to action potential duration to 90% repolarisation (APD₉₀) and resting membrane potential (RMP) prior to metabolic inhibition.

(A) Time to APD₉₀ for cardiomyocytes superfused with 2-30mM glucose prior to metabolic inhibition.

(B) The effect of 2-30mM glucose on the RMP prior to metabolic inhibition.

Data presented as mean \pm s.e.m. Data for 2mM glucose (orange bar, N=7 hearts, 7 experiments/ cardiomyocytes), 5mM glucose (red bar, N=5, 7), 10mM glucose (blue bar, N=6, 7), 15mM glucose (yellow bar, N= 4, 7), 20mM glucose (green bar, N=5, 7) and 30mM glucose (purple bar, N=3, 7). *P<0.05 (one-way ANOVA with Fisher's post-hoc test).

3.2.3 The effect of elevated extracellular glucose concentration on SarcK_{ATP} channel activity

During metabolic inhibition, activation of the SarcK_{ATP} channels causes an increase in potassium conductance which clamps the membrane potential close to E_k and causes the action potential to fail (Lederer *et al.*, 1989). As both the time to contractile and action potential failure were delayed in those isolated cardiomyocytes exposed to elevated extracellular glucose concentrations, it was hypothesised that SarcK_{ATP} channel activation in isolated cardiomyocytes may also be affected by perfusion with elevated extracellular glucose.

The activity of SarcK_{ATP} channels in cardiomyocytes was investigated using a patch clamp technique. Cardiomyocytes in the whole-cell configuration were superfused with a single glucose concentration (between 2-30mM) for between 3-6 minutes prior to SFT-MI. To record the SarcK_{ATP} channel activity, cardiomyocytes were clamped at a holding potential of 0mV to inactivate voltage gated ion channels (Na^+ , Ca^{2+} and K^+) and superfused with SFT-MI. Time to the SarcK_{ATP} activation was measured from these continuous recording, by measuring the point at which the outward current had increased by 20pA, as an increase in current by 20pA would be detectable against the steady-state outward current measured prior to SFT-MI.

Figure 3.6A shows representative traces of membrane current recorded from a single cardiomyocyte perfused under normoglycaemic (5mM glucose) or hyperglycaemic conditions (20mM glucose), prior to perfusion with SFT-MI, the development of an outward current during perfusion with SFT-MI indicating opening of SarcK_{ATP} channels. Acute increases in extracellular glucose from normoglycaemic (5mM glucose) to hyperglycaemic concentrations (10-30mM glucose) resulted in a concentration-dependent increase in the time to SarcK_{ATP} channel activation (Figure 3.6B) from $101.0 \pm 6.2s$ (5mM glucose) to $109.0 \pm 11.9s$ (10mM glucose, $P=0.57$), $118.3 \pm 7.2s$ (15mM glucose, $P=0.23$), $142.5 \pm 13.89s$ (20mM glucose, $P<0.01$) and $142.8 \pm 10.5s$ (30mM glucose, $P<0.01$). Reducing extracellular glucose to a hypoglycaemic concentration (2mM glucose) had no affect on the time to SarcK_{ATP} channel activation compared to normoglycaemic conditions ($79.25 \pm 13.5s$ $P=0.10$).

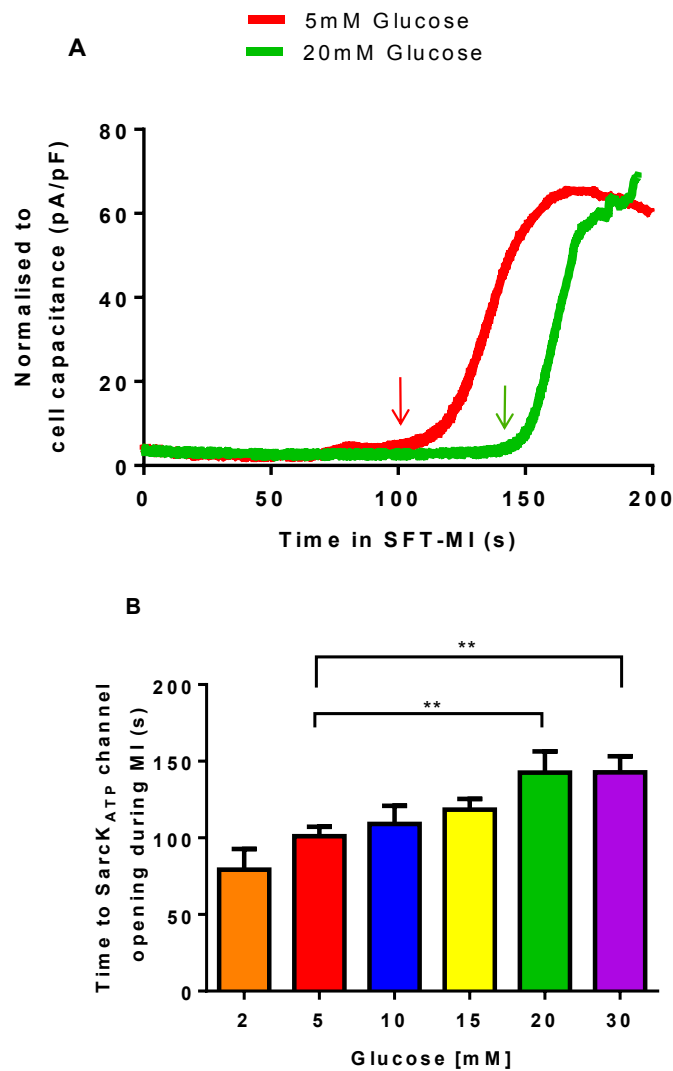


Figure 3.6 The effects of acute changes in extracellular glucose on SarcK_{ATP} current activation during metabolic inhibition.

(A) Example traces of whole cell SarcK_{ATP} channel current recorded from a single cardiomyocyte pre-incubated in either 5mM or 20mM glucose as indicated, and subject to metabolic inhibition. Each trace is normalised to the cell capacitance (pA/pF). Time to the SarcK_{ATP} current activation during SFT-MI was measured at the point at which the outward basal current had increased by 20pA (as indicated by the arrows).

(B) Time to SarcK_{ATP} current activation during metabolic inhibition (MI) for cardiomyocytes pre-incubated with 2-30mM glucose.

Data presented as mean \pm s.e.m. Data for 2mM glucose (orange bar, N=4 hearts, 8 experiments/cardiomyocytes), 5mM glucose (red bar, N=7, 12), 10mM glucose (blue bar, N=5, 6), 15mM glucose (yellow bar, N=4, 6), 20mM glucose (green bar, N=3, 6) and 30mM glucose (purple bar, N=3, 6). **P<0.01(one-way ANOVA with Fisher's post-hoc test).

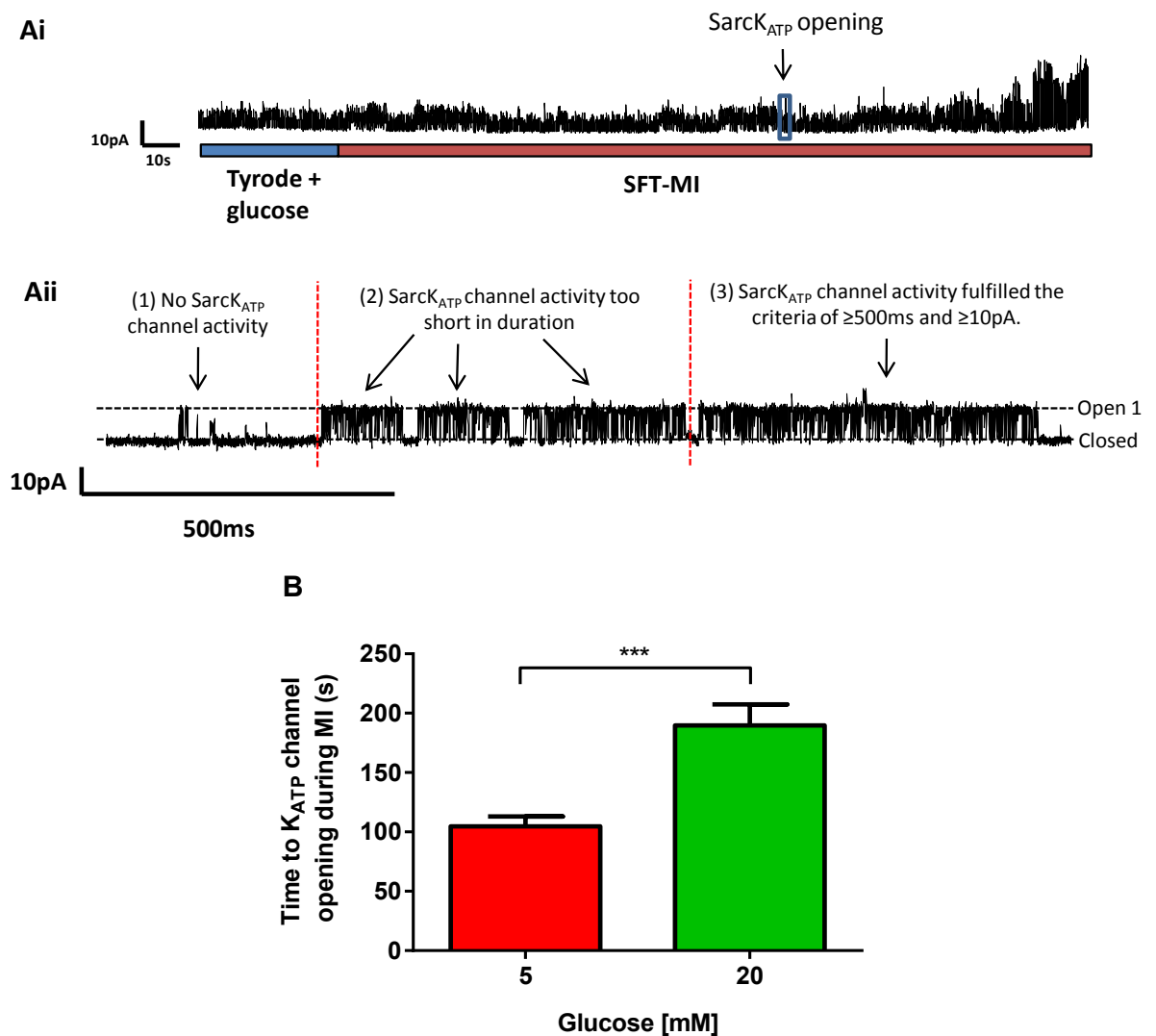


Figure 3.7 The effects of 5mM and 20mM glucose on single channel activity of SarcK_{ATP} during metabolic inhibition recorded using the cell-attached configuration.

(Ai) An example of a cell-attached trace recorded from a single cardiomyocyte pre-incubated in 5mM glucose prior to and during metabolic inhibition. The blue box indicates where the trace was expanded from to create Aii.

(Aii) Expansion of the area within the blue box of the example trace from A(i) showing (1) a region of no SarcK_{ATP} channel activity; (2) opening of SarcK_{ATP} channels $< 500\text{ms}$ and (3) opening of a SarcK_{ATP} channel at $\geq 500\text{ms}$ and $\geq 10\text{pA}$ during metabolic inhibition (SFT-MI), which met the criteria used in these study to determine SarcK_{ATP} channel activity.

(B) The effect of acute application of 5mM and 20mM glucose, on the time to opening of single SarcK_{ATP} channels during metabolic inhibition.

Data presented as mean \pm s.e.m. For the cell-attached data, 5mM glucose (red bar, N=8 hearts, 8 experiments/cardiomyocytes) and 20mM glucose (green bar, N=5, 5). *** $P < 0.001$ (Unpaired T-test).

In the whole cell configuration, intracellular dialysis occurs and may result in the loss of co-factors and changes in ATP levels. To check that the current measured (shown in Figure 3.6B) was $\text{Sarck}_{\text{ATP}}$, cell-attached recordings were conducted. Using this protocol, the conductance of the single channels measured can be calculated and compared to previously published values. The time to $\text{Sarck}_{\text{ATP}}$ channel opening was recorded from cardiomyocytes held at +40mV (as described in the methods section 2.5.2.1), while being perfused with either 5mM or 20mM glucose prior to superfusion with SFT-MI. An example of a cell-attached trace recorded from a cardiomyocyte perfused with Tyrode containing 5mM glucose (normoglycaemic conditions) followed by perfusion with SFT-MI can be seen in Figure 3.7Ai/ii. Time to $\text{Sarck}_{\text{ATP}}$ opening was measured as the first $\geq 500\text{ms}$ burst of $\text{Sarck}_{\text{ATP}}$ -like channel activity with a single channel current of $\geq 10\text{pA}$ (Brennan *et al.*, 2015). Figure 3.7B shows the mean data from such experiments, where the time to activation of $\text{Sarck}_{\text{ATP}}$ channels during perfusion with SFT-MI was determined for cardiomyocytes under normoglycaemic and hyperglycaemic conditions. Hyperglycaemic conditions significantly delayed the time to $\text{Sarck}_{\text{ATP}}$ opening from $104 \pm 8.4 \text{ s}$ (5mM glucose) to $189.6 \pm 17.9\text{s}$ (20mM glucose, $P < 0.001$).

These data indicate that hyperglycaemic conditions (20-30mM) significantly prolongs the time to $\text{Sarck}_{\text{ATP}}$ channel activation during SFT-MI, which may reflect slower ATP depletion at the cell surface membrane.

3.2.4 The effect of elevated extracellular glucose on intracellular ATP depletion during metabolic inhibition

The findings reported in this chapter ($\text{Sarck}_{\text{ATP}}$ channel active and rigor development) suggest ATP levels remain above critical levels for longer under hyperglycaemic conditions, this could be due to a delay in the ATP-depletion during metabolic inhibition; therefore the fluorescent indicator Magnesium Green (Mg^{2+} -Green) was used to assess the change in intracellular ATP during perfusion with SFT-MI and re-energisation. This indicator measures free cytoplasmic Mg^{2+} which under normal physiological conditions is predominantly bound to ATP. During ischaemia, ATP is depleted (hydrolysed) and Mg^{2+} is released, as a result free Mg^{2+} rises within the

cytosol of the cardiomyocyte. This is detected by binding to the Mg^{2+} -Green indicator resulting in an increase in fluorescence (Leyssens *et al.*, 1996), this allows relative changes in intracellular ATP to be indirectly measured using Mg^{2+} as a surrogate. Cardiomyocytes previously loaded with Mg^{2+} -Green (see methods section 2.6) were treated according to the protocol shown in Figure 3.1.

Figure 3.8 shows recordings of Mg^{2+} -Green fluorescence from three cardiomyocytes under normoglycaemic conditions (5mM glucose-A) and three cardiomyocytes under hyperglycaemic conditions (20mM glucose-Ai) prior to perfusion with SFT-MI and during re-energisation. Due to the Mg^{2+} -Green indicator being a non-ratiometric dye, in these recordings cardiomyocytes were quiescent (not electrically stimulated), to prevent movement artefacts and the fluorescence was normalised to fluorescence intensity at the start of the experiment (F/F_0). Under normoglycaemic conditions (5mM glucose), perfusion with SFT-MI initially resulted in a slow rise in fluorescence, then a rapid increase in fluorescence, which relates to the cardiomyocytes undergoing rigor contraction, followed by a slower increase in fluorescence. Initially upon re-energisation there was a further smaller increase in fluorescence, which started to decline in the latter stages of re-energisation (Figure 3.8). Under hyperglycaemic conditions (20mM glucose), a similar profile in time-dependent changes in fluorescence was evident. However during re-energisation the decline in fluorescence appeared to be more gradual than in 5mM glucose (Figure 3.8).

Figure 3.9A shows the average data from these experiments, in which the fluorescence of Mg^{2+} -Green (normalised to the start of the experiment) at the end of MI (600s) and at end of re-energisation (1200s) were measured. These data show that at the end of MI the difference in F/F_0 for those under hyperglycaemic conditions was significantly lower at $1.05 \pm 0.01F/F_0$, compared to those under normoglycaemic conditions at $1.12 \pm 0.03F/F_0$ ($P < 0.05$). At the end of re-energisation F/F_0 was also significantly lower under hyperglycaemic conditions at $1.04 \pm 0.02F/F_0$ compared to $1.14 \pm 0.04F/F_0$ ($P < 0.05$) for those under normoglycaemic conditions.

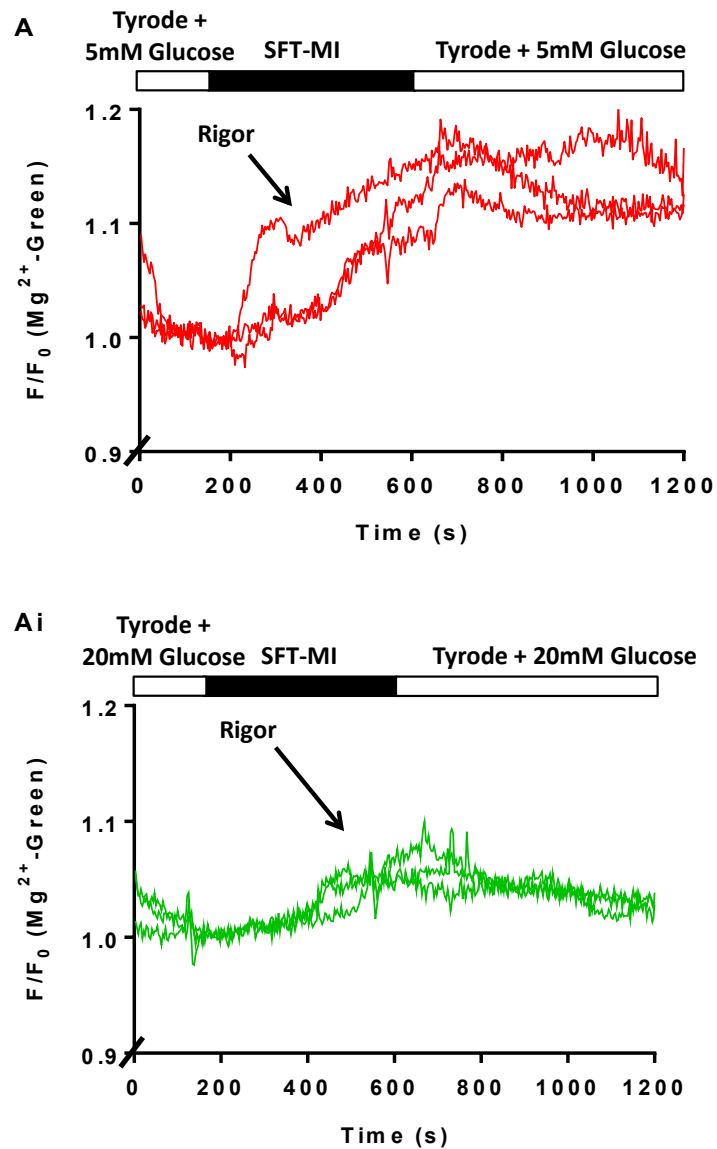


Figure 3.8 The effect of an acute elevation in extracellular glucose on Mg^{2+} -Green fluorescence in isolated cardiomyocytes exposed to metabolic inhibition and re-energisation.

- (A) Example traces showing the time course of changes in Mg^{2+} -Green fluorescence acutely exposed to 5mM glucose prior to metabolic inhibition and re-energisation.
- (Ai) Example trace showing the time course of changes in Mg^{2+} -Green fluorescence acutely exposed to 20mM glucose prior to metabolic inhibition and re-energisation.
- In both traces the expected time for the development of rigor contracture are indicated by arrows.

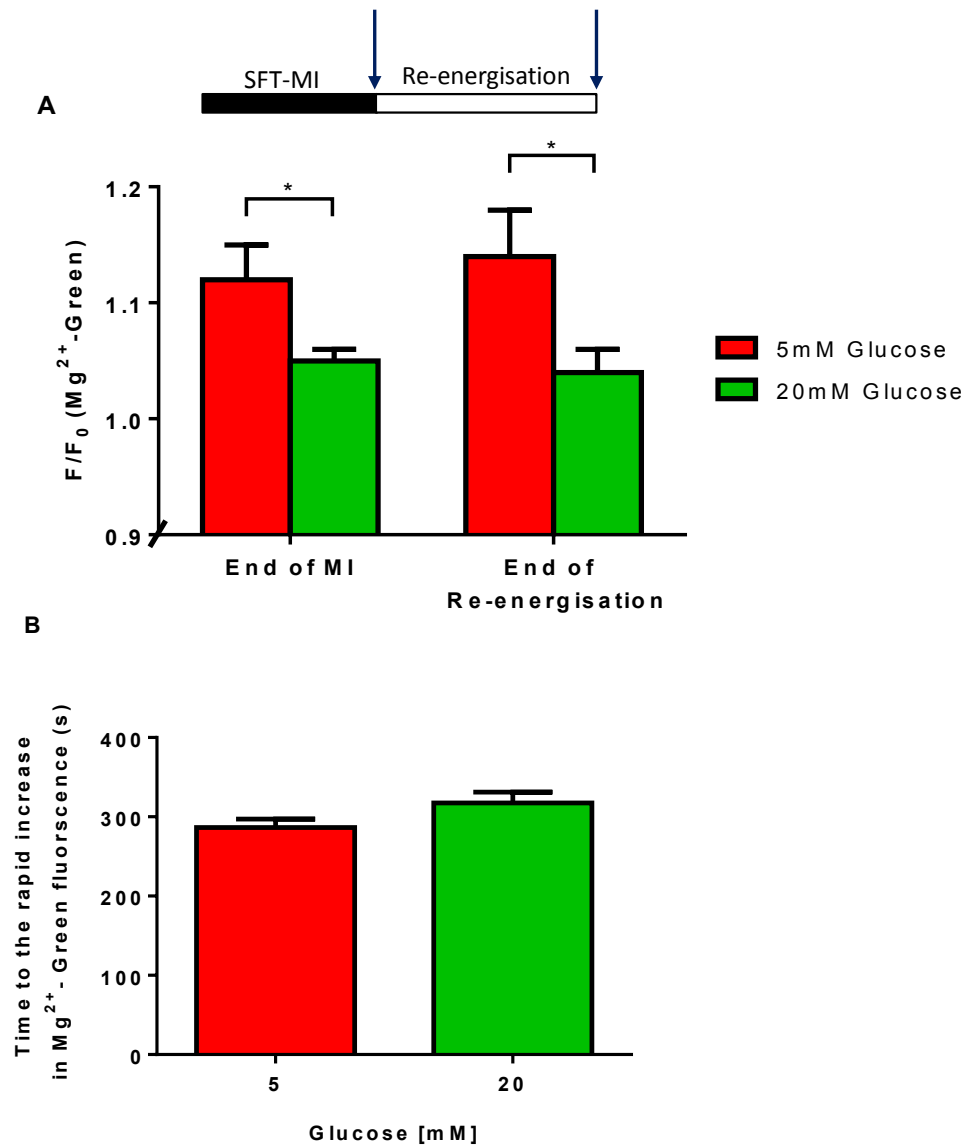


Figure 3.9 The effect of an acute elevation in extracellular glucose on Mg²⁺-Green fluorescence in isolated cardiomyocytes exposed to metabolic inhibition and re-energisation.

- (A) The effect of 5mM or 20mM glucose on Mg²⁺-Green fluorescence at the end of metabolic inhibition (MI) and at the end of re-energisation (as indicated on the schematic).
- (B) The effect of 5mM or 20mM glucose on the time to the rapid increase in Mg²⁺-Green fluorescence.

Data presented as mean \pm s.e.m. For 5mM glucose (red bar, N= 3 hearts, 9 fields of view, 41 cardiomyocytes) and 20mM glucose (green bar, N= 3, 8, 47). *P<0.05 (Unpaired T-test).

As shown in Figure 3.8A/Ai during SFT-MI following the slow increase in Mg^{2+} -Green fluorescence, there was a rapid increase in Mg^{2+} -Green fluorescence. The mean time to the rapid increase in Mg^{2+} -Green fluorescence during SFT-MI, for cardiomyocytes under normoglycaemic and hyperglycaemic conditions is shown in Figure 3.9B. These data show that hyperglycaemic conditions had no effect on the time to the rapid increase in fluorescence compared to those under normoglycaemic conditions with $317.4 \pm 13.7s$ (20mM glucose) versus $286.6 \pm 10.5s$ (5mM glucose, $P=0.10$).

These results show that cardiomyocytes under normoglycaemic conditions, exhibited an increase in Mg^{2+} -Green fluorescence during metabolic inhibition and re-energisation, compared to those under hyperglycaemic conditions.

3.2.5 The effects of elevated extracellular glucose on intracellular calcium within isolated cardiomyocytes subjected to metabolic inhibition and re-energisation

Previously in this chapter it was shown that acute hyperglycaemic conditions increased the percentage of contractile recovery, which could suggest improved Ca^{2+} regulation during metabolic inhibition and re-energisation. However it has also been shown that acute hyperglycaemic conditions delays the time to action potential failure, which could result in further accumulation of intracellular calcium ($[Ca^{2+}]_i$), which can contribute to re-energisation injury. Therefore the effects of acute hyperglycaemic conditions on calcium homeostasis were investigated. The fluorescence emission ratio (340:380nm) of the calcium dye Fura-2, was used as an index to changes in $[Ca^{2+}]_i$ within isolated cardiomyocytes.

3.2.5.1 Measurements of intracellular calcium as a marker of cell injury

Cardiomyocytes previously loaded with Fura-2 were treated according to the protocol outlined in Figure 3.1 and stimulated to contract at 1Hz by EFS.

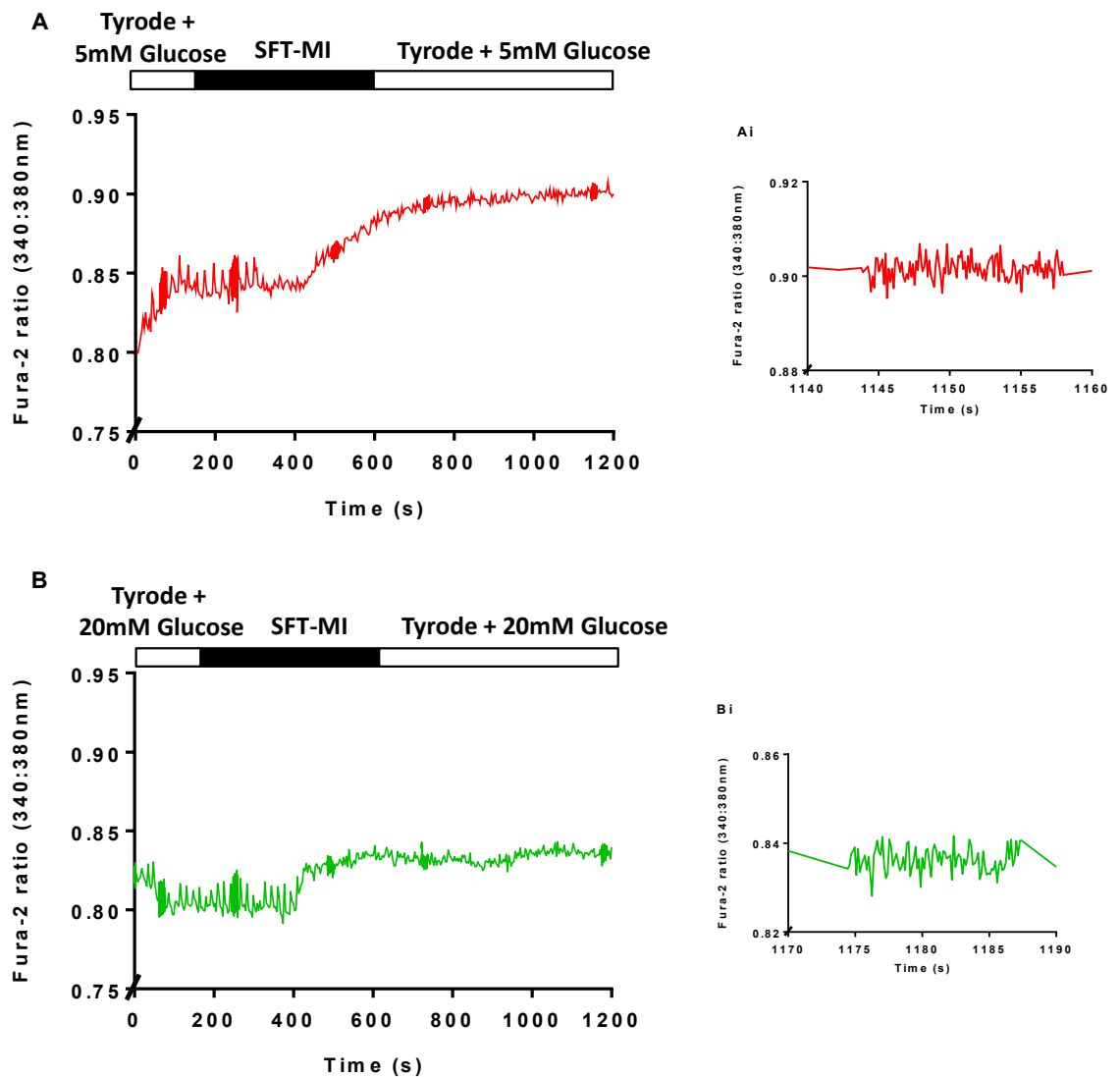


Figure 3.10 The effect of acute changes in extracellular glucose on the intracellular calcium in isolated cardiomyocytes during metabolic inhibition and re-energisation.

- (A) Example trace recording of the Fura-2 ratio (340:380nm) for a cardiomyocyte exposed to 5mM glucose prior to metabolic inhibition and during re-energisation.
- (Ai) A zoomed in areas of (A) showing the Fura-2 ratio (340:380nm) near to the end of re-energisation to illustrate the Ca^{2+} transient which would be used to determine recovery. In the example shown there was no recovery of Ca^{2+} transients.
- (B) Example trace recording of the Fura-2 ratio (340:380nm) for a cardiomyocyte exposed to 20mM glucose prior to metabolic inhibition and during re-energisation.
- (Bi) A zoomed in areas of (B) showing the Fura-2 ratio (340:380nm) near to the end of re-energisation to illustrate the Ca^{2+} transient which would be used to determine recovery. In the example shown there was no recovery of Ca^{2+} transients.

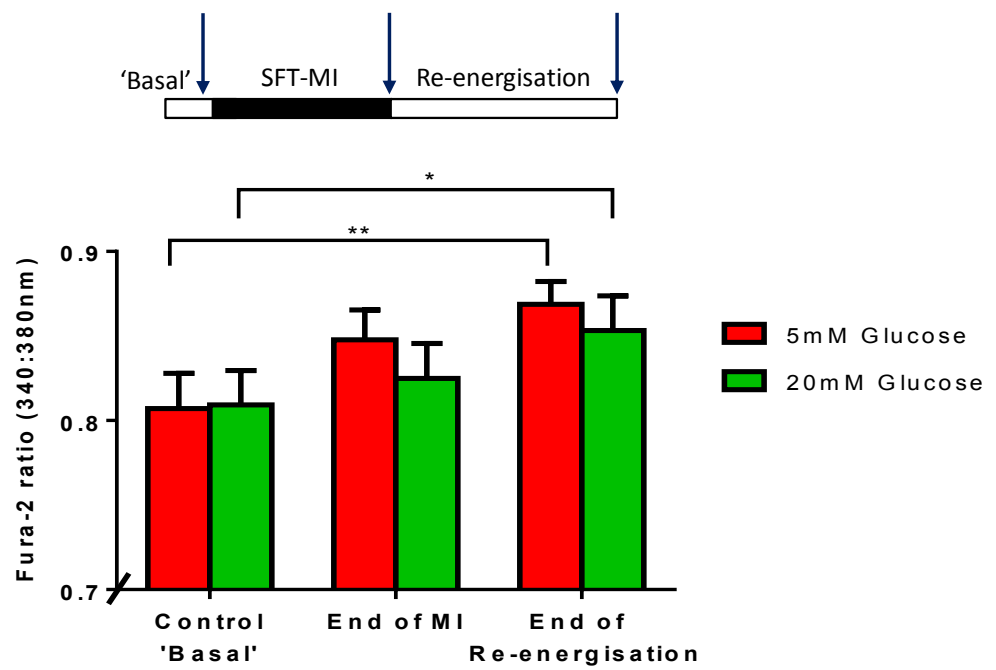
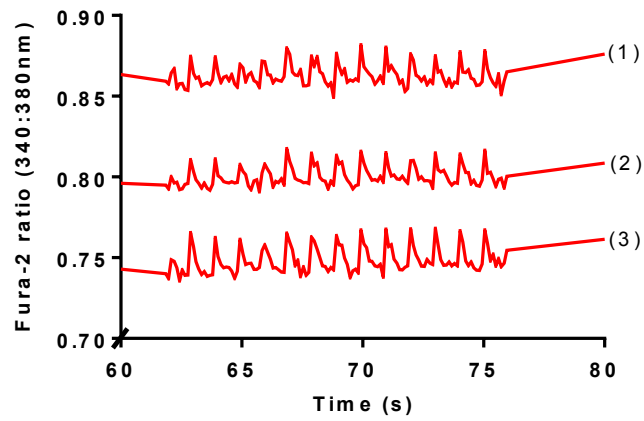


Figure 3.11 The effect of acute changes in extracellular glucose on the intracellular calcium in isolated cardiomyocytes during metabolic inhibition and re-energisation.

The effect of 5mM or 20mM glucose on the Fura-2 ratios at control 'basal' (start of metabolic inhibition), the end of metabolic inhibition (MI) and at the end of re-energisation (as indicated on the schematic).

Data presented as mean \pm s.e.m. For 5mM glucose (red bars, N= 4 hearts, 10 fields of views, 60 cardiomyocytes) and for 20mM glucose (green bars, N= 4, 9, 58). *P<0.05, **P<0.01 (one-way ANOVA with Fisher's repeated measures post-hoc test).

A



Ai

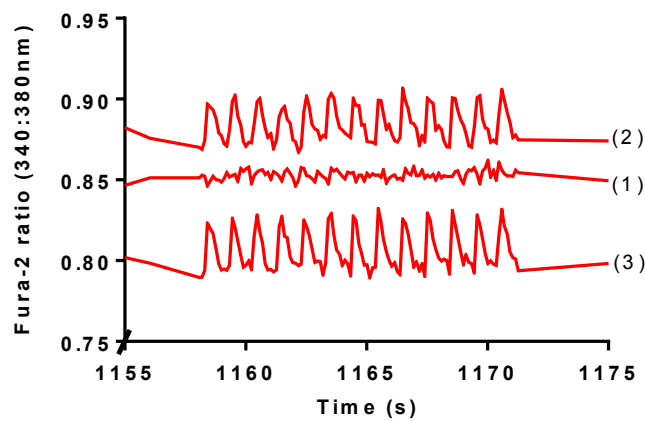


Figure 3.12 Capturing of Ca^{2+} transients during metabolic inhibition and re-energisation to determine recovery.

- (A) Example trace recordings of the Fura-2 ratios (340:380nm) captured prior to metabolic inhibition to illustrate the presence of Ca^{2+} transients (1-3) in synchrony with the EFS.
- (Ai) Example trace recordings of the Fura-2 ratios (340:380nm) captured towards the end of re-energisation to illustrate those from (A) that had either recovered Ca^{2+} transients (2 and 3) in time with the EFS or had not recovered (1).

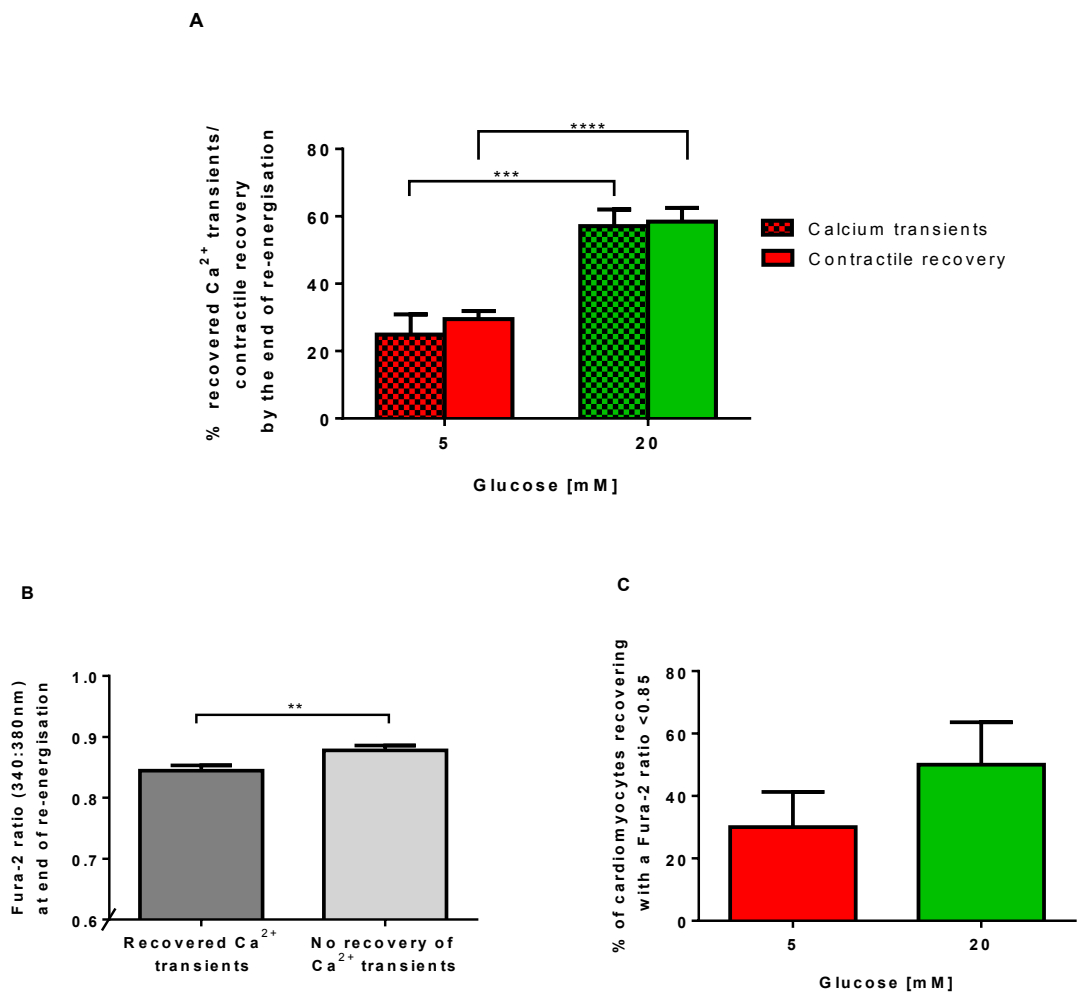


Figure 3.13 The effects of acute changes in extracellular glucose on the recovery of electrically evoked calcium transients following metabolic inhibition and re-energisation.

- (A) The percentage of cardiomyocytes recovering calcium transients compared to recovery of contractile function in 5mM and 20mM glucose by the end of 10 minutes re-energisation.
- (B) The Fura-2 ratio at the end of re-energisation (10 min) for those cardiomyocytes which either recovered calcium transients in response to EFS or not.
- (C) The percentage of cardiomyocytes in either 5mM or 20mM glucose, that recovered with a Fura-2 ratio <0.85 by the end of 10 minutes of re-energisation.

Data presented as mean \pm s.e.m. For 5mM glucose (red bars, N= 4 hearts, 10 fields of view, 60 cardiomyocytes) and for 20mM glucose (green bars, N= 4, 9, 58). **P<0.01, ***P<0.001, ****P<0.0001 (Unpaired T-test).

Figure 3.10A shows a Fura-2 ratio recorded from one cardiomyocyte under normoglycaemic conditions (5mM glucose), and shows the time course of changes in the Fura-2 ratio during metabolic inhibition and re-energisation. Perfusion with SFT-MI resulted in failure of Ca^{2+} -transients, followed by a steady increase in the diastolic Fura-2 ratio ($[\text{Ca}^{2+}]_i$). Upon re-energisation there was a further steady increase in Fura-2 ($[\text{Ca}^{2+}]_i$). Figure 3.10Ai shows the Ca^{2+} -transient captured towards the end of re-energisation which would be used as described in section 3.2.5.2 to calculate the percentage of cardiomyocytes that regained Ca^{2+} -transients. Under hyperglycaemic conditions (20mM glucose) (Figure 3.10B), a similar profile in time-dependent changes in the Fura-2 ratio were noted but the steady increase in Fura-2 was delayed and during re-energisation the increase in Fura-2 was more gradual. Figure 3.10Bi shows the Ca^{2+} -transients captured towards the end of re-energisation.

Figure 3.11 shows the average Fura-2 ratio (340:380nm) recorded immediately prior to MI as control 'basal' (180s), at the end of MI (600s) and at the end of re-energisation (1200s). Acute hyperglycaemic conditions had no affect on the 'basal' Fura-2 ratio at 0.81 ± 0.02 (20mM glucose) versus 0.81 ± 0.02 (5mM glucose, $P=0.94$). Acute hyperglycaemic conditions also had no affect on the Fura-2 ratio during SFT-MI; the ratio was 0.82 ± 0.02 for 20mM glucose versus 0.85 ± 0.02 for 5mM glucose ($P=0.41$). Similarly the Fura-2 ratio after 10 minutes of re-energisation was unchanged by acute hyperglycaemic conditions, with 0.85 ± 0.02 for 20mM glucose versus 0.87 ± 0.01 for 5mM glucose ($P=0.53$). However, at the end of the re-energisation period both normoglycaemic and hyperglycaemic conditions exhibited a significantly higher Fura-2 ratio compared to the Fura-2 ratio observed under 'basal' conditions ($P<0.01$ and $P<0.05$ respectively).

3.2.5.2 Is the recovery of contractile activity linked to maintained Ca^{2+} -homeostasis following metabolic inhibition and re-energisation?

Recovery of contractile function reflected by Ca^{2+} -transients indicates protection against metabolic inhibition and re-energisation, which has been shown to reflect maintenance of low diastolic Ca^{2+} (Rodrigo & Standen, 2005, Rodrigo & Samani, 2008). Therefore the presence of Ca^{2+} -transients in synchrony with the EFS at the beginning

of each experiment and their ability to recovery these at the end of re-energisation, was used to indicate recovery of the cardiomyocyte and the Fura-2 ratio below which this occurs was also determined. Figure 3.12A shows examples of Ca^{2+} -transient captured in synchrony with the EFS prior to metabolic inhibition from three cardiomyocytes perfused with 5mM glucose, and Figure 3.12Ai shows the same traces recorded towards the end of re-energisation to illustrate if Ca^{2+} -transients had recovered or not. Overall the Fura-2 ratio allowed quantification of the percentage of cardiomyocytes that are protected.

The overall recovery of Ca^{2+} -transients (Figure 3.13A) was significantly higher under hyperglycaemic conditions ($57.1 \pm 4.9\%$) compared to normoglycaemic conditions ($26.9 \pm 5.4\%$, $P < 0.001$). These recoveries reflected the recovery of contraction, which were $58.4 \pm 4.1\%$ for 20mM glucose and $29.5 \pm 2.4\%$ for 5mM glucose.

Figure 3.13B shows the average Fura-2 ratios present at the end of re-energisation, for cardiomyocytes either recovering Ca^{2+} -transients or not. For both normoglycaemic and hyperglycaemic conditions, cardiomyocytes recovering Ca^{2+} -transients had a lower Fura-2 ratio of 0.84 ± 0.01 ($P < 0.01$), compared to 0.88 ± 0.01 for those not recovering Ca^{2+} -transients. Therefore it was decided that cardiomyocytes recovering Ca^{2+} -transients with a Fura-2 ratio < 0.85 had maintained a viable $[\text{Ca}^{2+}]_i$. The data in Figure 3.13C, shows that the percentage of cardiomyocytes with a Fura-2 ratio < 0.85 , which will have recovered Ca^{2+} -transients by the end of re-energisation did not differ between those cardiomyocytes maintained under normoglycaemic ($30.0 \pm 11.3\%$) or hyperglycaemic conditions ($50.0 \pm 13.6\%$, $P = 0.27$).

These data suggests that under hyperglycaemic conditions (20mM glucose), a higher proportion of cardiomyocytes regain synchronous Ca^{2+} -transients by the end of re-energisation. This suggests that these cardiomyocytes would have regained contractile function. However hyperglycaemic conditions had no significant effect on calcium homeostasis during metabolic inhibition and re-energisation.

3.2.6 The effects of acute changes in extracellular fructose on the contractile function of isolated cardiomyocytes

Fructose is a glycolytic metabolic substrate transported into the cytosol of cardiomyocytes via GLUT 5 and 11, which then enters the glycolytic pathway at the rate limiting enzyme Phosphofructokinase-1 (PFK-1) as indicated in Figure 1.6 (Mellor et al., 2010).

To determine the effects of an acute increase in extracellular fructose on contractile function, isolated cardiomyocytes were perfused with Tyrode solution containing either 5mM or 20mM fructose with 5mM pyruvate and subjected to metabolic inhibition and re-energisation. The 5mM fructose Tyrode solution was osmotically balanced with mannitol and the SFT solutions used within the fructose data sets were osmotically balanced with sucrose (see section 2.7.2.2).

Acutely elevating extracellular fructose from 5mM to 20mM had no effect on the time to contractile failure (Figure 3.14A) with 151.9 ± 17.7 s versus 192.5 ± 7.0 s ($P=0.06$) respectively. The time to rigor (Figure 3.14B) was also not affected with 303.6 ± 8.6 s (20mM fructose) versus 269.7 ± 36.7 s (5mM fructose, $P=0.39$).

By the end of 10 minutes re-energisation, acutely elevating extracellular fructose from 5mM to 20mM had no affect on the percentage of 'non-hypercontracted' cardiomyocytes (Figure 3.15A) with $83.4 \pm 3.2\%$ versus $76.5 \pm 5.5\%$ ($P=0.31$) respectively, but did significantly increased the percentage of cardiomyocytes regaining contractile function (Figure 3.15B) from $33.3 \pm 2.7\%$ (5mM fructose) to $65.8 \pm 3.6\%$ (20mM fructose, $P<0.0001$).

These data suggest that perfusing with an elevated extracellular fructose concentration (20mM) only impacts during re-energisation by increasing contractile recovery.

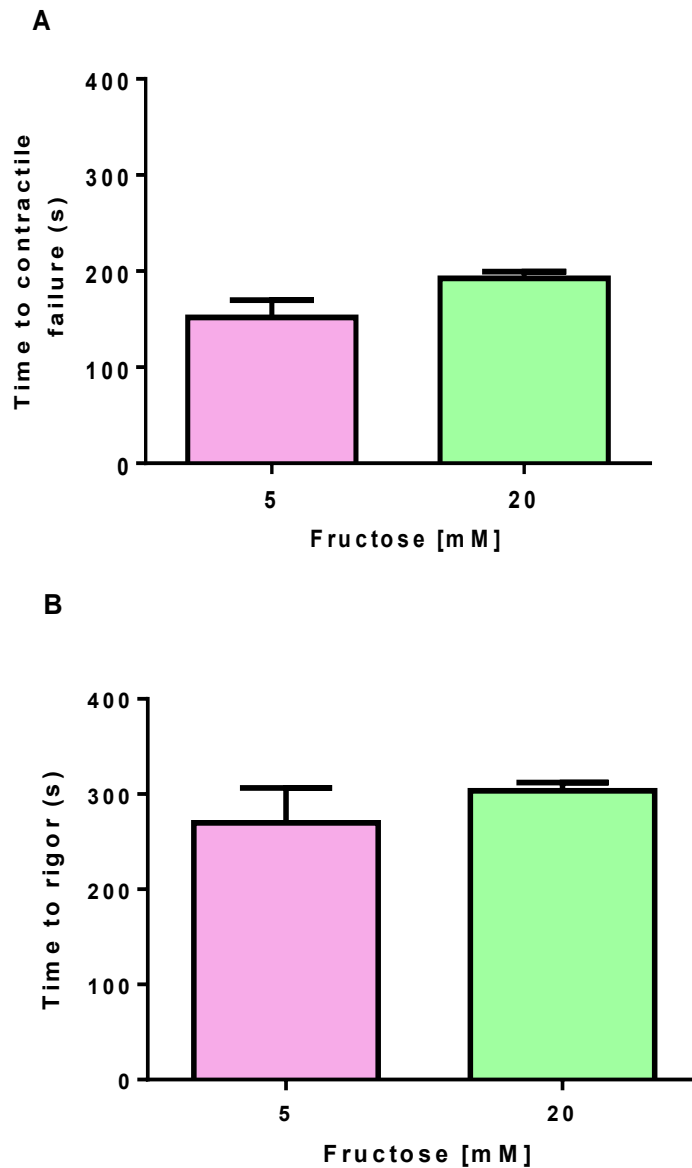


Figure 3.14 The effects of acute changes in extracellular fructose on the contractile function of isolated cardiomyocytes subjected to metabolic inhibition and re-energisation.

(A) Time to contractile failure from the onset of metabolic inhibition for cardiomyocytes superfused with 5mM or 20mM fructose and 5mM pyruvate.
 (B) Time to rigor contracture from the onset of metabolic inhibition for cardiomyocytes superfused with 5mM or 20mM fructose and 5mM pyruvate.
 Data presented as mean \pm s.e.m. For 5mM fructose (pink bar, N= 4 hearts, 6 fields of view, 147 cardiomyocytes) and 20mM fructose (green bar, N= 5, 6, 189).

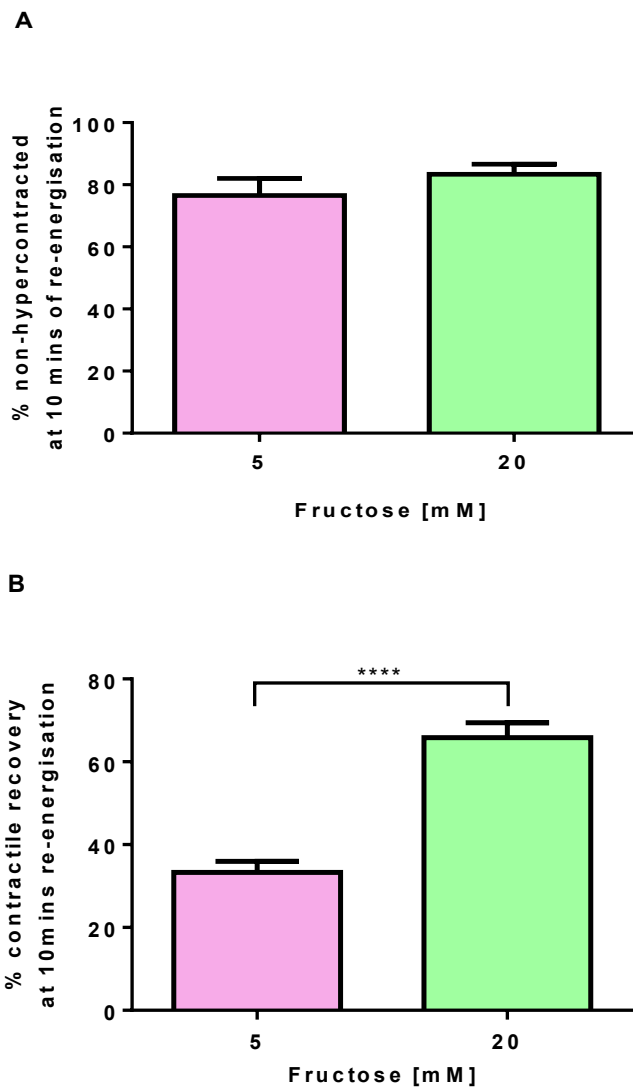


Figure 3.15 The effects of acute changes in extracellular fructose on recovery of isolated cardiomyocytes subjected to metabolic inhibition and re-energisation.

(A) The percentage of 'non-hypercontracted' cardiomyocytes by the end of 10 minutes of re-energisation for cardiomyocytes superfused with 5mM or 20mM fructose and 5mM pyruvate.

(B) The percentage of cardiomyocytes regaining contractile function in response to EFS, by the end of 10 minutes of re-energisation for cardiomyocytes superfused with 5mM or 20mM fructose and 5mM pyruvate.

Data presented as mean \pm s.e.m. For 5mM fructose (pink bar, N= 4 hearts, 6 fields of view, 147 cardiomyocytes) and 20mM fructose (green bar, N= 5, 6, 189).

****P<0.0001 (Unpaired T-test).

3.3 Discussion

The experiments described in this chapter were designed to investigate the effects of acute changes in extracellular glycolytic metabolic substrates (glucose and fructose) on the contractile and electrical responses of isolated cardiomyocytes, to metabolic inhibition and re-energisation. This was achieved by perfusing isolated rat ventricular cardiomyocytes with acute changes in glucose and fructose, prior to metabolic inhibition “ischaemia” and during re-energisation “reperfusion”. As the normal blood glucose concentration of rats is 5.2mM (Johnson-Delaney, 2008), 5mM glucose was used as the control glucose concentration (normoglycaemic conditions), while glucose concentrations ≥ 10 mM were used to mimic hyperglycaemic conditions and 2mM glucose was used as a hypoglycaemic concentration.

During ischaemia, anaerobic glycolysis is known to continue therefore the effects of acute hypoglycaemic and hyperglycaemic glucose concentrations and an acutely elevated fructose concentration (20mM) on isolated cardiomyocytes were examined. Data in this study show that perfusion under hyperglycaemic glucose conditions, prior to metabolic inhibition and during re-energisation, delayed the failure of contractile activity and rigor development during metabolic inhibition and increased contractile recovery by the end of re-energisation. Perfusion with an elevated fructose concentration also increased contractile recovery by the end of re-energisation. Acute hyperglycaemic conditions also delayed both action potential failure and $\text{SarCK}_{\text{ATP}}$ channel activation during metabolic inhibition. However there was no impact on APD_{90} or the RMP. Fluorescence imaging revealed acute hyperglycaemia had no effect on maintenance of $[\text{Ca}^{2+}]_i$, however changes in ATP levels which may underlie these results were suggested by Mg^{2+} -Green fluorescence. Under acute hyperglycaemic conditions smaller increases in Mg^{2+} -Green fluorescence were observed at the end of metabolic inhibition and the re-energisation period which could suggest less ATP depletion.

Hypoglycaemic conditions only hyperpolarised the RMP and had no effect on any of the other parameters measured.

3.3.1 Do acute changes in extracellular glucose prior to metabolic inhibition impact on ATP depletion during metabolic inhibition?

3.3.1.1 Perfusion with elevated glucose delays contractile failure, action potential failure and $\text{SarCK}_{\text{ATP}}$ opening

During metabolic inhibition, contractile failure occurs due to shortening and eventual failure of the APD as a result of depleted ATP levels causing opening of $\text{SarCK}_{\text{ATP}}$ channels (Figure 3.16) (Lederer *et al.*, 1989).

In this study, a concentration dependent delay in the time to contractile failure under acute hyperglycaemic conditions was observed during metabolic inhibition. The observed delay can be associated with the concentration dependent delay in time to action potential failure during metabolic inhibition, also observed in this study, under acute hyperglycaemic conditions. These results show acute elevations in glucose enable cardiomyocytes to contract and maintain action potentials for longer, which could be due to maintained ATP levels delaying $\text{SarCK}_{\text{ATP}}$ channel opening as proposed in Figure 3.17.

It was hypothesised that the delay in ATP depletion, may be due to increased glycolytic flux (via the Glut transporters) prior to and in the very early stages of metabolic inhibition (via glycolysis and oxidative phosphorylation, as prior to metabolic inhibition, cardiomyocytes were also perfused with 5mM pyruvate), which increase total [ATP] and ATP pools. ATP pools close to the sarcolemmal membrane and the myofibrils could also be maintained prior to metabolic inhibition by the PCr transfer shuttle. Previous studies have shown that during ischaemia, perfusion with 11.1mM glucose (a concentration sufficient to ensure adequate glucose uptake in the absence of insulin and alternate substrates) (King & Opie, 1998b), leads to a glycolytic flux of $1.17\mu\text{moles glucose units/g/min}$, resulting in a total ATP production of $7.4\mu\text{mol/g/min}$ (Bricknell & Opie, 1978). Perfusion with high glucose and insulin (19.5mM glucose and $250\mu\text{U/ml}$ insulin or 10mM glucose/ 140mU/l insulin), during low-flow ischaemia has also been shown to increase glycolysis, resulting in increased [ATP] and [PCr] and a higher free-energy of ATP hydrolysis (ΔG_{ATP}) (Vanoverschelde *et al.*, 1994; Cave *et al.*,

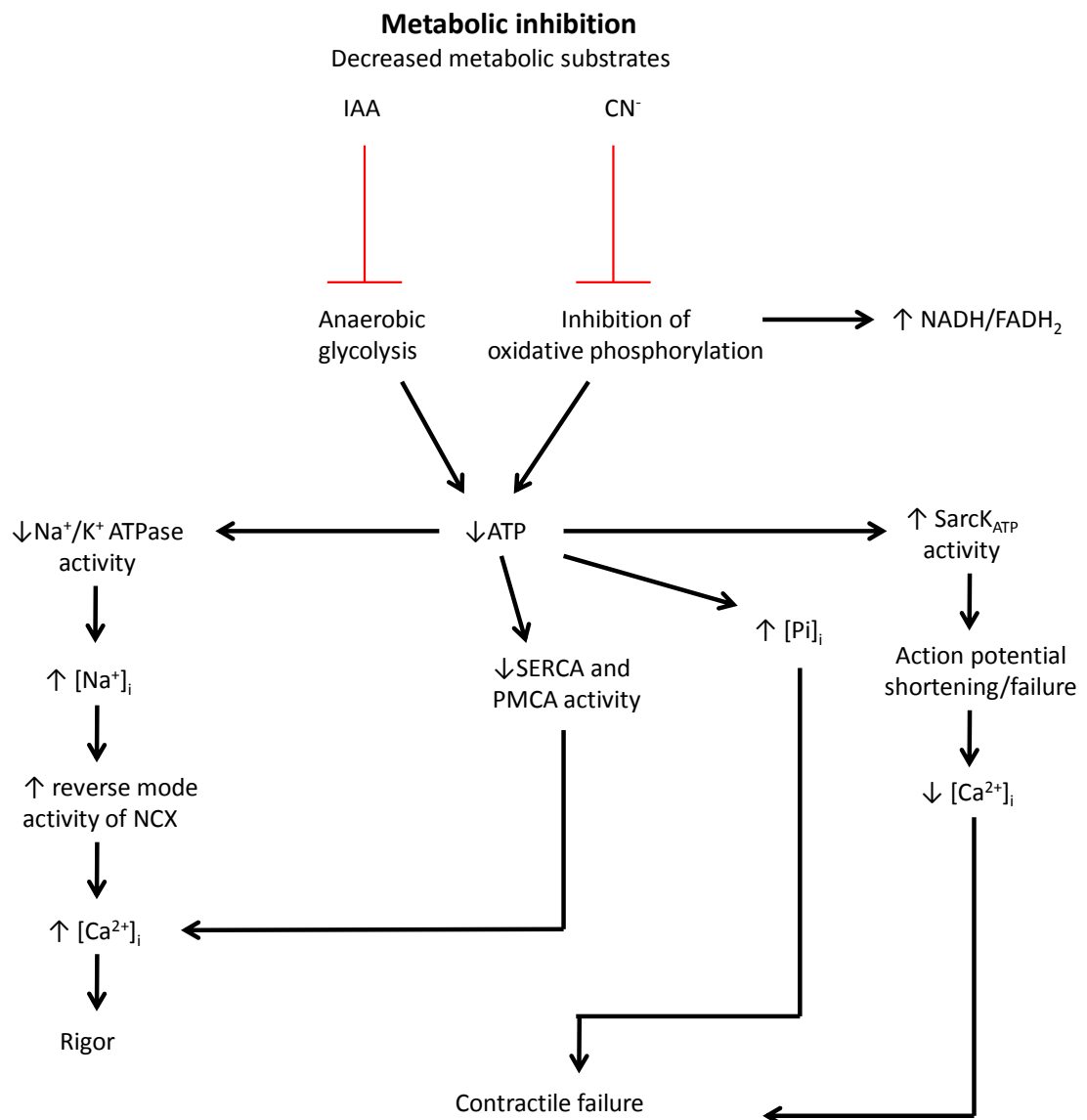


Figure 3.16 The effects of metabolic Inhibition.

The metabolic poisons IAA and CN^- inhibit the two different ATP production sites resulting in a decrease in ATP, which affect a number of the ATP-dependent transporters/pumps affecting contractile function.

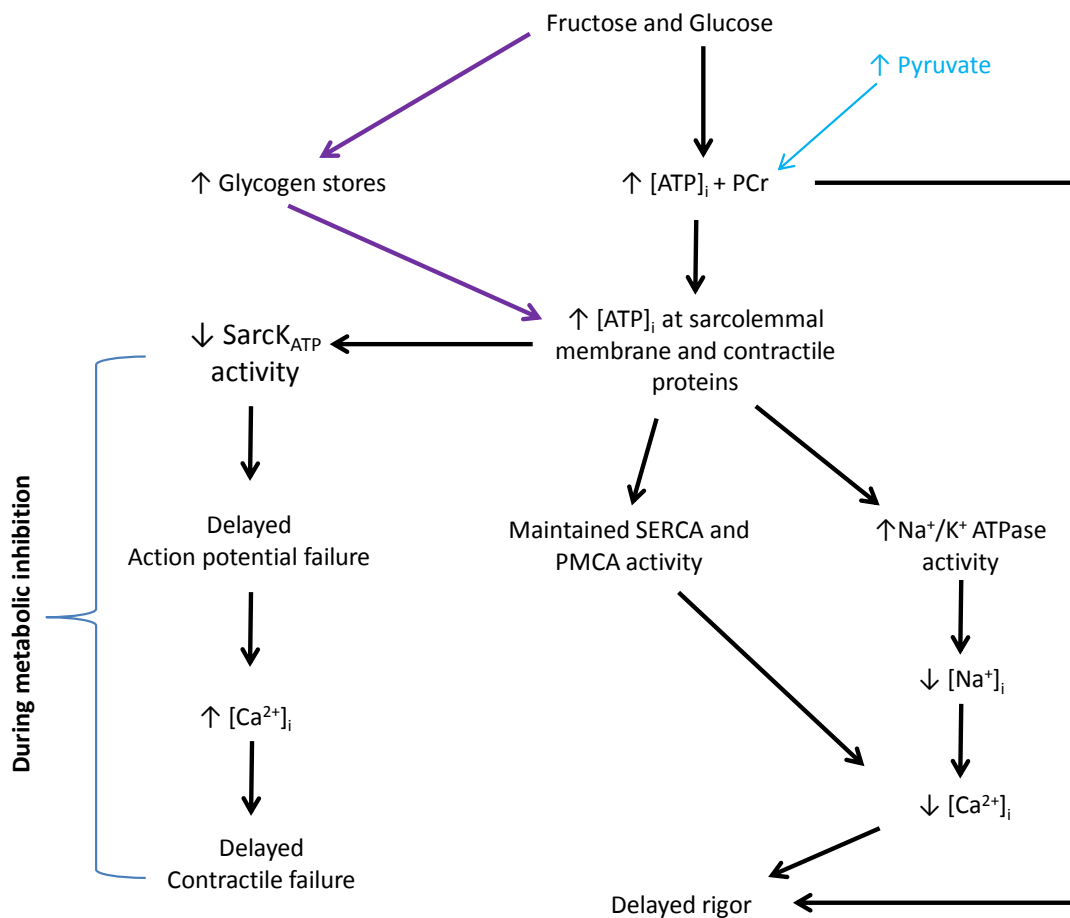


Figure 3.17 The hypothesised mechanisms behind cardioprotection seen when perfusing with elevated glucose, fructose and pyruvate prior to metabolic inhibition.

The diagram shows the hypothesised pathways being activated by increasing availability of ATP. Prior to metabolic inhibition glucose could be increasing the glycogen stores. Elevated pyruvate would increase ATP and PCr which would aid contractile function prior to metabolic inhibition. During metabolic inhibition anaerobic glycolytic ATP production would be the main source of ATP.

2000). These results show elevated glucose is sufficient to maintain both ATP and PCr and by increasing ΔG_{ATP} would support improved SERCA activity. However increased glycolysis during ischaemia increases lactate production and lowers pH (Owen *et al.*, 1990; Vanoverschelde *et al.*, 1994; Cave *et al.*, 2000), which can affect contraction of cardiomyocytes. In the model of low-flow ischaemia, lactate will not accumulate, as perfusion must fall to <5% in order for accumulation to occur (Cave *et al.*, 2000). This is similar to the model of superfusion used in this study and could indicate accumulation of lactate and protons may be prevented. In this study, pH was not measured, but it could be assumed due to increased glycolytic flux acidic conditions may occur; however Dizon *et al.* (1998) found when using IAA as has been used in this study, pH does not change significantly due to less lactate production (Dizon *et al.*, 1998). Therefore it could be assumed pH may not change greatly in this study.

The failure of an action potential can be attributed to opening of $\text{SarcK}_{\text{ATP}}$ channels where increased efflux of K^+ ions diminishes the plateau, driving the RMP back towards E_k causing hyperpolarisation of the membrane potential and shortening of the APD (Figure 3.16). $\text{SarcK}_{\text{ATP}}$ channels are closely associated with glycolytic enzymes (Dhar-Chowdhury *et al.*, 2005; Jovanovic *et al.*, 2005; Hong *et al.*, 2011). As these channels act as metabolic sensors and open when the ratio of $[\text{ATP}]/[\text{ADP}]$ falls, maintained ATP production (i.e. slower ATP depletion) in close proximity to these channels would be expected to delay their activation. This hypothesis fits with the observed delays under hyperglycaemic conditions of the time to $\text{SarcK}_{\text{ATP}}$ channel activation and channel current opening in both whole-cell and cell-attached patch clamp configurations, which suggests under hyperglycaemic conditions, ATP levels are maintained or there is a slower depletion of ATP during metabolic inhibition in close proximity to the $\text{SarcK}_{\text{ATP}}$ channels. The ATP causing this effect is likely to be glycolytically derived, due to the increased glucose concentrations. In addition glycolytic ATP rather than ATP from oxidative phosphorylation has previously been shown to inhibit $\text{SarcK}_{\text{ATP}}$ channels (Weiss & Lamp, 1987). The $\text{SarcK}_{\text{ATP}}$ channels recorded in this study open 35-50s before the action potential fails. This is expected as opening of $\text{SarcK}_{\text{ATP}}$ causes failure of the action potential. Earlier $\text{SarcK}_{\text{ATP}}$ activation

compared to action potential failure could also be due to $\text{Sarck}_{\text{ATP}}$ activation being measured as soon as the basal outward steady-state current had increased by >20pA.

In this study, acute elevations in extracellular glucose had no impact on either the APD_{90} or the RMP. This is in contrast to work by Sims *et al* (2014), who found that in isolated cardiomyocytes, elevating extracellular glucose caused a graded prolongation in APD_{90} and a concentration-dependent depolarisation of the membrane potential (statistical significance reached for both parameters at 15mM and 20mM) (Sims *et al.*, 2014). They suggest these effects may be due to activation of $\text{PKC}\alpha$ and $\text{PKC}\beta$, as inhibition of these PKC isoforms prevented these effects. The difference between studies could be due to the length of time the cardiomyocytes were perfused with each respective glucose concentration. In this thesis cardiomyocytes were settled (for 10 minutes) and perfused for 3-6 minutes in each respective glucose prior to SFT-MI, and these parameters were measured from 20 consecutive action potentials prior to SFT-MI. While it is unclear in the Sims *et al* (2014) study how long the incubation and perfusion time period with each glucose was for. If it was a longer period this could suggest the detrimental effect is due to longer exposure to elevated glucose.

3.3.1.2 Elevated glucose prevents ATP depletion but does not prevent a Ca^{2+} overload

To examine whether acute changes in glucose concentration did modulate ATP levels, the fluorescence indicator Mg^{2+} -Green was used. During metabolic inhibition under both normoglycaemic and hyperglycaemic conditions, there is initially a slow rise in Mg^{2+} -Green fluorescence this could indicate the mitochondria starting to depolarise (Rodrigo & Standen, 2005). This is possible as 2mM CN^- and 1mM IAA has previously been shown to cause an immediate depolarisation of mitochondria (via TMRE fluorescence), which was maintained until CN^- and IAA were removed (Lawrence *et al.*, 2001). Following this phase, a rapid increase in fluorescence occurred, which could indicate the mitochondria has depolarised, and is the point at which rigor begins due to F_0/F_1 ATP synthase being stimulated to work in reverse due to the depolarisation (Rodrigo & Standen, 2005). Previously the onset of the rapid increase in fluorescence has been found to relate to shortening in cell length which represents rigor (Lawrence

et al., 2001). Hyperglycaemic conditions did not affect the time to the start of the rapid increase in fluorescence, suggesting mitochondrial depolarisation is not delayed, as a result ATP production is not maintained. This finding does not correlate with the delay in rigor contracture also observed in this study. However, following the rapid phase, a slower increase in fluorescence was observed this could represent completion of rigor (Lawrence *et al.*, 2001). This observed profile coincides with a profile observed in a previous whole heart study, where perfusion with no glucose during ischaemia shows a similar 3 phase loss of ATP (Cross *et al.*, 1995), which could suggest the observed phase changes in Mg^{2+} -Green fluorescence are related to ATP depletion and in the case of hyperglycaemic conditions, could relate to a delay or maintained ATP production.

The collective Mg^{2+} -Green data also implies hyperglycaemic conditions alter ATP depletion during metabolic inhibition. Therefore the amount of free Mg^{2+} available to bind to Mg^{2+} -Green is lower compared to those perfused with 5mM glucose and could imply that perfusion with elevated glucose is maintaining ATP production. However caution is required when interpreting the Mg^{2+} -Green data, this is because the indicator Mg^{2+} -Green is not good for quantitative measurements as shown in Section 3.2.4, only qualitative measurements. This is because this indicator cannot show absolute ATP levels between cardiomyocytes, and as a non-ratiometric dye cannot deal with changes in cell size which would occur as the cardiomyocytes go through the metabolic inhibition and re-energisation protocol (i.e. rigor and hypercontracture).

Collectively these results suggest the observed delays in $Sarck_{ATP}$ channel activation, action potential and contractile failure during metabolic inhibition, under acute hyperglycaemic conditions, may be a result of delayed ATP depletion. The observed delays are proposed to arise from glycolytic ATP because many of the glycolytic enzymes are closely associated with the sarcolemmal membrane and SR membranes (Dhar-Chowdhury *et al.*, 2005; Jovanovic *et al.*, 2005; Hong *et al.*, 2011; Xu *et al.*, 1995; Pierce & Philipson, 1985). This means glycolytically derived ATP, rather than the mitochondrial derived ATP, is believed to regulate a number of ionic pumps, exchangers and transporters (Na^+/K^+ ATPase, NCX and SERCA) as well as $Sarck_{ATP}$ channels. Therefore continued anaerobic glycolysis during ischaemia could limit ATP

depletion within the sarcolemmal membrane area and maintain ionic homeostasis and contraction via improved Ca^{2+} regulation and maintenance of the action potential. Maintained glycolytic ATP levels in close proximity to the ATP-dependent Na^+/K^+ ATPase would be expected to prevent the Na^+ accumulation and the subsequent increase in $[\text{Ca}^{2+}]_i$ caused by reverse-mode activity of the NCX which occurs during metabolic inhibition and therefore reduce “ischaemic damage”. Previous studies have shown glycolytic ATP (derived from glucose or glycogen) maintains Na^+/K^+ ATPase activity during ischaemia, preventing Na^+ accumulation, resulting in maintained contraction (Van Emous *et al.*, 2001; Cross *et al.*, 1995; Dizon *et al.*, 1998).

Although the activity of Na^+/K^+ ATPase was not investigated, changes in $[\text{Ca}^{2+}]_i$ were measured using the ratio-metric indicator Fura-2. A similar profile of changes in Fura-2 were observed as previously seen in isolated rat cardiomyocytes, where during metabolic inhibition $[\text{Ca}^{2+}]_i$ increases (Rodrigo & Standen, 2005). There was no observed difference between Fura-2 ratios under normoglycaemic and hyperglycaemic conditions during metabolic inhibition, suggesting acute hyperglycaemic conditions do not prevent Ca^{2+} entry. This may signify Na^+/K^+ ATPase activity is not maintained by the end of metabolic inhibition. However it is proposed the observed no difference in Fura-2 ratios is related to the hyperglycaemic conditions delaying $\text{SarCK}_{\text{ATP}}$ opening, preventing earlier action potential failure and as a result maintained Ca^{2+} entry for longer.

3.3.1.3 The effect of elevated glucose on the development of rigor

The suggestion of maintained ATP and/or Na^+/K^+ ATPase activity could also affect development of rigor contracture (Figure 3.17). During metabolic inhibition, acute hyperglycaemic conditions delayed the time to rigor contracture in a concentration-dependent manner. There was no delay in the time to rigor with 30mM glucose. This was unexpected and could indicate faster ATP depletion near the myofibrils. The ATP required to prevent rigor was previously believed to be mitochondrial derived, as the mitochondria rather than the glycolytic enzymes are localised close to the myofibrils, and the ATP transferred by the creatine phosphate shuttle has preferential access to the myosin ATPase over other Mg^{2+} -ATP. In addition, during ischaemia PCr levels

rapidly decline and oxidative phosphorylation is inhibited, this prevents transfer of high-energy phosphates from the mitochondria to the myofibrils, resulting in local ATP levels at the myofibrils declining and ADP accumulating which was believed to stimulate rigor (Veksler *et al.*, 1997). Therefore the lack of delay with 30mM could suggest this glucose concentration is either preventing PCr formation or having an effect on the creatine phosphate shuttle's ability to transfer ATP to the myofibrils.

However when ATP production from oxidative phosphorylation is intact but glycolytic ATP production is inhibited, rigor still occurs, but at higher ATP levels compared to when ATP produced is only glycolytically derived. This implies glycolytic ATP rather than mitochondrial ATP is responsible for the development of rigor (Bricknell *et al.*, 1981) as outlined in Figure 3.17.

Previous studies have shown during low-flow ischaemia, perfusion with elevated glucose prevents ischaemic contracture (rigor) (Vanoverschelde *et al.*, 1994; Cross *et al.*, 1995; Bricknell *et al.*, 1981), while increasing the glucose concentration perfused from 0-11mM, delays ischaemic contracture (Owen *et al.*, 1990). These findings suggest rigor occurs when anaerobic glycolysis ceases and have been suggested to occur due to compartmentalisation of ATP in pools close to the contractile proteins (Bricknell *et al.*, 1981), which enable the contractile machinery to maintain function. The role of anaerobic glycolysis in preventing/delaying rigor development is indicated further by the findings that inhibiting glycolysis with 2-Deoxy-D-glucose or IAA either prior to and/or during ischaemia results in early rigor contracture, as a result of decreased glycolytic flux (Owen *et al.*, 1990, Kingsley *et al.*, 1991).

In addition, hearts perfused with 11mM glucose prior to no-flow ischaemia, developed rigor at >8 minutes into the ischaemic period, due to the absence of glucose during ischaemia, this suggests a role for glycogen (Kingsley *et al.*, 1991). Another study has shown perfusing with glucose (11mM) and insulin (24nmol/L), prior to ischaemia, increases internal glycogen levels. This resulted in delays in ischaemic contracture and maintained lactate efflux until ischaemic contracture developed compared to those perfused with a glucose free Krebs-Henseleit buffer containing isoproterenol to deplete glycogen levels (Cross *et al.*, 1996). This shows glycolysis continues until

glycogen is depleted. In this study as rigor did not occur immediately and was delayed with elevated glucose concentrations ($\geq 20\text{mM}$), this could suggest glycogen is involved, with the elevating glucose concentrations increasing internal glycogen stores. This is possible, as when glycolytic flux is increased, glucose-6-phosphate is converted into glycogen via glycogen synthase (Figure 3.18). Then upon metabolic inhibition (when the ATP/glycolytic flux decreases) despite the presence of IAA, glycogen would be released and converted back into glucose-6-phosphate by glycogen phosphorylase (Figure 3.18), resulting in production of additional ATP molecules and maintained glycolytic flux until the latter stages of metabolic inhibition. However, rats have low glycogen stores (King & Opie, 1998a, Williams *et al.*, 2000) and within the first few minutes of ischaemia the majority of glycogen stores are believed to be broken down and not contribute greatly to glycolytic flux after this time (King & Opie, 1998a). However, during short ischaemic periods, glycogen is not fully depleted, and contracture avoided (Cross *et al.*, 1996).

Therefore it is hypothesised perfusion with elevated glucose, increases ATP pools at the sarcolemmal membrane and may also increase glycogen stores within the cardiomyocytes, so that upon perfusion with metabolic inhibition a small amount of ATP production is maintained via anaerobic glycolysis and thus ATP depletion is delayed.

3.3.2 Perfusion with elevated extracellular glucose upon re-energisation prevents re-energisation injury

3.3.2.1 Can elevated glucose prevent hypercontracture?

Upon re-energisation, removal of CN^- restores the ETC and repolarises the mitochondrial membrane potential, which drives F_0/F_1 ATPase to recommence ATP production. If this occurs whilst Ca^{2+} levels are still elevated, hypercontracture can occur (Rodrigo & Standen, 2005) (Figure 3.19). The severity of hypercontracture determines whether cardiomyocytes relax from hypercontracture, the state of mPTPs then determine whether the cardiomyocytes remain in a quiescent state or regain contractile recovery, as opening of mPTP results in cell death, while closure supports recovery of contraction. Increasing extracellular glucose ($\geq 20\text{mM}$ glucose), resulted in

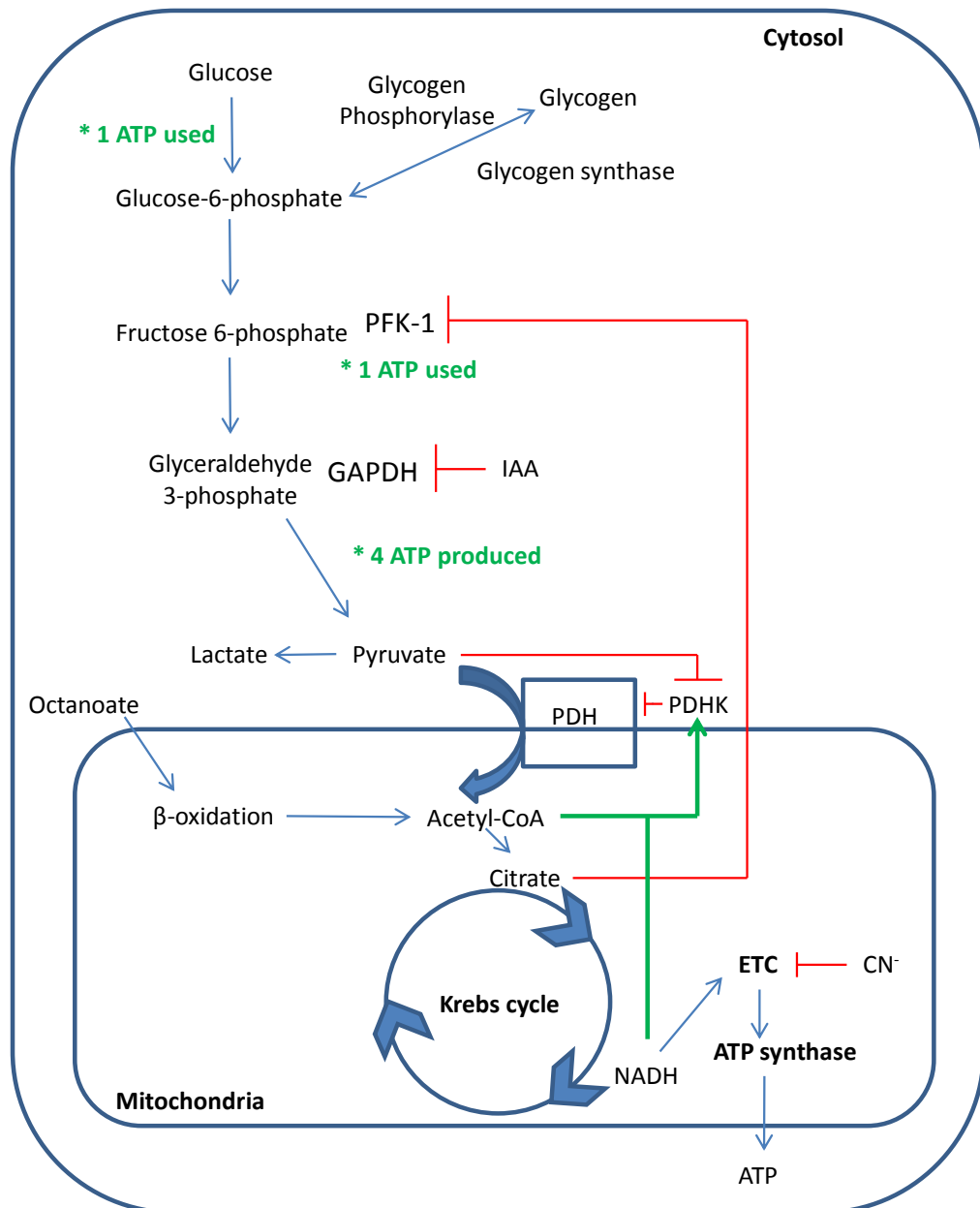


Figure 3.18 Regulation of enzymes involved in both cytosolic and mitochondrial ATP production.

The diagram represents how both PDH and PFK-1 can be inhibited (indicated in red) or stimulated (indicated by green) by products of the Krebs cycle, pyruvate and acetyl-CoA. The concentration of pyruvate would affect the level of PDHK inhibition, which would go onto affect how much PDH is inhibited. Inhibition of PFK-1 would inhibit glycolysis. The diagram also shows where the metabolic poisons (IAA and CN⁻) inhibit glycolysis and ETC respectively.

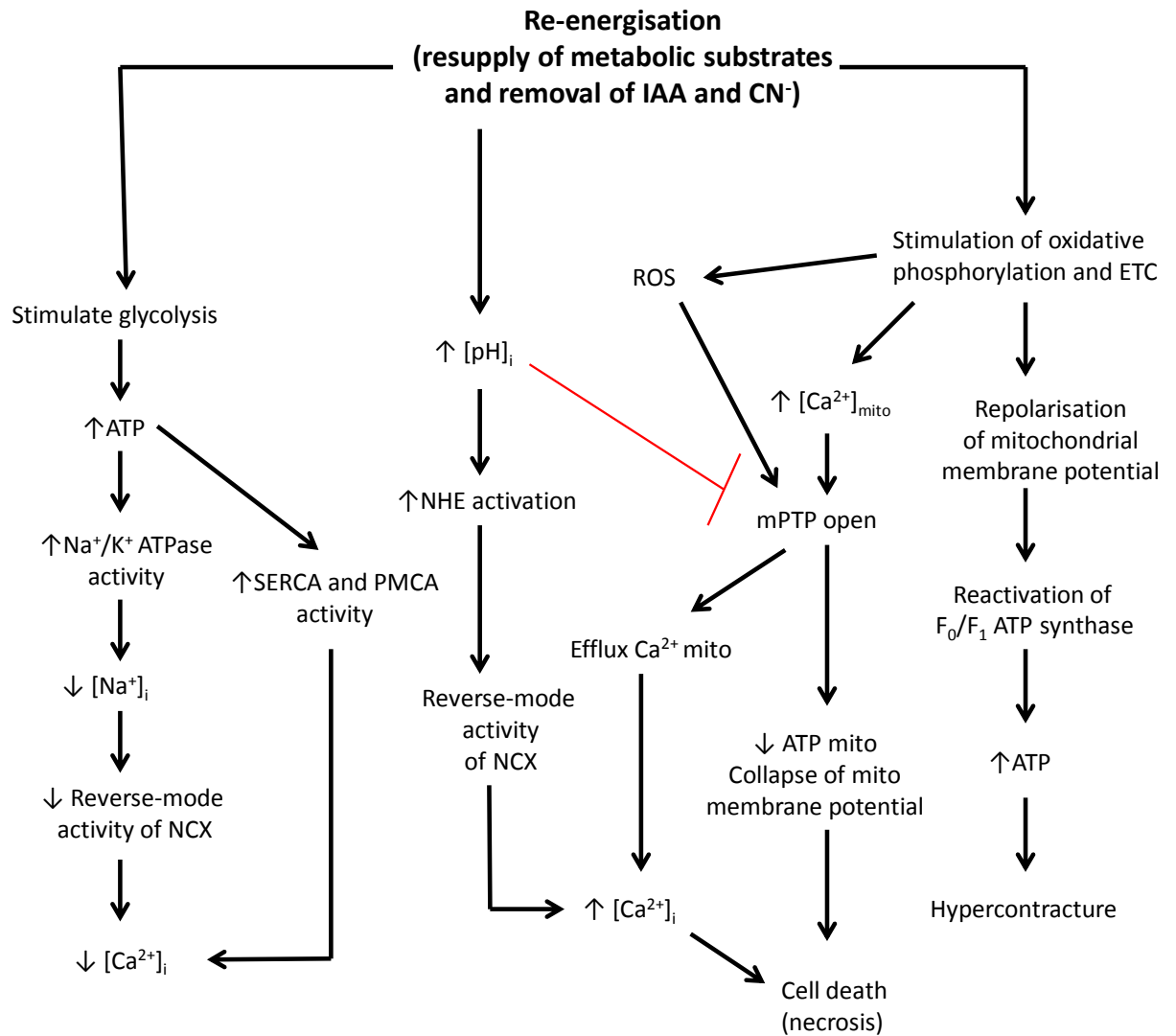


Figure 3.19 The effects of re-energisation

The diagram shows the various pathways stimulated by the removal of IAA and CN⁻ and the resupply of metabolic substrates. Both cytosolic and mitochondrial pathways are activated giving rise to hypercontracture and cell death. Mito =mitochondrial. Diagram adapted from Rodrigo *et al.*, 2002.

an increase in the percentage of 'non-hypercontracted' cardiomyocytes by the end of 10 minutes of re-energisation. Due to reperfusion induced hypercontracture requiring mitochondria re-energisation and increased ATP production via oxidative phosphorylation, but not Ca^{2+} influx or opening of mPTP (Rodrigo & Standen, 2005). This result could suggest perfusion with elevated glucose during re-energisation, is initially resulting in greater glycolytic ATP production compared to oxidative phosphorylation ATP production. As a result of the reduced stimulation of oxidative phosphorylation, less severe hypercontracture would occur and could be causing the increase in 'non-hypercontracted' cardiomyocytes (Figure 3.20). However, perfusion with 30mM glucose had no effect on the percentage of 'non-hypercontracted' cardiomyocytes suggesting these cardiomyocytes may of had a similar ATP and/or $[\text{Ca}^{2+}]_i$ level as those perfused with 5mM glucose.

3.3.2.2 Re-energisation with elevated glucose improves ATP production but does not alter Ca^{2+} levels

A delay in stimulation of oxidative phosphorylation with hyperglycaemic glucose concentrations is possible as during re-energisation a slow decline in Mg^{2+} -Green fluorescence was observed, but this was not until the latter stages of re-energisation. This late decline could correlate with delayed repolarisation of the mitochondria, resulting in delayed oxidative phosphorylation ATP production, which would result in less hypercontracture (Rodrigo & Standen, 2005). As the decline was more gradual under hyperglycaemic conditions; this could indicate repolarisation of the mitochondria happens sooner resulting in improved ATP production. The difference in Mg^{2+} -Green fluorescence was lower under hyperglycaemic conditions compared to normoglycaemic conditions, which could also indicate improved recovery of ATP.

Improved glycolytic ATP production with hyperglycaemic glucose concentrations may be expected to prevent the Ca^{2+} overload associated with re-energisation and lower $[\text{Ca}^{2+}]_i$, this is due to glycolytic ATP being involved in maintaining Ca^{2+} homeostasis, in particular maintaining SERCA activity (Xu *et al.*, 1995; Kockskamper *et al.*, 2005; Zima *et al.*, 2006). During ischaemia, ADP levels increase, decreasing SERCA activity. However the close proximity of many of the glycolytic enzymes to the SR membrane

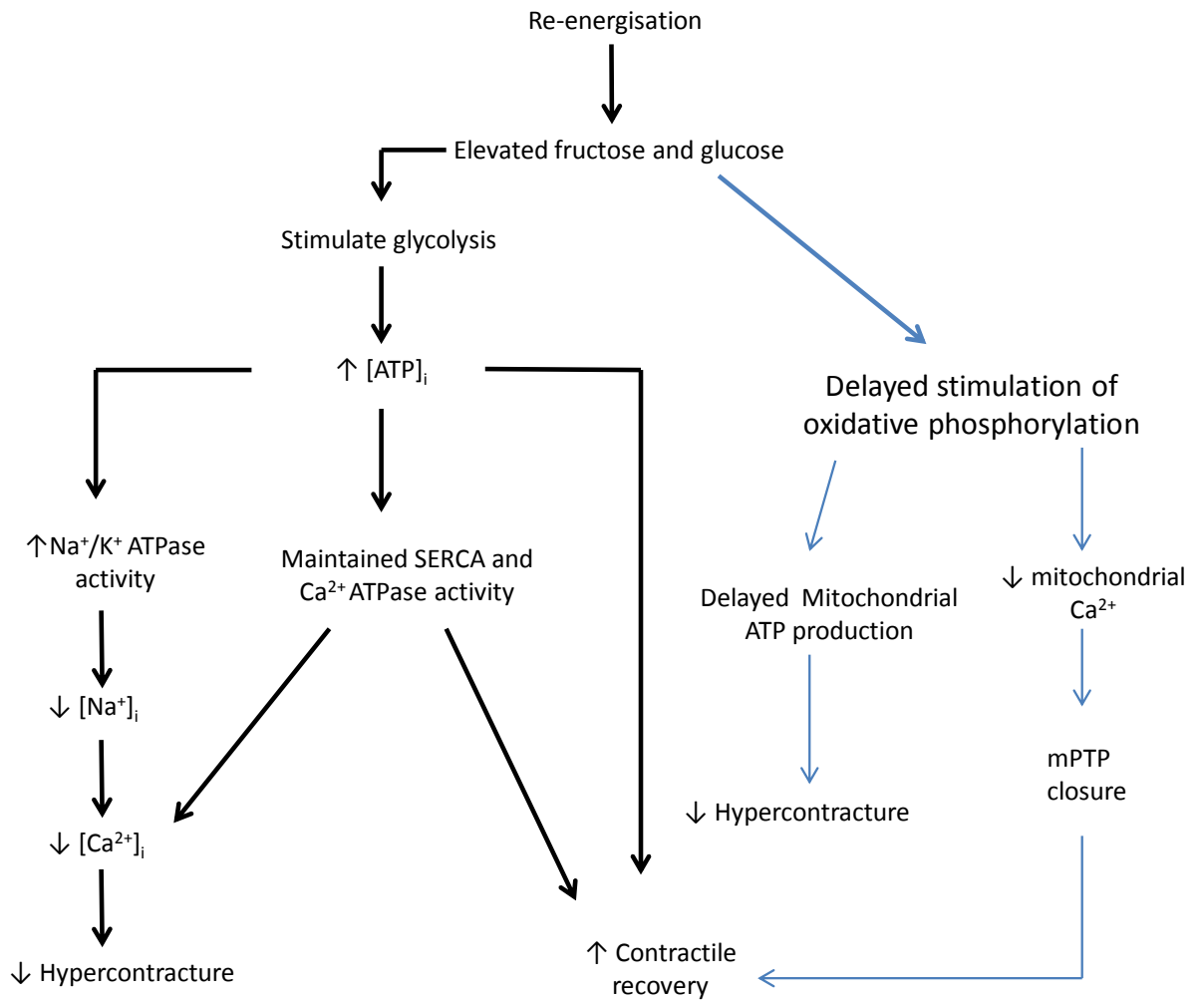


Figure 3.20 The hypothesised mechanisms behind cardioprotection seen with elevated metabolic substrates during re-energisation.

The diagram shows the hypothesised pathways elevated fructose and glucose are stimulating upon re-energisation. Pathways activated in the cytosol are indicated in black, while those in possibly stimulated by glucose in the mitochondria are indicated in blue.

means local concentrations of ATP would remain elevated and support Ca^{2+} homeostasis (Zima *et al.*, 2006).

In isolated rat cardiomyocytes during reperfusion, $[\text{Ca}^{2+}]_i$ has been shown to transiently fall upon reperfusion, then steadily increase (Rodrigo & Standen, 2005). In this study a similar profile was observed with both glucose concentrations showing higher Fura-2 ratios at the end of re-energisation compared to the Fura-2 ratio recorded at basal. There was no difference in the Fura-2 ratios between normoglycaemic and hyperglycaemic conditions by the end of 10 minutes of re-energisation, suggesting hyperglycaemia does not improve Ca^{2+} homeostasis or prevent Ca^{2+} overload associated with re-energisation. The lack of reduction in $[\text{Ca}^{2+}]_i$ could relate to the time length of re-energisation, as during global ischaemia $[\text{Ca}^{2+}]_i$ increases and further increases in early reperfusion, but recovers during later reperfusion (15-20 minutes) (Jeremy *et al.*, 1992), suggesting had the period of "re-energisation" in this study been longer than 10 minutes, a reduction in $[\text{Ca}^{2+}]_i$ may have been seen. Elevated $[\text{Ca}^{2+}]_i$ during re-energisation, could lead to mitochondrial overload, this would result in uncoupling of oxidative phosphorylation (Jeremy *et al.*, 1993). As a result, pyruvate would be converted into lactate, raising $[\text{pH}]_i$, which could prevent reactivation of the contractile machinery but could also prevent mPTP opening.

Although Ca^{2+} homeostasis was not improved under hyperglycaemic conditions, there was a significant increase in the percentage of cardiomyocytes recovering Ca^{2+} transients. This recovery correlated with contractile recovery data. The percentage of cardiomyocytes recovering with a low Fura-2 ratio (<0.85) following metabolic inhibition and re-energisation was not different between hyperglycaemic and normoglycaemic conditions. Previously a correlation between inhibition of Ca^{2+} influx or mPTP opening (during the first 10 minutes of re-energisation), has been found to increase the percentage of cardiomyocytes recovering with lower $[\text{Ca}^{2+}]_i$ and recovering contracting in response to EFS (Rodrigo & Standen, 2005). This suggest the higher recovery under hyperglycaemic conditions could be as a result of inhibition of the reverse mode NCX due to re-established Na^+/K^+ ATPase activity immediately upon

re-energisation, or due to a delay in mitochondrial repolarisation causing inhibition of mPTP (Figure 3.20).

3.3.2.3 Perfusion with elevated glucose improves contractile recovery during re-energisation

The effect of perfusion with hyperglycaemic glucose concentrations prior to metabolic inhibition and during re-energisation was to increase the percentage of cardiomyocytes recovering contractile function. This fits with previous whole heart studies, which have shown perfusing with elevated glucose (11-30mM) with or without 1000 μ U/140mU insulin, prior to ischaemia and during reperfusion improves functional recovery. This has been attributed to elevated glucose increasing ATP via glycolysis (Vanoverschelde *et al.*, 1994; Wang *et al.*, 2005; Jeremy *et al.*, 1992; Bricknell & Opie, 1978). The improved contractile recovery could also be due to elevated glycolytic ATP production stimulating Na⁺/K⁺ ATPase to work immediately upon re-energisation, therefore reducing potential re-energisation injury as indicated in Figure 3.20. Glycolytic ATP (derived from glucose or glycogen), has previously been associated with maintaining Na⁺/K⁺ ATPase activity during ischaemia, preventing Na⁺ accumulation, resulting in improved contractile recovery upon reperfusion (Van Emous *et al.*, 2001; Cross *et al.*, 1995; Dizon *et al.*, 1998). Functional recovery and prevention of Ca²⁺ overload in the post-ischaemic heart has been shown to require intact glycolysis in early reperfusion, even if oxidative phosphorylation substrates such as pyruvate or acetate are available (Jeremy *et al.*, 1993; Jeremy *et al.*, 1992). The Fura-2 data in this study suggest hyperglycaemic conditions do not prevent the Ca²⁺ overload. As contractile recovery is increased though, it could be proposed that Ca²⁺ entry is limited which aids recovery. In addition, this study used rats cardiomyocytes, which could contribute to the recovery rates, as rat cardiomyocytes have more resistance to metabolic inhibition (2.5mM NaCN and no glucose) compared to those from guinea pigs (Williams *et al.*, 2000). This resistance could mean increased recovery with elevated glucose concentrations is likely to be a reflection of increased glycolytic flux as all cardiomyocytes would have a standard recovery level. The length of time of exposure to hyperglycaemia can also impact on post-ischaemic recovery, with longer periods of induction stimulating apoptotic cell death and increased production of free

radicals (Brownlee, 2005; Fiordaliso *et al.*, 2001; Mapanga *et al.*, 2014) which can be toxic to cardiomyocytes. However as the perfusate used also contained pyruvate, a powerful antioxidant, any ROS being produced may be successfully scavenged preventing cell death (Mallet, 2000).

A previous study has shown perfusing isolated cardiomyocytes with 20mM glucose results in a similar percentage recovery as those perfused with 5mM glucose but a higher percentage of hypercontracture (Sims *et al.*, 2014). This contradicts the observations in this thesis and could relate to differences in the time length of incubation with glucose prior to the experiments. Without detailed information on the duration of incubation with elevated glucose prior to the experiments, and information on the parameters measure prior to SFT-MI (i.e. time to contractile failure and rigor development) and exactly how the data was analysed it is difficult to explain why the results differ between the two sets of experiments. For example if incubation time and parameters measured prior to SFT-MI were known a comparison could be made as to whether the effect is due to longer exposure to elevated glucose.

3.3.3 The impact of acute hypoglycaemic conditions prior to metabolic inhibition and during re-energisation

Hypoglycaemia can be just as detrimental to an impaired myocardium following an AMI, so prevention of hypoglycaemia is an important issue in a clinical setting. Acute hypoglycaemic conditions were achieved by perfusing with 2mM glucose. This resulted in no effect on the time to contractile, action potential failure, on the time to rigor, or on APD₉₀ compared to normoglycaemic conditions (5mM glucose). These results suggest that perfusion with a hypoglycaemic glucose concentration of 2mM results in similar levels of ATP as those perfused under normoglycaemic conditions and therefore the effects of metabolic inhibition would be similar to those seen in Figure 3.16. As hypoglycaemia had no effect of on SarCK_{ATP} channel activation compared to normoglycaemia, this could suggest ATP levels are similar to those perfused under normoglycaemic conditions.

Acute hypoglycaemic conditions significantly hyperpolarised the RMP this could indicate an increase in K⁺ conductance, a previous study on the guinea pig

hippocampal neurones suggest glucose depletion causes an increase in K^+ conductance (Spuler *et al.*, 1988). To fully establish the cause of this hyperpolarisation more experiments would be required.

Perfusing with an acute hypoglycaemic glucose concentration also had no effect on the percentage of cardiomyocytes either being 'non-hypercontracted' or regaining contractile function by the end of 10 minutes of re-energisation compared to those under normoglycemic conditions. These results suggest perfusion with an acute hypoglycaemic glucose concentration is detrimental to the cardiomyocytes and thus "ischaemic and reperfusion" injury mechanisms as outlined in Figure 3.19 cannot be prevented. Inducing hypoglycaemia with insulin before and after an AMI in canine myocardium has also been shown to result in increased necrosis and creatine kinase release and elevated ST-segment (Libby *et al.*, 1975). This study suggests hypoglycaemia has a detrimental effect on the cardiac tissue and is in line with our findings.

3.3.4 The effect of perfusion with elevated fructose during metabolic inhibition and re-energisation

As fructose feeds into glycolysis at a different point to glucose (at PFK-1), it was hypothesised that elevated fructose may result in similar results as elevated glucose. Fructose, like glucose, can be metabolised anaerobically during metabolic inhibition, but would be inhibited by IAA suggesting any effect fructose has would be prior to, or in the very early stages of, metabolic inhibition and these would recommence upon removal of IAA.

Although a delay in contractile failure was observed when elevating extracellular fructose from 5mM to 20mM, this did not reach significance ($P=0.06$). It is proposed that a significant delay may have been achieved had a large N number been obtained. This finding could suggest elevated fructose may be able to support contraction which is in agreement with Mellor *et al* (2011), who found that an acute application of fructose (11mM) to cardiomyocytes supported ECC, they propose fructose is achieving this by generating ATP which either supports SERCA or the Na^+/K^+ ATPase, resulting in maintained activity of the NCX (Mellor *et al.*, 2011). However elevating extracellular

fructose had no effect on the time to rigor, which could suggest elevating fructose can improve ATP levels at the sarcolemmal membrane but not the myofibrils, suggesting rigor development here may be reliant on mitochondrial ATP.

Perfusing with elevated fructose upon re-energisation would be expected to re-establish glycolytic ATP production. Elevating fructose had no effect on the percentage of 'non-hypercontracted' cardiomyocytes by the end of 10 minutes of re-energisation. Due to fructose feeding in below glucose hexokinase, fructose metabolism can be less controlled. Therefore with elevated fructose higher NADH/FADH₂ levels were expected which would lead to increased stimulation of oxidative phosphorylation when re-energisation commenced, therefore a greater percentage of hypercontracture was expected which would have reduced the level of 'non-hypercontracture'.

Perfusion with elevated fructose prior to metabolic inhibition and during re-energisation increased the percentage of cardiomyocytes recovering contractile function, compared to those perfused with 5mM fructose, this suggest a role for elevated fructose in cardioprotection. It is proposed that fructose has similar effects as glucose upon re-energisation as outlined in Figure 3.20. However as the exact mechanisms by which fructose and glucose are working is not established here, it cannot be ruled out fructose is working via independent mechanisms to glucose. Short periods of fructose application have been suggested to be protective, due to fructose having a direct effect, possibly via increasing glycogen stores or by activity MitoK_{ATP} (Jordan *et al.*, 2003). Fructose could be increasing glycogen stores in our cardiomyocytes as the heart, like the liver, contains fructokinase which converts fructose to glycogen. However fructokinase activity within the heart is minimal (Bais *et al.*, 1985) suggesting this may not impact greatly. If fructose was activating MitoK_{ATP}, this could imply similar pathways to IPC such as preventing mPTP opening are being activated (as indicated in Figure 1.13). Fructose preventing mPTP opening is a similar proposed mechanism for the effects of elevated glucose (Figure 3.20).

CHAPTER FOUR

The role of oxidative phosphorylation metabolic substrates in isolated cardiomyocytes subjected to metabolic inhibition and re-energisation

4. The role of oxidative phosphorylation metabolic substrates in isolated cardiomyocytes subjected to metabolic inhibition and re-energisation

4.1 Introduction

Under normal physiological conditions, a higher proportion of the ATP required for the myocardium to maintain proper function comes from mitochondrial oxidative phosphorylation (i.e. metabolism of fatty acids and pyruvate). In chapter 3, it was demonstrated that perfusing isolated cardiomyocytes, prior to metabolic inhibition and during re-energisation, with elevated concentrations of glycolytic metabolic substrates (glucose and fructose), resulted in a metabolic-dependent cardioprotection, as seen by an increase in the percentage of cardiomyocytes recovering contractile function by the end of re-energisation.

Aerobic glucose metabolism produces a limited amount of ATP (approximately 31 ATP/1 glucose or fructose molecule) and reducing agents.

However the initial glycolysis stage results in the production of pyruvate, which enters the Krebs cycle and produces larger quantities of reducing agents (which maintain the ETC) and ATP. As a result this study aims to investigate the impact of metabolic substrates (pyruvate and fatty acid) which feed directly into the Krebs cycle.

Previous whole heart ischaemia and reperfusion studies have shown that perfusion with 1.2mM palmitate (long chain fatty acid) and glucose (11mM), prior to no flow ischaemia and during reperfusion, reduced the rate of glucose oxidation (during reperfusion) compared to those perfused solely with glucose (11mM) throughout the protocol. This suggests that fatty acids were the preferred substrate as indicated by the ATP production rate (Lopaschuk *et al.*, 1990). This supports findings by Johnston *et al* (1990), who observed that reperfusion with 2mM palmitate (following pre-ischaemic perfusion with 5mM glucose), resulted in a small increase in ATP but greater contractile dysfunction, compared to those reperfused with either glucose (10mM) or glucose and palmitate (Johnston & Lewandowski, 1991). However perfusion with 0.5mM palmitate prior to global ischaemia and during reperfusion has also been shown to be detrimental, in terms of increased LDH release and more severe

arrhythmias upon reperfusion, compared to those perfused with 11mM glucose (Bricknell & Opie, 1978). These results suggest that although fatty acids are still favoured by the myocardium following ischaemia, their presence upon reperfusion (without glucose) can be detrimental. This may be due to fatty acid oxidation inhibiting glucose oxidation. As a result it has been suggested that stimulation of glucose oxidation (either directly by pyruvate or pharmacological stimulation of PDH) could be beneficial, possibly due to the fact that pyruvate can effectively increase glucose oxidation by supplying the mitochondria with a more readily available substrate for ATP production.

Rats fed pyruvate (0.5g/kg/day) for 4 weeks, prior to ischaemia and reperfusion, are able to restore arterial pressure during reperfusion and levels of creatine phosphokinase-MB isoenzyme and the antioxidant glutathione, and also restore catalase activity compared to rats not fed pyruvate (Arya *et al.*, 2006). Pharmacological stimulation of the mitochondrial located enzyme, pyruvate dehydrogenase (PDH), which converts pyruvate into acetyl-CoA, via inhibition of PDH Kinase (PDHK) with dichloroacetate (DCA), has also been found to reduce infarct size, improve cardiac function and increase glucose oxidation during reperfusion (Ussher *et al.*, 2012).

Due to these reported effects of pyruvate and fatty acid, and the impact that these substrates have on the ETC, the experiments carried out in this chapter were designed to investigate the impact of pyruvate and fatty acid (both of which feed directly into Krebs), on the contractile function and cellular responses of isolated cardiomyocytes to metabolic inhibition and re-energisation.

The results in this chapter will describe the effects of acute changes (prior to metabolic inhibition and during re-energisation) in extracellular pyruvate (to a physiological and a supraphysiological concentration) and of a medium chain fatty acid (octanoate), in association with either a normoglycaemic (5mM glucose) or hyperglycaemic (20mM glucose) extracellular glucose concentration, on the contractile and electrical responses of isolated cardiomyocytes, during metabolic inhibition and re-energisation.

In this chapter, the data recorded under normoglycaemic conditions (5mM glucose) in sections 4.2.1-4.2.6 were recorded on the same day, this allows for a direct

comparison of the data. However the data recorded under hyperglycaemic conditions (20mM glucose) were not recorded on the same day. Therefore the control data (5mM glucose/5mM pyruvate) for each data set will be shown and the difference between these controls assessed statistically to confirm day-to-day repeatability. Each treatment group will then be normalised to its own control and a percentage change in the specific variable calculated to allow a statistical comparison to be performed. For section 4.2.7 which investigated the effect of octanoate, both data sets were not recorded on the same day and as a result all data were normalised to their respective control before a statistical comparison was performed.

4.2 Results

4.2.1 The effect of reducing extracellular pyruvate on isolated cardiomyocytes exposed to metabolic inhibition and re-energisation

Pyruvate can suppress oxidation of glucose at concentrations as little as 1mM (Moreno *et al.*, 2010) and as perfusion with 5mM pyruvate inhibits glycolysis, as indicated by a decrease in the rate of glycolytic ATP production (Bricknell & Opie, 1978). It was decided that the extracellular pyruvate concentration would be reduced to a submillimolar concentration of 0.5mM, which is at the higher end of the normal physiological pyruvate range of 0.3-0.5mM (Longmore, 1968).

To determine the effects of reducing extracellular pyruvate in association with either normoglycaemic or hyperglycaemic conditions, on the contractile function of isolated cardiomyocytes during metabolic inhibition and re-energisation, isolated cardiomyocytes were subjected to the protocol as described in section 3.2.1 and shown in Figure 3.1. The same variables outlined in section 3.2.1 were measured as markers of ischaemic injury (time to contractile failure and rigor contracture from the onset of metabolic inhibition) and the same markers of protection against re-energisation injury (percentage of 'non-hypercontracted' cardiomyocytes and percentage recovery by the end of 10 minutes of re-energisation) were calculated.

The time-dependent effects of an acute reduction in extracellular pyruvate in association with acute changes in extracellular glucose are shown in Figure 4.1 and

show a similar profile of contractile failure and partial recovery on re-energisation as those perfused with 5mM pyruvate.

Reducing extracellular pyruvate from 5mM to 0.5mM under normoglycaemic conditions significantly reduced the time to contractile failure (Figure 4.2A), from 196.7 ± 9.7 s to 157.2 ± 9.0 s ($P < 0.05$) respectively.

The control data (5mM glucose/5mM pyruvate) for the time to contractile failure is shown in Figure 4.2B. The control time to contractile failure recorded on the same day as those perfused with 20mM glucose and 5mM pyruvate was 193.5 ± 9.3 s, this was not significantly different to the controls recorded on the same day as those perfused with 20mM glucose and 0.5mM pyruvate (196.7 ± 9.7 s, $P = 0.82$).

Under hyperglycaemic conditions, prior to normalisation the time to contractile failure (Figure 4.2C), for those recorded with 5mM pyruvate was 223.0 ± 8.8 s and 170.4 ± 3.0 s for those recorded with 0.5mM pyruvate. Once normalised, using the respective control data, the percentage change in the time to contractile failure (Figure 4.2D) was significantly reduced for those perfused with 0.5mM pyruvate ($85.1 \pm 4.7\%$) compared to 5mM pyruvate ($116.9 \pm 9.4\%$, $P < 0.05$).

The effects of reducing extracellular pyruvate from 5mM to 0.5mM under normoglycaemic conditions was to significantly reduce the time to rigor (Figure 4.3A), from 307.2 ± 9.1 s to 244.9 ± 5.8 s ($P < 0.001$) respectively.

The control time to rigor (Figure 4.3B) recorded on the same day as those perfused 20mM glucose and 5mM pyruvate was 310.7 ± 20.1 s, this was not significantly different to the controls recorded on the same day as those perfused with 20mM glucose and 0.5mM pyruvate (307.2 ± 9.1 s, $P = 0.89$).

Under hyperglycaemic conditions, prior to normalisation the time to rigor (Figure 4.3C), for those recorded with 5mM pyruvate was 325.7 ± 17.2 s and 250.4 ± 4.7 s for those recorded with 0.5mM pyruvate. Following normalisation, the percentage change in time to rigor (Figure 4.3D) was significantly reduced when extracellular pyruvate was reduced from 5mM ($105.7 \pm 5.3\%$) to 0.5mM pyruvate ($80.9 \pm 3.1\%$, $P < 0.01$).

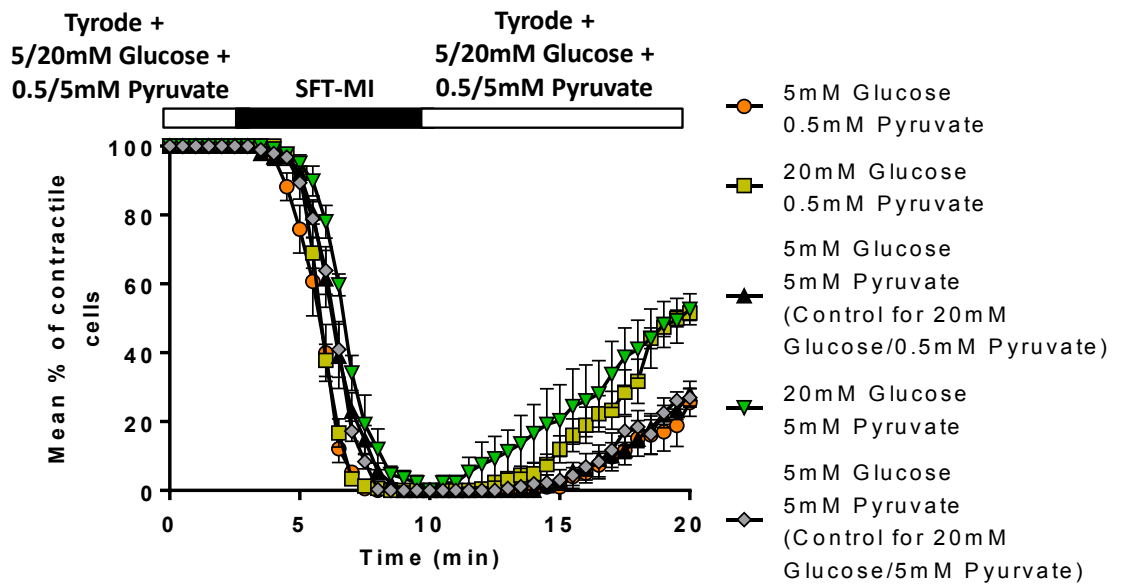


Figure 4.1 The effect of an acute reduction in extracellular pyruvate on the response of isolated cardiomyocytes to metabolic inhibition and re-energisation in response to acute changes in extracellular glucose.

Time course of the percentage of cardiomyocytes contracting in response to EFS, during perfusion with SFT-MI and re-energisation. Prior to SFT-MI and during the 10 minutes of re-energisation cardiomyocytes were superfused with Tyrode solution containing 5mM or 20mM glucose with either 0.5mM or 5mM pyruvate. Data represented as mean \pm s.e.m. Data for 5mM glucose, 5mM pyruvate (black bar, N=4 hearts, 4 fields of view, 154 cardiomyocytes) and 0.5mM pyruvate (orange bar, N=4, 6, 133). Control data (5mM glucose/5mM pyruvate) for the 20mM glucose/5mM pyruvate data (grey bar, N=5, 5, 189) and for 20mM glucose/0.5mM pyruvate (black bar, N=4, 4, 154). Data for 20mM glucose, 5mM pyruvate (green bar, N=5, 5, 108) and 0.5mM pyruvate (yellow bar, N=4, 6, 169).

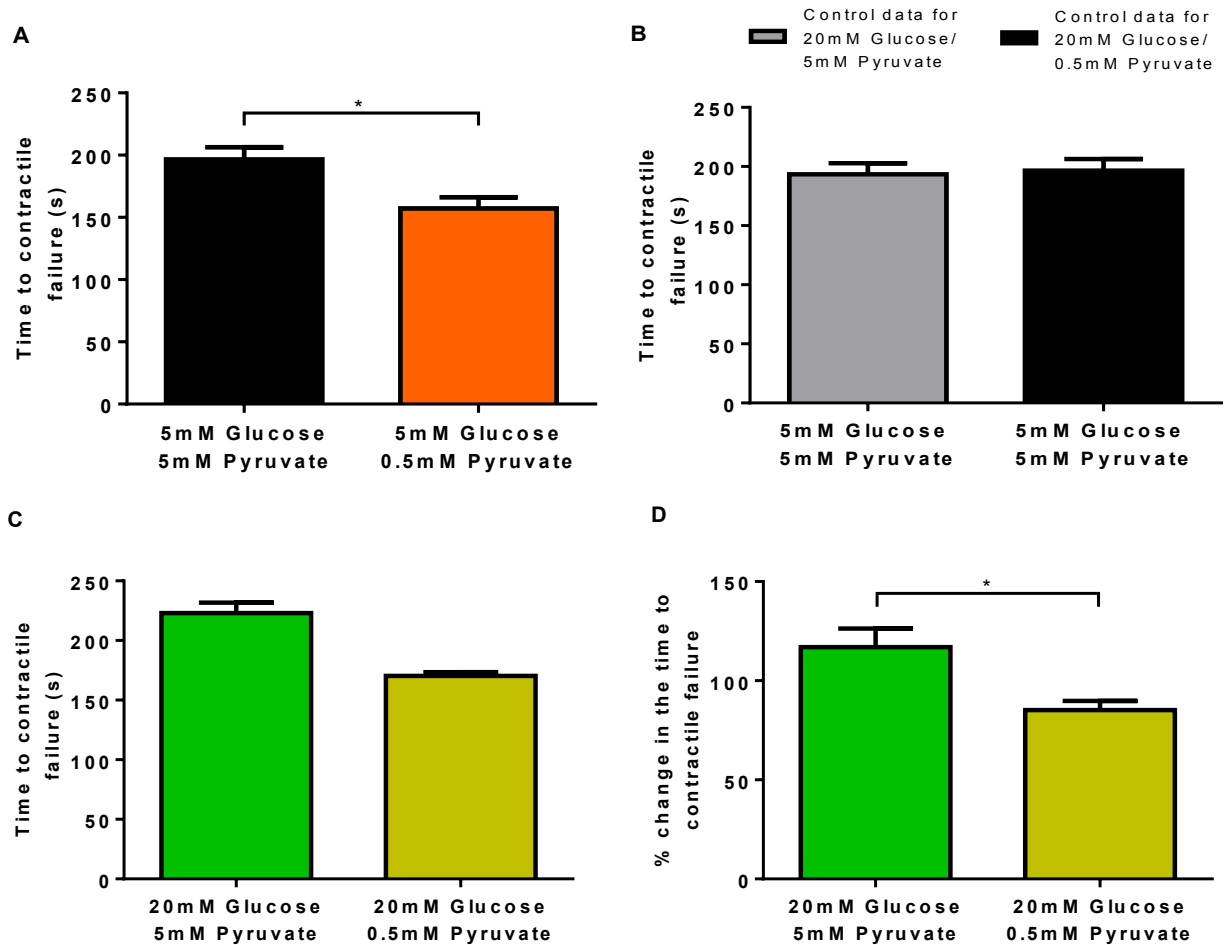


Figure 4.2 The effect of a reduction in extracellular pyruvate on the time to contractile failure during metabolic inhibition in response to acute changes in extracellular glucose.

- (A) Time to contractile failure from the onset of metabolic inhibition for cardiomyocytes superfused with 5mM glucose and either 5mM or 0.5mM pyruvate.
- (B) Time to contractile failure from the onset of metabolic inhibition for the control data (5mM glucose/5mM pyruvate) recorded at the beginning of each day for the 20mM glucose data sets.
- (C) Time to contractile failure from the onset of metabolic inhibition for cardiomyocytes superfused with 20mM glucose and either 5mM or 0.5mM pyruvate.
- (D) Normalised time to contractile failure for the 20mM glucose data sets represented as a % change in the time to contractile failure. Each 20mM glucose treatment group was normalised to its corresponding control, the 5mM pyruvate data (green bar) was normalised to the grey bar in (B) and the 0.5mM pyruvate data (yellow bar) was normalised to the black bar in (B).

Data represented as mean \pm s.e.m. Data for 5mM glucose, 5mM pyruvate (black bar, N=4 hearts, 4 fields of view, 154 cardiomyocytes) and 0.5mM pyruvate (orange bar, N=4, 6, 133). Control data (5mM glucose/5mM pyruvate) for the 20mM glucose/5mM pyruvate data (grey bar, N=5, 5, 189) and for 20mM glucose/0.5mM pyruvate (black bar, N=4, 4, 154). Data for 20mM glucose, 5mM pyruvate (green bar, N=5, 5, 108) and 0.5mM pyruvate (yellow bar, N=4, 6, 169). *P<0.05 (Unpaired T-test).

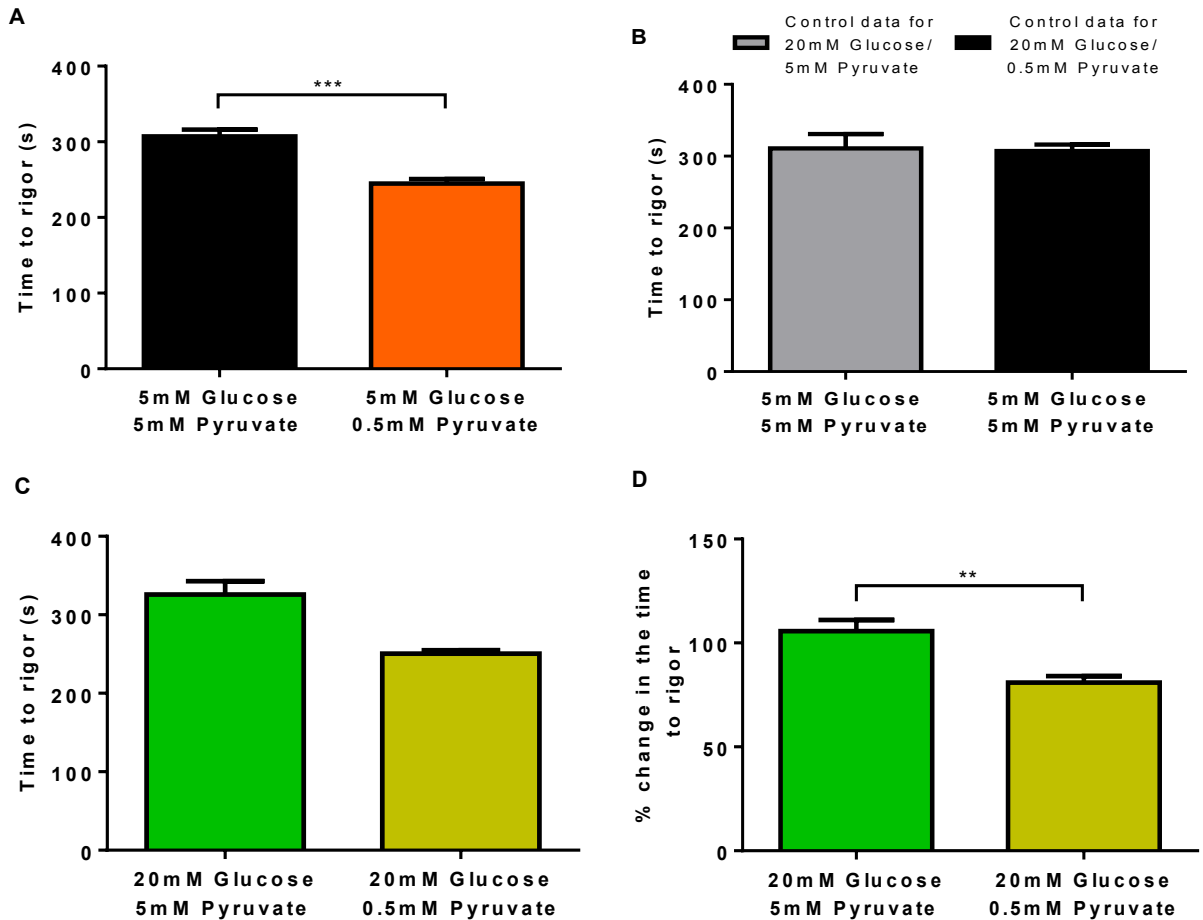


Figure 4.3 The effect of a reduction in extracellular pyruvate on the time to rigor contracture during metabolic inhibition in response to acute changes in extracellular glucose.

- (A) Time to rigor contracture from the onset of metabolic inhibition for cardiomyocytes superfused with 5mM glucose and either 5mM or 0.5mM pyruvate.
- (B) Time to rigor from the onset of metabolic inhibition for the control data (5mM glucose/5mM pyruvate) recorded at the beginning of each day for the 20mM glucose data sets.
- (C) Time to rigor contracture from the onset of metabolic inhibition for cardiomyocytes superfused with 20mM glucose and either 5mM or 0.5mM pyruvate.
- (D) Normalised time to rigor for the 20mM glucose data sets represented as a % change in the time to rigor. Each 20mM glucose treatment group was normalised to its corresponding control, the 5mM pyruvate data (green bar) was normalised to the grey bar in (B) and the 0.5mM pyruvate data (yellow bar) was normalised to the black bar in (B).

Data represented as mean \pm s.e.m. Data for 5mM glucose, 5mM pyruvate (black bar, N=4 hearts, 4 fields of view, 154 cardiomyocytes) and 0.5mM pyruvate (orange bar, N=4, 6, 133). Control data (5mM glucose/5mM pyruvate) for the 20mM glucose/5mM pyruvate data (grey bar, N=5, 5, 189) and for 20mM glucose/0.5mM pyruvate (black bar, N=4, 4, 154). Data for 20mM glucose, 5mM pyruvate (green bar, N=5, 5, 108) and 0.5mM pyruvate (yellow bar, N=4, 6, 169). ** $P < 0.01$, *** $P < 0.001$ (Unpaired T-test).

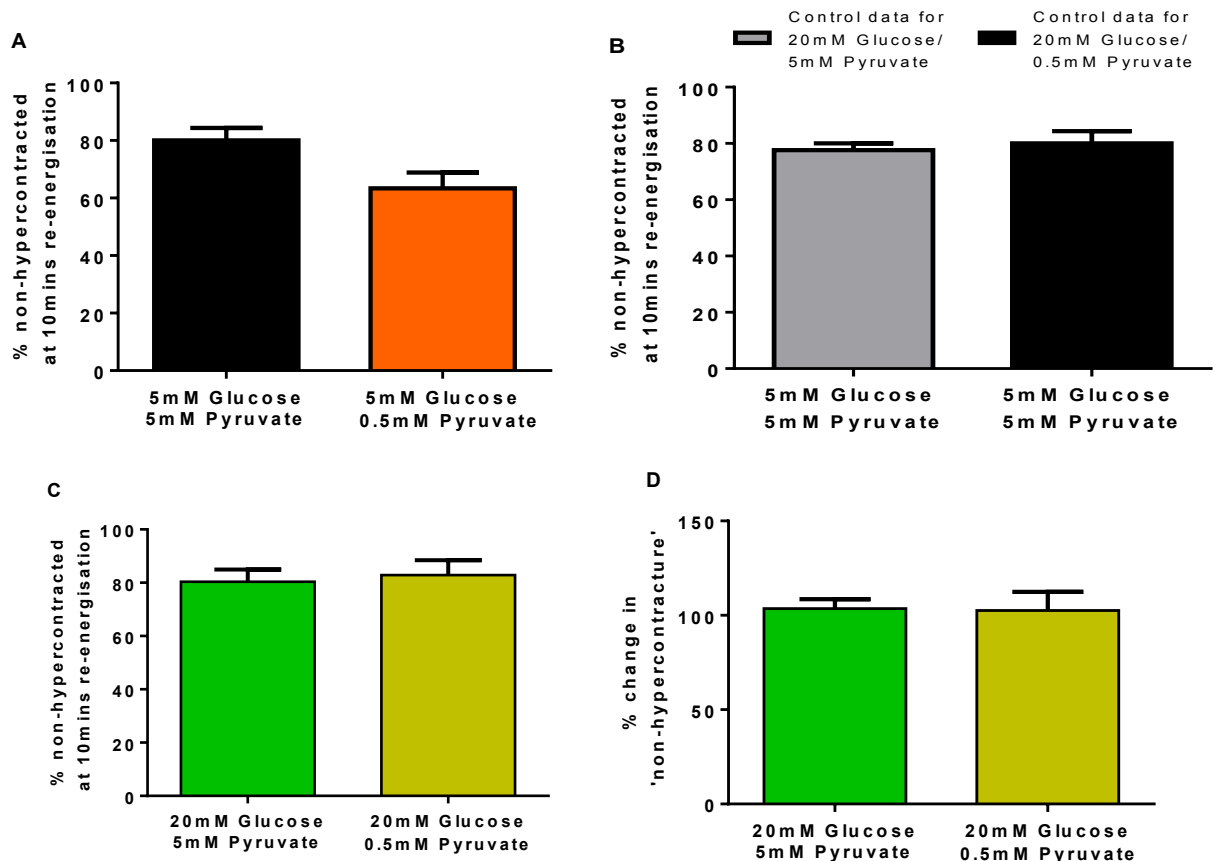


Figure 4.4 The effect of a reduction in extracellular pyruvate on the viability of isolated cardiomyocytes to metabolic inhibition and re-energisation in response to acute changes in extracellular glucose.

- (A) The percentage of cardiomyocytes relaxed from hypercontracted 'non-hypercontracted' by the end of 10 minutes of re-energisation following superfusion with 5mM glucose and either 5mM or 0.5mM pyruvate.
- (B) The percentage of cardiomyocytes relaxed from hypercontracted 'non-hypercontracted' by the end of 10 minutes of re-energisation for the control data (5mM glucose/5mM pyruvate) recorded at the beginning of each day for the 20mM glucose data sets.
- (C) The percentage of cardiomyocytes relaxed from hypercontracted 'non-hypercontracted' by the end of 10 minutes of re-energisation following superfusion with 20mM glucose and either 5mM or 0.5mM pyruvate.
- (D) Normalised percentage of 'non-hypercontracted' cardiomyocytes for the 20mM glucose data sets represented as a % change in 'non-hypercontracture'. Each 20mM glucose treatment group was normalised to its corresponding control, the 5mM pyruvate data (green bar) was normalised to the grey bar in (B) and the 0.5mM pyruvate data (yellow bar) was normalised to the black bar in (B).

Data represented as mean \pm s.e.m. Data for 5mM glucose, 5mM pyruvate (black bar, N=4 hearts, 4 fields of view, 154 cardiomyocytes) and 0.5mM pyruvate (orange bar, N=4, 6, 133). Control data (5mM glucose/5mM pyruvate) for the 20mM glucose/5mM pyruvate data (grey bar, N=5, 5, 189) and for 20mM glucose/0.5mM pyruvate (black bar, N=4, 4, 154). Data for 20mM glucose, 5mM pyruvate (green bar, N=5, 5, 108) and 0.5mM pyruvate (yellow bar, N=4, 6, 169).

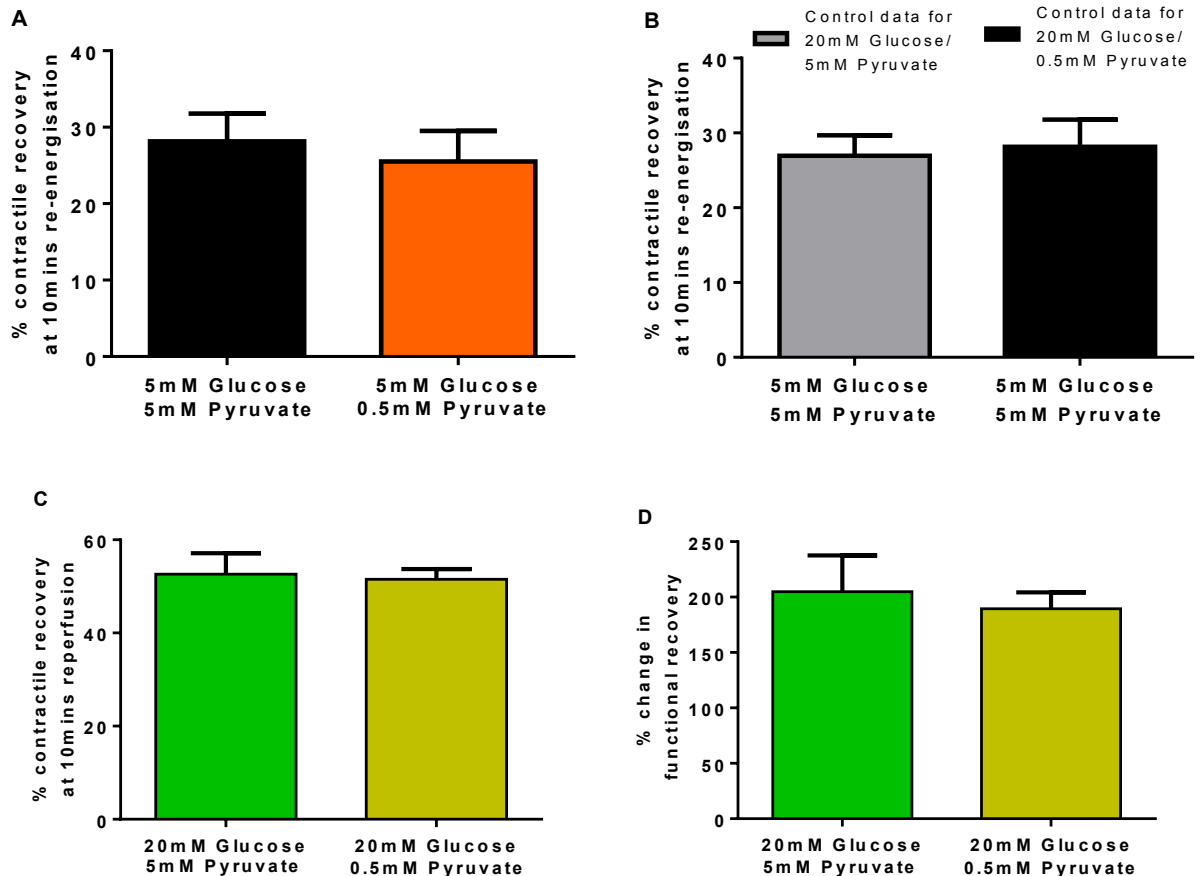


Figure 4.5 The effect of a reduction in extracellular pyruvate on the recovery of isolated cardiomyocytes to metabolic inhibition and re-energisat in response to acute changes in extracellular glucose.

- (A) The percentage of cardiomyocytes regaining contractile function in response to EFS by the end of 10 minutes of re-energisat following superfusion with 5mM glucose and either 5mM or 0.5mM pyruvate.
- (B) The percentage of cardiomyocytes regaining contractile function in response to EFS by the end of 10 minutes of re-energisat for the control data (5mM glucose/5mM pyruvate) recorded at the beginning of each day for the 20mM glucose data sets.
- (C) The percentage of cardiomyocytes regaining contractile function in response to EFS by the end of 10 minutes of re-energisat following superfusion with 20mM glucose and either 5mM or 0.5mM pyruvate.
- (D) Normalised contractile recovery for the 20mM glucose data sets represented as a % change in functional recovery. Each 20mM glucose treatment group was normalised to its corresponding control, the 5mM pyruvate data (green bar) was normalised to the grey bar in (B) and the 0.5mM pyruvate data (yellow bar) was normalised to the black bar in (B).

Data represented as mean \pm s.e.m. Data for 5mM glucose, 5mM pyruvate (black bar, N=4 hearts, 4 fields of view, 154 cardiomyocytes) and 0.5mM pyruvate (orange bar, N=4, 6, 133). Control data (5mM glucose/5mM pyruvate) for the 20mM glucose/5mM pyruvate data (grey bar, N=5, 5, 189) and for 20mM glucose/0.5mM pyruvate (black bar, N=4, 4, 154). Data for 20mM glucose, 5mM pyruvate (green bar, N=5, 5, 108) and 0.5mM pyruvate (yellow bar, N=4, 6, 169).

Reducing extracellular pyruvate from 5mM to 0.5mM under normoglycaemic conditions had no effect on the percentage of 'non-hypercontracted' cardiomyocytes (Figure 4.4A), with $80.1 \pm 4.3\%$ versus $63.3 \pm 5.8\%$ ($P=0.06$) respectively.

The control percentage of 'non-hypercontracted' cardiomyocytes (Figure 4.4B) recorded on the same day as those perfused with 20mM glucose and 5mM pyruvate was $77.6 \pm 2.4\%$, this was not significantly different to those controls recorded on the same day as those perfused with 20mM glucose and 0.5mM pyruvate ($80.1 \pm 4.3\%$, $P=0.61$).

Prior to normalisation the percentage of 'non-hypercontracted' cardiomyocytes under hyperglycaemic conditions (Figure 4.4C) was $80.3 \pm 4.6\%$ for those recorded with 5mM pyruvate and $82.8 \pm 5.6\%$ for those recorded with 0.5mM pyruvate. Once normalised, the percentage change in 'non-hypercontracture' (Figure 4.4D) shows reducing pyruvate from 5mM to 0.5mM had no effect with $103.6 \pm 5.0\%$ versus $102.6 \pm 9.9\%$ ($P=0.94$) respectively.

Under normoglycaemic conditions, reducing extracellular pyruvate from 5mM to 0.5mM had no effect on the percentage of contractile recovery (Figure 4.5A), with $28.1 \pm 3.6\%$ versus $25.5 \pm 4.0\%$ ($P=0.66$) respectively.

The control percentage of contractile recovery (Figure 4.5B), recorded on the same day as those perfused with 20mM glucose and 5mM pyruvate was $26.9 \pm 2.8\%$, this was not significantly different to those recorded on the same day as those perfused with 20mM glucose and 0.5mM pyruvate ($28.1 \pm 3.6\%$, $P=0.79$).

Prior to normalisation the percentage of contractile recovery for hyperglycaemic conditions (Figure 4.5C), for those recorded with 5mM pyruvate was $52.6 \pm 4.5\%$ and $51.5 \pm 2.2\%$ for those recorded with 0.5mM pyruvate. Following normalisation, there was no effect on the percentage change in contractile recovery (Figure 4.5D) with reducing extracellular pyruvate from 5mM ($204.9 \pm 32.7\%$) to 0.5mM ($189.5 \pm 19.9\%$, $P=0.66$).

In summary, these data suggest that perfusing with a reduced pyruvate concentration (0.5mM) under both normoglycaemic and hyperglycaemic conditions, reduces the

time to contractile failure and rigor contracture during metabolic inhibition, but had no effect on the variables measured during re-energisation.

4.2.2 The effects of reduced pyruvate on cardiac action potential behaviour during metabolic inhibition

In the contractile function experiments, perfusing isolated cardiomyocytes with 0.5mM pyruvate reduced the time to contractile failure; therefore it was hypothesised the action potential failure time during metabolic inhibition would also be reduced, as it has been shown that action potential failure during metabolic inhibition can cause contractile failure. To investigate this, action potentials were recorded (using the whole-cell patch-clamp technique) from isolated cardiomyocytes perfused with 0.5mM pyruvate, in association with either a normoglycaemic or hyperglycaemic glucose concentration.

Figure 4.6 shows action potentials recorded before and during perfusion with SFT-MI, selected to illustrate the changes that occur during metabolic inhibition. This figure concludes with the complete failure of the stimulus to trigger an action potential in the cardiomyocyte.

Reducing extracellular pyruvate from 5mM to 0.5mM under normoglycaemic conditions had no effect on the time to action potential failure (Figure 4.7A), with 142.0 ± 15.1 s (5mM pyruvate) versus 140.2 ± 9.8 s (0.5mM pyruvate, $P=0.92$).

The control (5mM glucose/5mM pyruvate) time to action potential failure (Figure 4.7B) recorded on the same day as those perfused with 20mM glucose and 5mM pyruvate was 149.0 ± 4.6 s, this was not significantly different to the controls recorded on the same day as those perfused with 0.5mM pyruvate (140.5 ± 13.5 s, $P=0.53$).

Under hyperglycaemic conditions, prior to normalisation the time to action potential failure (Figure 4.7C), for those recorded with 5mM pyruvate was 177.9 ± 10.2 s and 166.5 ± 10.5 s for those recorded with 0.5mM pyruvate. Once normalised, using the respective control data, the percentage change in the time to action potential failure (Figure 4.7D) shows reducing extracellular pyruvate from 5mM ($122.6 \pm 8.5\%$) to 0.5mM pyruvate ($129 \pm 14.3\%$), had no effect ($P=0.67$).

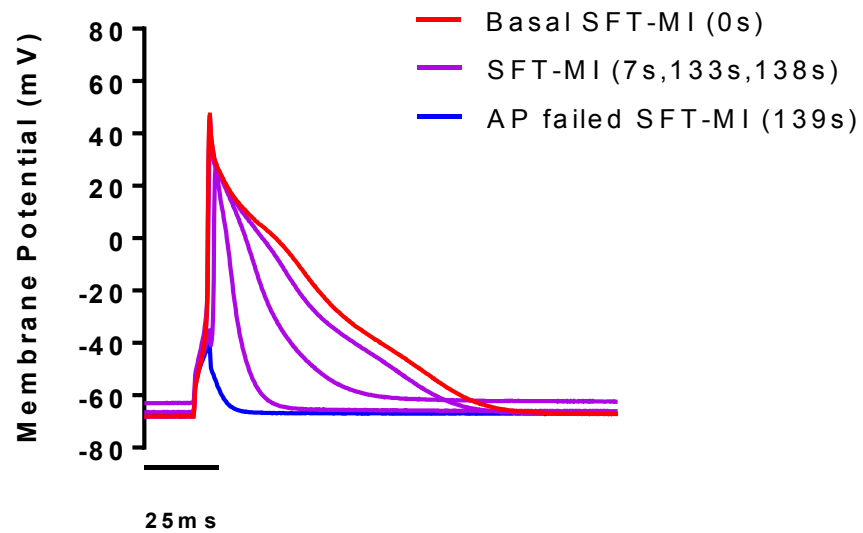


Figure 4.6 The effects of an acute reduction in extracellular pyruvate on the time to action potential failure during metabolic inhibition in response to acute changes in extracellular glucose.

Example traces of action potentials from a cardiomyocyte superfused with 0.5mM pyruvate and 5mM glucose prior to metabolic inhibition, showing shortening and eventual failure of the action potential.

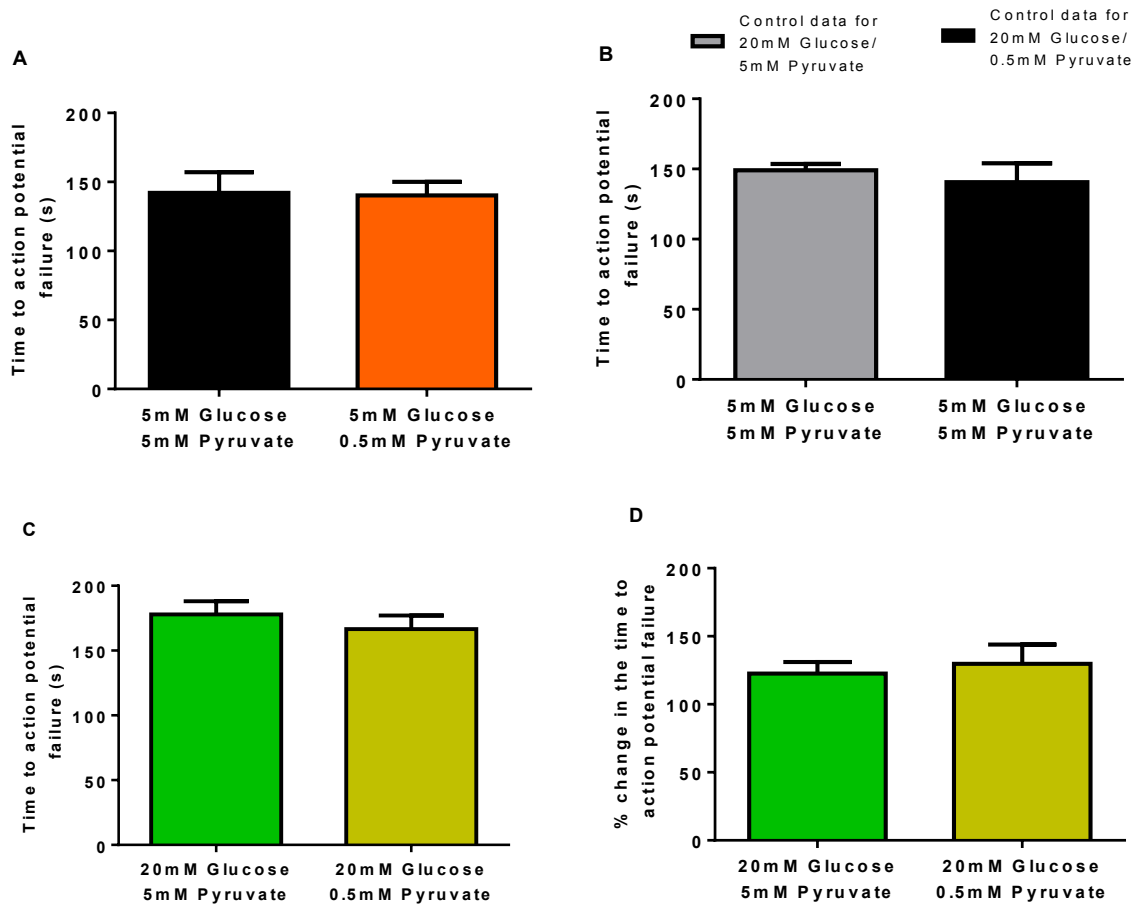


Figure 4.7 The effects of an acute reduction in extracellular pyruvate on the time to action potential failure during metabolic inhibition in response to acute changes in extracellular glucose.

- (A) The time to action potential failure for cardiomyocytes superfused with 5mM glucose and either 5mM or 0.5mM pyruvate prior to metabolic inhibition.
- (B) The time to action potential failure for the control data (5mM glucose/5mM pyruvate) recorded at the beginning of each day for the 20mM glucose data sets.
- (C) The time to action potential failure for cardiomyocytes superfused with 20mM glucose and either 5mM or 0.5mM pyruvate prior to metabolic inhibition.
- (D) Normalised time to action potential failure for the 20mM glucose data sets represented as a % change in time to action potential failure. Each 20mM glucose treatment group was normalised to its corresponding control, the 5mM pyruvate data (green bar) was normalised to the grey bar in (B) and the 0.5mM pyruvate data (yellow bar) was normalised to the black bar in (B).

Data represented as mean \pm s.e.m. Data for 5mM glucose, 5mM pyruvate (black bar, N=3 hearts, 3 experiments) and 0.5mM pyruvate (orange bar, N=3, 6). Control data (5mM glucose/5mM pyruvate) for the 20mM glucose/5mM pyruvate data (grey bar, N=5, 5) and for 20mM glucose/0.5mM pyruvate (black bar, N=4, 4). Data for 20mM glucose, 5mM pyruvate (green bar, N=5, 7) and 0.5mM pyruvate (yellow bar, N=4, 6).

From the same cardiomyocytes recorded for action potential failure times, 20 consecutive action potentials prior to SFT-MI were measured for APD₉₀ and RMP.

Under normoglycaemic conditions, reducing extracellular pyruvate from 5mM to 0.5mM had no effect on the APD₉₀ (Figure 4.8A), with $85.7 \pm 4.3\text{ms}$ versus $92.0 \pm 13.4\text{ms}$ ($P=0.76$) respectively.

The control APD₉₀ (Figure 4.8B), recorded on the same day as those perfused with 20mM glucose and 5mM pyruvate was $83.5 \pm 23.5\text{ms}$, this was not significantly different to the control APD₉₀ recorded on the same day as those perfused with 0.5mM pyruvate ($89.2 \pm 33.3\text{ms}$, $P=0.89$) respectively.

Under hyperglycaemic conditions, prior to normalisation the APD₉₀ (Figure 4.8C) for those recorded with 5mM pyruvate was $91.4 \pm 14.3\text{ms}$ and $65.7 \pm 13.3\text{ms}$ for those recorded with 0.5mM pyruvate. Following normalisation, the percentage change in APD₉₀ (Figure 4.8D) shows reducing extracellular pyruvate from 5mM to 0.5mM had no effect with $119.2 \pm 19.4\%$ versus $97.7 \pm 24.3\%$ ($P=0.50$) respectively.

Reducing extracellular pyruvate from 5mM to 0.5mM under normoglycaemic conditions had no effect on the RMP (Figure 4.9A), with $-60.4 \pm 2.7\text{mV}$ versus $-59.6 \pm 3.5\text{mV}$ ($P=0.88$) respectively.

The control RMP (Figure 4.9B) recorded on the same day as those perfused with 20mM glucose and 5mM pyruvate was $-68.9 \pm 1.5\text{mV}$, this was not significantly different to those controls recorded on the same day as those perfused with 0.5mM pyruvate ($-68.9 \pm 1.6\text{mV}$, $P=1.0$).

Prior to normalisation the RMPs for those under hyperglycaemic conditions (Figure 4.9C), were $-69.3 \pm 1.4\text{mV}$ for those recorded with 5mM pyruvate and $-67.0 \pm 1.2\text{mV}$ for those recorded with 0.5mM pyruvate. Once normalised, the percentage change in the RMP (Figure 4.9D) shows reducing extracellular pyruvate from 5mM ($101.0 \pm 2.1\%$) to 0.5mM pyruvate ($97.3 \pm 1.7\%$, $P=0.20$) had no effect.

These data suggest that reducing pyruvate to 0.5mM had no effect on action potential behaviour under either normoglycaemic or hyperglycaemic conditions.

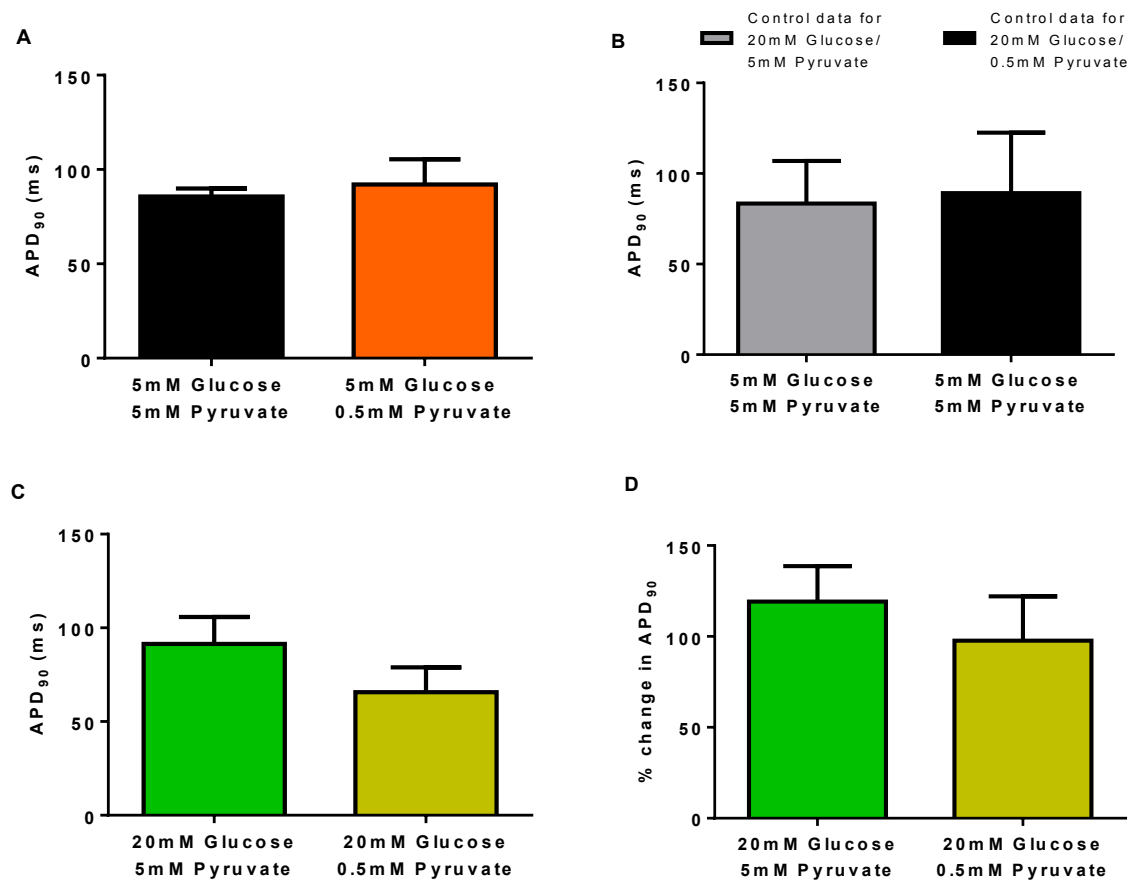


Figure 4.8 The effects of an acute reduction in extracellular pyruvate on APD₉₀ prior to metabolic inhibition in response to acute changes in extracellular glucose.

- (A) APD₉₀ for cardiomyocytes superfused with 5mM glucose and either 5mM or 0.5mM pyruvate prior to metabolic inhibition.
- (B) APD₉₀ for the control data (5mM glucose/5mM pyruvate) recorded at the beginning of each day for the 20mM glucose data sets.
- (C) APD₉₀ for cardiomyocytes superfused with 20mM glucose and either 5mM or 0.5mM pyruvate prior to metabolic inhibition.
- (D) Normalised APD₉₀ for the 20mM glucose data sets represented as a % change in APD₉₀. Each 20mM glucose treatment group was normalised to its corresponding control, the 5mM pyruvate data (green bar) was normalised to the grey bar in (B) and the 0.5mM pyruvate data (yellow bar) was normalised to the black bar in (B).

Data represented as mean \pm s.e.m. Data for 5mM glucose, 5mM pyruvate (black bar, N=3 hearts, 3 experiments) and 0.5mM pyruvate (orange bar, N=3, 6). Control data (5mM glucose/5mM pyruvate) for the 20mM glucose/5mM pyruvate data (grey bar, N=5, 5) and for 20mM glucose/0.5mM pyruvate (black bar, N=4, 4). Data for 20mM glucose, 5mM pyruvate (green bar, N=5, 7) and 0.5mM pyruvate (yellow bar, N=4, 6).

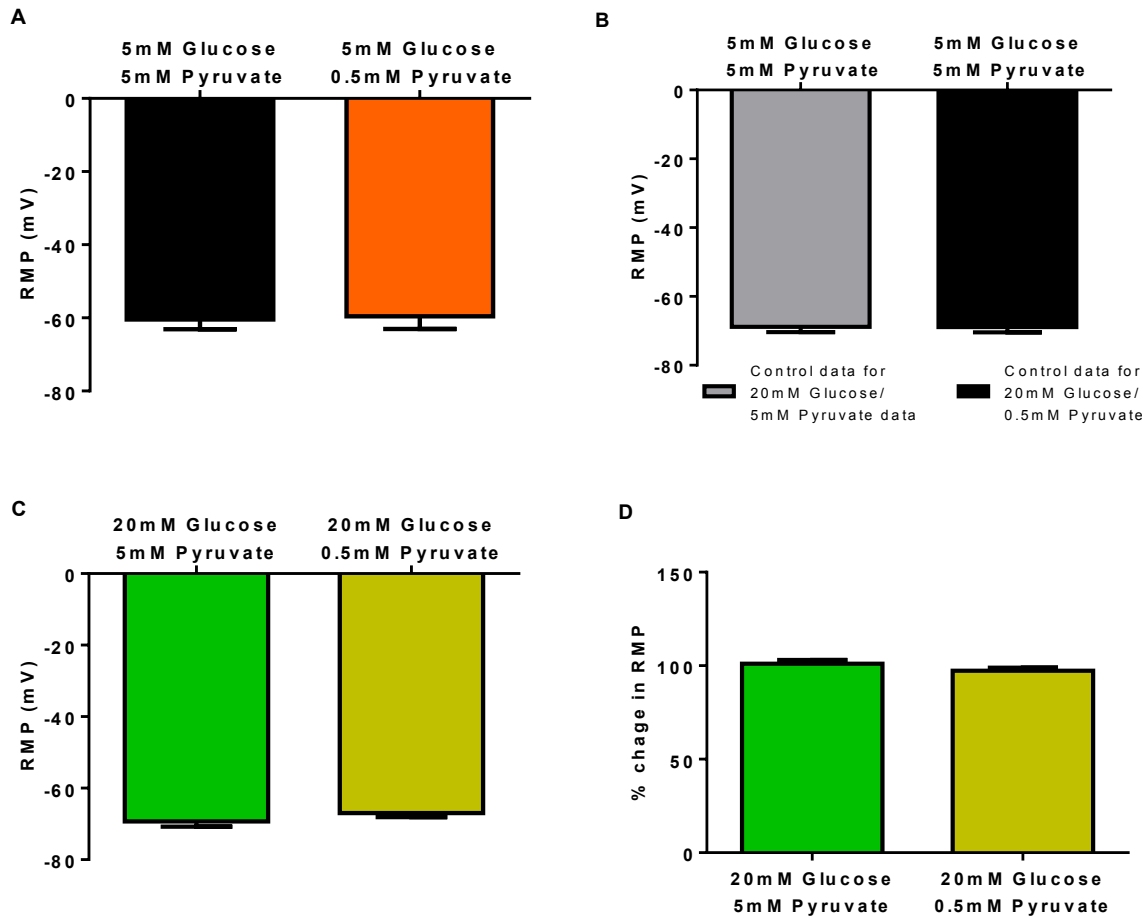


Figure 4.9 The effects of an acute reduction in extracellular pyruvate on the resting membrane potential prior to metabolic inhibition in response to acute changes in extracellular glucose.

- (A) The RMP for cardiomyocytes superfused with 5mM glucose and either 5 or 0.5mM pyruvate prior to metabolic inhibition.
- (B) The RMP for the control data (5mM glucose/5mM pyruvate) recorded at the beginning of each day for the 20mM glucose data sets.
- (C) The RMP for cardiomyocytes superfused with 20mM glucose and either 5 or 0.5mM pyruvate prior to metabolic inhibition.
- (D) Normalised RMP for the 20mM glucose data sets represented as a % change in membrane potential. Each 20mM glucose treatment group has been normalised to its corresponding control data set, the lower pyruvate data (yellow bar) have been normalised to the black bar in (B) and the 20mM glucose data (green bar) has been normalised to the grey bar in (B).

Data represented as mean \pm s.e.m. Data for 5mM glucose, 5mM pyruvate (black bar, N=3 hearts, 3 experiments) and 0.5mM pyruvate (orange bar, N=3, 6). Control data (5mM glucose/5mM pyruvate) for the 20mM glucose/5mM pyruvate data (grey bar, N=5, 5) and for 20mM glucose/0.5mM pyruvate (black bar, N=4, 4). Data for 20mM glucose, 5mM pyruvate (green bar, N=5, 7) and 0.5mM pyruvate (yellow bar, N=4, 6).

4.2.3 The effect of reduced pyruvate on SarcK_{ATP} channel activity during metabolic inhibition

As mentioned previously, opening of SarcK_{ATP} channels during metabolic inhibition can cause failure of the action potential. As the times to action potential failure were not affected by reducing pyruvate from 5mM to 0.5mM, it was hypothesised that time to SarcK_{ATP} channel activation would also not be affected. SarcK_{ATP} channel activation for cardiomyocytes perfused with 0.5mM pyruvate under normoglycaemic (5mM glucose) or hyperglycaemic (20mM glucose) conditions were measured using the whole-cell patch-clamp technique. Cardiomyocytes were perfused for 3-6 minutes with a single glucose concentration until a whole-cell configuration had been achieved. Once capacitance had been calculated, the perfusate was switched to SFT-MI. The time to SarcK_{ATP} channel activity was measured as the point at which the observed basal outward current had increased by 20pA.

Figure 4.10 shows representative traces of membrane current recorded from single cardiomyocytes perfused under normoglycaemic conditions (5mM-Ai), or perfused under hyperglycaemic conditions (20mM-Aii), with either 0.5mM pyruvate or 5mM pyruvate, prior to perfusion with SFT-MI, showing the development of an outward current during perfusion with SFT-MI indicating opening of SarcK_{ATP} channels. Example traces for the control data are cited in the appendix.

Reducing extracellular pyruvate from 5mM to 0.5mM under normoglycaemic conditions had no effect on the time to SarcK_{ATP} channel activation during SFT-MI (Figure 4.11A), with 107.0 ± 11.1 s versus 120.1 ± 7.5 s ($P=0.33$) respectively.

The control (5mM glucose/5mM pyruvate) time to SarcK_{ATP} channel activation during SFT-MI (Figure 4.11B) recorded on the same day as those perfused with 20mM glucose and 5mM pyruvate was 98.8 ± 4.5 s, this was not significantly different to the controls recorded on the same day as those perfused with 20mM glucose and 0.5mM pyruvate (114.3 ± 11.6 s, $P=0.26$).

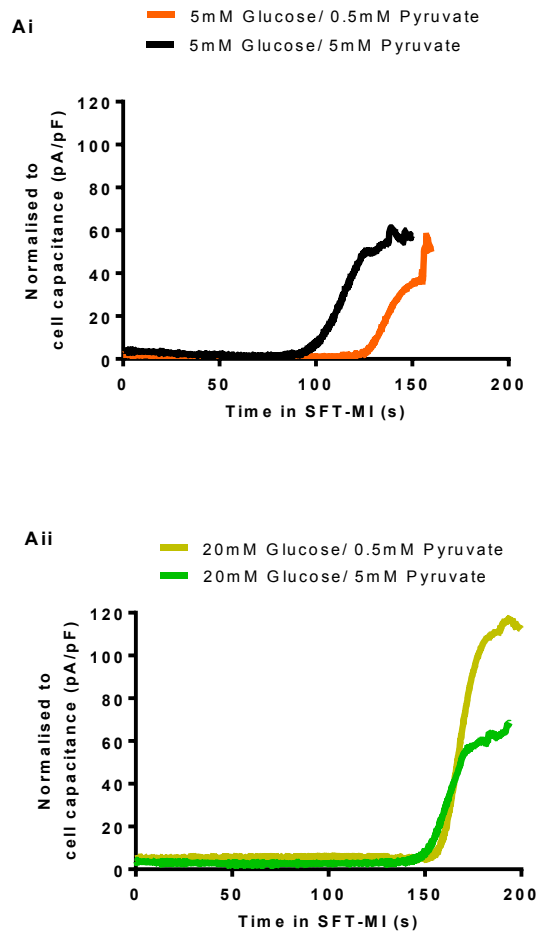


Figure 4.10 The effects of an acute reduction in extracellular pyruvate on $\text{SarcK}_{\text{ATP}}$ current activation during metabolic inhibition in response to acute changes in extracellular glucose.

(A) Example traces of whole-cell $\text{SarcK}_{\text{ATP}}$ channels recorded from a single cardiomyocyte pre-incubated in 5 mM glucose (Ai) with either 0.5mM or 5mM pyruvate or pre-incubated in 20mM glucose (Aii) with either 0.5mM or 5mM pyruvate, prior to superfusion with metabolic inhibition. Each trace is normalised to the cell capacitance. Time to the $\text{SarcK}_{\text{ATP}}$ current activation during SFT-MI was measured at the point at which the basal outward current had increased by 20pA.

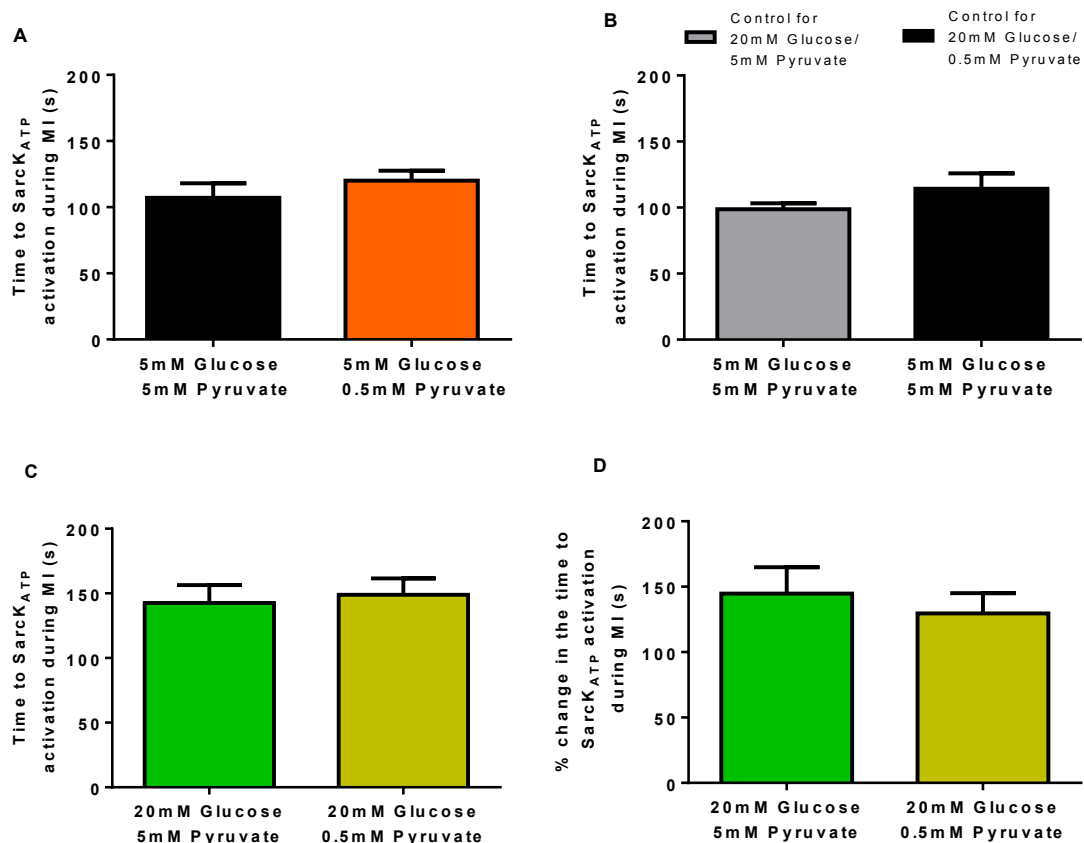


Figure 4.11 The effects of an acute reduction in extracellular pyruvate on SarcK_{ATP} current activation during metabolic inhibition in response to acute changes in extracellular glucose.

(A) Time to SarcK_{ATP} current activation during metabolic inhibition (MI) for cardiomyocytes pre-incubated in 5mM glucose with either 0.5mM or 5mM pyruvate.

(B) Time to SarcK_{ATP} current activation during metabolic inhibition (MI) for the control data (5mM glucose/5mM pyruvate) recorded at the beginning of each day for the 20mM glucose data sets.

(C) Time to SarcK_{ATP} current activation during metabolic inhibition (MI) for cardiomyocytes pre-incubated in 20mM glucose with either 0.5mM or 5mM pyruvate.

(D) Normalised time to SarcK_{ATP} current activation for the 20mM glucose data sets represented as a % change in the time to SarcK_{ATP} current activation. Each 20mM glucose treatment group was normalised to its corresponding control, the 5mM pyruvate data (green bar) was normalised to the grey bar in (B) and the 0.5mM pyruvate data (yellow bar) was normalised to the black bar in (B).

Data represented as mean \pm s.e.m. Data for 5mM glucose, 5mM pyruvate (black bar, N=5 hearts, 5 experiments) and 0.5mM pyruvate (orange bar, N=5, 9). Control data (5mM glucose/5mM pyruvate) for the 20mM glucose/5mM pyruvate data (grey bar, N=4, 4) and for 20mM glucose/0.5mM pyruvate (black bar, N=4, 4). Data for 20mM glucose, 5mM pyruvate (green bar, N=4, 6) and 0.5mM pyruvate (yellow bar, N=4, 9).

Under hyperglycaemic conditions, prior to normalisation (Figure 4.11C), the time to SarcK_{ATP} channel activation during SFT-MI, for those recorded with 5mM pyruvate was 142.5 ± 13.9 s and 148.9 ± 12.7 s for those recorded with 0.5mM pyruvate. Once normalised, using the respective control data, the percentage change in the time to SarcK_{ATP} channel activation during SFT-MI (Figure 4.11D) shows reducing extracellular pyruvate from 5mM to 0.5mM had no effect with $144.8 \pm 20.1\%$ compared to $129.6 \pm 15.5\%$ ($P=0.55$) respectively.

These data suggest reducing extracellular pyruvate from 5mM to 0.5mM has no effect on the time to SarcK_{ATP} activation under both normoglycaemic and hyperglycaemic conditions.

4.2.4 The effect of reduced extracellular pyruvate on Mg²⁺-Green fluorescence

In the previous section, it was shown that reducing pyruvate to 0.5mM did not significantly affect SarcK_{ATP} activation. To investigate whether reducing pyruvate to 0.5mM was having any affect on intracellular ATP levels during metabolic inhibition and re-energisation, the fluorescent indicator Mg²⁺-Green was used as previously described (see section 3.2.4), as this indicator can act as a surrogate for measuring ATP levels.

Figure 4.12 shows recordings of Mg²⁺-Green fluorescence from three cardiomyocytes perfused with 5mM pyruvate (Figure 4.12Ai) or 0.5mM pyruvate (Figure 4.12Aii) under normoglycaemic conditions (5mM glucose), and from three cardiomyocytes perfused with 5mM pyruvate (Figure 4.12Bi) or 0.5mM pyruvate (Figure 4.12Bii) under hyperglycaemic conditions (20mM glucose), prior to perfusion with SFT-MI and during re-energisation. In these recording cardiomyocytes were quiescent and not electrically stimulated, to prevent movement artefacts as the Mg²⁺-Green indicator is a non-ratiometric dye. Fluorescence was normalised to fluorescence intensity at the start of the experiment (F/F_0). The profile for changes in Mg²⁺-Green fluorescence under both glycaemic conditions with 5mM pyruvate was the same as previously described in section 3.2.4. Compared to this, perfusion with 0.5mM pyruvate under normoglycaemia during SFT-MI resulted in a smaller steadier increase in fluorescence followed by a later, less pronounced rapid increase. During re-energisation the

fluorescence remained elevated, although at lower intensity than seen in 5mM pyruvate. Under hyperglycaemic conditions during SFT-MI a smaller steady increase in fluorescence was observed, with the rapid increase occurring sooner. During re-energisation the fluorescence remained elevated at a similar intensity as seen in 5mM pyruvate. This may be a reflection of the smaller increase in fluorescence during metabolic inhibition. Example recordings of Mg^{2+} -Green fluorescence for the controls are cited in the appendix.

Reducing extracellular pyruvate from 5mM to 0.5mM under normoglycaemic conditions had no effect on F/F_0 at the end of MI (Figure 4.13A), with $1.06 \pm 0.02F/F_0$ versus $1.04 \pm 0.01F/F_0$ ($P=0.25$) respectively. There was also no effect at the end of re-energisation, with $1.04 \pm 0.02F/F_0$ versus $1.04 \pm 0.01F/F_0$ ($P=0.65$) respectively.

The control data (5mM glucose/5mM pyruvate) for F/F_0 at the end of MI and at the end of re-energisation is shown in Figure 4.13B. The control F/F_0 at the end of MI recorded on the same day as those perfused with 20mM glucose and 5mM pyruvate was $1.08 \pm 0.04F/F_0$, this was not significantly different to F/F_0 controls recorded on the same day as those perfused with 0.5mM pyruvate ($1.06 \pm 0.02F/F_0$, $P=0.66$). The control F/F_0 at the end of re-energisation recorded on the same day as those perfused with 20mM glucose and 5mM pyruvate was $1.06 \pm 0.04F/F_0$, this was not significantly different the F/F_0 control recorded on the same day as those perfused with 0.5mM pyruvate ($1.04 \pm 0.02F/F_0$, $P=0.60$).

Under hyperglycaemic conditions, prior to normalisation the F/F_0 at the end of MI (Figure 4.13C) was $1.05 \pm 0.01F/F_0$ for those recorded with 5mM pyruvate and $1.04 \pm 0.01F/F_0$ for those recorded with 0.5mM pyruvate. While the F/F_0 at the end of re-energisation was $1.04 \pm 0.01F/F_0$ for those recorded with 5mM pyruvate and $1.03 \pm 0.01F/F_0$ for those recorded with 0.5mM pyruvate. Once normalised, using the respective control data, the percentage change in F/F_0 at the end of MI and at the end of re-energisation (Figure 4.13D) shows reducing pyruvate from 5mM to 0.5mM had no effect on either the F/F_0 at the end of MI with $97.2 \pm 2.2\%$ versus $98.2 \pm 0.8\%$ ($P=0.64$) respectively or on the F/F_0 at the end of re-energisation with $97.8 \pm 2.2\%$ compared to $99.9 \pm 1.0\%$ ($P=0.36$) respectively.

During SFT-MI following the initial slow increase in Mg^{2+} -Green fluorescence, there was a rapid increase in Mg^{2+} -Green fluorescence. Under normoglycaemic conditions, reducing extracellular pyruvate from 5mM to 0.5mM had no effect on the time to the rapid increase in Mg^{2+} -Green fluorescence (Figure 4.14A), with $285.7 \pm 12.4\text{s}$ versus $295.8 \pm 7.7\text{s}$ ($P=0.52$) respectively.

The control (5mM glucose/5mM pyruvate) time to the rapid increase in Mg^{2+} -Green fluorescence (Figure 4.14B) recorded on the same day as those perfused with 20mM glucose and 5mM pyruvate was $302.3 \pm 8.8\text{s}$, this was not significantly different to the controls recorded on the same day as those perfused with 0.5mM pyruvate ($285.7 \pm 12.4\text{s}$, $P=0.34$).

Prior to normalisation the time to the rapid increase in Mg^{2+} -Green fluorescence (Figure 4.14C), for those recorded under hyperglycaemic conditions with 5mM pyruvate was $317.4 \pm 13.7\text{s}$ and $313.4 \pm 10.6\text{s}$ for those recorded with 0.5mM pyruvate. Once normalised, using the respective control data, the percentage change in the time to the rapid increase in Mg^{2+} -Green fluorescence (Figure 4.14D) shows reducing pyruvate from 5mM to 0.5mM had no effect with $104.2 \pm 4.1\%$ versus $109.5 \pm 3.6\%$ ($P=0.34$) respectively.

These results show that under normoglycaemic and hyperglycaemic conditions, reducing pyruvate to 0.5mM had no effect on Mg^{2+} -Green fluorescence observed during metabolic inhibition or re-energisation.

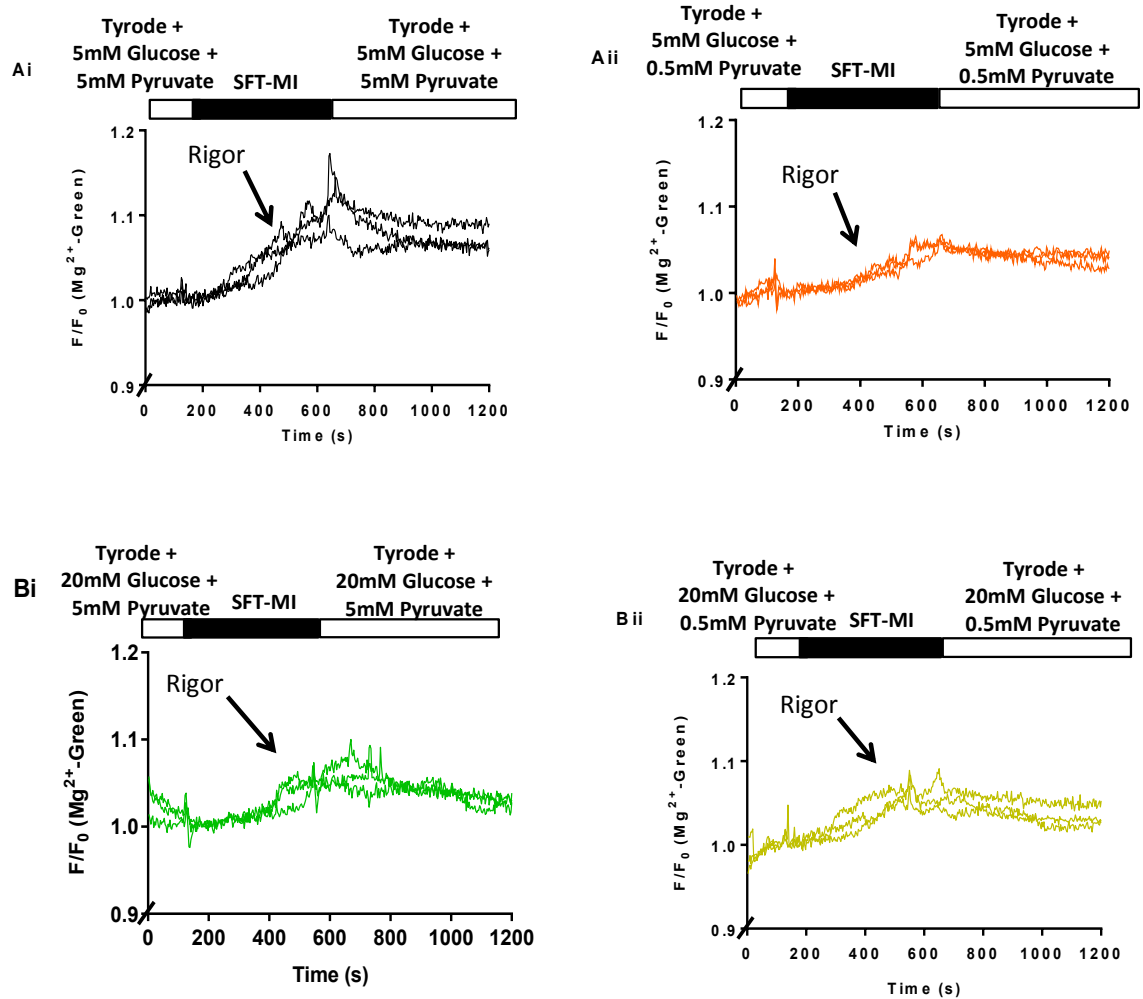


Figure 4.12 The impact of acute changes in extracellular pyruvate on the fluorescence of Mg^{2+} -Green in isolated cardiomyocytes during metabolic inhibition and re-energisation in response to acute changes in extracellular glucose.

- (A) Example traces showing the time course of changes in Mg^{2+} -Green fluorescence acutely exposed to 5mM glucose and 5mM pyruvate (Ai) and 5mM glucose and 0.5mM pyruvate (Aii) before metabolic inhibition and during re-energisation.
- (B) Example traces showing the time course of changes in Mg^{2+} -Green fluorescence acutely exposed to 20mM glucose and 5mM pyruvate (Bi) and 20mM glucose and 0.5mM pyruvate (Bii) before metabolic inhibition and during re-energisation.

In all traces the expected time for the development of rigor are indicated by arrows.

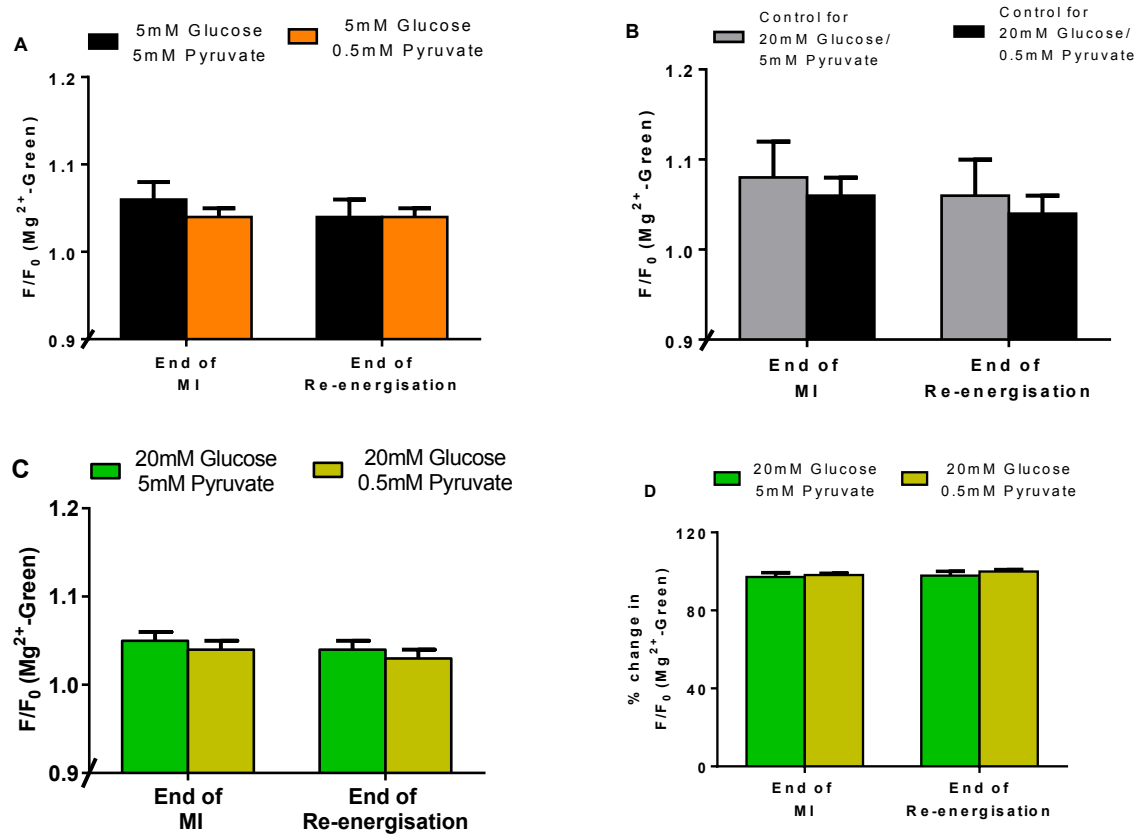


Figure 4.13 The impact of an acute reduction in extracellular pyruvate on the fluorescence of Mg^{2+} -Green in isolated cardiomyocytes during metabolic inhibition and re-energisation in response to acute changes in extracellular glucose.

- (A) The changes in Mg^{2+} -Green fluorescence at the end of metabolic inhibition (MI) and at the end of re-energisation, for cardiomyocytes superfused with 5mM glucose and either 0.5mM or 5mM pyruvate.
- (B) The changes in Mg^{2+} -Green fluorescence at the end of metabolic inhibition (MI) and at the end of re-energisation, for cardiomyocytes superfused with 5mM glucose and 5mM pyruvate, recorded at the beginning of each day for the 20mM glucose data sets.
- (C) The changes in Mg^{2+} -Green fluorescence at the end of metabolic inhibition (MI) and at the end of re-energisation, for cardiomyocytes superfused with 20mM glucose and either 0.5mM or 5mM pyruvate.
- (D) Normalised Mg^{2+} -Green fluorescence for the 20mM glucose data sets represented as a % change in Mg^{2+} -Green fluorescence. Each 20mM glucose treatment group was normalised to its corresponding control, the 5mM pyruvate data (green bar) was normalised to the grey bar in (B) and the 0.5mM pyruvate data (yellow bar) was normalised to the black bar in (B).

Data represented as mean \pm s.e.m. Data for 5mM glucose, 5mM pyruvate (black bar, N=3 hearts, 3 fields of view, 26 cardiomyocytes) and 0.5mM pyruvate (orange bar, N=3, 9, 61). Control data (5mM glucose/5mM pyruvate) for the 20mM glucose/5mM pyruvate data (grey bar, N=3, 3, 19) and for 20mM glucose/0.5mM pyruvate (black bar, N=3, 3, 26). Data for 20mM glucose, 5mM pyruvate (green bar, N=3, 8, 42) and 0.5mM pyruvate (yellow bar, N=3, 10, 78).

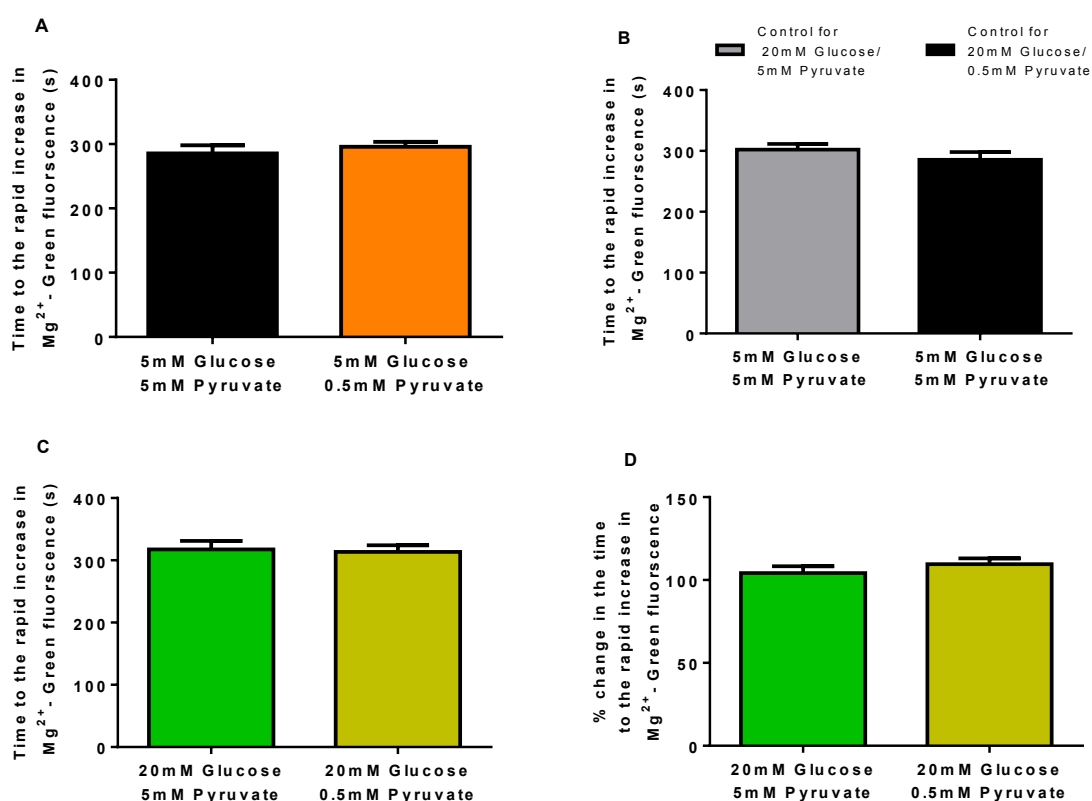


Figure 4.14 The impact of an acute reduction in extracellular pyruvate on the time to the rapid increase in Mg^{2+} -Green fluorescence in isolated cardiomyocytes during metabolic inhibition in response to acute changes in extracellular glucose.

- (A) The time to the rapid increase in Mg^{2+} -Green fluorescence, for cardiomyocytes superfused with 5mM glucose and either 0.5mM or 5mM pyruvate.
- (B) The time to the rapid increase in Mg^{2+} -Green fluorescence, for cardiomyocytes superfused with 5mM glucose and 5mM pyruvate, recorded at the beginning of each day for the 20mM glucose data sets.
- (C) The time to the rapid increase in Mg^{2+} -Green fluorescence, for cardiomyocytes superfused with 20mM glucose and either 0.5mM or 5mM pyruvate.
- (D) Normalised time to the rapid increase in Mg^{2+} -Green fluorescence for the 20mM glucose data sets represented as a % change in the time to the rapid increase in Mg^{2+} -Green fluorescence. Each 20mM glucose treatment group was normalised to its corresponding control, the 5mM pyruvate data (green bar) was normalised to the grey bar in (B) and the 0.5mM pyruvate data (yellow bar) was normalised to the black bar in (B).

Data represented as mean \pm s.e.m. Data for 5mM glucose, 5mM pyruvate (black bar, N=3 hearts, 3 fields of view, 26 cardiomyocytes) and 0.5mM pyruvate (orange bar, N=3, 9, 61). Control data (5mM glucose/5mM pyruvate) for the 20mM glucose/5mM pyruvate data (grey bar, N=3, 3, 19 and for 20mM glucose/0.5mM pyruvate (black bar, N=3, 3, 26). Data for 20mM glucose, 5mM pyruvate (green bar, N=3, 8, 42) and 0.5mM pyruvate (yellow bar, N=3, 10, 78).

4.2.5 The modifying effect of reduced extracellular pyruvate on intracellular calcium in response to metabolic inhibition and re-energisation in association with acute changes in glucose

Previously in this chapter it has been shown that reducing pyruvate from 5mM to 0.5mM under both normoglycaemic and hyperglycaemic glucose concentrations had no effect on contractile recovery. As contractile recovery has been linked to improved calcium regulation, to investigate whether reducing pyruvate had an effect on $[Ca^{2+}]_i$ during metabolic inhibition and re-energisation, the ratiometric calcium dye Fura-2 and the protocol for calcium imaging experiments previously described in section 3.2.5 was used.

4.2.5.1 Measurements of intracellular calcium as a marker of cell injury

Figure 4.15 shows Fura-2 ratios from cardiomyocytes under normoglycaemic conditions (5mM glucose) perfused with 5mM (Figure 4.15Ai) or 0.5mM (Figure 4.15Aii) pyruvate and from cardiomyocytes under hyperglycaemic conditions (20mM glucose) perfused with 5mM (Figure 4.15Bi) or 0.5mM (Figure 4.15Bii) pyruvate, prior to metabolic inhibition and during re-energisation and shows the time course of changes in the Fura-2 ratio during the metabolic inhibition and re-energisation protocol. For both 5mM or 0.5mM pyruvate, under normoglycaemic conditions, perfusion with SFT-MI, resulted in failure of Ca^{2+} -transients, followed by a steady increase in the diastolic Fura-2 ratio ($[Ca^{2+}]_i$). However during re-energisation, perfusion with 5mM pyruvate resulted in an initial decline in Fura-2 ($[Ca^{2+}]_i$) in some cardiomyocytes before a steady increase developed, while perfusion with 0.5mM pyruvate resulted in a further steady increase in Fura-2 ($[Ca^{2+}]_i$). Perfusion with 5mM or 0.5mM pyruvate, under hyperglycaemic conditions resulted in a similar profile in time-dependent changes in Fura-2 ratios. However with 0.5mM pyruvate a rapid, rather than steady, increase in diastolic Fura-2 ratio ($[Ca^{2+}]_i$) was observed during perfusion with SFT-MI and re-energisation resulted in a steady increase in Fura-2 ratio ($[Ca^{2+}]_i$). Example Fura-2 recordings for the control data and examples of the Ca^{2+} transients captured at the end of re-energisation are cited in the appendix.

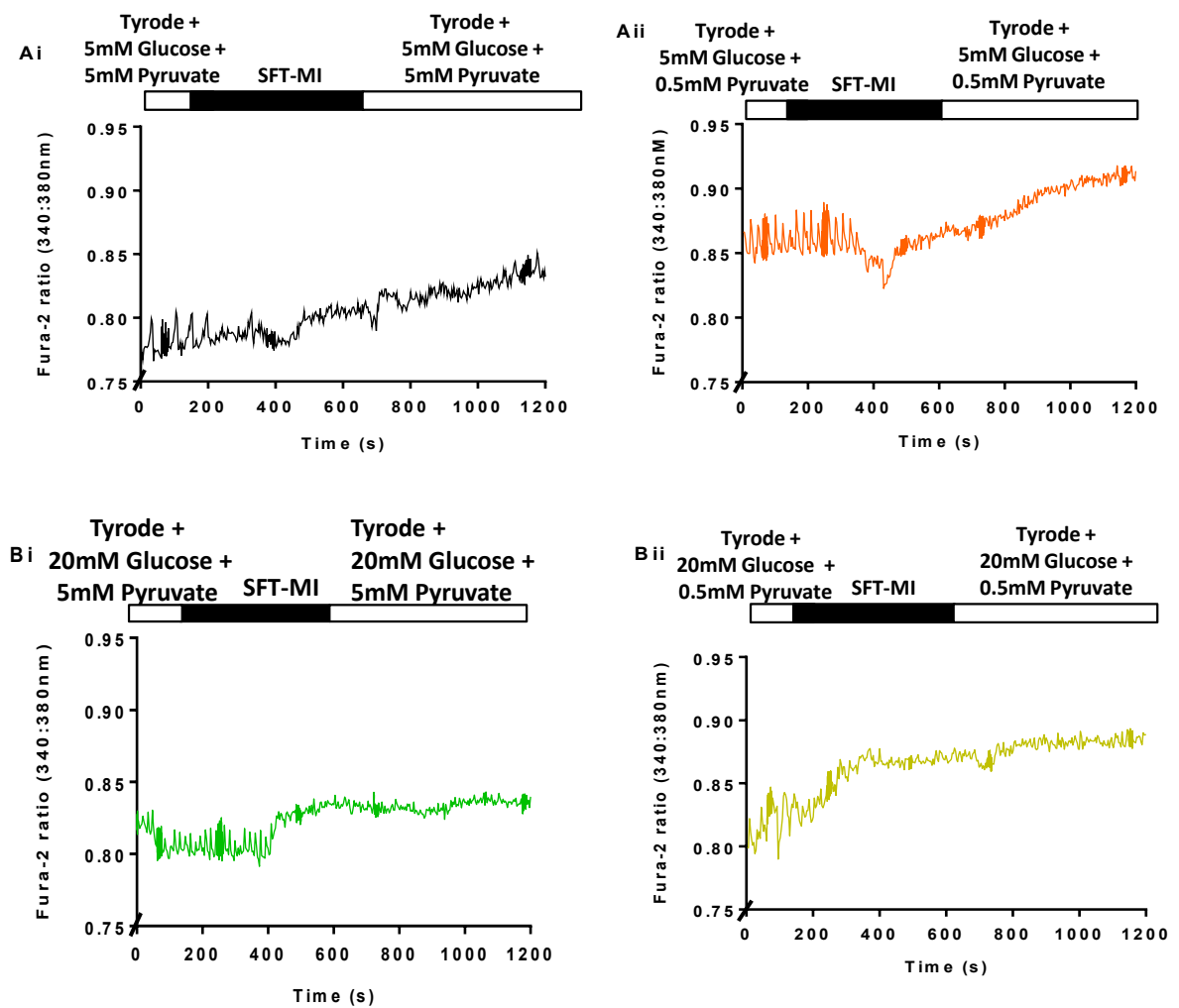


Figure 4.15 The impact of acute changes in extracellular pyruvate on intracellular calcium in isolated cardiomyocytes during metabolic inhibition and re-energisation in response to acute changes in extracellular glucose.

- (A) Example trace recording of the Fura-2 ratio (340:380nm) for a cardiomyocyte exposed to 5mM glucose and 5mM pyruvate (Ai) and 5mM glucose and 0.5mM pyruvate (Aii), prior to metabolic inhibition and during re-energisation.
- (B) Example trace recording of the Fura-2 ratio (340:380nm) for a cardiomyocyte exposed to 20mM glucose and 5mM pyruvate (Bi) and 20mM glucose and 0.5mM pyruvate (Bii), prior to metabolic inhibition and during re-energisation.

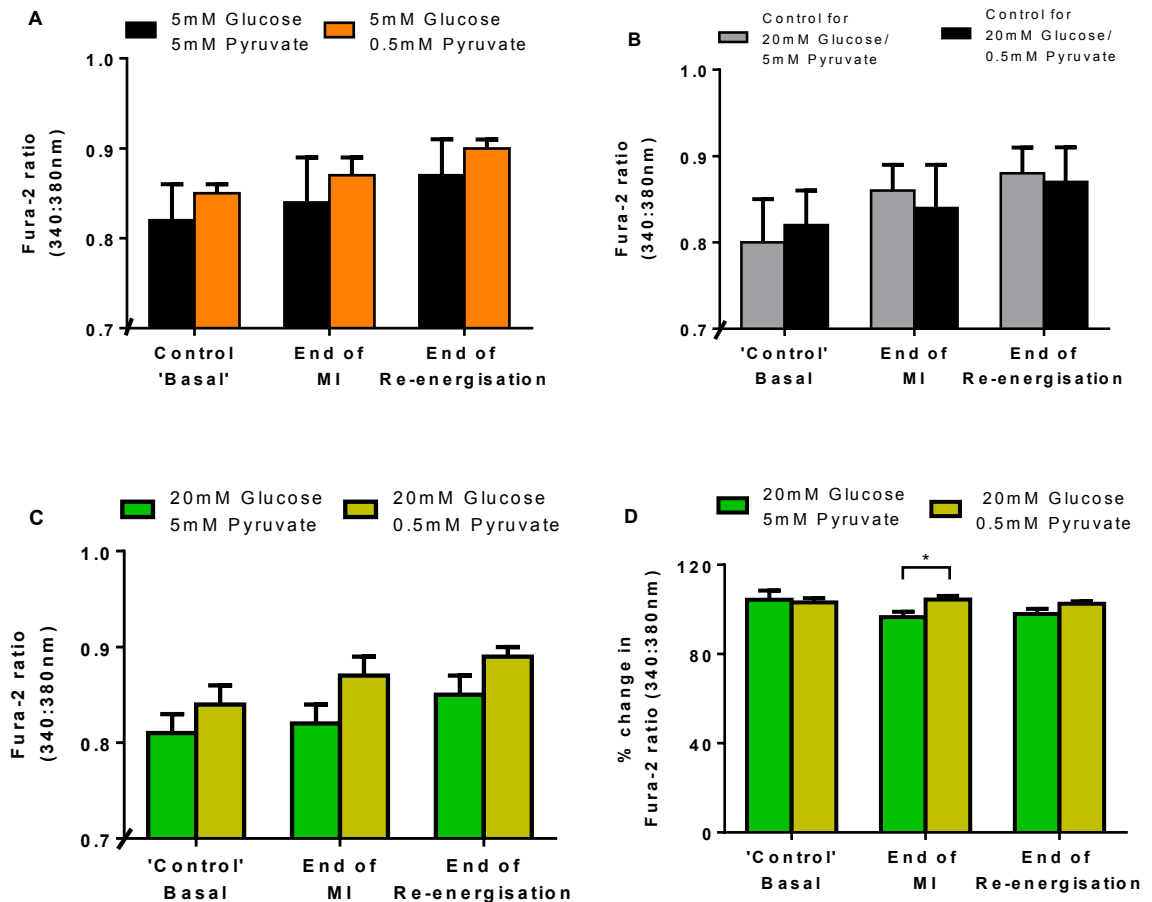


Figure 4.16 The impact of acute changes in extracellular pyruvate on intracellular calcium in isolated cardiomyocytes during metabolic inhibition and re-energisation in response to acute changes in extracellular glucose.

- (A) The Fura-2 ratios at control 'basal', the end of metabolic inhibition (MI) and at the end of re-energisation, for cardiomyocytes superfused with 5mM glucose and either 0.5mM or 5mM pyruvate.
- (B) The Fura-2 ratios at control 'basal', the end of metabolic inhibition (MI) and at the end of re-energisation, recorded at the beginning of each day for the 20mM glucose data sets.
- (C) The Fura-2 ratios at control 'basal', the end of metabolic inhibition (MI) and at the end of re-energisation, for cardiomyocytes superfused with 20mM glucose and either 0.5mM or 5mM pyruvate.
- (D) Normalised Fura-2 ratios for the 20mM glucose data sets represented as a % change in Fura-2 ratios. Each 20mM glucose treatment group was normalised to its corresponding control data set, the 5mM pyruvate data (green bars) was normalised to the grey bars in (B) and the 0.5mM pyruvate data (yellow bars) was normalised to the black bars in (B).

Data represented as mean \pm s.e.m. Data for 5mM glucose, 5mM pyruvate (black bar, N=3 hearts, 3 fields of view, 27 cardiomyocytes) and 0.5mM pyruvate (orange bar, N=3, 9, 57). Control data (5mM glucose/5mM pyruvate) for the 20mM glucose/5mM pyruvate data (grey bar, N=4, 4, 28) and for 20mM glucose/0.5mM pyruvate (black bar, N=3, 3, 27). Data for 20mM glucose, 5mM pyruvate (green bar, N=4, 9, 58) and 0.5mM pyruvate (yellow bar, N=3, 9, 75). *P<0.05 (Unpaired T-test).

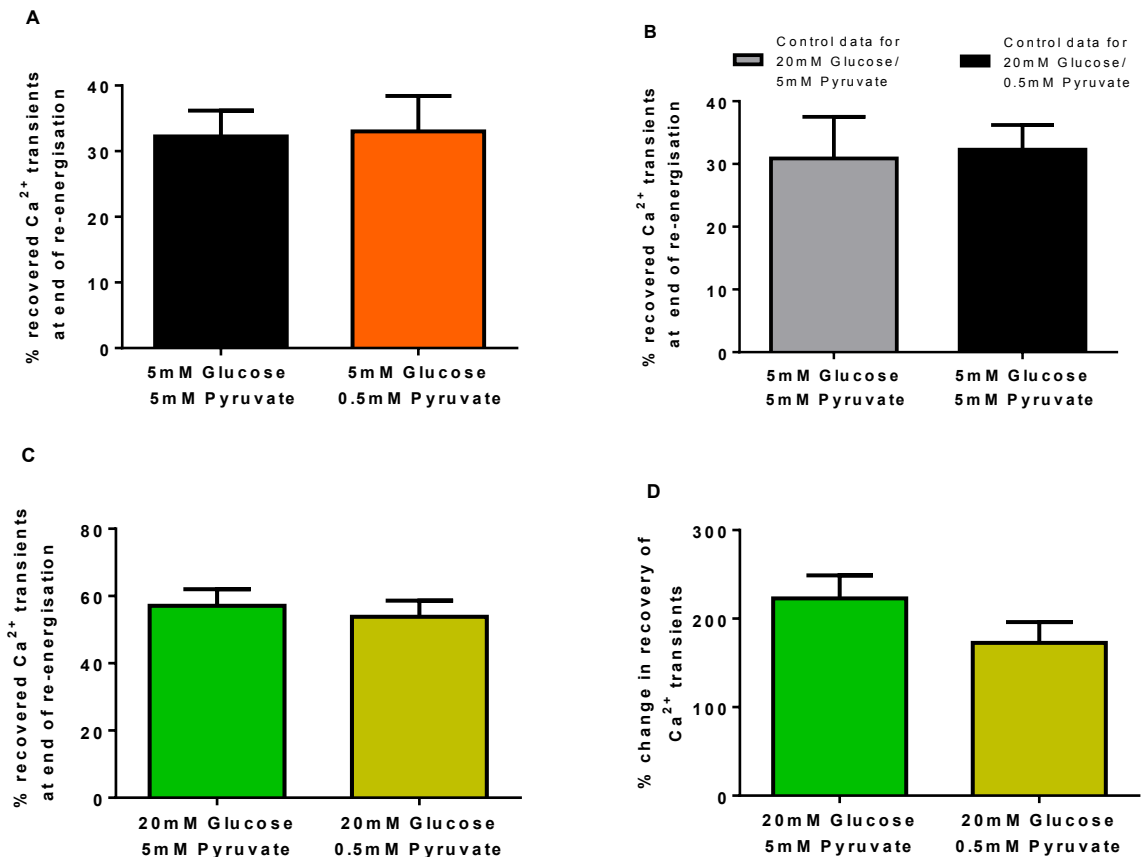


Figure 4.17 The effects of an acute reduction in extracellular pyruvate on the recovery of electrically evoked calcium transients following metabolic inhibition and re-energisation in response to acute changes in extracellular glucose.

- (A) The percentage of cardiomyocytes recovering calcium transients, by the end of 10 minutes re-energisation, for cardiomyocytes superfused with 5mM glucose and either 0.5mM or 5mM pyruvate.
- (B) The percentage of cardiomyocytes recovering calcium transients, by the end of 10 minutes re-energisation, for the cardiomyocytes superfused with 5mM glucose and 5mM pyruvate recorded at the beginning of each day of the 20mM glucose data sets.
- (C) The percentage of cardiomyocytes recovering calcium transients, by the end of 10 minutes re-energisation, for cardiomyocytes superfused with 20mM glucose and either 0.5mM or 5mM pyruvate.
- (D) Normalised Fura-2 ratios for the 20mM glucose data sets represented as a % change in the percentage of cardiomyocytes recovering calcium transients by the end of 10 minutes re-energisation. Each 20mM glucose treatment group was normalised to its corresponding control data set, the 5mM pyruvate data (green bar) was normalised to the grey bar in (B) and the 0.5mM pyruvate data (yellow bar) was normalised to the black bar in (B).

Data represented as mean \pm s.e.m. Data for 5mM glucose, 5mM pyruvate (black bar, N=3 hearts, 3 fields of view, 27 cardiomyocytes) and 0.5mM pyruvate (orange bar, N=3, 9, 57). Control data (5mM glucose/5mM pyruvate) for the 20mM glucose/5mM pyruvate data (grey bar, N=4, 4, 28) and for 20mM glucose/0.5mM pyruvate (black bar, N=3, 3, 27). Data for 20mM glucose, 5mM pyruvate (green bar, N=4, 9, 58) and 0.5mM pyruvate (yellow bar, N=3, 9, 75).

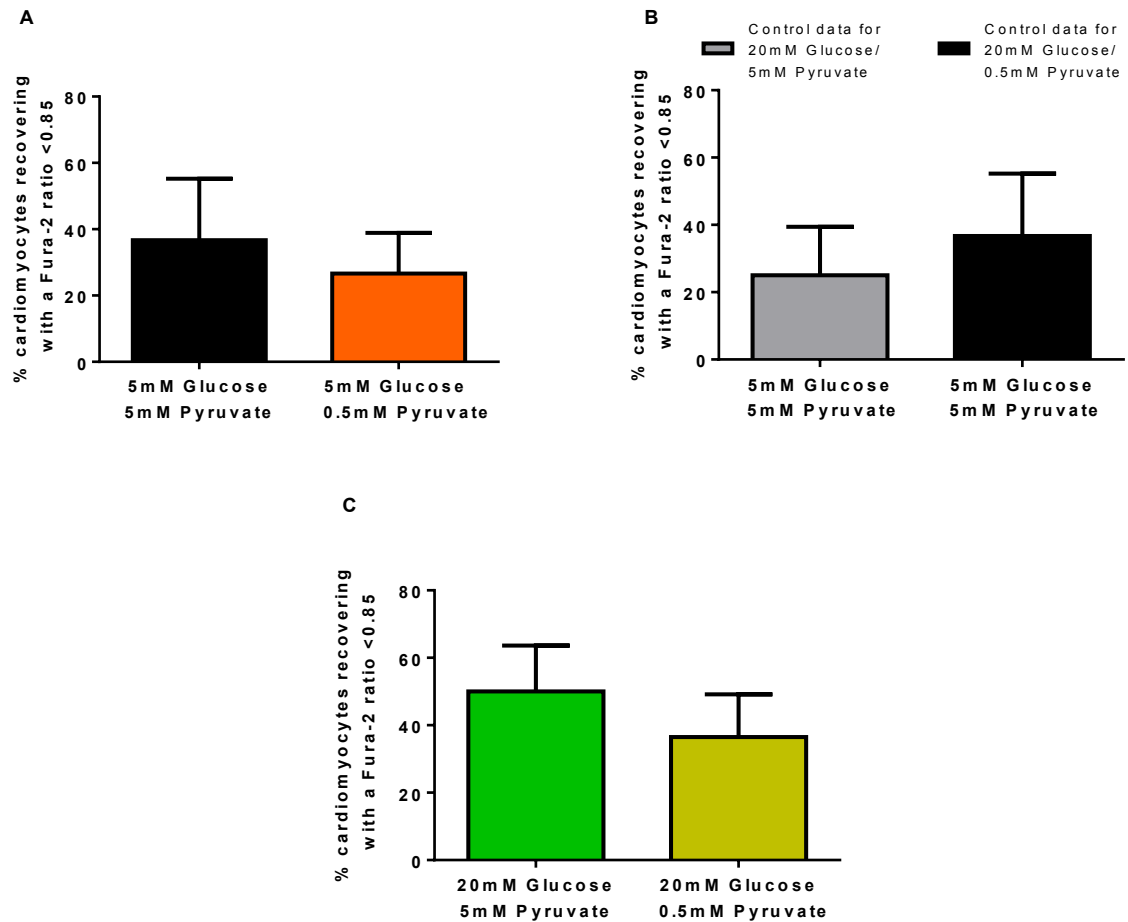


Figure 4.18 The effects of an acute reduction in extracellular pyruvate on the recovery of electrically evoked calcium transients following metabolic inhibition and re-energisation in response to acute changes in extracellular glucose.

- (A) The percentage of cardiomyocytes, that recovered a Fura-2 ratio <0.85 by the end of 10 minutes of re-energisation, for cardiomyocytes superfused with 5mM glucose and either 0.5mM or 5mM pyruvate.
- (B) The percentage of cardiomyocytes, that recovered a Fura-2 ratio <0.85 by the end of 10 minutes of re-energisation, for cardiomyocytes superfused with 5mM glucose and 5mM pyruvate., recorded at the beginning of each day of the 20mM glucose data sets.
- (C) The percentage of cardiomyocytes, that recovered a Fura-2 ratio <0.85 by the end of 10 minutes of re-energisation, for cardiomyocytes superfused with 20mM glucose and either 0.5mM or 5mM pyruvate.

Data represented as mean \pm s.e.m. Data for 5mM glucose, 5mM pyruvate (black bar, N=3 hearts, 3 fields of view, 27 cardiomyocytes) and 0.5mM pyruvate (orange bar, N=3, 9, 57). Control data (5mM glucose/5mM pyruvate) for the 20mM glucose/5mM pyruvate data (grey bar, N=4, 4, 28) and for 20mM glucose/0.5mM pyruvate (black bar, N=3, 3, 27). Data for 20mM glucose, 5mM pyruvate (green bar, N=4, 9, 58) and 0.5mM pyruvate (yellow bar, N=3, 9, 75).

Under normoglycaemic conditions, reducing pyruvate from 5mM to 0.5mM had no effect on any of the Fura-2 ratios (Figure 4.16A). The 'basal' Fura-2 ratios were 0.82 ± 0.04 (5mM pyruvate) versus 0.85 ± 0.01 (0.5mM pyruvate, $P=0.49$); the Fura-2 ratios at the end of MI were 0.84 ± 0.05 (5mM pyruvate) versus 0.87 ± 0.02 (0.5mM pyruvate, $P=0.47$) and the Fura-2 ratios at the end of re-energisation were 0.87 ± 0.04 (5mM pyruvate) versus 0.90 ± 0.01 (0.5mM pyruvate, $P=0.28$).

The control Fura-2 ratios recorded at 'basal', at the end of MI and at the end of re-energisation (Figure 4.16B), recorded on the same day as those perfused with 20mM glucose and 5mM pyruvate were 0.80 ± 0.05 , ('basal'); 0.86 ± 0.03 (at the end of MI), and 0.88 ± 0.03 (at the end of re-energisation), these were not significantly different to the control Fura-2 ratios recorded at these times on the same day as those perfused with 0.5mM pyruvate, with 0.82 ± 0.04 , ('basal', $P=0.76$); 0.84 ± 0.05 (at the end of MI, $P=0.70$), 0.87 ± 0.04 (at the end of re-energisation, $P=0.93$).

Under hyperglycaemic conditions, prior to normalisation the Fura-2 ratios (Figure 4.16C), for those recorded with 5mM pyruvate were 0.81 ± 0.02 ('basal'); 0.82 ± 0.02 (at the end of MI), and 0.85 ± 0.02 (at the end of re-energisation) and 0.84 ± 0.02 , ('basal'); 0.87 ± 0.02 (at the end of MI), and 0.89 ± 0.01 (at the end of re-energisation) for those recorded with 0.5mM pyruvate. Following normalisation, the percentage change in the Fura-2 ratios (Figure 4.16D) shows reducing extracellular pyruvate from 5mM to 0.5mM had no effect at 'basal' with $104.3 \pm 4.1\%$ versus $103.2 \pm 1.8\%$ ($P=0.80$) respectively and at the end of re-energisation with $97.9 \pm 2.3\%$ versus $102.5 \pm 1.2\%$ ($P=0.10$) respectively. However at the end of MI, reducing extracellular pyruvate significantly increased the percentage change in Fura-2 with $96.5 \pm 2.4\%$ (5mM pyruvate) versus $104.4 \pm 1.6\%$ (0.5mM pyruvate, $P<0.05$).

4.2.5.2 Does reducing pyruvate impact on the recovery of contraction and the corresponding lower resting $[Ca^{2+}]_i$?

To determine whether reducing pyruvate has an impact on the recovery of Ca^{2+} transients, cardiomyocytes were analysed for their ability to produce regular synchronous Ca^{2+} transients at the start of the experiment and their ability to recover these by the end of re-energisation (as with the data in section 3.2.5). This allowed me

to establish if reducing pyruvate was impacting on Ca^{2+} regulation. Analysing the Ca^{2+} transients also allowed me to establish if recovery of contractile function was being reflected by recovery of Ca^{2+} transients.

Under normoglycaemic conditions, reducing extracellular pyruvate from 5mM to 0.5mM had no effect on the overall recovery of Ca^{2+} transients (Figure 4.17A), with $32.3 \pm 3.9\%$ versus $33.0 \pm 5.4\%$ ($P=0.94$) respectively.

The control percentage of cardiomyocytes recovering Ca^{2+} transients (Figure 4.17B) recorded on the same day as those perfused with 20mM glucose and 5mM pyruvate was $30.9 \pm 6.6\%$, this was not significantly different to the controls recorded on the same day as those perfused with 0.5mM pyruvate ($32.3 \pm 3.9\%$, $P=0.88$).

Prior to normalisation, the percentage of cardiomyocytes recovering Ca^{2+} transients under hyperglycaemic conditions (Figure 4.17C), for those recorded with 5mM pyruvate was $57.1 \pm 4.9\%$ and $53.8 \pm 4.8\%$ for those recorded with 0.5mM pyruvate. Once normalised, using the respective control data, the percentage change in the recovery of Ca^{2+} transients (Figure 4.17D) shows reducing extracellular pyruvate from 5mM to 0.5mM had no effect with $222.9 \pm 26.0\%$ versus $172.5 \pm 23.7\%$ ($P=0.17$) respectively.

The percentage of cardiomyocytes which recovered Ca^{2+} transients with a Fura-2 ratio <0.85 was then calculated (as previously calculated in section 3.2.5.2). Reducing pyruvate from 5mM to 0.5mM under normoglycaemic conditions, had no effect on the recovery of Ca^{2+} transients with a Fura-2 ratio <0.85 (Figure 4.18A), with $36.7 \pm 18.6\%$ versus $26.7 \pm 12.2\%$ ($P=0.68$) respectively.

The control percentage of cardiomyocytes recovering Ca^{2+} transients with a Fura-2 ratio <0.85 (Figure 4.18B) recorded on the same day as those perfused with 20mM glucose and 5mM pyruvate was $25 \pm 14.4\%$, this was not significantly different to the controls recorded on the same day as those perfused with 20mM glucose and 0.5mM pyruvate ($36.7 \pm 18.6\%$, $P=0.63$).

Due to one of the control days recorded with 5mM pyruvate having 0% recover Ca^{2+} transients with a Fura-2 ratio <0.85 , the hyperglycaemic data was unable to be

normalised. However due to the controls showing no significance, a direct comparison of the hyperglycaemic data was deemed acceptable in this instance and shows reducing extracellular pyruvate from 5mM to 0.5mM pyruvate had no effect on the percentage of cardiomyocytes recovering Ca^{2+} transients with a Fura-2 ratio <0.85 (Figure 4.18C) with $50.0 \pm 13.6\%$ versus $36.5 \pm 12.6\%$ ($P=0.48$) respectively.

These results suggest that reducing pyruvate to 0.5mM under hyperglycaemic conditions results in significantly higher Fura-2 ratio ($[\text{Ca}^{2+}]_i$ level) by the end of metabolic inhibition compared to 5mM pyruvate. Meanwhile, reducing pyruvate under normoglycaemic conditions had no effect. Reducing pyruvate to 0.5mM also had no effect on the percentage of cardiomyocytes, regaining synchronous Ca^{2+} transients by the end of re-energisation under either glycaemic condition.

4.2.6 The effects of an acute elevation in extracellular pyruvate on the contractile function of isolated cardiomyocytes

The effects of a supraphysiological concentration of pyruvate (10mM) have previously been reported with Dennis *et al* (1979) showing that applying 10mM pyruvate to isolated rat hearts stimulates nearly 100% activity of the pyruvate dehydrogenase (PDH) enzyme complex (Dennis *et al.*, 1979). In addition, a previous whole heart mouse study has shown, perfusion with 10mM pyruvate (with or without 15mM glucose) prior to ischaemia can prolong the time to ischaemic contracture and improved post-ischaemic functional recovery (Flood *et al.*, 2003).

To determine the effects on contractile function of acutely increasing extracellular pyruvate from 5mM to 10mM, in association with acute changes in extracellular glucose (5mM or 20mM), isolated cardiomyocytes were subjected to the metabolic inhibition and re-energisation protocol. The same markers of ischaemic injury were measured and the same markers of re-energisation protection were also calculated as previously mentioned (see section 4.2.1).

The time-dependent effects of acute elevations in extracellular pyruvate in association with acute changes in extracellular glucose are shown in Figure 4.19.

Elevating extracellular pyruvate from 5mM to 10mM under normoglycaemic conditions significantly delayed the time to contractile failure (Figure 4.20A) from 186.3 ± 8.0 s to 221.7 ± 6.3 s ($P < 0.01$) respectively.

The control (5mM glucose/5mM pyruvate) time to contractile failure (Figure 4.20B) recorded on the same day as those perfused with 20mM glucose and 5mM pyruvate was 193.5 ± 9.3 s, this was not significantly different to the controls recorded on the same day as those perfused with 20mM glucose and 10mM pyruvate (186.3 ± 8.0 s, $P = 0.57$).

Prior to normalisation, the time to contractile failure under hyperglycaemic conditions (Figure 4.20C), for those recorded with 5mM pyruvate was 223.0 ± 8.8 s and 212.0 ± 9.9 s for those recorded with 10mM pyruvate. Once normalised, using the respective control data, the percentage change in the time to contractile failure (Figure 4.20D) shows elevating extracellular pyruvate from 5mM to 10mM had no effect with $116.9 \pm 9.4\%$ versus $113.4 \pm 3.5\%$ ($P = 0.70$) respectively.

Elevating extracellular pyruvate from 5mM to 10mM under normoglycaemic conditions had no effect on the time to rigor (Figure 4.21A), with 307.7 ± 4.0 s versus 318.8 ± 3.9 s ($P = 0.09$) respectively.

The control time to rigor (Figure 4.21B), recorded on the same day as those perfused with 20mM glucose and 5mM pyruvate was 310.7 ± 20.1 s, this was not significantly different to those controls recorded on the same day as those perfused with 10mM pyruvate (307.7 ± 4.0 s, $P = 0.89$).

Under hyperglycaemic conditions, prior to normalisation the time to rigor (Figure 4.21C), was 325.7 ± 17.2 s for those recorded with 5mM pyruvate and 312.5 ± 8.6 s for those recorded with 10mM pyruvate. Following normalisation, the percentage change in time to rigor (Figure 4.21D) shows elevating extracellular pyruvate from 5mM to 10mM had no effect with $105.7 \pm 5.3\%$ versus $101.4 \pm 2.4\%$ ($P = 0.43$) respectively.

Elevating extracellular pyruvate from 5mM to 10mM under normoglycaemic conditions had no effect on the percentage of 'non-hypercontracted' cardiomyocytes (Figure 4.22A), with $74.4 \pm 4.3\%$ versus $78.5 \pm 3.2\%$ ($P = 0.44$) respectively.

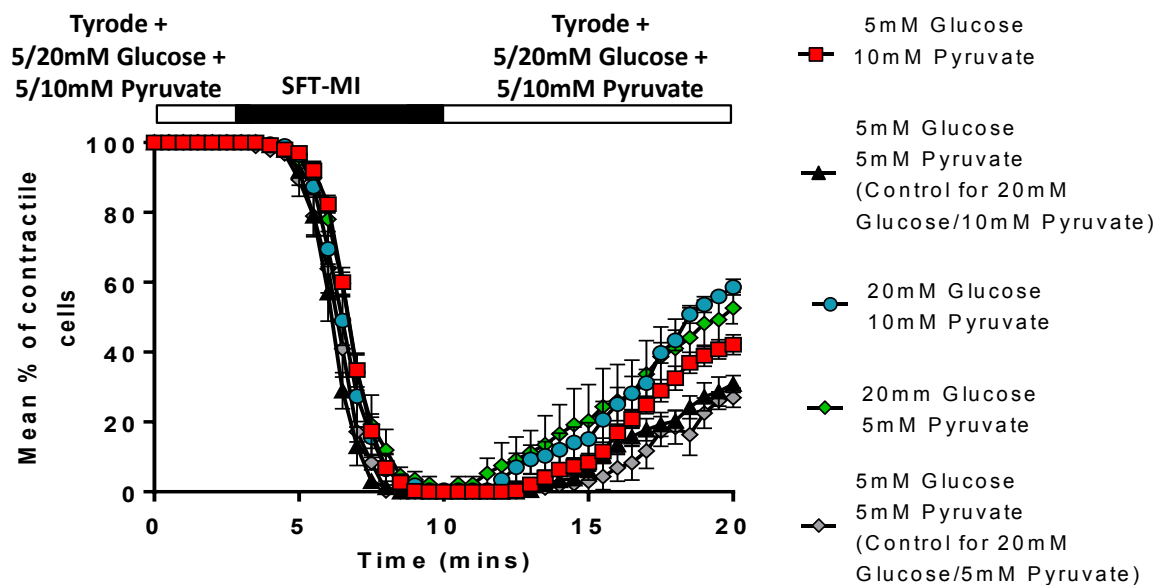


Figure 4.19 The effects of an acute elevation in extracellular pyruvate on the contractile function of isolated cardiomyocytes to metabolic inhibition and re-energisation in response to acute changes in extracellular glucose.

Time course of the percentage of cardiomyocytes contracting in response to EFS, during perfusion with SFT-MI and re-energisation. Prior to SFT-MI and during the 10 minutes of re-energisation cardiomyocytes were superfused with Tyrode solution containing either 5mM or 20mM glucose with either 5mM or 10mM pyruvate. Data represented as mean \pm s.e.m. Data for 5mM glucose, 5mM pyruvate (black bar, N=5 hearts, 5 fields of view, 200 cardiomyocytes) and 10mM pyruvate (red bar, N=5, 9, 275). Control data (5mM glucose/5mM pyruvate) for the 20mM glucose/5mM pyruvate data (grey bar, N=5, 5, 189) and for 20mM glucose/10mM pyruvate (black bar, N=5, 5, 200). Data for 20mM glucose, 5mM pyruvate (green bar, N=5, 5, 108) and 10mM pyruvate (blue bar, N=5, 7, 215).

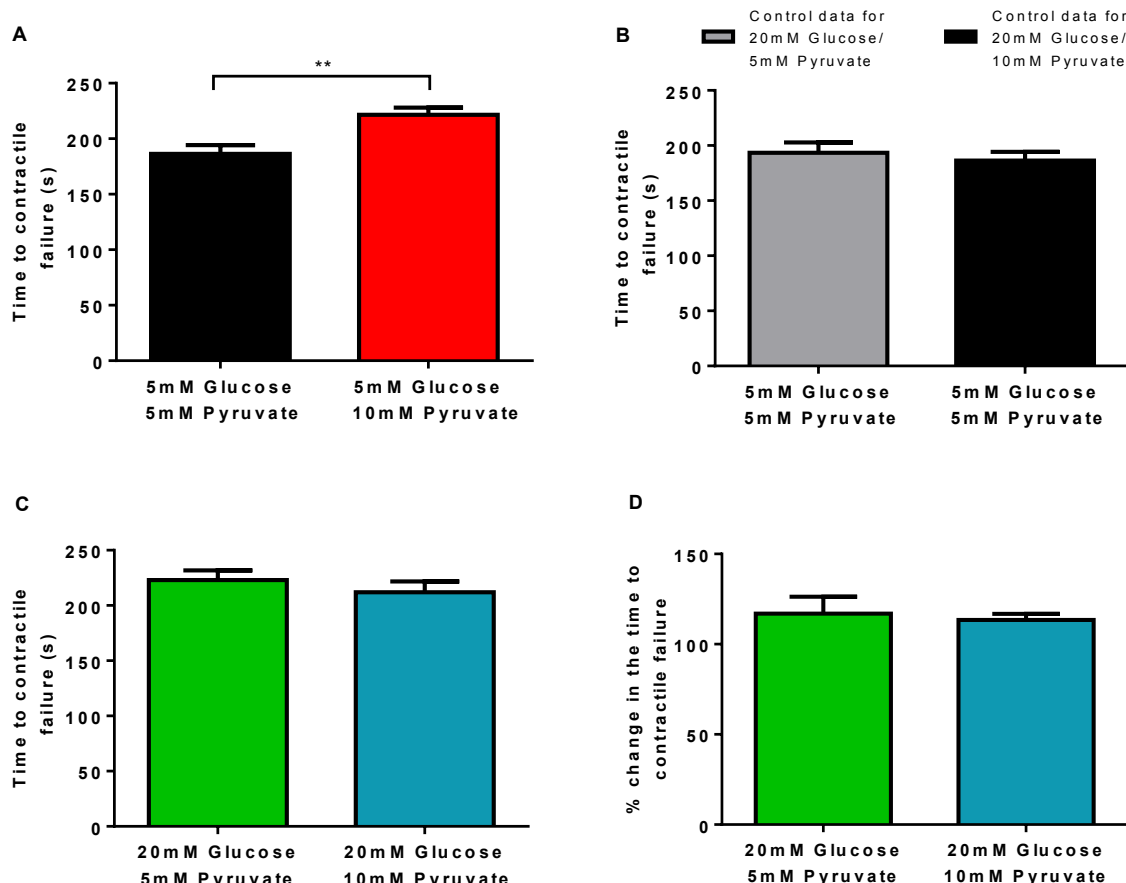


Figure 4.20 The effect of an acute elevation in extracellular pyruvate on the time to contractile failure during metabolic inhibition in response to acute changes in extracellular glucose.

- (A) Time to contractile failure from the onset of metabolic inhibition for cardiomyocytes superfused with 5mM glucose and either 5mM or 10mM pyruvate.
- (B) Time to contractile failure from the onset of metabolic inhibition for the control data (5mM glucose/5mM pyruvate) recorded at the beginning of each day for the 20mM glucose data sets.
- (C) Time to contractile failure from the onset of metabolic inhibition for cardiomyocytes superfused with 20mM glucose and either 5mM or 10mM pyruvate.
- (D) Normalised time to contractile failure for the 20mM glucose data sets represented as a % change in the time to contractile failure. Each 20mM glucose treatment group was normalised to its corresponding control, the 5mM pyruvate data (green bar) was normalised to the grey bar in (B) and the 10mM pyruvate data (blue bar) was normalised to the black bar in (B).

Data represented as mean \pm s.e.m. Data for 5mM glucose, 5mM pyruvate (black bar, N=5 hearts, 5 fields of view, 200 cardiomyocytes) and 10mM pyruvate (red bar, N=5, 9, 275). Control data (5mM glucose/5mM pyruvate) for the 20mM glucose/5mM pyruvate data (grey bar, N=5, 5, 189) and for 20mM glucose/10mM pyruvate (black bar, N=5, 5, 200). Data for 20mM glucose, 5mM pyruvate (green bar, N=5, 5, 108) and 10mM pyruvate (blue bar, N=5, 7, 215). *P<0.05 (Unpaired T-test).

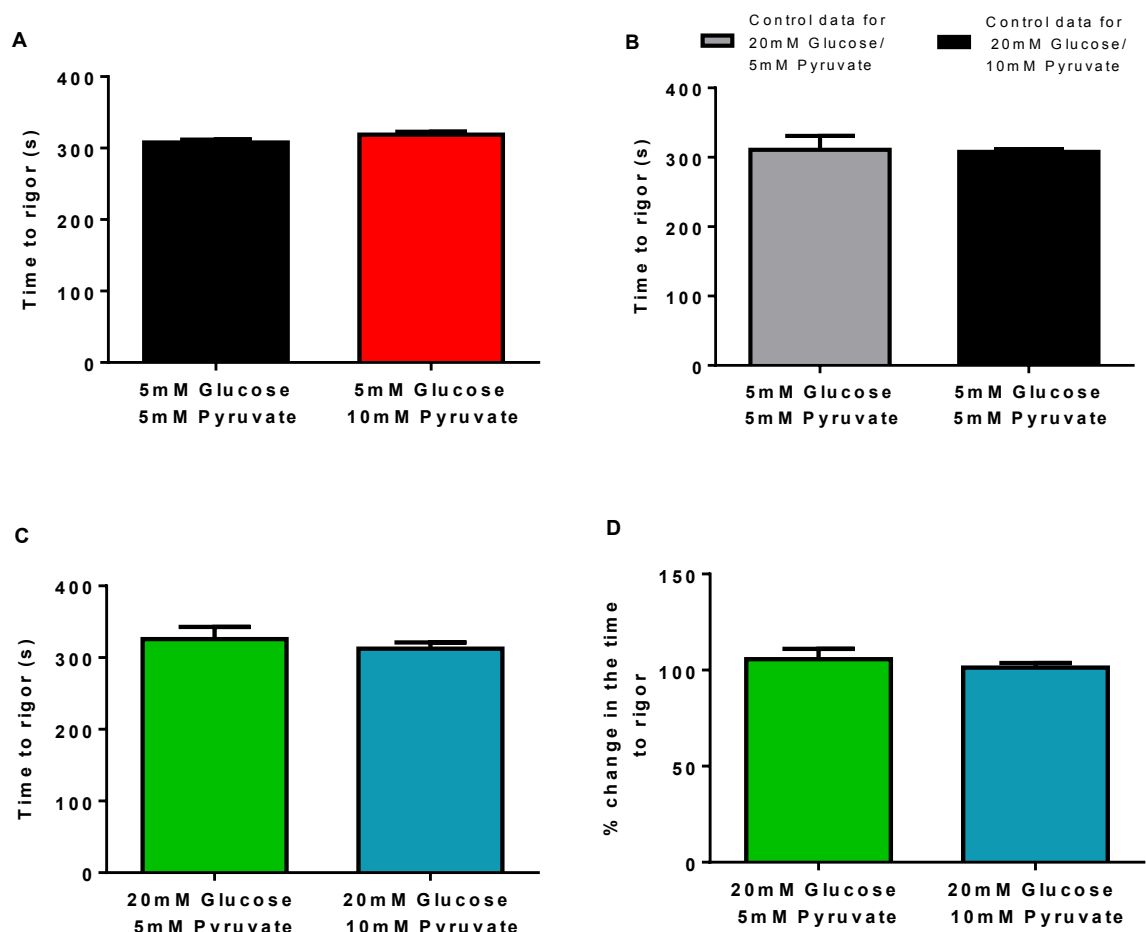


Figure 4.21 The effect of an acute elevation in extracellular pyruvate on the time to rigor contracture to metabolic inhibition in response to acute changes in extracellular glucose.

- (A) Time to rigor contracture from the onset of metabolic inhibition for cardiomyocytes superfused with 5mM glucose and either 5mM or 0.5mM pyruvate.
- (B) Time to rigor from the onset of metabolic inhibition for the control data (5mM glucose/5mM pyruvate) recorded at the beginning of each day for the 20mM glucose data sets.
- (C) Time to rigor contracture from the onset of metabolic inhibition for cardiomyocytes superfused with 20mM glucose and either 5mM or 0.5mM pyruvate.
- (D) Normalised time to rigor for the 20mM glucose data sets represented as a % change in the time to rigor. Each 20mM glucose treatment group was normalised to its corresponding control, the 5mM pyruvate data (green bar) was normalised to the grey bar in (B) and the 0.5mM pyruvate data (blue bar) was normalised to the black bar in (B).

Data represented as mean \pm s.e.m. Data for 5mM glucose, 5mM pyruvate (black bar, N=5 hearts, 5 fields of view, 200 cardiomyocytes) and 10mM pyruvate (red bar, N=5, 9, 275). Control data (5mM glucose/5mM pyruvate) for the 20mM glucose/5mM pyruvate data (grey bar, N=5, 5, 189) and for 20mM glucose/10mM pyruvate (black bar, N=5, 5, 200). Data for 20mM glucose, 5mM pyruvate (green bar, N=5, 5, 108) and 10mM pyruvate (blue bar, N=5, 7, 215).

The control percentage of 'non-hypercontracted' cardiomyocytes (Figure 4.22B) recorded on the same day as those perfused with 20mM glucose and 5mM pyruvate was $77.6 \pm 2.4\%$, this was not significantly different to the controls recorded on the same day as those perfused with 10mM pyruvate $74.4 \pm 4.3\%$ ($P=0.53$).

Prior to normalisation, the percentage of 'non-hypercontracted' cardiomyocytes under hyperglycaemic conditions (Figure 4.22C), was $80.3 \pm 4.6\%$ for those recorded with 5mM pyruvate and $83.2 \pm 3.0\%$ for those recorded with 10mM pyruvate. Once normalised, the percentage change in 'non-hypercontracture' (Figure 4.22D) shows elevating extracellular pyruvate from 5mM to 10mM had no effect with $103.6 \pm 5.0\%$ versus $111.4 \pm 5.1\%$ ($P=0.32$) respectively.

Under normoglycaemic conditions, elevating extracellular pyruvate from 5mM to 10mM significantly increased the percentage of contractile recovery (Figure 4.23A), from $30.8 \pm 2.5\%$ to $42.1 \pm 2.9\%$ ($P<0.05$) respectively.

The control percentage of contractile recovery (Figure 4.23B), recorded on the same day as those perfused with 20mM glucose and 5mM pyruvate was $26.9 \pm 2.8\%$, this was not significantly different to the controls recorded on the same day as those perfused with 10mM pyruvate ($30.8 \pm 2.5\%$, $P=0.32$).

Under hyperglycaemic conditions, the percentage of contractile recovery prior to normalisation (Figure 4.23C), was $52.6 \pm 4.5\%$ for those recorded with 5mM pyruvate and $58.7 \pm 2.3\%$ for those recorded with 10mM pyruvate. Following normalisation, the percentage change in contractile recovery (Figure 4.23D) shows elevating extracellular pyruvate from 5mM to 10mM had no effect with $204.9 \pm 32.7\%$ versus $207.6 \pm 25.8\%$ ($P=0.95$) respectively.

These data suggest that elevating extracellular pyruvate under normoglycaemic conditions delayed contractile failure and improved contractile recovery. While under hyperglycaemic conditions elevating extracellular pyruvate had no additional effect.

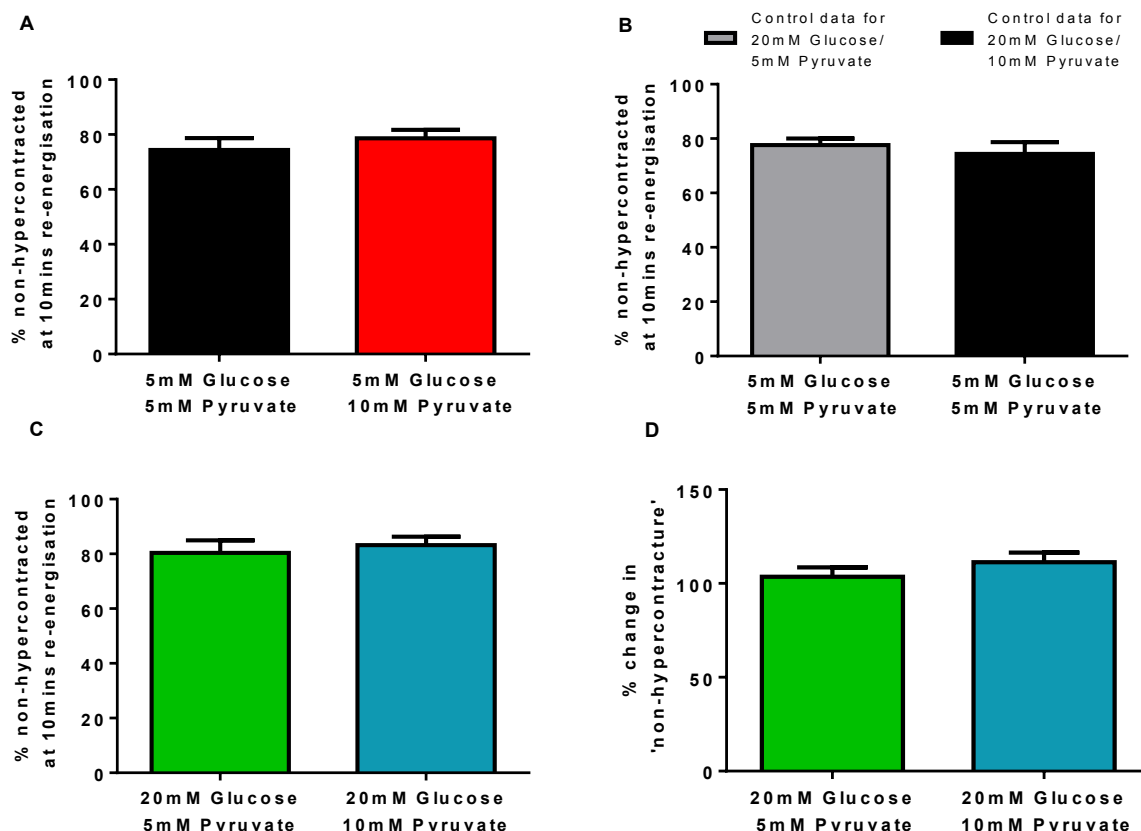


Figure 4.22 The effect of an acute elevation in extracellular pyruvate on the viability of isolated cardiomyocytes to metabolic inhibition and re-energisation in response to acute changes in extracellular glucose.

- (A) The percentage of cardiomyocytes relaxed from hypercontracted 'non-hypercontracted' by the end of 10 minutes of re-energisation following superfusion with 5mM glucose and either 5mM or 10mM pyruvate.
- (B) The percentage of cardiomyocytes relaxed from hypercontracted 'non-hypercontracted' by the end of 10 minutes of re-energisation for the control data (5mM glucose/5mM pyruvate) recorded at the beginning of each day for the 20mM glucose data sets.
- (C) The percentage of cardiomyocytes relaxed from hypercontracted 'non-hypercontracted' by the end of 10 minutes of re-energisation following superfusion with 20mM glucose and either 5mM or 10mM pyruvate.
- (D) Normalised percentage of 'non-hypercontracted' cardiomyocytes for the 20mM glucose data sets represented as a % change in 'non-hypercontracture'. Each 20mM glucose treatment group was normalised to its corresponding control, the 5mM pyruvate data (green bar) was normalised to the grey bar in (B) and the 10mM pyruvate data (blue bar) was normalised to the black bar in (B).

Data represented as mean \pm s.e.m. Data for 5mM glucose, 5mM pyruvate (black bar, N=5 hearts, 5 fields of view, 200 cardiomyocytes) and 10mM pyruvate (red bar, N=5, 9, 275). Control data (5mM glucose/5mM pyruvate) for the 20mM glucose/5mM pyruvate data (grey bar, N=5, 5, 189) and for 20mM glucose/10mM pyruvate (black bar, N=5, 5, 200). Data for 20mM glucose, 5mM pyruvate (green bar, N=5, 5, 108) and 10mM pyruvate (blue bar, N=5, 7, 215).

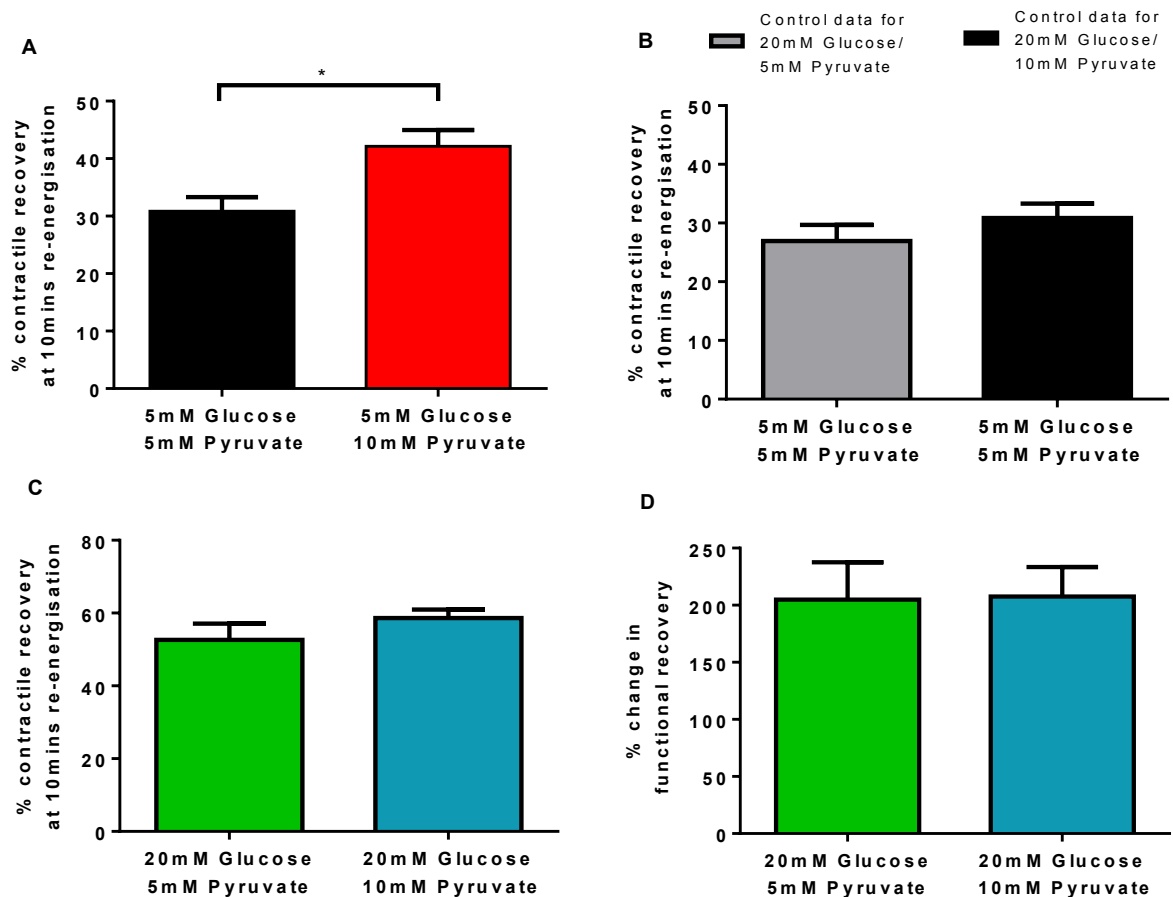


Figure 4.23 The effect of an acute elevation in extracellular pyruvate on the recovery of isolated cardiomyocytes to metabolic inhibition and re-energisation in response to acute changes in extracellular glucose.

- (A) The percentage of cardiomyocytes regaining contractile function in response to EFS by the end of 10 minutes of re-energisation following superfusion with 5mM glucose and either 5mM or 10mM pyruvate.
- (B) The percentage of cardiomyocytes regaining contractile function in response to EFS by the end of 10 minutes of re-energisation for the control data (5mM glucose/5mM pyruvate) recorded at the beginning of each day for the 20mM glucose data sets.
- (C) The percentage of cardiomyocytes regaining contractile function in response to EFS by the end of 10 minutes of re-energisation following superfusion with 20mM glucose and either 5mM or 10mM pyruvate.
- (D) Normalised contractile recovery for the 20mM glucose data sets represented as a % change in functional recovery. Each 20mM glucose treatment group was normalised to its corresponding control, the 5mM pyruvate data (green bar) was normalised to the grey bar in (B) and the 10mM pyruvate data (blue bar) was normalised to the black bar in (B).

Data represented as mean \pm s.e.m. Data for 5mM glucose, 5mM pyruvate (black bar, N=5 hearts, 5 fields of view, 200 cardiomyocytes) and 10mM pyruvate (red bar, N=5, 9, 275). Control data (5mM glucose/5mM pyruvate) for the 20mM glucose/5mM pyruvate data (grey bar, N=5, 5, 189) and for 20mM glucose/10mM pyruvate (black bar, N=5, 5, 200). Data for 20mM glucose, 5mM pyruvate (green bar, N=5, 5, 108) and 10mM pyruvate (blue bar, N=5, 7, 215). *P<0.05 (Unpaired T-test).

4.2.7 Fatty acid metabolism prevents the cardioprotection previously elicited by elevated extracellular glucose

The normal physiological blood fatty acid concentration is 0.2-0.6mM (Lopaschuk *et al.*, 2010). Fatty acids are the preferred metabolic substrate for the myocardium under normal physiological conditions. However during ischaemia, fatty acid oxidation ceases and anaerobic glycolysis becomes the main source of ATP production. Upon reperfusion mitochondrial oxidative phosphorylation is re-instated, and the fatty acids which would have built up during ischaemia can be metabolised. This can lead to inhibition of glucose oxidation (i.e. metabolism of pyruvate) and can be detrimental. Therefore the effects of a physiological concentration of fatty acid on isolated cardiomyocytes, under both normoglycaemic and hyperglycaemic conditions were investigated. The fatty acid used in these experiments was octanoate (C₈), which is a medium chain length fatty acid and cycles through β -oxidation 3 times (summarised in Figure 4.24).

4.2.7.1 Replacement of pyruvate for octanoate

In previous experiments the only direct oxidative phosphorylation metabolic substrate perfused to cardiomyocytes was pyruvate. Therefore initially a set of experiments were carried out with octanoate in the absence of pyruvate (0mM), to determine the effects of octanoate as the only directly available oxidative phosphorylation metabolic substrate, on the contractile function of isolated cardiomyocytes under normoglycaemic and hyperglycaemic conditions.

To determine the effects of octanoate (0.5mM) in the absence of pyruvate (0mM) on contractile function with acute increases in extracellular glucose, isolated cardiomyocytes were subjected to metabolic inhibition and re-energisation (as described in section 4.2.1). As the concentration of octanoate used was 0.5mM these results were compared to those perfused with 0.5mM pyruvate (data previously described in chapter 4.2.1). The effects of octanoate in associated with acute changes in extracellular glucose, had a similar time-dependent (Figure 4.25) profile of contractile failure but a lower recovery on re-energisation compared to those perfused with 0.5mM pyruvate.

The control (5mM glucose/5mM pyruvate) time to contractile failure (Figure 4.26A) recorded on the same day as those perfused with 0.5mM pyruvate was $196.7 \pm 9.7s$, this was not significantly different to the controls recorded on the same day as those perfused with and 0.5mM octanoate and 0mM pyruvate ($201.9 \pm 11.0s$, $P=0.74$).

Under normoglycaemic conditions, the time to contractile failure prior to normalisation (Figure 4.26B), was $157.2 \pm 9.0s$ for those recorded with 0.5mM pyruvate and $166.4 \pm 10.3s$ for those recorded with 0.5mM octanoate. Under hyperglycaemic conditions, prior to normalisation the time to contractile failure (Figure 4.26B), for those recorded with 0.5mM pyruvate was $170.4 \pm 3.0s$ and $175.3 \pm 6.1s$ for those recorded with 0.5mM octanoate.

Following normalisation, the percentage change in the time to contractile failure (Figure 4.26C) shows replacing pyruvate with octanoate under normoglycaemic or hyperglycaemic conditions had no effect, with $80.5 \pm 3.9\%$ (5mM glucose/0.5mM pyruvate) versus $83.4 \pm 8.2\%$ (5mM glucose/0.5mM octanoate, $P=0.74$), and $85.1 \pm 4.7\%$ (20mM glucose/0.5mM pyruvate) versus $90.2 \pm 4.8\%$ (20mM glucose/0.5mM octanoate, $P=0.47$).

The control time to rigor (Figure 4.27A) recorded on the same day as those perfused with 0.5mM pyruvate was $307 \pm 9.1s$, this was not significantly different to those controls recorded on the same day as those perfused with 0.5mM octanoate ($337 \pm 18.5s$, $P=0.16$).

Prior to normalisation the time to rigor (Figure 4.27B), under normoglycaemic conditions, was $244.9 \pm 5.8s$ for those recorded with 0.5mM pyruvate and $275.2 \pm 16.0s$ for those recorded with 0.5mM octanoate. Under hyperglycaemic conditions, the time to rigor was $250.4 \pm 4.7s$ for those recorded with 0.5mM pyruvate and $278.2 \pm 16.7s$ for those recorded with 0.5mM octanoate.

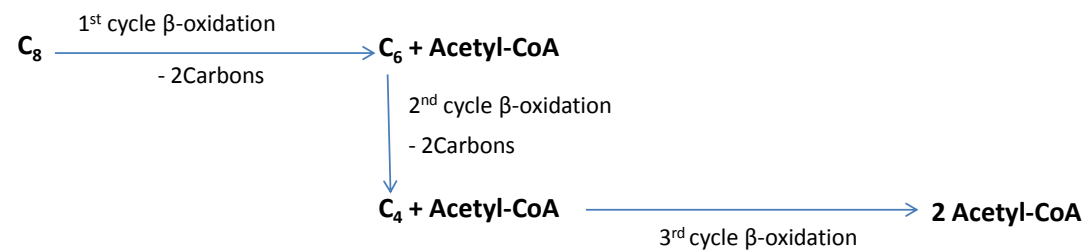
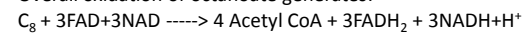


Figure 4.24 β -oxidation of octanoate

Octanoate (C_8) is a medium chain length fatty acid, which undergoes 3 cycles of β -oxidation to generate 4 molecules of acetyl-CoA, which can then feed into the Krebs cycle.

Overall oxidation of octanoate generates:



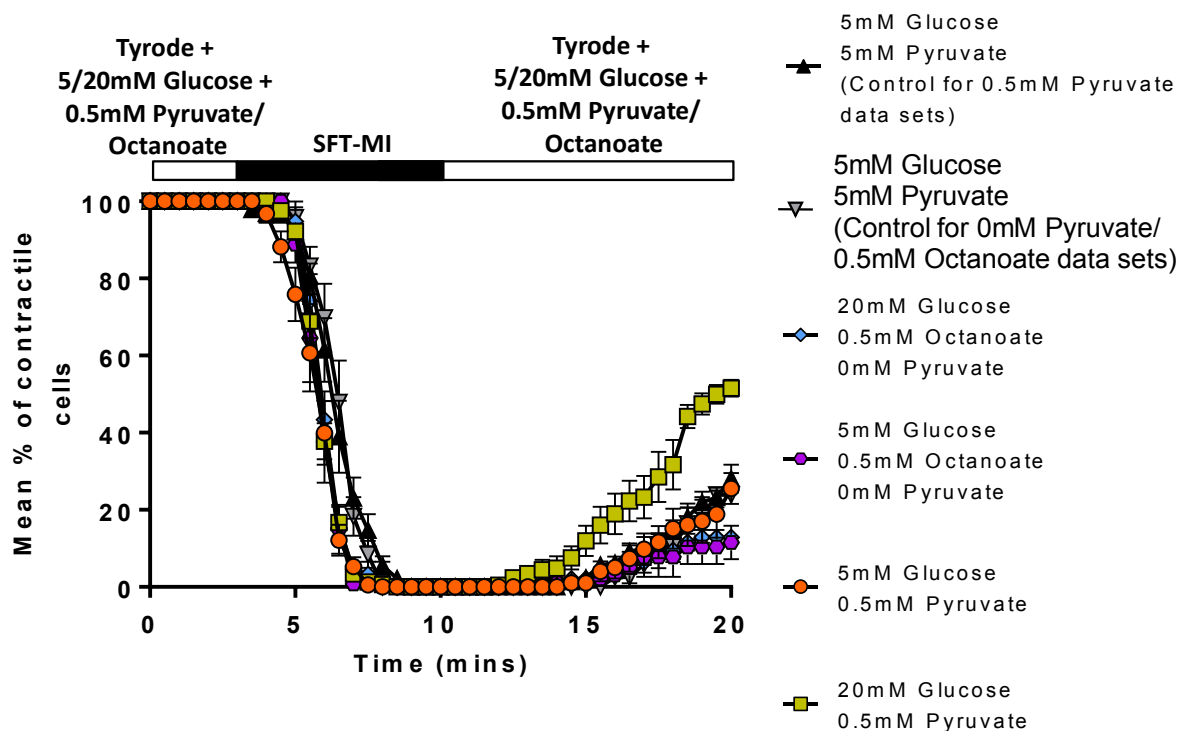


Figure 4.25 The effects of replacing pyruvate with octanoate on the contractile function of isolated cardiomyocytes to metabolic inhibition and re-energisation in response to acute changes in extracellular glucose.

Time course of the percentage of cardiomyocytes contracting in response to EFS, during perfusion with SFT-MI and re-energisation. Prior to SFT-MI and during the 10 minutes of re-energisation cardiomyocytes were superfused with Tyrode solution containing 5mM or 20mM glucose with either 5mM or 0mM pyruvate, with or without 0.5mM octanoate. Data represented as mean \pm s.e.m. Control data (5mM glucose/5mM pyruvate) for the 0.5mM pyruvate data sets (black bar, N=4 hearts, 4 fields of view, 154 cardiomyocytes) and the 0.5mM octanoate data sets (grey bar, N=3, 3, 54). Data for 0.5mM pyruvate, 5mM glucose (orange bar, N=4, 6, 133) and 20mM glucose (yellow bar N=4, 6, 169). Data for 0.5mM octanoate, 5mM glucose (purple bar, N=3, 5, 96) and 20mM glucose (blue bar, N=3, 3, 156).

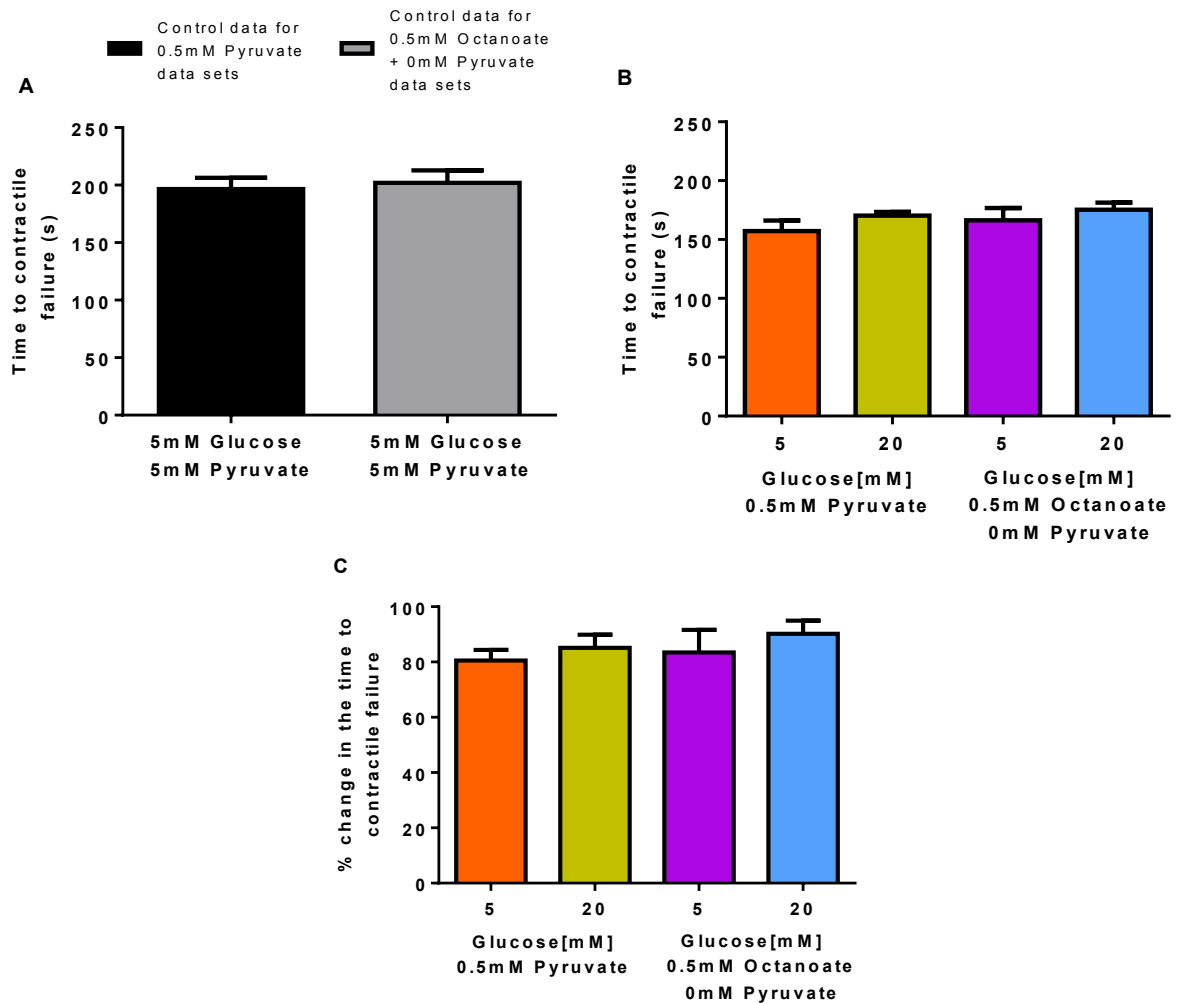


Figure 4.26 The effects of replacing pyruvate with octanoate and acute changes in extracellular glucose on the time to contractile failure during metabolic inhibition.

- (A) Time to contractile failure from the onset of metabolic inhibition for the control data (5mM glucose/5mM pyruvate) recorded at the beginning of each day for each data set.
- (B) Time to contractile failure from the onset of metabolic inhibition for cardiomyocytes superfused with 5mM or 20mM glucose, with either 0.5mM pyruvate or 0.5mM octanoate and 0mM pyruvate.
- (C) Normalised time to contractile failure for all data sets represented as a % change in the time to contractile failure. Each treatment group was normalised to its corresponding control data set, the 0.5mM pyruvate data sets (orange and yellow bars) were normalised to the black bar in (A) and the octanoate data sets (purple and blue bars) were normalised to the grey bar in (A). Data represented as mean \pm s.e.m. Control data (5mM glucose/5mM pyruvate) for the 0.5mM pyruvate data sets (black bar, N=4 hearts, 4 fields of view, 154 cardiomyocytes) and the 0.5mM octanoate data sets (grey bar, N=3, 3, 54). Data for 0.5mM pyruvate, 5mM glucose (orange bar, N=4, 6, 133) and 20mM glucose (yellow bar N=4, 6, 169). Data for 0.5mM octanoate, 5mM glucose (purple bar, N=3, 5, 96) and 20mM glucose (blue bar, N=3, 3, 156).

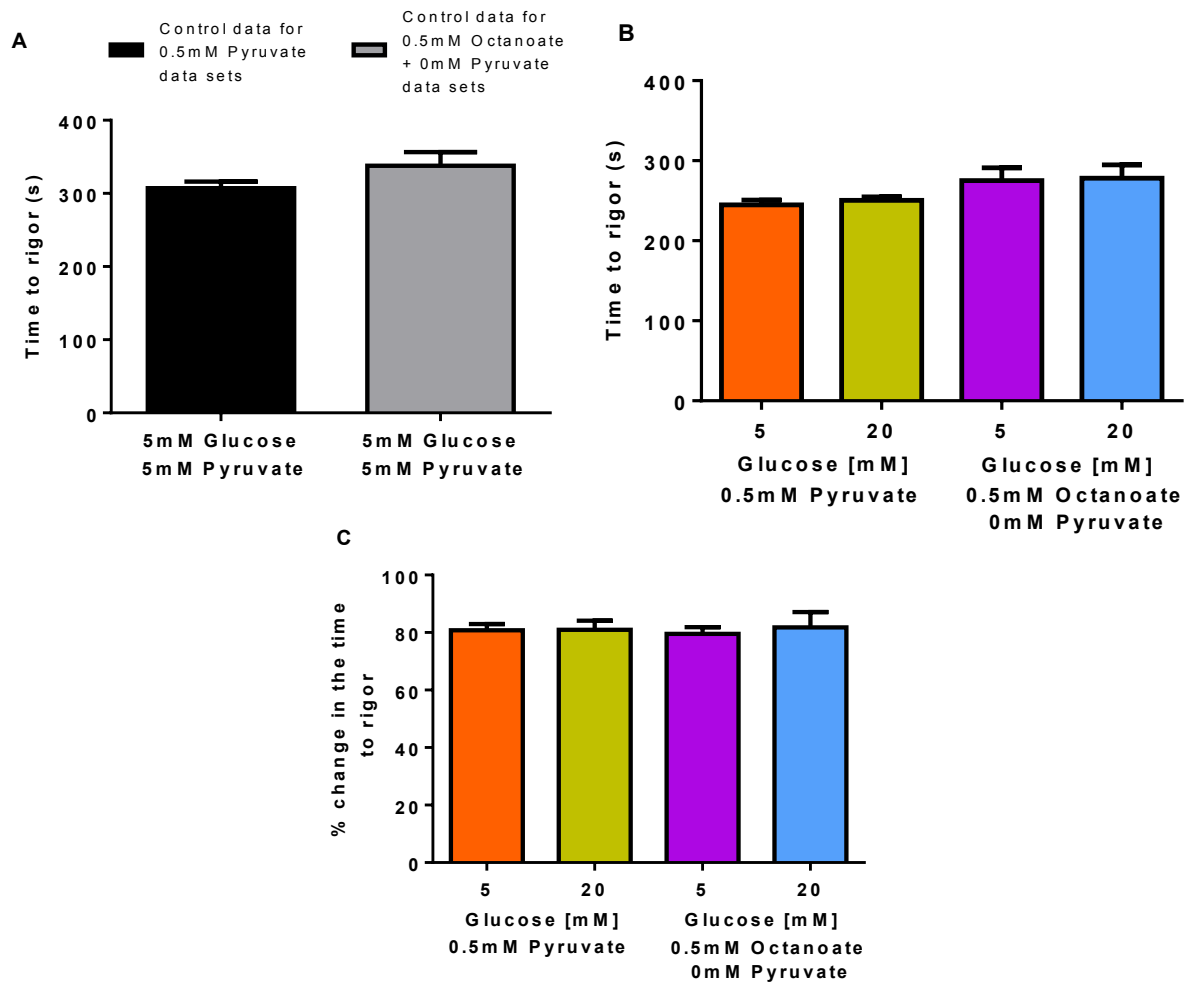


Figure 4.27 The effect of replacing pyruvate with octanoate and acute changes in extracellular glucose on the time to rigor contracture during metabolic inhibition.

- (A) Time to rigor from the onset of metabolic inhibition for the control data (5mM glucose/5mM pyruvate) recorded at the beginning of each day for each data set.
- (B) Time to rigor contracture from the onset of metabolic inhibition for cardiomyocytes superfused with 5mM or 20mM glucose, with either 0.5mM pyruvate or 0.5mM octanoate and 0mM pyruvate.
- (C) Normalised time to rigor contracture for all data sets represented as a % change in the time to rigor contracture. Each treatment group was normalised to its corresponding control data set, the lower pyruvate data sets (orange and yellow bars) were normalised to the black bar in (A) and the 0.5mM octanoate data sets (purple and blue bars) were normalised to the grey bar in (A).

Data represented as mean \pm s.e.m. Control data (5mM glucose/5mM pyruvate) for the 0.5mM pyruvate data sets (black bar, N=4 hearts, 4 fields of view, 154 cardiomyocytes) and the 0.5mM octanoate data sets (grey bar, N=3, 3, 54). Data for 0.5mM pyruvate, 5mM glucose (orange bar, N=4, 6, 133) and 20mM glucose (yellow bar N=4, 6, 169). Data for 0.5mM octanoate, 5mM glucose (purple bar, N=3, 5, 96) and 20mM glucose (blue bar, N=3, 3, 156).

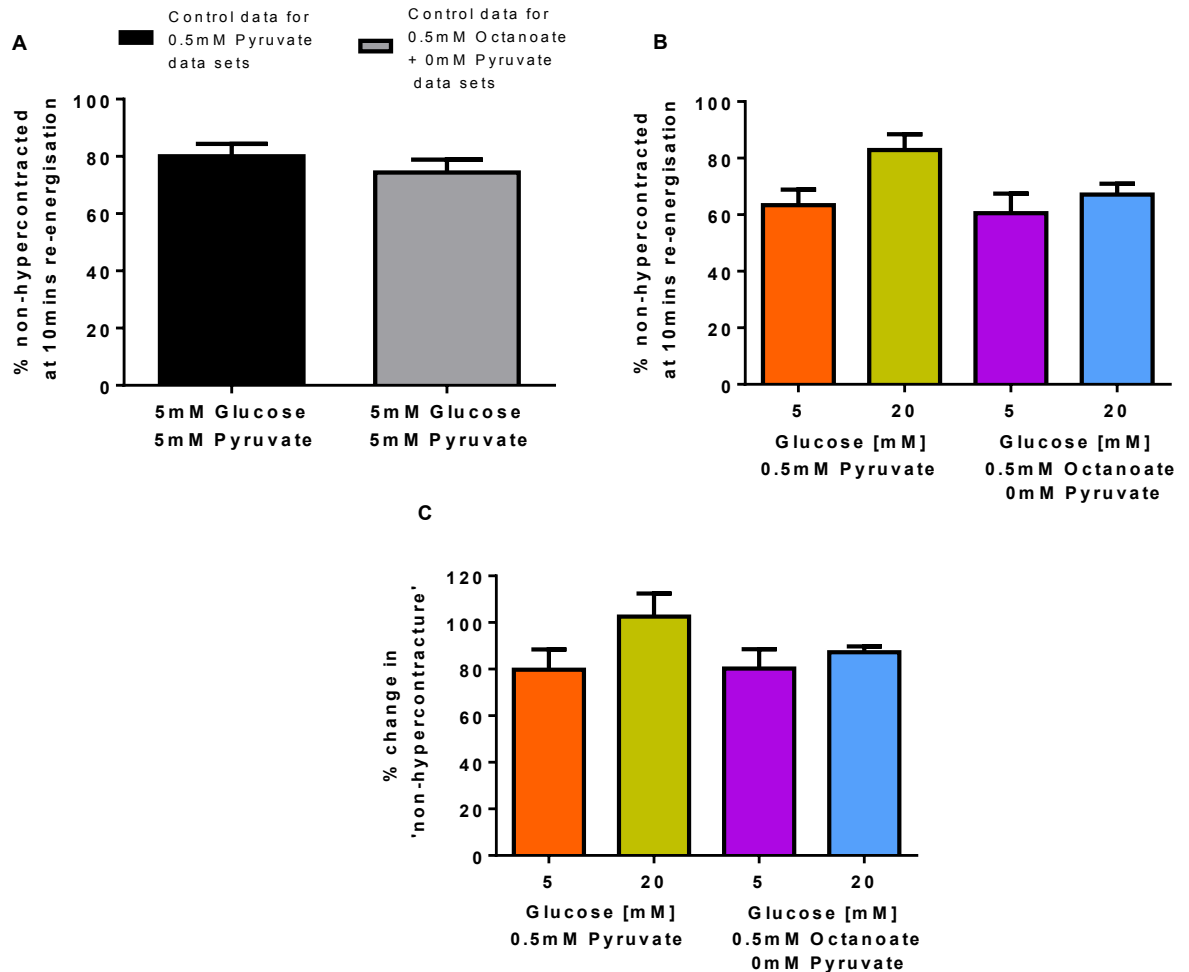


Figure 4.28 The effect of replacing pyruvate with octanoate and acute changes in extracellular glucose on the viability of isolated cardiomyocytes to metabolic inhibition and re-energisation.

- (A) The percentage of cardiomyocytes relaxed from hypercontracted 'non-hypercontracted' by the end of 10 minutes of re-energisation for the control data (5mM glucose/5mM pyruvate) recorded at the beginning of each day for each data set.
- (B) The percentage of cardiomyocytes relaxed from hypercontracted 'non-hypercontracted' by the end of 10 minutes of re-energisation, following superfusion with 5mM or 20mM glucose, with either 0.5mM pyruvate or 0.5mM octanoate and 0mM pyruvate.
- (C) Normalised percentage of 'non-hypercontracted' cardiomyocytes for both data sets represented as a % change in 'non-hypercontracture'. Each treatment group was normalised to its corresponding control data set, the 0.5mM pyruvate data sets (orange and yellow bars) were normalised to the black bar in (A) and the 0.5mM octanoate data sets (purple and blue bars) were normalised to the grey bar in (A).

Data represented as mean \pm s.e.m. Control data (5mM glucose/5mM pyruvate) for the 0.5mM pyruvate data sets (black bar, N=4 hearts, 4 fields of view, 154 cardiomyocytes) and the 0.5mM octanoate data sets (grey bar, N=3, 3, 54). Data for 0.5mM pyruvate, 5mM glucose (orange bar, N=4, 6, 133) and 20mM glucose (yellow bar N=4, 6, 169). Data for 0.5mM octanoate, 5mM glucose (purple bar, N=3, 5, 96) and 20mM glucose (blue bar, N=3, 3, 156).

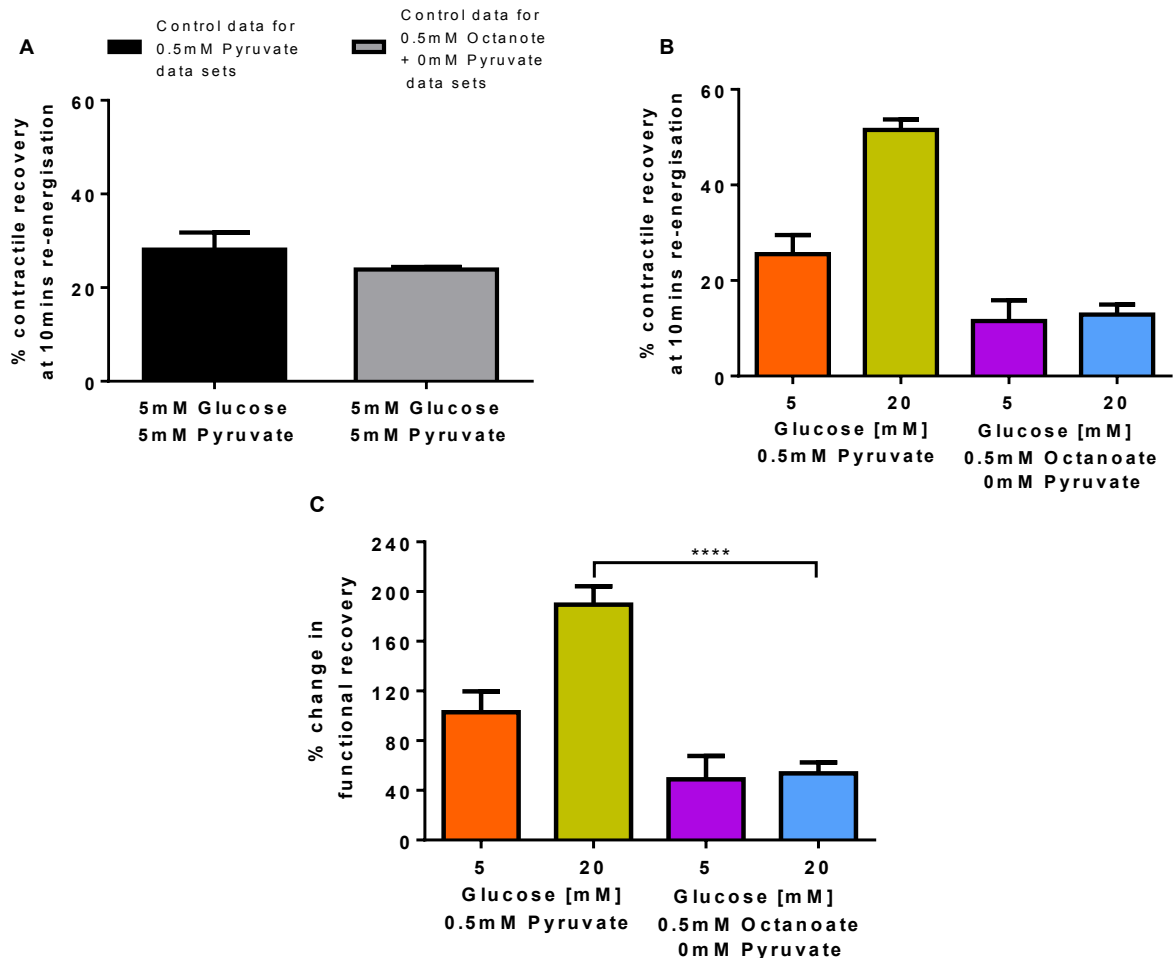


Figure 4.29 The effect of replacing pyruvate with octanoate and acute changes in extracellular glucose on the recovery of isolated cardiomyocytes to metabolic inhibition and re-energisation.

- (A) The percentage of cardiomyocytes regaining contractile function in response to EFS by the end of 10 minutes of re-energisation for the control data (5mM glucose/5mM pyruvate) recorded at the beginning of each day for each data set.
- (B) The percentage of cardiomyocytes regaining contractile function in response to EFS by the end of 10 minutes of re-energisation, following superfusion with 5mM or 20mM glucose, with either 0.5mM pyruvate or 0.5mM octanoate and 0mM pyruvate.
- (C) Normalised contractile recovery for both data sets represented as a % change in functional recovery. Each treatment group was normalised to its corresponding control data set, the 0.5mM pyruvate data sets (orange and yellow bars) were normalised to the black bar in (A) and the 0.5mM octanoate data sets (purple and blue bars) were normalised to the grey bar in (A).

Data represented as mean \pm s.e.m. Control data (5mM glucose/5mM pyruvate) for the 0.5mM pyruvate data sets (black bar, N=4 hearts, 4 fields of view, 154 cardiomyocytes) and the 0.5mM octanoate data sets (grey bar, N=3, 3, 54). Data for 0.5mM pyruvate, 5mM glucose (orange bar, N=4, 6, 133) and 20mM glucose (yellow bar N=4, 6, 169). Data for 0.5mM octanoate, 5mM glucose (purple bar, N=3, 5, 96) and 20mM glucose (blue bar, N=3, 3, 156). ****P<0.0001 (Unpaired T-test).

Once normalised, the percentage change in the time to rigor (Figure 4.27C) shows replacing pyruvate with octanoate had no effect under normoglycaemic or hyperglycaemic conditions, with $80.8 \pm 2.2\%$ (5mM glucose/0.5mM pyruvate) versus $79.6 \pm 2.3\%$ (5mM glucose/0.5mM octanoate, $P=0.71$) and with $80.9 \pm 3.1\%$ (20mM glucose/0.5mM pyruvate) versus $81.8 \pm 5.4\%$ (20mM glucose/0.5mM octanoate, $P=0.89$).

The control percentage of 'non-hypercontracted' cardiomyocytes (Figure 4.28A) for those recorded on the same day as those perfused with 0.5mM pyruvate was $80.1 \pm 4.3\%$, this was not significantly different to those recorded on the same day as those perfused with 0.5mM octanoate ($74.4 \pm 4.5\%$, $P=0.41$).

Under normoglycaemic conditions, prior to normalisation the percentage of 'non-hypercontracted' cardiomyocytes (Figure 4.28B), for those recorded with 0.5mM pyruvate was $63.3 \pm 5.5\%$ and $60.5 \pm 6.9\%$ for those recorded with 0.5mM octanoate. Under hyperglycaemic conditions, prior to normalisation the percentage of 'non-hypercontracted' cardiomyocytes (Figure 4.28B), for those recorded with 0.5mM pyruvate was $82.8 \pm 5.6\%$ and $67.1 \pm 3.8\%$ for those recorded with 0.5mM octanoate.

Once normalised, the percentage change in 'non-hypercontracture' (Figure 4.28C) shows replacing pyruvate with octanoate under normoglycaemic or hyperglycaemic conditions, had no effect with $79.7 \pm 8.7\%$ (5mM glucose/0.5mM pyruvate) versus $80.3 \pm 8.2\%$ (5mM glucose/0.5mM octanoate, $P=0.96$) and $102.6 \pm 9.9\%$ (20mM glucose/0.5mM pyruvate) versus $87.2 \pm 2.6\%$ (20mM glucose/0.5mM octanoate, $P=0.16$).

The control percentage of contractile recovery (Figure 4.29A), recorded on the same day as those perfused with 0.5mM pyruvate was $28.1 \pm 3.6\%$, this was not significantly different to the controls recorded on the same day as those perfused with 0.5mM octanoate ($23.9 \pm 0.6\%$, $P=0.37$).

Under normoglycaemic conditions, prior to normalisation the percentage of contractile recovery (Figure 4.29B), was $25.5 \pm 4.0\%$ for those recorded with 0.5mM pyruvate and $11.5 \pm 4.3\%$ for those recorded with 0.5mM octanoate. Under

hyperglycaemic conditions, prior to normalisation the percentage of contractile recovery (Figure 4.29B), for those recorded with 0.5mM pyruvate was $51.5 \pm 2.2\%$ and $12.9 \pm 2.1\%$ for those recorded with 0.5mM octanoate.

Once normalised, the percentage change in contractile recovery (Figure 4.29C) shows replacing pyruvate with octanoate under normoglycaemic conditions had no effect with $102.9 \pm 16.8\%$ (0.5mM pyruvate) versus $49.0 \pm 18.7\%$ (0.5mM octanoate, $P=0.06$). While under hyperglycaemic conditions, replacing pyruvate with octanoate significantly reduced the percentage of contractile recovery with $189.5 \pm 14.9\%$ (0.5mM pyruvate) versus $53.7 \pm 19.9\%$ (0.5mM octanoate, $P<0.0001$).

4.2.7.2 The addition of pyruvate on the actions of octanoate

Following on from those experiments with 0mM pyruvate, a set of experiments were carried out with 0.5mM octanoate and 5mM pyruvate, under both normoglycaemic and hyperglycaemic conditions. These results were compared to those perfused with 0mM pyruvate + 0.5mM octanoate (previously described in section 4.2.7.1). The effects of octanoate in the presence of 5mM pyruvate were investigated using the same protocols as those experiments with 0mM pyruvate.

The time -dependent effects of the addition of pyruvate on octanoate in association with acute changes in extracellular glucose, is shown in Figure 4.30 and shows a similar profile of contractile failure and a low recovery on re-energisation as those perfused with 0.5mM octanoate and 0mM pyruvate.

The control (5mM glucose/5mM pyruvate) time to contractile failure (Figure 4.31A) recorded on the same day as those perfused with 0.5mM octanoate and 0mM pyruvate was $201.9 \pm 11.0s$, this was not significantly different to those controls recorded on the same day as those perfused with 0.5mM octanoate and 5mM pyruvate ($186.6 \pm 10.7s$, $P=0.37$).

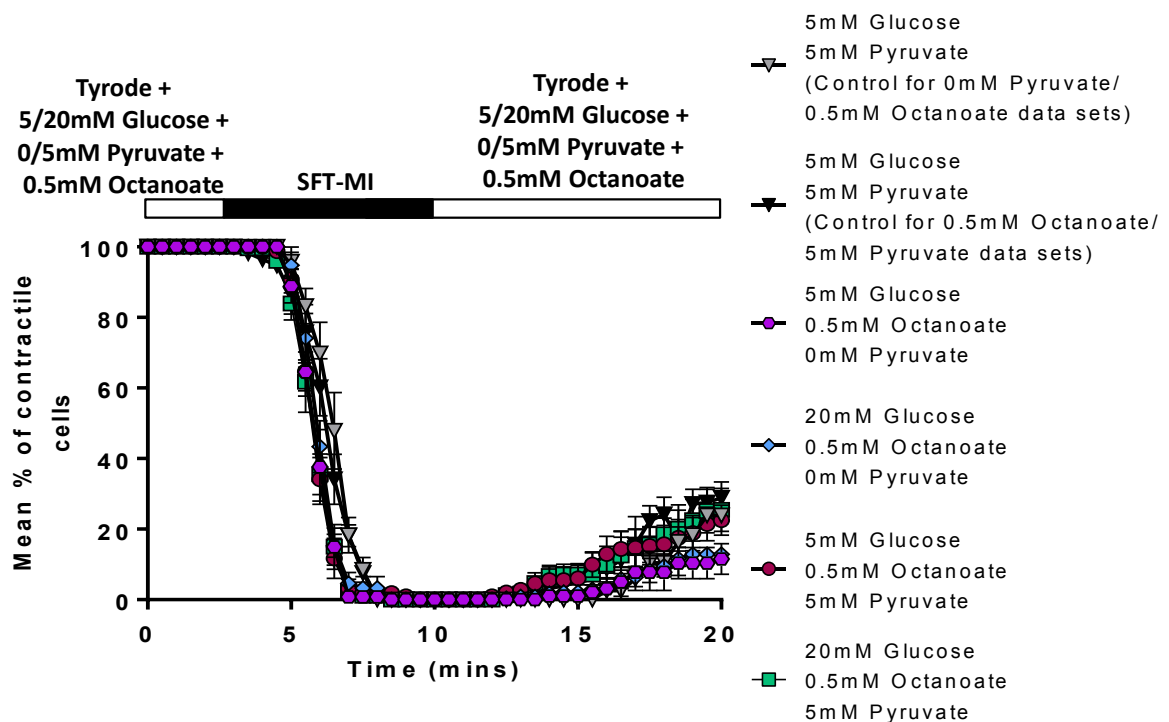


Figure 4.30 The impact of the addition of pyruvate on the effects of octanoate on the contractile function of isolated cardiomyocytes to metabolic inhibition and re-energisation in response to acute changes in extracellular glucose.

Time course of the percentage of cardiomyocytes contracting in response to EFS, during perfusion with SFT-MI and re-energisation. Prior to SFT-MI and during the 10 minutes of re-energisation cardiomyocytes were superfused with Tyrode solution containing either 5mM or 20mM glucose, with either 0.5mM pyruvate and 0.5mM octanoate or 5mM pyruvate and 0.5mM octanoate. Control cardiomyocytes were perfused with 5mM glucose and 5mM pyruvate. Data represented as mean \pm s.e.m. Control data (5mM glucose/5mM pyruvate) for the 0.5mM octanoate with 0mM pyruvate data sets (grey bar, N=3 hearts, 3 fields of view, 54 cardiomyocytes) and for the 0.5mM octanoate data with 5mM pyruvate sets (black bar, N=3, 3, 152). Data for 0.5mM octanoate with 0mM pyruvate, 5mM glucose (purple bar, N=3, 5, 96) and 20mM glucose (blue bar, N=3, 6, 156). Data for 0.5mM octanoate with 5mM pyruvate, 5mM glucose (mauve bar, N= 3, 6, 175) and 20mM glucose (green bar, N= 3, 6, 174).

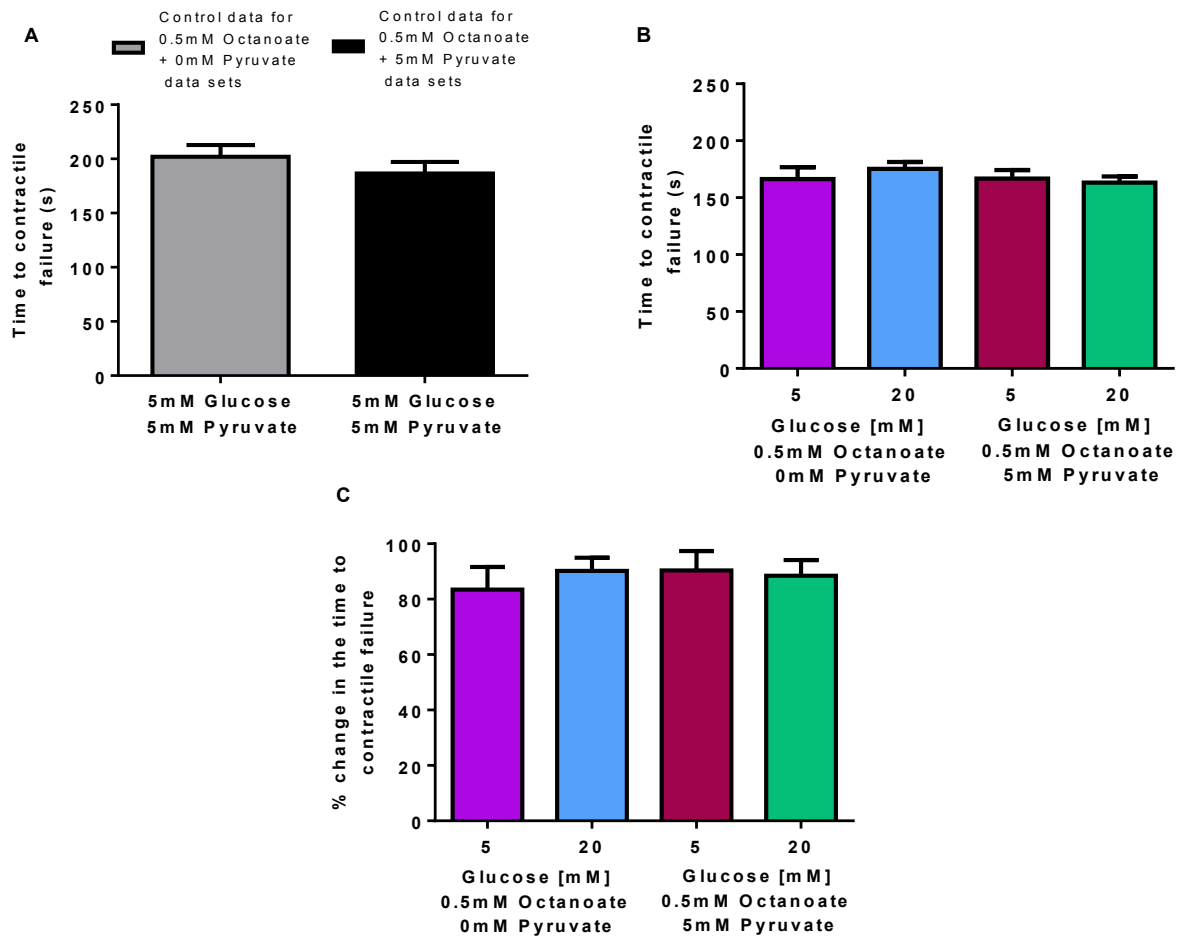


Figure 4.31 The impact of the addition of pyruvate on the effects of octanoate on the time to contractile failure during metabolic inhibition in response to acute changes in extracellular glucose.

- (A) Time to contractile failure from the onset of metabolic inhibition for the control data (5mM glucose/5mM pyruvate) recorded at the beginning of each day for each data set.
- (B) Time to contractile failure from the onset of metabolic inhibition for cardiomyocytes superfused with 5mM or 20mM glucose with either 0.5mM octanoate and 0mM pyruvate or 0.5mM octanoate and 5mM pyruvate.
- (C) Normalised time to contractile failure for both data sets represented as a % change in the time to contractile failure. Each octanoate treatment group was normalised to its corresponding control data set, the 0.5mM octanoate with 0mM pyruvate data sets (purple and blue bars) were normalised to the grey bar in (A) and the 0.5mM octanoate with 5mM pyruvate data sets (mauve and green bar) were normalised to the black bar in (A).

Data represented as mean \pm s.e.m. Control data (5mM glucose/5mM pyruvate) for the 0.5mM octanoate with 0mM pyruvate data sets (grey bar, N=3 hearts, 3 fields of view, 54 cardiomyocytes) and for the 0.5mM octanoate data with 5mM pyruvate sets (black bar, N=3, 3, 152). Data for 0.5mM octanoate with 0mM pyruvate, 5mM glucose (purple bar, N=3, 5, 96) and 20mM glucose (blue bar, N=3, 6, 156). Data for 0.5mM octanoate with 5mM pyruvate, 5mM glucose (mauve bar, N= 3, 6, 175) and 20mM glucose (green bar, N= 3, 6, 174).

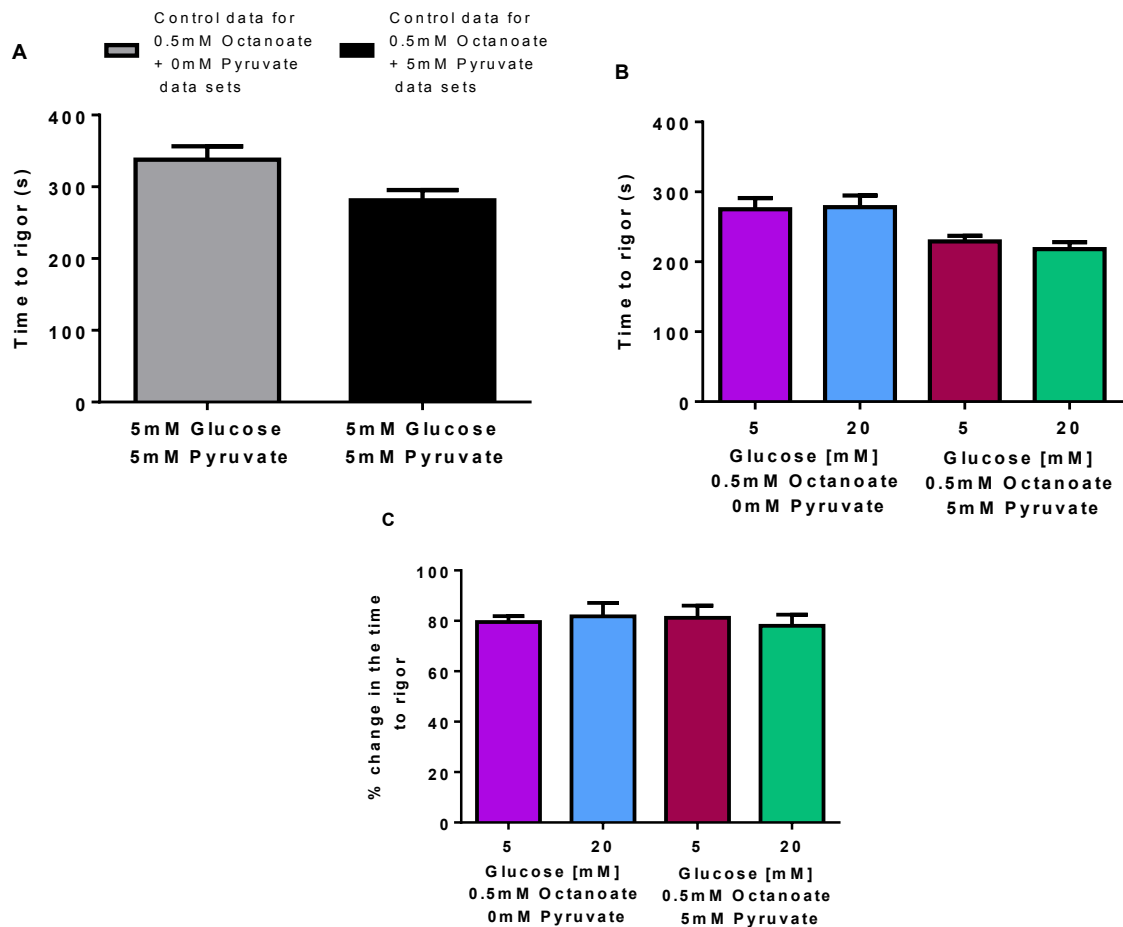


Figure 4.32 The impact of the addition of pyruvate on the effects of octanoate on the time to rigor during metabolic inhibition in response to acute changes in extracellular glucose.

- (A) Time to rigor from the onset of metabolic inhibition for the control data (5mM glucose/5mM pyruvate) recorded at the beginning of each day for each data set.
- (B) Time to rigor contracture from the onset of metabolic inhibition for cardiomyocytes superfused with 5mM or 20mM glucose with either 0.5mM octanoate and 0mM pyruvate or 0.5mM octanoate and 5mM pyruvate.
- (C) Normalised time to rigor for both data sets represented as a % change in the time to rigor. Each octanoate treatment group was normalised to its corresponding control data set, the 0.5mM octanoate with 0mM pyruvate data sets (purple and blue bars) were normalised to the grey bar in (A) and the 0.5mM octanoate with 5mM pyruvate data sets (mauve and green bar) were normalised to the black bar in (A).

Data represented as mean \pm s.e.m. Control data (5mM glucose/5mM pyruvate) for the 0.5mM octanoate with 0mM pyruvate data sets (grey bar, N=3 hearts, 3 fields of view, 54 cardiomyocytes) and for the 0.5mM octanoate data with 5mM pyruvate sets (black bar, N=3, 3, 152). Data for 0.5mM octanoate with 0mM pyruvate, 5mM glucose (purple bar, N=3, 5, 96) and 20mM glucose (blue bar, N=3, 6, 156). Data for 0.5mM octanoate with 5mM pyruvate, 5mM glucose (mauve bar, N= 3, 6, 175) and 20mM glucose (green bar, N= 3, 6, 174).

Under normoglycaemic conditions, prior to normalisation the time to contractile failure (Figure 4.31B) for those recorded with 0.5mM octanoate and 0mM pyruvate was 166.4 ± 10.3 s and 166.9 ± 7.5 s for those recorded with 0.5mM octanoate and 5mM pyruvate. Under hyperglycaemic conditions, prior to normalisation the time to contractile failure (Figure 4.31B) for those recorded with 0.5mM octanoate and 0mM pyruvate was 175.3 ± 6.1 s and 163.3 ± 5.4 s for those recorded with 0.5mM octanoate and 5mM pyruvate.

Once normalised, the percentage change in the time to contractile failure (Figure 4.31C) shows under normoglycaemic and hyperglycaemic conditions, the addition of pyruvate (5mM) to the octanoate perfusate had no effect with $83.4 \pm 8.2\%$ (5mM glucose/0.5mM octanoate/0mM pyruvate) versus $90.4 \pm 7.0\%$ (5mM glucose/0.5mM octanoate/5mM pyruvate, $P=0.53$) and $90.2 \pm 4.8\%$ (20mM glucose/0.5mM octanoate/0mM pyruvate) versus $88.4 \pm 5.7\%$ (20mM glucose/0.5mM octanoate/5mM pyruvate, $P=0.82$).

The control time to rigor (Figure 4.32A) recorded on the same day as those perfused with 0.5mM octanoate and 0mM pyruvate was 337.9 ± 18.5 s, this was not significantly different to those controls recorded on the same day as those perfused with 0.5mM octanoate and 5mM pyruvate (281.0 ± 14.4 s, $P=0.07$)

Prior to normalisation, the time to rigor (Figure 4.32B) under normoglycaemic conditions was 275.2 ± 16.0 s for those recorded with 0.5mM octanoate and 0mM pyruvate and 278.2 ± 16.7 s for those recorded with 0.5mM octanoate and 5mM pyruvate. Under hyperglycaemic conditions, the time to rigor for those recorded with 0.5mM octanoate and 0mM pyruvate was 278.2 ± 16.7 s and 218.2 ± 10.0 s for those recorded with 0.5mM octanoate and 5mM pyruvate.

Following normalisation, the percentage change in time to rigor (Figure 4.32C), shows the addition of pyruvate (5mM) to the octanoate perfusate, under normoglycaemic and hyperglycaemic conditions had no effect with $79.6 \pm 2.3\%$ (5mM glucose/0.5mM octanoate/0mM pyruvate) versus $81.2 \pm 4.8\%$ (5mM glucose/0.5mM octanoate/5mM pyruvate, $P=0.78$), and $81.8 \pm 5.4\%$ (20mM glucose/0.5mM octanoate/0mM pyruvate) versus $78.0 \pm 4.4\%$ (20mM glucose/0.5mM octanoate/5mM pyruvate, $P=0.60$).

The control percentage of 'non-hypercontracted' cardiomyocytes (Figure 4.33A) recorded on the same day as those perfused with 0.5mM octanoate and 0mM pyruvate was $74.4 \pm 4.5\%$, this was not significantly different to those recorded on the same day as those perfused with 0.5mM octanoate and 5mM pyruvate ($78.5 \pm 1.4\%$, $P=0.43$).

Under normoglycaemic conditions, prior to normalisation the percentage of 'non-hypercontracted' cardiomyocytes (Figure 4.33B), for those recorded with 0.5mM octanoate and 0mM pyruvate was $60.5 \pm 6.9\%$ and $72.8 \pm 3.1\%$ for those recorded with 0.5mM octanoate and 5mM pyruvate. Under hyperglycaemic conditions, prior to normalisation the percentage of 'non-hypercontracted' cardiomyocytes (Figure 4.33B), for those recorded with 0.5mM octanoate and 0mM pyruvate was $67.1 \pm 3.8\%$ and $74.0 \pm 7.7\%$ for those recorded with 0.5mM octanoate and 5mM pyruvate.

Once normalised, the percentage change in 'non-hypercontracture' (Figure 4.33C) shows under normoglycaemic and hyperglycaemic conditions, the addition of pyruvate (5mM) to the octanoate perfusate had no effect with $80.3 \pm 8.2\%$ (5mM glucose/0.5mM octanoate/0mM pyruvate) versus $93.3 \pm 4.0\%$ (5mM glucose/0.5mM octanoate/5mM pyruvate, $P=0.17$), and $87.2 \pm 2.6\%$ (20mM glucose/0.5mM octanoate/0mM pyruvate) versus $94.1 \pm 9.6\%$ (20mM glucose/0.5mM octanoate/5mM pyruvate, $P=0.51$).

The control percentage of contractile recovery (Figure 4.34A), recorded on the same day as those perfused with 0.5mM octanoate and 0mM pyruvate was $23.9 \pm 0.6\%$, this was not significantly different to the controls recorded on the same day as those perfused with 0.5mM octanoate and 5mM pyruvate ($28.9 \pm 4.5\%$, $P=0.33$).

Under normoglycaemic conditions, prior to normalisation the percentage of contractile recovery for those recorded with 0.5mM octanoate and 0mM pyruvate was $11.5 \pm 4.3\%$ and $22.5 \pm 4.3\%$ for those recorded with 0.5mM octanoate and 5mM pyruvate (Figure 4.34B). Under hyperglycaemic conditions, prior to normalisation the percentage of contractile recovery for those recorded with 0.5mM octanoate and 0mM pyruvate was $12.9 \pm 2.1\%$ and $25.5 \pm 6.1\%$ for those recorded with 0.5mM octanoate and 5mM pyruvate (Figure 4.34B).

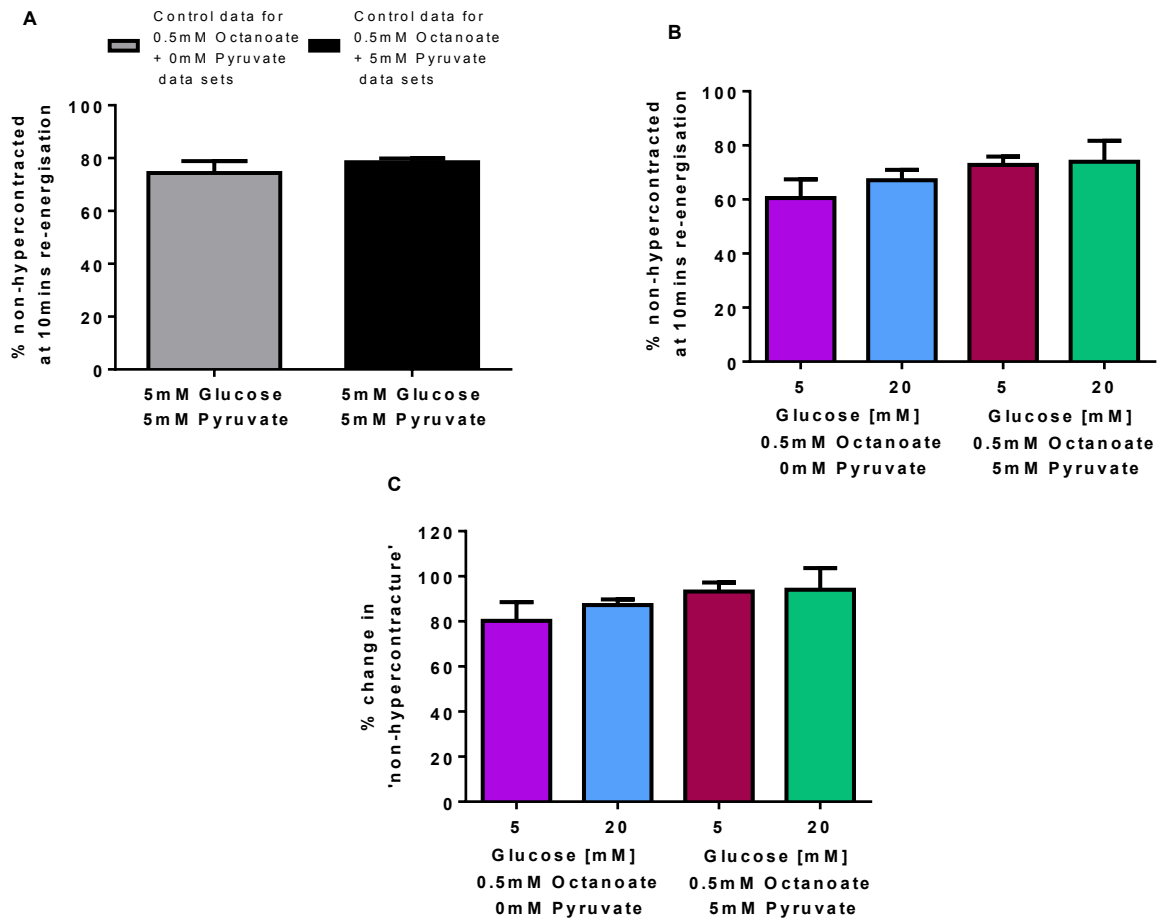


Figure 4.33 The impact of the addition of pyruvate on the effects of octanoate on the viability of isolated cardiomyocytes to metabolic inhibition and re-energisation in response to acute changes in extracellular glucose.

- (A) The percentage of cardiomyocytes relaxed from hypercontracted 'non-hypercontracted' by the end of 10 minutes of re-energisation for the control data (5mM glucose/5mM pyruvate) recorded at the beginning of each day for both data sets.
- (B) The percentage of cardiomyocytes relaxed from hypercontracted 'non-hypercontracted' by the end of 10 minutes of re-energisation following superfusion with 5mM or 20mM glucose with either 0.5mM octanoate and 0mM pyruvate or 0.5mM octanoate and 5mM pyruvate.
- (C) Normalised percentage of 'non-hypercontracted' cardiomyocytes for both data sets represented as a % change in 'non-hypercontracture'. Each octanoate treatment group was normalised to its corresponding control data set, the 0.5mM octanoate with 0mM pyruvate data sets (purple and blue bars) were normalised to the grey bar in (A) and the 0.5mM octanoate with 5mM pyruvate data sets (mauve and green bar) were normalised to the black bar in (A).

Data represented as mean \pm s.e.m. Control data (5mM glucose/5mM pyruvate) for the 0.5mM octanoate with 0mM pyruvate data sets (grey bar, N=3 hearts, 3 fields of view, 54 cardiomyocytes) and for the 0.5mM octanoate data with 5mM pyruvate sets (black bar, N=3, 3, 152). Data for 0.5mM octanoate with 0mM pyruvate, 5mM glucose (purple bar, N=3, 5, 96) and 20mM glucose (blue bar, N=3, 6, 156). Data for 0.5mM octanoate with 5mM pyruvate, 5mM glucose (mauve bar, N= 3, 6, 175) and 20mM glucose (green bar, N= 3, 6, 174).

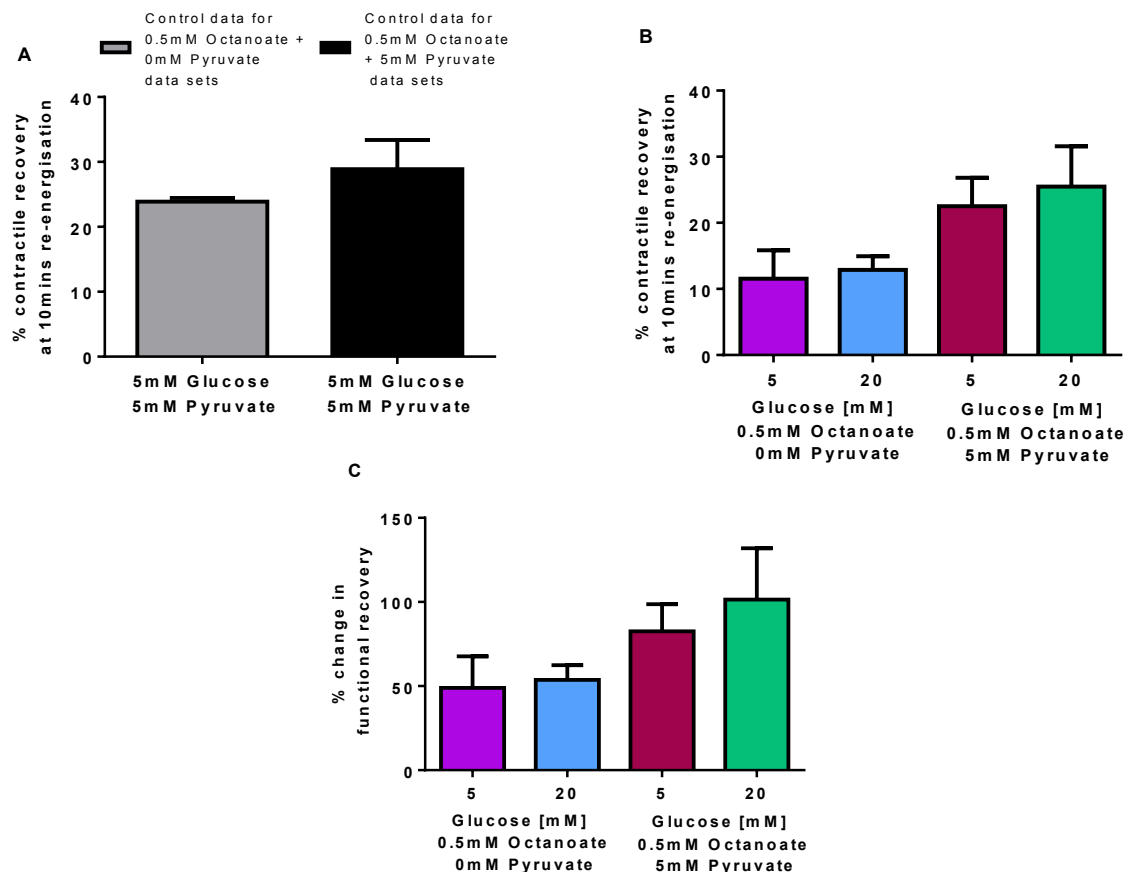


Figure 4.34 The impact of the addition of pyruvate on the effects of octanoate on the recovery of isolated cardiomyocytes to metabolic inhibition and re-energisation in response to acute changes in extracellular glucose.

- (A) The percentage of cardiomyocytes regaining contractile function in response to EFS by the end of 10 minutes of re-energisation for the control data (5mM glucose/5mM pyruvate) recorded at the beginning of each day for each data set.
- (B) The percentage of cardiomyocytes regaining contractile function in response to EFS by the end of 10 minutes of re-energisation, following superfusion with 5mM or 20mM glucose with either 0.5mM octanoate and 0mM pyruvate or 0.5mM octanoate and 5mM pyruvate.
- (C) Normalised contractile recovery for both data sets represented as a % change in functional recovery. Each octanoate treatment group was normalised to its corresponding control data set, the 0.5mM octanoate with 0mM pyruvate data sets (purple and blue bars) were normalised to the grey bar in (A) and the 0.5mM octanoate with 5mM pyruvate data sets (mauve and green bar) were normalised to the black bar in (A).

Data represented as mean \pm s.e.m. Control data (5mM glucose/5mM pyruvate) for the 0.5mM octanoate with 0mM pyruvate data sets (grey bar, N=3 hearts, 3 fields of view, 54 cardiomyocytes) and for the 0.5mM octanoate data with 5mM pyruvate sets (black bar, N=3, 3, 152). Data for 0.5mM octanoate with 0mM pyruvate, 5mM glucose (purple bar, N=3, 5, 96) and 20mM glucose (blue bar, N=3, 6, 156). Data for 0.5mM octanoate with 5mM pyruvate, 5mM glucose (mauve bar, N= 3, 6, 175) and 20mM glucose (green bar, N= 3, 6, 174).

Following normalisation, the percentage change in contractile recovery (Figure 4.34C) shows adding pyruvate (5mM) to the octanoate perfusate under normoglycaemic or hyperglycaemic conditions had no effect with $49.0 \pm 4.3\%$ (5mM glucose/0.5mM octanoate/0mM pyruvate) versus $82.5 \pm 16.2\%$ (5mM glucose/0.5mM octanoate/5mM pyruvate, $P=0.21$), and $53.7 \pm 8.8\%$ (20mM glucose/0.5mM octanoate/0mM pyruvate) versus $101.5 \pm 30.4\%$ (20mM glucose/0.5mM octanoate/5mM pyruvate, $P=0.16$).

These data shows that replacing pyruvate (0.5mM) with octanoate (0.5mM), under normoglycaemic conditions had no effect. However under hyperglycaemic conditions, although there was no effect during metabolic inhibition, there was a reduction in the protection against re-energisation injury. The addition of 5mM pyruvate to the octanoate perfusate had no effect on any of the measured variables. Overall octanoate appears to eliminate the previous protection observed under hyperglycaemic conditions.

4.3 Discussion

The experiments in this chapter were designed to investigate the effects of acute changes in substrates metabolised via oxidative phosphorylation (namely, pyruvate and octanoate) on isolated cardiomyocytes in response to either normoglycaemic or hyperglycaemic conditions during metabolic inhibition and re-energisation. These two metabolic substrates are readily converted into acetyl-CoA and produce NADH/FADH₂ which drives the ETC for oxidative phosphorylation to generate larger quantities of ATP. However they are not metabolised during ischaemia due to the anaerobic conditions. Therefore, changes in their concentration could impact on the previously observed effects of glucose (Chapter 3).

For this chapter, the data recorded under normoglycaemic conditions in section 4.2.1-4.2.6 were recorded on the same day so a direct comparison of the data was made. However the data recorded under hyperglycaemic conditions and the data in section 4.2.7, had to be normalised before a comparison could occur. The controls for the hyperglycaemic data show there was no significance between values obtained on different days; nevertheless, data were compared by calculating the percentage change compared with the (daily) control; these will be discussed below.

Data in this study shows that perfusing with a reduced extracellular pyruvate concentration, prior to metabolic inhibition and during re-energisation, under both normoglycaemic and hyperglycaemic conditions, had adverse effects on the impact of metabolic inhibition but no effect during re-energisation. During metabolic inhibition there was also no impact on either the time to action potential failure or $\text{SarCK}_{\text{ATP}}$ channel activation. Reducing extracellular pyruvate had no effect on Mg^{2+} -Green fluorescence, indicating there was no effect on ATP levels during metabolic inhibition and re-energisation but did result in higher $[\text{Ca}^{2+}]_i$ levels by the end of metabolic inhibition under hyperglycaemic conditions only. However there was no effect on the percentage of cardiomyocytes recovering Ca^{2+} - transients or those recovering with a lower Fura-2 ratio.

Elevating extracellular pyruvate to 10mM, under normoglycaemic conditions, delayed the time to contractile failure and improved contractile recovery, but under hyperglycaemic conditions there was no effect.

The replacement of pyruvate with the fatty acid octanoate (0.5mM) in the perfusate prior to metabolic inhibition and during re-energisation prevented the cardioprotection previously observed under hyperglycaemic conditions. This was not modified by the addition of 5mM pyruvate.

4.3.1 Impact of pyruvate during metabolic inhibition

Under non-ischaemic conditions, exogenous pyruvate is transported into cardiomyocytes and metabolised to aid ATP production via oxidative phosphorylation (Linn *et al.*, 1969; Utter & Keech, 1963; Kerbey *et al.*, 1976), however during metabolic inhibition this is prevented.

4.3.1.1 The effect of reducing pyruvate prior to metabolic inhibition

Reducing extracellular pyruvate to a physiological concentration of 0.5mM in the perfusate reduced the time to contractile failure under both glycaemic conditions, compared to those perfused with Tyrode solution containing 5mM pyruvate. These rapid contractile failures could relate to a decrease in ATP levels, this would be expected as reducing pyruvate from 5mM to 0.5mM could be expected to result in less

ATP production. Less ATP production could be possible as 0.5mM pyruvate has previously been shown to decrease PDH activity (Dennis *et al.*, 1979), this would reduce NADH production via the Krebs cycle, resulting in less stimulation of ATP production via oxidative phosphorylation. Therefore reducing pyruvate could be decreasing mitochondrial ATP production, leading to decreased PCr formation and could therefore lead to less transfer to the myofibrils. This hypothesis that early contractile failure is occurring due to decreased PCr, coincides with previous studies that suggest early contractile failure during ischaemia is linked to a rapid decline in [PCr] rather than [ATP] (Allen & Orchard, 1987; Rauch *et al.*, 1994; Cross *et al.*, 1995; Kingsley *et al.*, 1991). The rapid decline in PCr could relate to PCr being used to buffer ATP during earlier ischaemia (Depre & Taegtmeyer, 2000; Nichols & Lederer, 1990b) and could also relate to the prevention of the transfer of PCr to the contractile proteins (myofibrils) from the mitochondria (Kingsley *et al.*, 1991; Veksler *et al.*, 1997).

These data suggest pyruvate does have a role in maintaining contraction, but due to pyruvate not being present either in the SFT-MI perfusate or being metabolised during metabolic inhibition, it is suggested any impact is prior to metabolic inhibition but it is enough of an impact to have an effect and that it is anaerobic glycolysis that maintains contraction during metabolic inhibition, which could explain why a difference in time still exists between the two glucose concentrations (i.e. 20mM glucose still maintains contraction longer than 5mM glucose).

Due to contractile failure being linked to action potential failure, it was expected that a similar trend observed for contractile failure would be observed for action potential failure. However reducing pyruvate to 0.5mM under either glycaemic condition had no effect on the time to action potential failure. These results may be due to the sample size being significantly lower than the contractile failure experiments. In addition to there being no effect on the time to action potential failure, there was no effect on the RMP or the APD₉₀. Together these data imply reducing pyruvate is not altering ATP levels to a concentration where activation of the SarcK_{ATP} channels could be affected. This is due to action potential failure being related to opening of the SarcK_{ATP} channels (Lederer *et al.*, 1989).

Reducing pyruvate had no effect on the time to $\text{Sarck}_{\text{ATP}}$ channel activation under either glycaemic condition. These results do reflect the action potential failure data and suggest reducing pyruvate does not affect the $[\text{ATP}]/[\text{ADP}]$ ratio that is in close proximity to the $\text{Sarck}_{\text{ATP}}$ channels and therefore their activity is not affected. This indicates reducing pyruvate is not affecting maintenance of glycolytic ATP production in regions close to the $\text{Sarck}_{\text{ATP}}$ channels, as it is glycolytic ATP production which has been proposed to regulate their opening due to the close proximity of the glycolytic enzymes to the $\text{Sarck}_{\text{ATP}}$ channels (Dhar-Chowdhury *et al.*, 2005; Jovanovic *et al.*, 2005; Hong *et al.*, 2011).

Based on the contractile failure data, it is possible there are changes in $[\text{ATP}]_i$, therefore the fluorescence indicator Mg^{2+} -Green was used to investigate whether reducing pyruvate was impacting on ATP. For both glycaemic conditions there was a less pronounced rapid increase in Mg^{2+} -Green fluorescence. This could indicate slower mitochondria depolarisation (Rodrigo & Standen, 2005; Lawrence *et al.*, 2001), as a result ATP production via oxidative phosphorylation may be delayed. However, reducing pyruvate had no effect on the time to the rapid increase in Mg^{2+} -Green fluorescence, suggesting there was no prevention in the start of mitochondrial depolarisation, which was expected as in addition to pyruvate being absent it cannot be metabolised during metabolic inhibition.

The possibility of a reduction in pyruvate decreasing $[\text{ATP}]_i$ during metabolic inhibition is not supported in this study, as under both glycaemic conditions, there was no effect on Mg^{2+} -Green fluorescence by the end of metabolic inhibition. These data indicate glucose is predominantly maintaining ATP levels during metabolic inhibition, which fits with the $\text{Sarck}_{\text{ATP}}$ data but not the contractile failure data, which could imply reducing pyruvate is only significantly affecting ATP levels at the myofibrils.

Due to the Mg^{2+} -Green data showing no effect on the time to the rapid increase in Mg^{2+} -Green fluorescence, it would be expected that the time to rigor would also not differ. However reducing pyruvate significantly reduced the time to rigor, suggesting reducing pyruvate is either affecting glycolytic ATP production, which is believed to prevent rigor development during ischaemia as seen in Figure 3.17 (Cross *et al.*, 1995; Owen *et al.*, 1990; Kingsley *et al.*, 1991) or it is stimulating rigor to occur before

anaerobic glycolysis ceases, which could indicate as with the contractile failure data, that the transport of ATP via the creatine phosphate shuttle to specific pools at the myofibrils is affected. This is possible as decreases in ATP levels at the myofibrils have been proposed to stimulate rigor (Veksler *et al.*, 1997).

As the Mg^{2+} -Green data implies reducing pyruvate has no impact on the maintenance of ATP levels; it could be hypothesised that the activity of many of the ATP-dependent ion pumps/transporters would remain the same and therefore Ca^{2+} -homeostasis would be unaffected. To identify if $[Ca^{2+}]_i$ was affected, the Ca^{2+} imaging fluorescence indicator Fura-2, was used to measure changes in $[Ca^{2+}]_i$. By the end of metabolic inhibition, only reducing pyruvate under hyperglycaemic conditions resulted in an increase in the Fura-2 ratio, which suggests under these conditions reducing pyruvate leads to unregulated Ca^{2+} homeostasis during metabolic inhibition, which does not fit with the Mg^{2+} -Green data suggesting no alteration in ATP levels or with the lack of effect on the action potential data. This higher Fura-2 ratio was unexpected but could be due to increased Ca^{2+} influx, or a decrease in Ca^{2+} removal from the cytosol via SERCA or PMCA, but this does not agree with the findings that glycolytic ATP is involved in maintaining SERCA activity and therefore maintains Ca^{2+} homeostasis (Xu *et al.*, 1995; Kockskamper *et al.*, 2005; Zima *et al.*, 2006).

4.3.1.2 The effect of elevating pyruvate prior to metabolic inhibition

Elevating pyruvate to a supraphysiological concentration of 10mM delayed the time to contractile failure under normoglycaemic conditions but not hyperglycaemic conditions compared to those perfused with 5mM pyruvate. This delay is proposed to relate to 10mM pyruvate increasing NADH and PCr levels, which would increase ATP levels (Zweier & Jacobus, 1987; Cavallini *et al.*, 1990; Mallet & Sun, 1999; Mellors *et al.*, 1999; Kerr *et al.*, 1999). This proposal is in agreement with a previous study that shows elevating pyruvate to 10mM in an isolated non-ischaemic heart, increases the PCr concentration to 18.3mM compared to 15.2mM with 16mM glucose, and results in an increase in flux from PCr to ATP (Zweier & Jacobus, 1987). Therefore the observed delay could relate to 10mM pyruvate stimulating maximum activity of PDH (Dennis *et al.*, 1979), resulting in increased acetyl-CoA, which would then go onto support higher

ATP production via oxidative phosphorylation prior to metabolic inhibition, and thus would increase PCr formation which would support contractile function. However as pyruvate is not present in the metabolic inhibition solution, this could imply during metabolic inhibition, as previously described, continual ATP production to support contractile function results from anaerobic glycolysis. A continuation of anaerobic glycolysis could be hypothesised to arise due to the elevated pyruvate in the perfusate stimulating the glucose present to be predominantly converted to increase glycogen stores within the cardiomyocytes to be used later during metabolic inhibition.

The improved contractility could also be attributed to 10mM pyruvate having its own independent effects such as decreasing Pi (Zweier & Jacobus, 1987) and increasing SERCA activity via increased ΔG_{ATP} (Zweier & Jacobus, 1987; Mellors *et al.*, 1999). 10mM pyruvate could also be increasing citrate levels, which could inhibit glycolysis at PFK-1 (Mallet & Sun, 1999) and thus decrease the ATP supply from glycolysis. However elevating pyruvate could also elevate NADH levels within the cardiomyocytes, this may result in inhibition of PDH (Cavallini *et al.*, 1990) (Figure 3.18), which could alleviate inhibition of PFK-1.

These findings suggest under normoglycaemic conditions elevating pyruvate could be increasing ATP, NADH and PCr levels which supports contractile function. The lack of effect under hyperglycaemic conditions could suggest this glucose concentration is generating the maximum ATP concentration required to prevent contractile failure. Alternatively pyruvate could be dominating prior to metabolic inhibition and actually inhibiting glycolysis at PFK-1, then during metabolic inhibition anaerobic glycolysis could be taking over. However from these studies which pathway is actually being activated cannot be deduced, and one could be masking the other.

In this study, elevating pyruvate had no effect on the time to rigor contracture under either glycaemic condition. These findings support the idea that glycolytic ATP production prevents rigor development rather than mitochondrial ATP (Bricknell *et al.*, 1981) as otherwise a delay in rigor would be expected had pyruvate been having an effect. However the data is in contrast to previous studies, which have shown

perfusion with 10mM pyruvate in the absence or presence of glucose delays ischaemic contracture during no-flow ischaemia (Flood *et al.*, 2003; Kerr *et al.*, 1999).

4.3.2 Pyruvate actions upon re-energisation following acute changes in pyruvate prior to metabolic inhibition and during reperfusion

Perfusion with pyruvate could be aiding recovery of the ETC, as pyruvate is an α -keto acid, which can reverse CN^- induced inhibition of Cyt C by reacting with CN^- to produce cyanohydrins (Cittadini *et al.*, 1971; Delhumeau *et al.*, 1994; Nuskova *et al.*, 2010). However, the different pyruvate concentrations (0.5mM, 5mM and 10mM) in our Tyrode solutions upon re-energisation may not significantly affect the recovery of Cyt C from CN^- inhibition, as a pyruvate concentration of $\geq 48\text{mM}$ is required to give maximum recovery of Cyt C activity (Delhumeau *et al.*, 1994; Nuskova *et al.*, 2010).

4.3.2.1 The effects of reducing pyruvate during re-energisation

Re-energisation with a reduced pyruvate concentration decreased the percentage of 'non- hypercontracture' by the end of 10 minutes of re-energisation under normoglycaemic conditions, this was close to statistical significance ($P=0.06$) and it is proposed had other experiments been performed significance may have been reached. This could suggest increased NADH levels upon re-energisation (Cavallini *et al.*, 1990), stimulating faster mitochondrial repolarisation (Rodrigo & Standen, 2005; Rodrigo *et al.*, 2002), leading to increased mitochondrial ATP production via F_0/F_1 ATP synthase as seen in Figure 3.19, which would stimulate more hypercontracture and therefore reduce the percentage of 'non-hypercontracted' cardiomyocytes. Surprisingly no effect was observed under hyperglycaemic conditions, a decrease was expected due to the increase in $[\text{Ca}^{2+}]_i$ observed during metabolic inhibition.

The fluorescence of Mg^{2+} -Green during re-energisation could indicate whether reducing pyruvate affects mitochondrial repolarisation. During re-energisation the Mg^{2+} -Green fluorescence under both glycaemic conditions remained elevated but at a lower intensity than 5mM pyruvate suggesting reducing pyruvate could be delaying repolarisation of mitochondria (Lawrence *et al.*, 2001), which would be expected to delay reactivation of F_0/F_1 ATP synthase leading to slower mitochondrial ATP

production. By the end of re-energisation, reducing pyruvate had no effect on Mg^{2+} -Green fluorescence under both glycaemic conditions; implying reducing pyruvate was not effecting re-establishment of mitochondrial ATP production compared to those perfused with 5mM pyruvate.

The Fura-2 ratios during re-energisation were also not affected by the reduction in pyruvate under either glycaemic conditions. As these observations indicate reducing pyruvate is not affecting Ca^{2+} homeostasis, it is proposed as in line with findings by Jeremy *et al* (1992) and Jeremy *et al* (1993) that glycolytic ATP produced rather than ATP from mitochondrial oxidation is essential upon re-energisation to prevent a “reperfusion” Ca^{2+} overload (Jeremy *et al.*, 1992; Jeremy *et al.*, 1993).

In addition to there being no effect on the Fura-2 ratios with reduced pyruvate, there was no effect on the percentage of cardiomyocytes recovering Ca^{2+} transient, or on the percentage of those recovering with a Fura-2 ratio <0.85 . Overall the data obtained with Fura-2 suggests pyruvate is not effecting Ca^{2+} homeostasis or the recovery of Ca^{2+} transient upon re-energisation. These results coincide with the finding that reducing extracellular pyruvate had no effect on the percentage of cardiomyocytes regaining contractile function by the end of re-energisation. This suggests it is the glucose concentration in the perfusate (with the hyperglycaemic glucose concentration showing the greatest improvement as before) and an intact glycolytic pathway as discussed previously in section 3.3.2 (Jeremy *et al.*, 1992; Jeremy *et al.*, 1993, Van Emous *et al.*, 2001; Cross *et al.*, 1995; Dizon *et al.*, 1998) that aids functional recovery upon re-energisation.

4.3.2.2 The effect of elevating pyruvate during re-energisation

Elevating pyruvate had no effect on the percentage of cardiomyocytes that were ‘non-hypercontracted’ by the end of re-energisation under either glycaemic condition. This was not expected as 10mM pyruvate was expected to increase NADH levels upon re-energisation (Cavallini *et al.*, 1990) especially in combination with 20mM glucose, which would be expected to stimulate more hypercontracture and therefore reduce the percentage of ‘non-hypercontracted’ cardiomyocytes via the mechanism outlined in 4.3.2.1 and as seen in Figure 3.19.

Elevated pyruvate improved contractile recovery under normoglycaemic conditions, which coincides with previous studies where perfusion with 10mM pyruvate prior to and after global no-flow ischaemia has been shown to improve post-ischaemic contractile function (Kerr *et al.*, 1999; Flood *et al.*, 2003). The ability of 10mM pyruvate to improve contractile function has been attributed to pyruvate improving ATP levels (Kerr *et al.*, 1999), as well as reducing opening of mPTP within the first few minutes of reperfusion and enabling complete re-sealing of any mPTPs that open (indicated by reduced entrapment of 2-deoxyglucose-6-phosphate) (Kerr *et al.*, 1999). Pyruvate's actions on mPTP have been postulated to relate to pyruvate decreasing pH or by decreasing ROS production, preventing $[Ca^{2+}]$ induced mPTP opening (Kerr *et al.*, 1999) as indicated in Figure 4.35. As the percentage recovery did not improve under hyperglycaemic conditions, it is suggested that although 10mM pyruvate maybe inhibiting mPTP and decreasing ROS production, this may not be enough to enhance the recovery previously observed with 20mM glucose and 5mM pyruvate. Alternatively 20mM glucose could be mimicking the result of pyruvate, or it could be that 10mM pyruvate is stimulating the recovery on its own and is in fact inhibiting glycolysis, but it is impossible to tell from these studies which substrate is having the effect.

4.3.3 Detrimental effects of octanoate upon re-energisation following metabolic inhibition

4.3.3.1 The actions of octanoate prior to metabolic inhibition and during re-energisation

Fatty acids provide the main source of ATP to the myocardium under normal physiological conditions. Within cardiomyocytes octanoate is metabolised by β -oxidation into acetyl CoA, which then enters the Krebs cycle as seen in Figure 3.18.

Due to pyruvate and octanoate both directly producing acetyl-CoA for oxidative phosphorylation, to establish what effects octanoate alone would have on the cardiomyocytes, pyruvate was replaced with octanoate. Replacement of a physiological pyruvate concentration (0.5mM), with a physiological concentration of octanoate (0.5mM) in the perfusate had no effect on the time to contractile failure, or

the time to rigor under either glycaemic condition. These results indicate prior to metabolic inhibition, octanoate is fulfilling the role previously observed with pyruvate as the main substrate providing acetyl-CoA to the Krebs cycle to generate NADH, which drives oxidative phosphorylation (Figure 3.18) to generate the ATP required to support contractile function and rigor prior to metabolic inhibition.

However, octanoate is expected to generate greater quantities of ATP, as it can produce 4 acetyl-CoA per molecule compared to 1 per molecule for pyruvate. Increased acetyl-CoA can lead to inhibition of glucose oxidation (via inhibiting PDH) and glycolysis (via subsequent increased citrate inhibiting PFK-1) prior to metabolic inhibition (Figure 3.18) (Kerbey *et al.*, 1976; Lopaschuk *et al.*, 1990; Neely *et al.*, 1972; Lopaschuk *et al.*, 1993). A previous study has shown octanoate can reduce glycolytic rate (Longnus *et al.*, 2001). This group perfused whole hearts with a similar octanoate concentration to the one used in this study of 0.6mM and showed octanoate at this concentration does produce a sufficient amount of acetyl-CoA to inhibit glycolysis and reduce the glycolytic rate (Longnus *et al.*, 2001). However as octanoate is not metabolised during metabolic inhibition, this inhibition could be relieved and would allow anaerobic glycolytic ATP production to recommence and support contractile function during metabolic inhibition (Figure 3.17).

Re-establishment of oxidative phosphorylation upon re-energisation allows octanoate metabolism to recommence, this can be detrimental even in the presence of glucose. In previous studies the effects of a long chain fatty acid palmitate (1.2mM) in the presence of 11mM glucose, was shown to be detrimental following a period of no-flow ischaemia by resulting in substantial reperfusion injury (Lopaschuk *et al.*, 1990; Johnston & Lewandowski, 1991). The detrimental effect of palmitate has been attributed to palmitate increasing acetyl-CoA levels, which inhibit PDH and thus inhibit glucose oxidation, resulting in uncoupling of glycolysis from glucose oxidation (Lopaschuk *et al.*, 1993).

Replacement of 0.5mM pyruvate with 0.5mM octanoate had no effect on the percentage of cardiomyocytes 'non-hypercontracted' by the end of re-energisation, under either glycaemic condition. These results suggest octanoate is not affecting

NADH levels during metabolic inhibition, therefore upon re-energisation oxidative phosphorylation could be being stimulated at the same rate as those perfused with 0.5mM pyruvate.

However there was a reduction in the percentage of cardiomyocytes regaining contractile function by the end of re-energisation that reached significance for hyperglycaemic conditions but not for normoglycaemic (this was close to statistical significance $P=0.06$, if another experiment had been carried out it is proposed significance may have been reached). This result may be due to octanoate increasing levels of NADH, which upon re-energisation stimulates oxidative phosphorylation triggering opening of mPTP (Figure 4.35) (Griffiths & Halestrap, 1995, Qian *et al.*, 1997, Di Lisa *et al.*, 2001). The absence of pyruvate may also be preventing the cardiomyocytes remaining slightly acidic upon re-energisation; this correction of acidity could also be stimulating opening of mPTPs and increasing cell death (Griffiths & Halestrap, 1995, Qian *et al.*, 1997, Di Lisa *et al.*, 2001). The reduced recovery may also indicate that octanoate is inhibiting glucose oxidation; as a result of increased acetyl-CoA, which would uncouple glucose oxidation and glycolysis. This is possible as octanoate has previously been shown to increase acetyl-CoA levels inhibiting PDH (Longnus *et al.*, 2001). Uncoupling of glucose oxidation and glycolysis results in increased lactate production, this leads to acidosis (Lopaschuk *et al.*, 1993), resulting in increased $[Na^+]_i$ accumulation and a subsequent Ca^{2+} overload which can cause reperfusion injury (Figure 4.35). In addition, octanoate increases citrate levels, which feedback and inhibit PFK-1 (Lopaschuk *et al.*, 1990; Neely *et al.*, 1972; Lopaschuk *et al.*, 1993) resulting in inhibition of glycolytic ATP production (Figure 3.18). Inhibition of glycolytic ATP production would disturb re-establishment of ionic homeostasis by reducing Na^+/K^+ ATPase and/or SERCA activity, resulting in re-energisation injury.

4.3.3.2 Potential benefits of stimulating glucose oxidation with pyruvate in the presence of octanoate prior to metabolic inhibition and during re-energisation

Previous studies have found that pharmacological stimulation of glucose oxidation via stimulation of PDH, by inhibiting PDHK with DCA, even in the presence of a fatty acid, improves recovery (Ussher *et al.*, 2012; Lopaschuk *et al.*, 1993). As pyruvate is known

to stimulate PDH (via inhibition of PDHK) (Kerbey *et al.*, 1976; Dennis *et al.*, 1979) it could be hypothesised that pyruvate could also improve recovery in the presence of a fatty acid. Therefore pyruvate was added back to the perfusate to identify if it would affect the response of the cardiomyocytes to octanoate.

The addition of 5mM pyruvate to the perfusate containing 0.5mM octanoate had no effect, under either glycaemic condition, on the time to contractile failure or rigor compared to those perfused with 0.5mM octanoate without pyruvate. It should be noted that the control rigor data had a P value of $P=0.07$ and increasing the 'n' value may affect the conclusion of these experiment. These results suggest the addition of pyruvate to the perfusate is not affecting the cardiomyocytes ability to maintain anaerobic glycolysis during metabolic inhibition, as anaerobic glycolysis is believed to maintain contraction and prevent rigor development (Cross *et al.*, 1995; Owen *et al.*, 1990; Kingsley *et al.*, 1991). These results were not expected, as it was hypothesised that these two metabolic substrates together could produce larger amounts of acetyl-CoA, resulting in larger quantities of citrate being produced via the Krebs cycle, which would feedback and inhibit glycolysis at PFK-1 even prior to metabolic inhibition (Figure 3.18). A previous study under normoxic conditions has shown the addition of a higher pyruvate concentration (2.5mM) to octanoate (0.2mM) increases citrate levels (Mallet & Sun, 1999), which supports the hypothesis that octanoate and pyruvate together can increase citrate levels. Mallet *et al* (1999) also observed that these two metabolic substrates caused an increase in PCr and $[ATP]/[ADP][P_i]$ and a decrease in Cr and P_i (Mallet & Sun, 1999), which implies these two metabolic substrates together produce adequate ATP and PCr levels, suggesting in this study that prior to metabolic inhibition, contraction and rigor are also supported by PCr.

As oxidative phosphorylation is reactivated upon re-energisation, if pyruvate was stimulating glucose oxidation a decrease in re-energisation injury would be expected. The addition of 5mM pyruvate to the perfusate containing 0.5mM octanoate had no effect on the percentage of cardiomyocytes 'non-hypercontracted' by the end of re-energisation under either glycaemic condition. This suggests upon re-energisation pyruvate and octanoate together do not result in higher mitochondrial ATP production, and thus no increase in hypercontracture.

The addition of pyruvate to the perfusate did not increase the percentage of cardiomyocytes regaining contractile function by the end of re-energisation under either glycaemic condition. The lack of improvement in contractile recovery following the addition of pyruvate suggests 5mM pyruvate is not increasing activity of PDH (via inhibition of PDHK) (see Figure 3.18) (Kerbey *et al.*, 1976; Dennis *et al.*, 1979) significantly to improve recovery and therefore the detrimental effect of octanoate is maintained. Had an improvement in PDH activity been achieved there would be improved coupling of glycolysis and glucose oxidation, thus preventing $[Na^+]_i$ accumulation and the subsequent Ca^{2+} overload. In addition, as pyruvate is known to stimulate acidosis, a reduction in cell death via prevention in mPTP opening was expected (Qian *et al.*, 1997; Di Lisa *et al.*, 2001; Griffiths & Halestrap, 1995). As recovery nearly double it could be hypothesised had the concentration of pyruvate added been higher (i.e. 10mM) the effect upon re-energisation may have been greater. This is due to finding that the activity and flux of PDH is greater with 10mM pyruvate than with a lower pyruvate concentration (0.5mM) even in the presence of octanoate (1mM) (Dennis *et al.*, 1979).

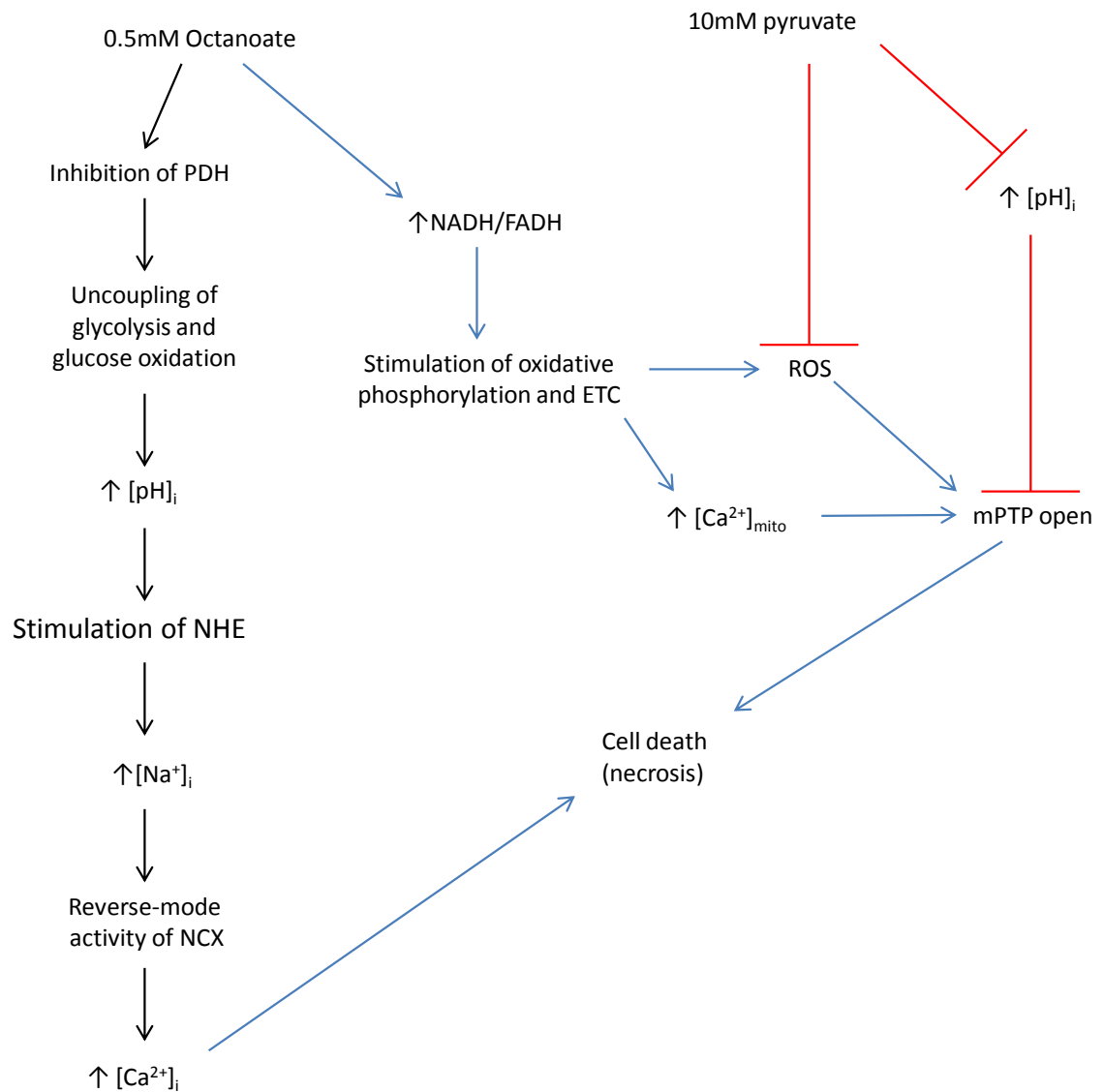


Figure 4.35 The hypothesised effects of octanoate and 10mM pyruvate during re-energisation.

The diagram shows the hypothesised pathways both in the cytosol (indicating by black arrows) and the mitochondria (indicated by blue arrows) activated by octanoate and 10mM pyruvate, both of which give rise to increased re-energisation injury. 10mM pyruvate could be inhibiting mPTP opening (indicated in red) by its antioxidant effect for scavenging or by increase pH.

CHAPTER FIVE

Metabolic pre and post conditioning of isolated cardiomyocytes

5. Metabolic pre and post conditioning of isolated cardiomyocytes

5.1 Introduction

Traditional ischaemic conditioning is achieved by subjecting a myocardium to non-lethal repetitive cycles of ischaemia and reperfusion, which can be applied either shortly before a longer period of lethal sustained ischaemia (ischaemic preconditioning), or after the main ischaemic event but before the onset of a prolonged period of reperfusion (ischaemic postconditioning). Both of these ischaemic conditioning types induce cardioprotection (Murry *et al.*, 1986; Zhao *et al.*, 2003) and have been adapted to be used in a clinical setting (i.e. remote IPC). The definitive mechanisms behind these protective processes have not been fully elucidated; however the potential mechanisms have been discussed in section 1.11.2. Both pre and postconditioning are believed to have an element based around metabolism, which has been discussed in section 1.11.3 (Tong *et al.*, 2000; Nishino *et al.*, 2004; Correa *et al.*, 2008; Ji *et al.*, 2013; Yabe *et al.*, 1997; Fralix *et al.*, 1992; Sargent *et al.*, 1994).

Previous whole heart studies investigating the effects on perfusion with elevated glucose did not examine the effects through to reperfusion (Owen *et al.*, 1990; Kingsley *et al.*, 1991). While studies investigating the effect of perfusion with elevated glucose solely during reperfusion are conflicting (Vanoverschelde *et al.*, 1994, Jeremy *et al.*, 1993; Jeremy *et al.*, 1992). The aim of this study was to gain a better understanding of the effects of elevating metabolic substrates either prior to metabolic inhibition or solely during re-energisation in isolated cardiomyocytes, and to assess whether at a cellular level metabolic pre/postconditioning may be achievable. However it should be noted that in a clinical setting the occurrence of AMI is unpredictable and that individuals presenting with an elevated blood glucose concentration prior to, during and after an AMI, are more likely to suffer with adverse outcomes. Thus, preconditioning is unlikely to be clinically relevant and postconditioning may not be clinically viable.

In chapter 3 and 4, it was shown that perfusing isolated cardiomyocytes with elevated extracellular metabolic substrates, prior to metabolic inhibition and during re-energisation imparts a concentration-dependent cardioprotection. Therefore this chapter was designed to investigate the effects on isolated cardiomyocytes, of elevating these metabolic substrates either prior to metabolic inhibition (preconditioning) or during re-energisation (postconditioning). The aim was to establish if elevating the available metabolic substrates at these times, can elicit a similar type of cardioprotection as seen with the traditional pre/post ischaemic conditioning and therefore whether metabolic pre/post conditioning could be clinically beneficial.

The results in this chapter will describe the cardioprotective benefits of elevating metabolic substrates for different durations either prior to (preconditioning) or after SFT-MI (postconditioning), on the contractile function and recovery of isolated cardiomyocytes following metabolic inhibition and re-energisation.

5.2 Results

5.2.1 The effects of preconditioning with elevated glucose on the contractile function of isolated cardiomyocytes

As previously described in chapter 3, perfusing isolated cardiomyocytes with a hyperglycaemic glucose concentration (20mM glucose) before metabolic inhibition and during re-energisation, resulted in $58.4 \pm 4.1\%$ of cardiomyocytes recovering contractile function by the end of 10 minutes re-energisation compared to $29.5 \pm 2.4\%$ under normoglycaemic conditions (5mM glucose). Therefore the aim of these experiments was to investigate whether preconditioning cardiomyocytes with a hyperglycaemic glucose concentration (20mM glucose) would also elicit cardioprotection compared to perfusion under normoglycaemic conditions throughout the protocol.

Cardiomyocytes were preconditioned (PC) for either 5 or 15 minutes with 20mM glucose and 5mM pyruvate prior to perfusion under normoglycaemic conditions with 5mM pyruvate for 5 minutes. Cardiomyocytes were re-energised with Tyrode

containing 5mM glucose and 5mM pyruvate. Figure 5.1 shows the protocols for the preconditioning experiments of different durations (5 and 15 minutes). The 5 minute preconditioning protocol was based on previous “pre-treatment” protocols used by the lab (Sims *et al.*, 2014). The 15 minute preconditioning protocol was designed with previous chapter protocols and the chapter 5 “control” protocol in mind, in which the cardiomyocytes were left to settle in the respective experimental Tyrode solutions for 10 minutes prior to EFS beginning, as I wanted to match these previous protocols.

Ischaemia and reperfusion were simulated in these experiments by metabolic inhibition and re-energisation (as previously described in section 3.2.1). Markers of ischaemic injury were taken as the times to contractile failure and rigor contracture from the onset of metabolic inhibition. Markers of re-energisation protection were calculated as the percentage of ‘non-hypercontracted’ cardiomyocytes and the percentage regaining contractile function in time with EFS by the end of the re-energisation. The same protocol and markers were used and measured for all preconditioning experiments.

The time-dependent effects of preconditioning isolated cardiomyocytes with a hyperglycaemic glucose concentration for either 5 or 15 minutes, followed by perfusion with normoglycaemic concentration prior to metabolic inhibition and during re-energisation are shown in Figure 5.2A. Preconditioning significantly delayed the time to contractile failure (Figure 5.2B) from 163.0 ± 10.1 s under normoglycaemic conditions to 193.5 ± 6.5 s (5 minutes preconditioning, $P < 0.05$) and 192.0 ± 10.2 s (15 minutes preconditioning, $P < 0.05$).

Preconditioning for 5 minutes significantly delayed the time to rigor (Figure 5.2C) from 270.2 ± 13.1 s under normoglycaemic conditions to 322.3 ± 18.2 s ($P < 0.05$). However, preconditioning for 15 minutes had no effect on the time to rigor at 282.7 ± 15.0 s ($P = 0.58$) compared to normoglycaemic conditions.

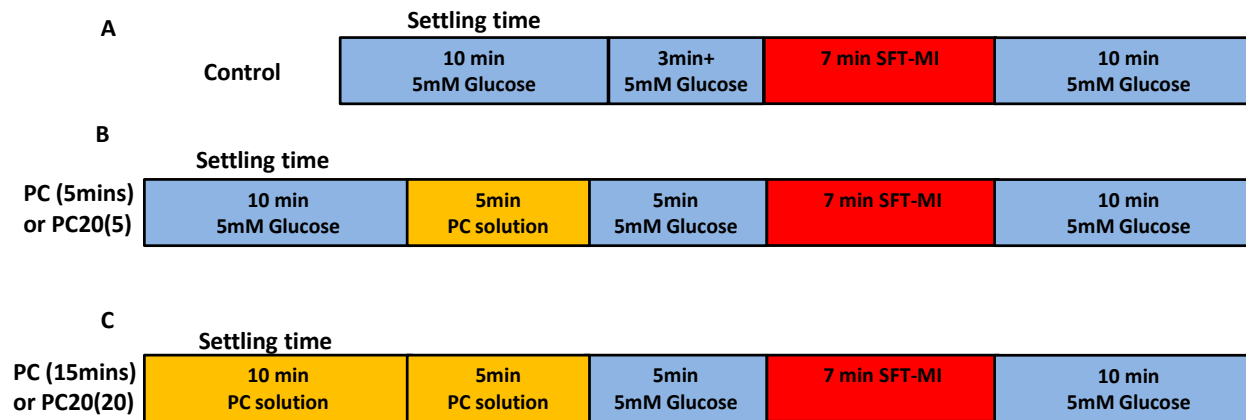


Figure 5.1 The metabolic contractile function and SarcK_{ATP} preconditioning protocols

(A) Control protocol: Cardiomyocytes were settled for 10 minutes in Tyrode solution containing 5mM glucose and then perfused with Tyrode solution containing 5mM glucose for 3 minutes (contractile experiments) or 3-6 minutes in the SarcK_{ATP} experiments. For the contractile failure experiments metabolic inhibition was then induced by perfusing with SFT-MI for 7 minutes, followed by 10 minutes of re-energisation with Tyrode solution containing 5mM glucose. For the SarcK_{ATP} experiments, SFT-MI was perfused until the end of the experiment.

(B) Protocol used for the 5 minute preconditioning (PC) experiments.

(C) Protocol used for the 15 minute preconditioning (PC) experiments.

In the SarcK_{ATP} experiments the PC solution was 20mM glucose and SFT-MI was perfused until the end of the experiment.

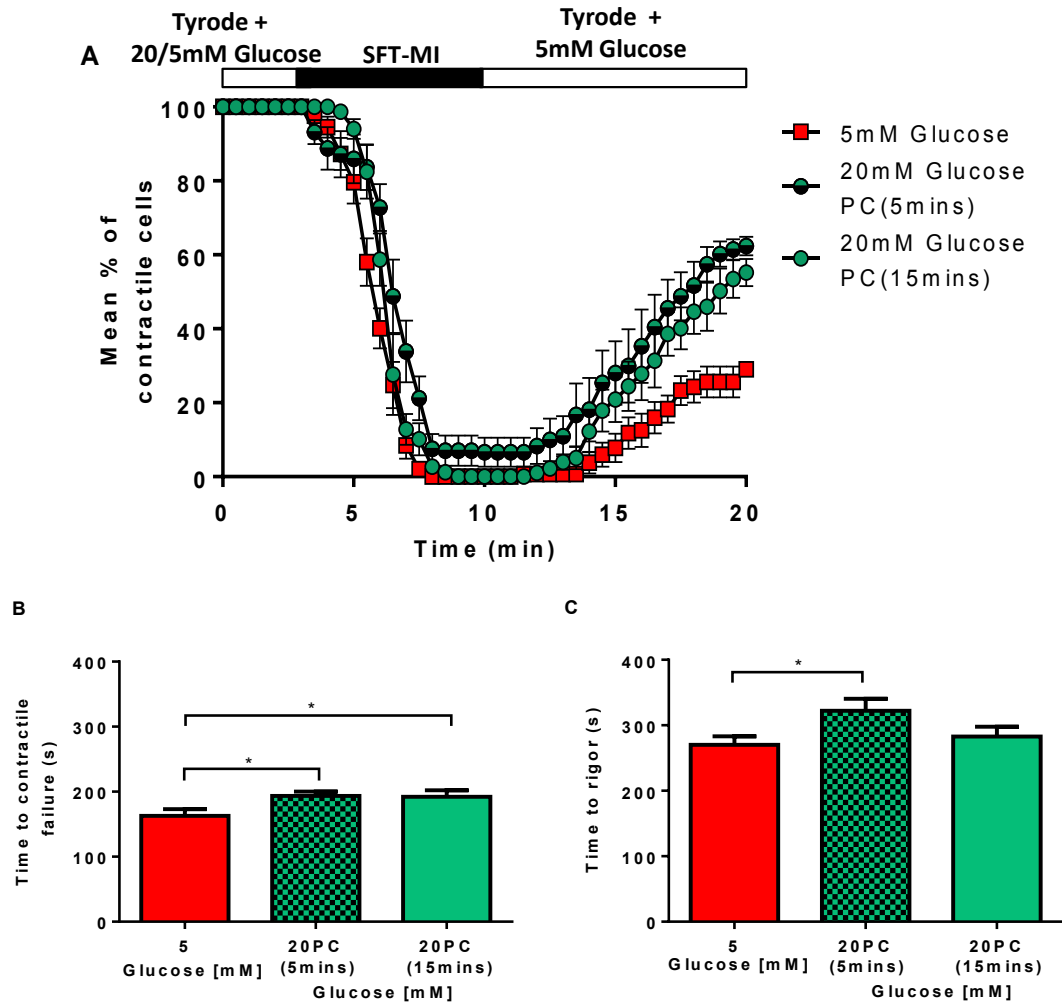


Figure 5.2 The effects of metabolic preconditioning with elevated glucose on the response of isolated cardiomyocytes to metabolic inhibition and re-energisation.

- (A) Time course showing the mean percentage of cardiomyocytes contracting in response to EFS, during superfusion with SFT-MI and re-energisation. Cardiomyocytes were preconditioned with 20mM glucose (20PC), for either 5 (PC(5mins)) or 15 minutes (PC(15mins)) followed by superfusion with 5mM glucose for 5 minutes, prior to superfusion with SFT-MI. During re-energisation cardiomyocytes were superfused with Tyrode containing 5mM glucose for all data sets.
- (B) Time to contractile failure from the onset of metabolic inhibition for cardiomyocytes superfused with 5mM glucose or preconditioned with 20mM glucose.
- (C) Time to rigor contracture from the onset of metabolic inhibition for cardiomyocytes superfused with 5mM glucose or preconditioned with 20mM glucose.
- Data presented as mean \pm s.e.m. Data for 5mM glucose (red bar, N= 6 hearts, 6 fields of view, 125 cardiomyocytes). Data for preconditioning, 20PC (5mins) (patterned green bar, N= 3, 6, 160) and 20PC (15mins) (green bar, N= 4, 6, 128). *P<0.05 (one-way ANOVA with Fisher's post-host test).

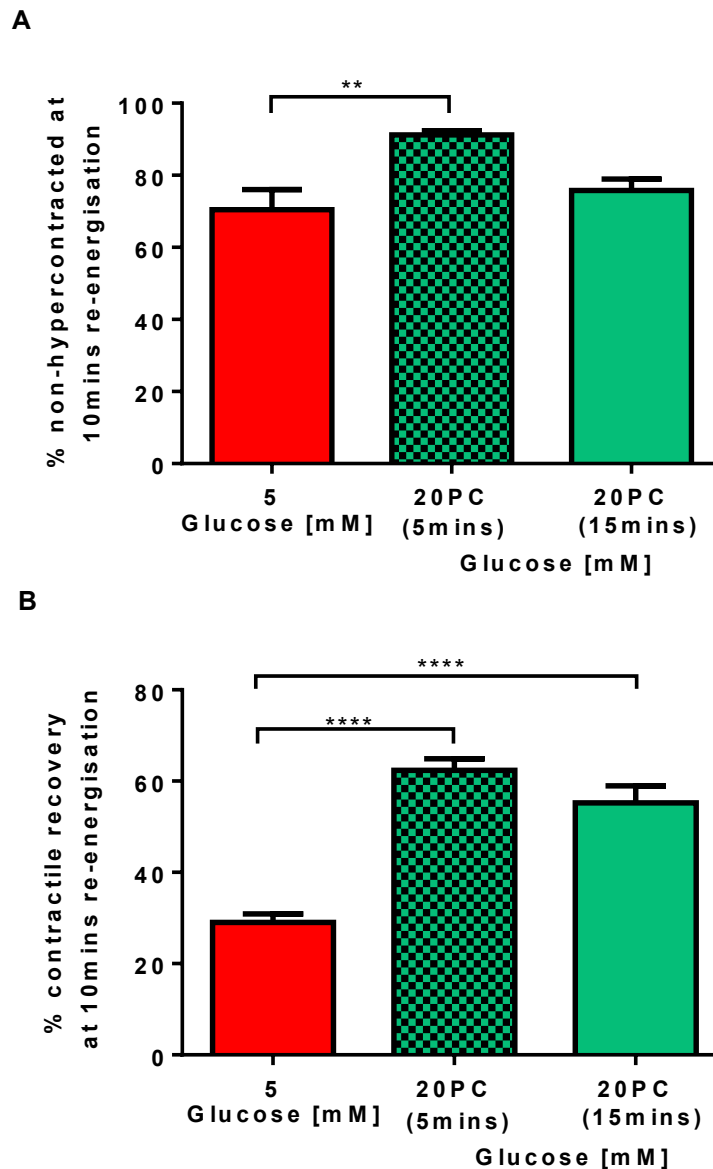


Figure 5.3 The effects of metabolic preconditioning with elevated glucose on the recovery of isolated cardiomyocytes subjected to metabolic inhibition and re-energisation.

- (A) The percentage of 'non-hypercontracted' cardiomyocytes by the end of 10 minutes re-energisation for cardiomyocytes superfused with 5mM glucose or preconditioned with 20mM glucose.
- (B) The percentage of cardiomyocytes regaining contractile function by the end of 10 minutes re-energisation for cardiomyocytes superfused with 5mM glucose or preconditioned with 20mM glucose.

Data presented as mean \pm s.e.m. Data for 5mM glucose (red bar, N= 6 hearts, 6 fields of view, 125 cardiomyocytes). Data for preconditioning, 20PC (5mins) (patterned green bar, N= 3, 6, 160), 20PC (15mins) (green bar, N= 4, 6, 128). **P<0.01, ****P<0.0001 (one-way ANOVA with Fisher's post-hoc test).

The percentage of 'non-hypercontracted' cardiomyocytes at the end of 10 minutes of re-energisation, was significantly increased following 5 minutes preconditioning (Figure 5.3A) from $70.5 \pm 5.6\%$ under normoglycaemic conditions to $91.2 \pm 1.1\%$ ($P < 0.01$). Paradoxically, preconditioning for 15 minutes, was without effect at $75.8 \pm 3.2\%$ ($P = 0.33$) compared to normoglycaemic conditions. Preconditioning significantly increased the percentage of cardiomyocytes regaining contractile function by the end of re-energisation (Figure 5.3B) from $29.0 \pm 1.9\%$ under normoglycaemic conditions to $62.4 \pm 2.5\%$ (5 minutes preconditioning, $P < 0.0001$) and $55.2 \pm 3.7\%$ (15 minutes preconditioning, $P < 0.0001$).

These data show that preconditioning isolated cardiomyocytes with a hyperglycaemic glucose concentration for either 5 or 15 minutes delays contractile failure and improves contractile recovery. Additionally preconditioning for 5 minutes also delayed rigor contracture and increased the percentage of 'non-hypercontracted' cardiomyocytes. Therefore these data suggest preconditioning with a hyperglycaemic glucose concentration is sufficient to impart a cardioprotective phenotype.

5.2.2 Preconditioning isolated cardiomyocytes with elevated glucose delays SarcK_{ATP} channel activity during metabolic inhibition

As previously described perfusing cardiomyocytes with a hyperglycaemic glucose concentration (20mM glucose) immediately prior to metabolic inhibition, caused a delay in SarcK_{ATP} activation (section 3.2.3). Therefore it was hypothesised that preconditioning isolated cardiomyocytes, with a hyperglycaemic glucose concentration prior to perfusion with a normoglycaemic glucose concentration, would also delay SarcK_{ATP} activation during metabolic inhibition.

To investigate whether preconditioning with a hyperglycaemic glucose concentration would delay SarcK_{ATP} channel activation, cardiomyocytes were subjected to the protocols outlined in Figure 5.1. Cardiomyocytes were preconditioned for either 5 (PC20(5)) or 15 minutes (PC20(20)) with 20mM glucose (the number in the end brackets illustrates what glucose concentration the cardiomyocytes were settled in). The SarcK_{ATP} channel activity during SFT-MI was recorded using the whole-cell patch clamp technique, with cardiomyocytes clamped at a holding potential of 0mV. The

time to the $\text{Sarck}_{\text{ATP}}$ current during perfusion with SFT-MI, was measured from these continuous records by measuring the point at which the observed basal outward steady-state current had increased by 20pA.

Figure 5.4A shows representative traces of membrane current recorded from a cardiomyocyte perfused with a normoglycaemic glucose concentration, and from cardiomyocytes preconditioned for either 5 or 15 minutes with a hyperglycaemic glucose concentration. The development of outward currents indicated opening of $\text{Sarck}_{\text{ATP}}$ channels; this was delayed in those cardiomyocytes preconditioned with 20mM glucose. Figure 5.4B shows the effect of preconditioning with 20mM glucose. Preconditioning for 5 minutes (PC20(5)) had no effect on the time to $\text{Sarck}_{\text{ATP}}$ channel activation with $129.5 \pm 10.2\text{s}$ versus $111.4 \pm 7.1\text{s}$ ($P=0.30$) for those perfused under normoglycaemic conditions. However preconditioning for 15 minutes (PC20(20)) significantly delayed the time to $\text{Sarck}_{\text{ATP}}$ channel activation to $161.3 \pm 15.7\text{s}$ ($P<0.01$) compared to normoglycaemic conditions.

These data show that preconditioning isolated cardiomyocytes with a hyperglycaemic glucose concentration for 15 minutes delays the time to $\text{Sarck}_{\text{ATP}}$ channel activation during metabolic inhibition.

5.2.3 The effects of preconditioning with elevated fructose on the contractile function of isolated cardiomyocytes

In chapter 3, it was demonstrated that perfusion with an elevated fructose concentration (20mM), before metabolic inhibition and during re-energisation, imparted a cardioprotective phenotype on isolated cardiomyocytes. Therefore the ability of fructose to precondition isolated cardiomyocytes was investigated; 15mM fructose was chosen to be combined with 5mM glucose, as this gave the Tyrode solution a total sugar concentration of 20mM, which was osmotically balanced with 20mM sucrose in the SFT solution.

The time dependent effects of preconditioning with 15mM fructose for 5 or 15 minutes, prior to metabolic inhibition and re-energisation are shown in Figure 5.5A. Preconditioning for 5 minutes had no effect on the time to contractile failure (Figure

5.5B) at 185.1 ± 3.6 s compared to 157.8 ± 9.5 s ($P=0.053$) under normoglycaemic conditions. However, preconditioning for 15 minutes significantly delayed the time to contractile failure at 208.8 ± 11.8 s ($P<0.01$). The time to rigor contracture (Figure 5.5C) was not affected by either preconditioning protocol with 318.5 ± 16.8 s (5 minutes preconditioning, $P=0.052$) and 289.0 ± 13.7 s (15 minutes preconditioning, $P=0.45$) compared to 272 ± 15.0 s recorded under normoglycaemic conditions.

Preconditioning for 5 minutes significantly increased the percentage of 'non-hypercontracted' cardiomyocytes by the end of 10 minutes of re-energisation (Figure 5.6A) from $69.7 \pm 6.9\%$ under normoglycaemic conditions to $88.4 \pm 3.1\%$ ($P<0.01$). However preconditioning for 15 minutes was without effect at $85.3 \pm 6.1\%$ ($P=0.07$) compared to normoglycaemic conditions. Both preconditioning times significantly increased the percentage of cardiomyocytes regaining contraction (Figure 5.6B), from $32.0 \pm 1.5\%$ under normoglycaemic conditions to $55.0 \pm 2.1\%$ (5 minutes preconditioning, $P<0.0001$) and $62.3 \pm 3.3\%$ (15 minutes preconditioning, $P<0.0001$).

These data show that preconditioning isolated cardiomyocytes with an elevated fructose concentration (15mM) for 15 minutes delayed the time to contractile failure. While preconditioning for 5 minutes increased the percentage of 'non-hypercontracted' cardiomyocytes. Both preconditioning times resulted in improved contractile recovery by the end of re-energisation, suggesting preconditioning with fructose is cardioprotective.

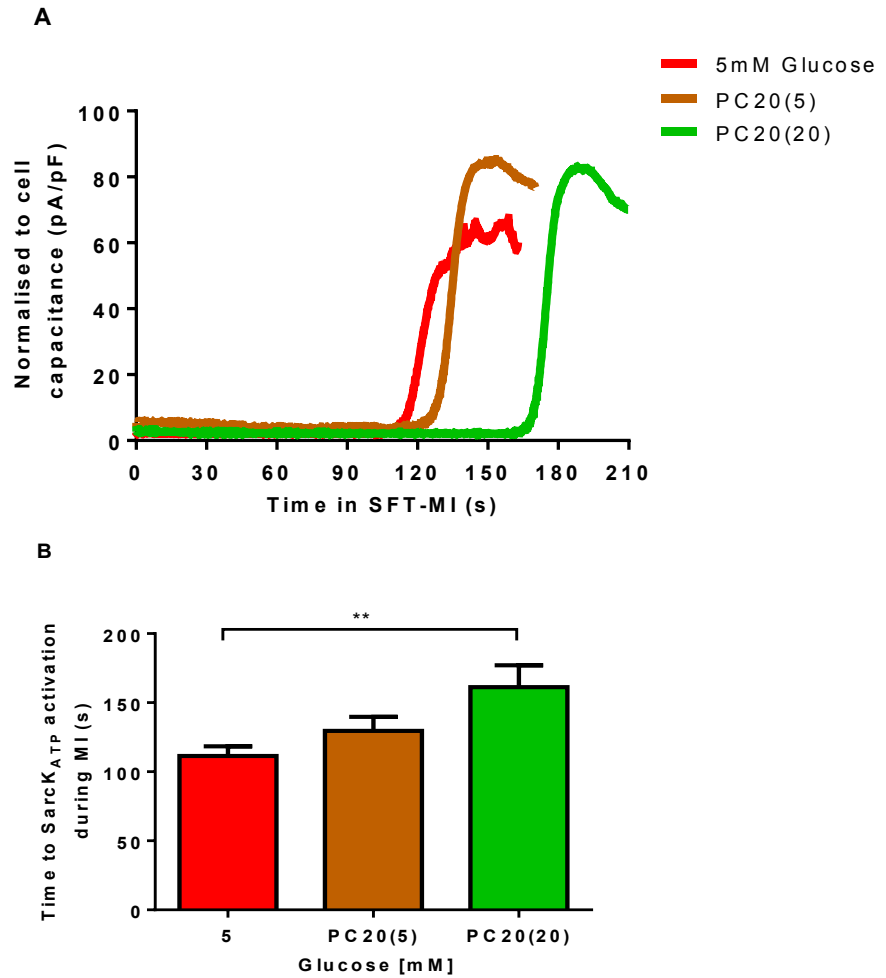


Figure 5.4 The effects of metabolic preconditioning with elevated glucose on SarcK_{ATP} current activation during metabolic inhibition.

- (A) Example traces of whole-cell SarcK_{ATP} channel current recorded from a single cardiomyocyte pre-incubated in 5mM glucose (red trace), or pre-incubated in 20mM glucose for either 5 (brown trace, PC20(5)) or 15 minutes (green trace, PC20(20)) before perfusion with 5mM glucose for 5 minute and then subjected to metabolic inhibition (MI). Each trace is normalised to cell capacitance (pA/pF). Time to the SarcK_{ATP} current activation during SFT-MI was measured at the point at which the outward basal current had increased by 20pA.
- (B) Time to SarcK_{ATP} current activation during metabolic inhibition (MI), for cardiomyocytes pre-incubated in 5mM or 20mM glucose for either 15 (PC20(20)) or 5 minutes (PC20(5)) before switching to 5mM glucose.

Data presents as mean \pm s.e.m. Data for 5mM glucose (red bar, N= 10 hearts, 10 experiments/cardiomyocytes). Data for preconditioning, PC20(5) (brown bar, N=6, 12), PC20(20) (green bar, N= 7, 13). **P<0.01 (one-way ANOVA with Fisher's post-hoc test).

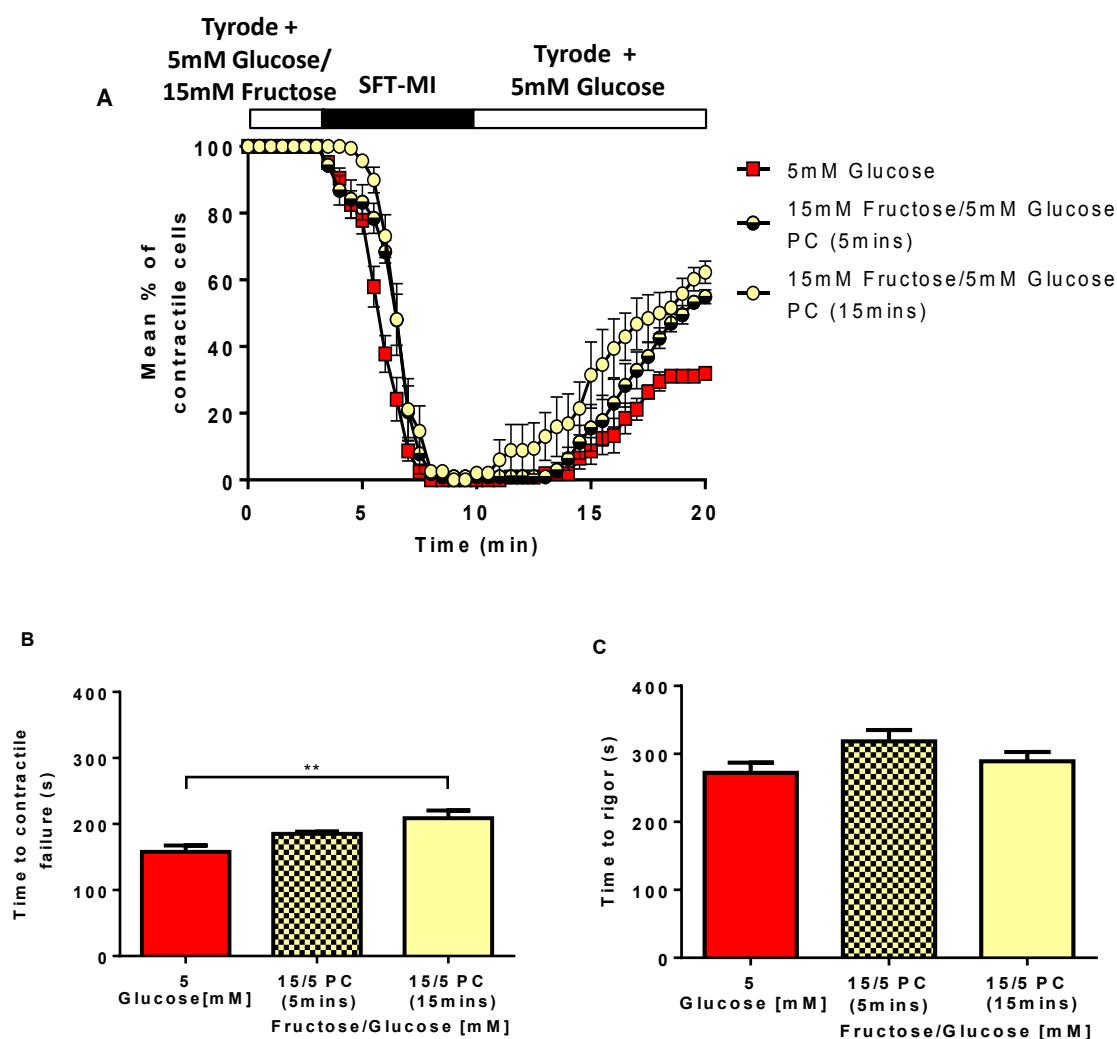


Figure 5.5 The effects of metabolic preconditioning with elevated fructose on the response of isolated cardiomyocytes to metabolic inhibition and re-energisation.

(A) Time course showing the mean percentage of cardiomyocytes contracting in response to EFS, during superfusion with SFT-MI and re-energisation. Cardiomyocytes were preconditioned with 15mM fructose/5mM glucose (15/5PC), for either 5 (PC(5mins)) or 15 minutes (PC(15mins)) followed by superfusion with 5mM glucose for 5 minutes, prior to superfusion with SFT-MI. During re-energisation cardiomyocytes were superfused with Tyrod containing 5mM glucose for all data sets.

(B) Time to contractile failure from the onset of metabolic inhibition for cardiomyocytes superfused with 5mM glucose or preconditioned with 15mM fructose/5mM glucose.

(C) Time to rigor contracture from the onset of metabolic inhibition for cardiomyocytes superfused with 5mM glucose or preconditioned with 15mM fructose/5mM glucose.

Data presented as mean \pm s.e.m. Data for 5mM glucose (red bar, N= 5 hearts, 5 fields of view, 116 cardiomyocytes). Data for preconditioning, 15/5PC (5mins) (patterned cream bar, N= 3, 5, 168), 15/5PC (15mins) (cream bar, N= 3, 5, 128). **P<0.01 (one-way ANOVA with Fisher's post-hoc test).

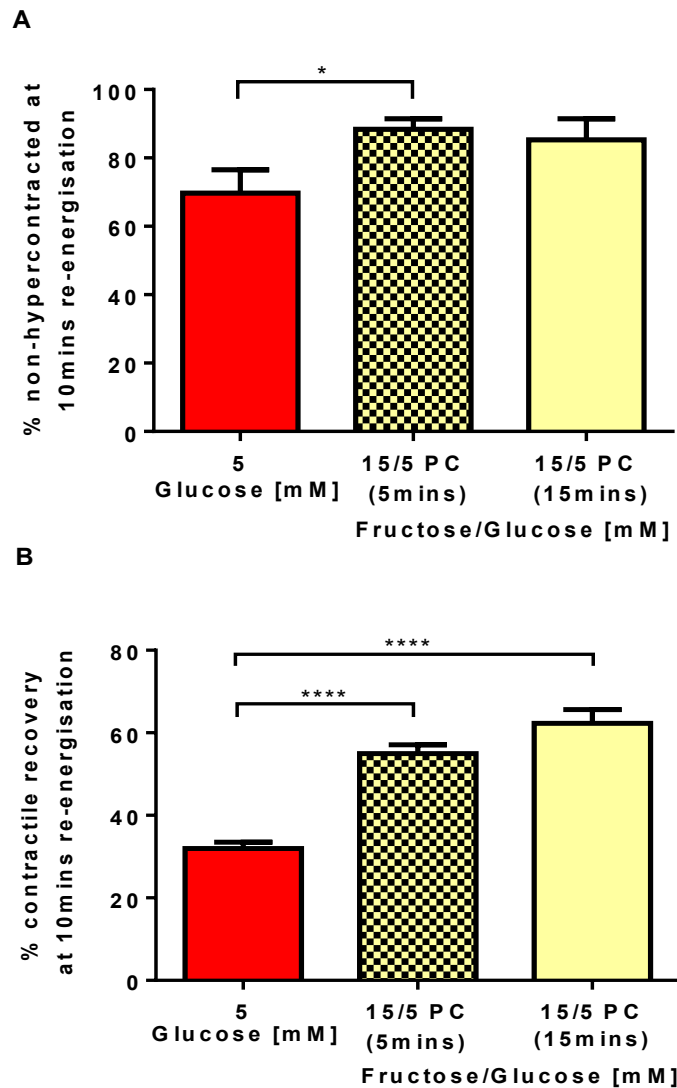


Figure 5.6 The effects of metabolic preconditioning with elevated fructose on the recovery of isolated cardiomyocytes subjected to metabolic inhibition and re-energisation.

(A) The percentage of 'non-hypercontracted' cardiomyocytes by the end of 10 minutes re-energisation for cardiomyocytes superfused with 5mM glucose or preconditioned with 15mM fructose/5mM glucose.

(B) The percentage of cardiomyocytes regaining contractile function by the end of 10 minutes re-energisation for cardiomyocytes superfused with 5mM glucose or preconditioned with 15mM fructose/5mM glucose.

Data presented as mean \pm s.e.m. Data for 5mM glucose (red bar, N= 5 hearts, 5 fields of view, 116 cardiomyocytes). Data for preconditioning, 15/5PC (5mins) (patterned cream bar, N= 3, 5, 168), 15/5PC (15mins) (cream bar, N= 3, 5, 128). *P<0.05, ****P<0.0001 (one-way ANOVA with Fisher's post-hoc test).

5.2.4 The effects of preconditioning with elevated pyruvate on the contractile function of isolated cardiomyocytes

In chapter 4, it was shown that a supraphysiological concentration of pyruvate (10mM) was cardioprotective under normoglycaemic conditions. Therefore these experiments aimed to investigate whether this combination of metabolic substrates could be effective in a preconditioning setting.

The time-dependent effects of preconditioning isolated cardiomyocytes with 10mM pyruvate and 5mM glucose is shown in Figure 5.7A. Preconditioning for 5 minutes significantly delayed the time to contractile failure (Figure 5.7B) from 157.3 ± 7.8 s (5mM glucose) under normoglycaemic conditions to 198.6 ± 7.8 s ($P < 0.05$). However preconditioning for 15 minutes had no effect on the time to contractile failure at 198.0 ± 21.0 s ($P = 0.053$).

Preconditioning for 5 minutes significantly delayed the time to rigor (Figure 5.7C) from 268.6 ± 12.8 s under normoglycaemic conditions to 321.7 ± 16.5 s ($P < 0.05$). However preconditioning for 15 minutes had no effect on the time to rigor contracture at 277.5 ± 23.0 s ($P = 0.74$) compared to normoglycaemic conditions.

Preconditioning for 5 minutes significantly increased the percentage of 'non-hypercontracted' cardiomyocytes by the end of 10 minutes of re-energisation (Figure 5.8A) with $85.3 \pm 2.9\%$ ($P < 0.05$) versus $70.2 \pm 5.6\%$ under normoglycaemic conditions. However the 15 minute preconditioning had no effect with $80.0 \pm 4.3\%$ ($P = 0.14$) compared to normoglycaemic conditions. Both preconditioning times significantly increased the percentage of cardiomyocytes regaining contractile function (Figure 5.8B) from $31.2 \pm 1.5\%$ under normoglycaemic conditions to $63.1 \pm 3.7\%$ (5 minutes preconditioning, $P < 0.0001$) and $56.7 \pm 6.2\%$ (15 minutes preconditioning, $P < 0.001$).

These data show that preconditioning isolated cardiomyocytes for 5 minutes with an elevated pyruvate concentration (10mM) delays contractile failure and rigor contracture and increased the percentage of cardiomyocytes 'non-hypercontracted' by the end of re-energisation. In addition these data show both preconditioning times increased the percentage of contractile recovery.

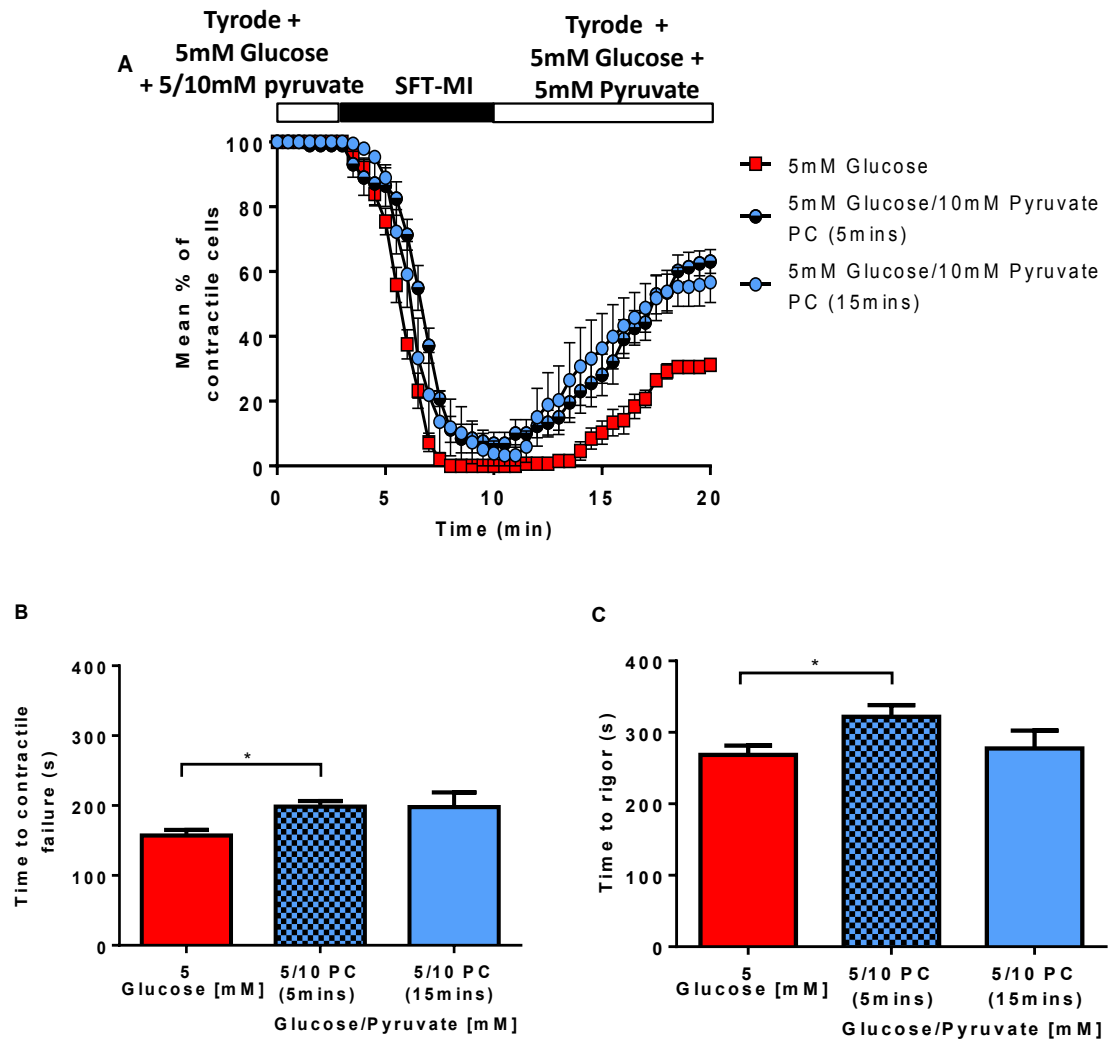


Figure 5.7 The effects of metabolic preconditioning with elevated pyruvate on the response of isolated cardiomyocytes to metabolic inhibition and re-energisation.

- (A) Time course showing the mean percentage of cardiomyocytes contracting in response to EFS, during superfusion with SFT-MI and re-energisation. Cardiomyocytes were preconditioned with 5mM glucose/10mM pyruvate (5/10PC), for either 5 (PC (5mins)) or 15 minutes (PC(15mins)), followed by superfusion with 5mM glucose/ 5mM pyruvate for 5 minutes, prior to superfusion with SFT-MI. During re-energisation cardiomyocytes were superfused with Tyrode containing 5mM glucose and 5mM pyruvate for all data sets.
- (B) Time to contractile failure from the onset of metabolic inhibition for cardiomyocytes superfused with 5mM glucose or preconditioned with 5mM glucose/10mM pyruvate.
- (C) Time to rigor contracture from the onset of metabolic inhibition for cardiomyocytes superfused with 5mM glucose or preconditioned with 5mM glucose/10mM pyruvate.

Data presented as mean \pm s.e.m. Data for 5mM glucose (red bar, N= 6 hearts, 6 fields of view, 127 cardiomyocytes). Data for preconditioning, 5/10PC (5mins) (patterned blue bar, N= 3, 6, 128), 5/10PC (15mins) (blue bar, N= 3, 6, 144). *P<0.05 (one-way ANOVA with Fisher's post-hoc test).

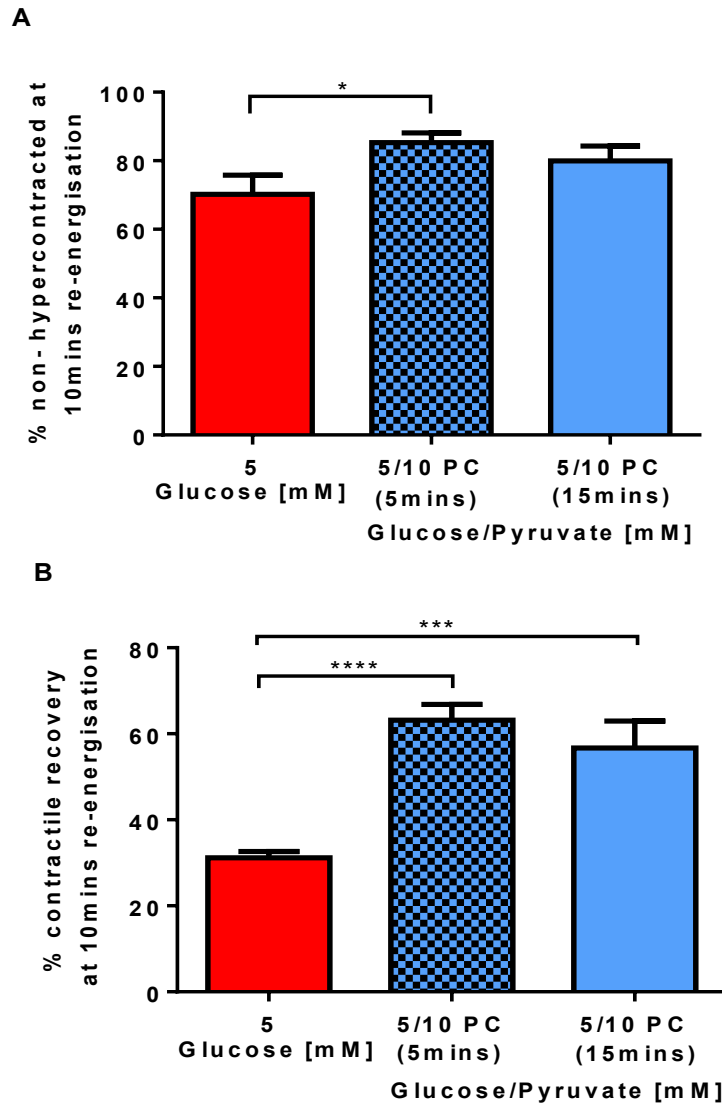


Figure 5.8 The effects of metabolic preconditioning with elevated pyruvate on the recovery of isolated cardiomyocytes subjected to metabolic inhibition and re-energisation.

- (A) The percentage of 'non-hypercontracted' cardiomyocytes by the end of 10 minutes re-energisation for cardiomyocytes superfused with 5mM glucose or preconditioned with 5mM glucose/10mM pyruvate.
- (B) The percentage of cardiomyocytes regaining contractile function by the end of 10 minutes re-energisation for cardiomyocytes superfused with 5mM glucose or preconditioned with 5mM glucose/10mM pyruvate.

Data presented as mean \pm s.e.m. Data for 5mM glucose (red bar, N= 6 hearts, 6 fields of view, 127 cardiomyocytes). Data for preconditioning, 5/10PC (5mins) (patterned blue, N= 3, 6, 128), 5/10PC (15mins) (blue bar, N= 3, 6, 144). *P<0.05, ***P<0.001, ****P<0.0001 (one-way ANOVA with Fisher's post-hoc test).

5.2.5 Postconditioning with elevated glucose limits re-energisation injury

Previously it was demonstrated that perfusing with a hyperglycaemic glucose concentration (20mM glucose), either prior to metabolic inhibition and during re-energisation or as a preconditioning treatment is cardioprotective. Therefore these experiments were designed to investigate whether perfusing cardiomyocytes with a hyperglycaemic glucose concentration only at the point of re-energisation (metabolic postconditioning), would also be cardioprotective.

Metabolic postconditioning was achieved by re-energising cardiomyocytes, after 7 minutes of metabolic inhibition, with a hyperglycaemic glucose concentration and 5mM pyruvate. Figure 5.9 shows the postconditioning protocols, in which isolated cardiomyocytes were stimulated to contract at 1Hz by EFS throughout. The postconditioning protocols were designed based on the idea that restabilising re-energisation ionic homeostasis is important to aid recovery and based on findings outlined in chapter 3, it is suggested elevated glucose may aid this. The 10 minute postconditioning protocol was designed based around previous protocols in which re-energised with the experimental Tyrode solution had been for the whole 10 minutes. Meanwhile, the 5 minute postconditioning protocol was designed based on the understanding that an intact glycolytic pathway initial upon re-energisation is crucial to recovery (Jeremy *et al.*, 1992).

As the duration of the postconditioning within this protocol varied between 5 and 10 minutes (see Figure 5.9). This allowed three factors to be investigated 1) if a hyperglycaemic glucose concentration was beneficial to cardiomyocytes during re-energisation 2) how long it was necessary for the hyperglycaemic glucose concentration to be present for during re-energisation and 3) if a hyperglycaemic glucose concentration could stimulate cardioprotection when available for only the first half of re-energisation. At the end of the protocol the same markers of ischaemic injury were measured and the same markers of re-energisation protection as previously mentioned were calculated (see section 5.2.1).

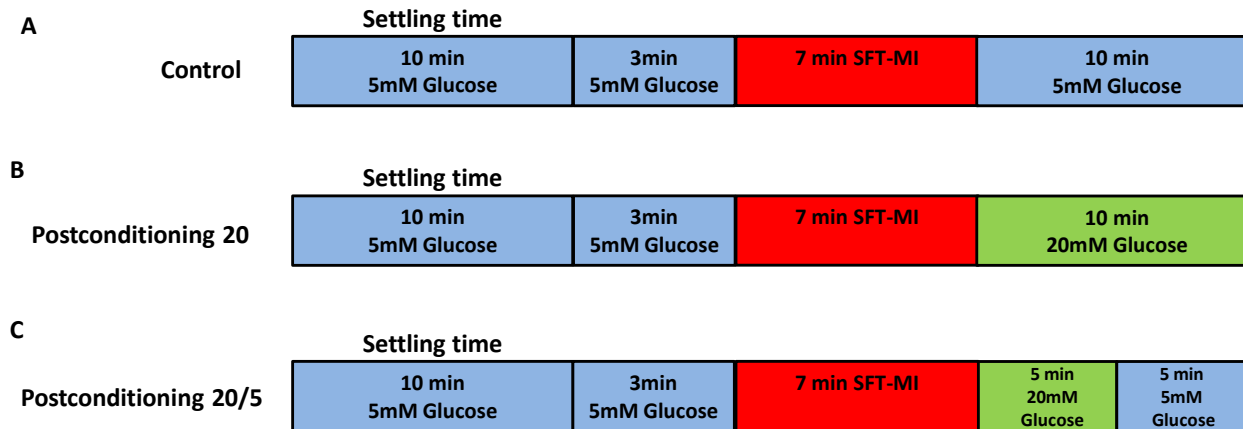


Figure 5.9 The metabolic postconditioning protocols

- (A) Control protocol: Cardiomyocytes were settled for 10 minutes in Tyrode solution containing 5mM glucose and then perfused with Tyrode solution containing 5mM glucose for 3 minutes. Metabolic inhibition was then induced by perfusing with SFT-MI for 7 minutes, followed by 10 minutes of re-energisation with Tyrode solution containing 5mM glucose.
- (B) Protocol used for the 10 minute postconditioning experiments, cardiomyocytes were perfused for the 10 minutes of re-energisation with Tyrode solution containing 20mM glucose.
- (C) Protocol used for the 5 minute postconditioning experiments, cardiomyocytes were perfused for the first 5 minutes of re-energisation with Tyrode solution containing 20mM glucose and for the last 5 minutes of re-energisation with Tyrode containing 5mM glucose.

The time-dependent effects of re-energising cardiomyocytes under either normoglycaemic or hyperglycaemic conditions for 5 or 10 minutes are shown in Figure 5.10A. Prior to metabolic inhibition all cardiomyocytes were perfused with Tyrode solution containing 5mM glucose and 5mM pyruvate. To ensure all cardiomyocytes were the same prior to metabolic inhibition, the time to contractile failure and rigor contracture were measured from the onset of metabolic inhibition. Both postconditioning data sets showed similar times to contractile failure and rigor contracture, as those under normoglycaemic conditions with no postconditioning. This was expected as all groups were perfused under normoglycaemic conditions prior to metabolic inhibition.

By the end of 10 minutes re-energisation, postconditioning with a hyperglycaemic glucose concentration had no effect on the percentage of 'non-hypercontracted' cardiomyocytes (Figure 5.10B) with $83.3 \pm 4.6\%$ (10 minutes postconditioning, $P=0.21$) and $85.8 \pm 1.1\%$ (5 minutes postconditioning, $P=0.10$) versus $76.3 \pm 0.8\%$ under normoglycaemic conditions. Postconditioning significantly increased the percentage of contractile recovery (Figure 5.10C) from $29.8 \pm 2.8\%$ under normoglycaemic conditions to $63.2 \pm 6.6\%$ (10 minutes postconditioning, $P<0.01$) and $62.8 \pm 4.8\%$ (5 minutes postconditioning, $P<0.01$).

These data show that upon re-energisation perfusing isolated cardiomyocytes with a hyperglycaemic glucose concentration improves contractile recovery and therefore could be cardioprotective. These data also suggest that to achieve this cardioprotection, postconditioning is required for only the first 5 minutes of re-energisation.

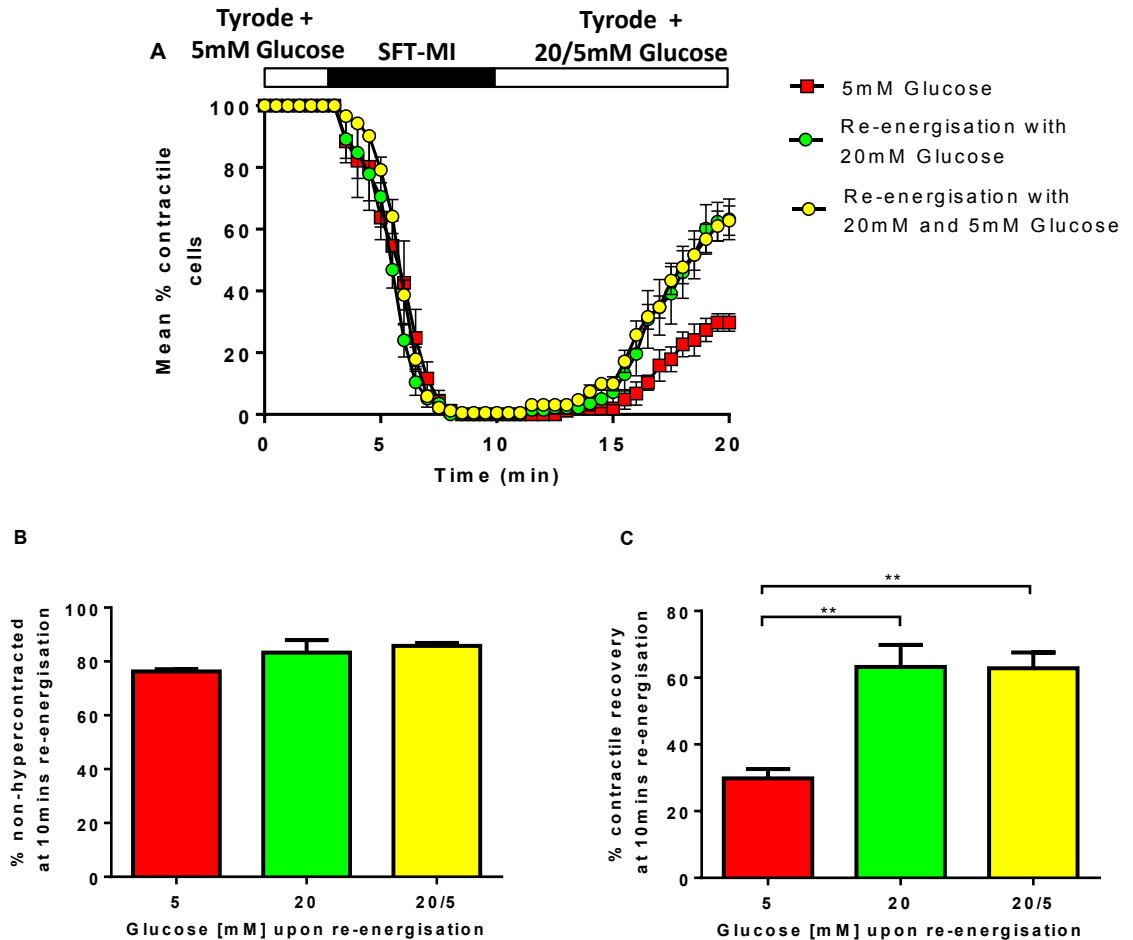


Figure 5.10 The effects of metabolic postconditioning with elevated glucose on the response and recovery of isolated cardiomyocytes subjected to metabolic inhibition and re-energisation.

- (A) Time course showing the mean percentage of cardiomyocytes contracting in response to EFS, during superfusion with SFT-MI and re-energisation. Prior to SFT-MI cardiomyocytes were superfused with Tyrode containing 5mM glucose and 5mM pyruvate. During re-energisation cardiomyocytes were superfused with Tyrode solution containing either 5 mM glucose for 10 minutes, 20mM glucose for 10 minutes or with 20mM glucose for the initial 5 minutes of re-energisation followed by 5mM glucose for the remaining 5 minutes of re-energisation.
- (B) The percentage of 'non-hypercontracted' cardiomyocytes by the end of 10 minutes re-energisation for cardiomyocytes superfused upon reperfusion with either 5mM or 20mM glucose.
- (C) The percentage of cardiomyocytes regaining contractile function by the end of 10 minutes re-energisation for cardiomyocytes superfused upon reperfusion with either 5mM or 20mM glucose.
- Data presented as mean \pm s.e.m. Data for 5mM glucose upon re-energisation (red bar, N= 3 hearts, 3 fields of views, 85 cardiomyocytes). Data for 20mM glucose upon re-energisation for 10 minutes (green bar, N= 3, 6, 115) and 20mM glucose for the initial 5 minutes of re-energisation followed by 5mM glucose for the remaining 5 minutes of re-energisation (yellow bar, N= 3, 6, 162). **P<0.01 (one-way ANOVA with Fisher's post-hoc test).

5.3 Discussion

This chapter investigated whether increasing the availability of metabolic substrates either before (preconditioning) or after (postconditioning) a period of metabolic inhibition would be cardioprotective to isolated cardiomyocytes, in the same respects as traditional pre/post-ischaemic conditioning.

The data described in this chapter shows that preconditioning isolated cardiomyocytes, with an elevated glycolytic substrate (glucose or fructose) or an elevated pyruvate concentration, for 5 minutes delays the time to contractile failure and rigor contracture during metabolic inhibition, while 15 minutes of preconditioning only delays the time to contractile failure. The delay in contractile failure observed for those preconditioned with 20mM glucose for 15 minutes, could be linked to the observed delay in $\text{SarCK}_{\text{ATP}}$ channel activation during metabolic inhibition. By the end of re-energisation, only those preconditioning for 5 minutes exhibited an increase in the percentage of 'non-hypercontracture'. However all preconditioning groups exhibited an increase in contractile recovery.

In addition, the postconditioning data shows that upon re-energisation, perfusing with a hyperglycaemic glucose concentration increased the percentage of contractile recovery.

5.3.1 Are metabolic pre and/or postconditioning relevant?

Previous findings in this study suggest elevated glucose, fructose or pyruvate (under normoglycaemic conditions) throughout the metabolic inhibition and re-energisation protocol may be protective to cardiomyocytes. It was hypothesised that this might be of clinical importance in the treatment, or management of an AMI, where a short treatment of elevated glucose might be cardioprotective. In addition it may give an understanding of what is happening at a cellular level in patients who present with hyperglycaemia at the time of an AMI. An elevated glucose concentration prior to an ischaemic insult would provide additional glycolytic substrate to allow anaerobic ATP synthesis to continue for longer during ischaemia. However as with application of IPC, it would be impossible to predict when an AMI would occur. Post-ischaemic treatment

with elevated glucose may be more clinically relevant as this could be applied directly after the period of sustained ischaemia. Unfortunately as hyperglycaemia is associated with a poor prognosis following an AMI, post-ischaemic treatment may not be clinically appropriate.

5.3.1.1 Metabolic preconditioning imparts cardioprotection

Metabolic preconditioning (for either 5 or 15 minutes) with any of the elevated metabolic substrates (glucose, fructose and pyruvate) delayed the time to contractile failure during metabolic inhibition, significance was either reached or was close at $P=0.053$ (for both 5 minute preconditioning with fructose and 15 minute preconditioning with pyruvate, for these two experiments it is proposed had another experiment been performed significance may have been reached). Together these results suggest elevating any of the metabolic substrates prior to metabolic inhibition is beneficial to the cardiomyocytes and coincides with previous findings outlined within this study (Section 3.2.1 and 4.2.6). As previously described in (Section 3.3.1) maintenance of glycolytic ATP levels during ischaemia reduces ischaemic damage and allows contraction to continue by maintaining ionic homeostasis via maintained activity of the Na^+/K^+ ATPase and preventing reverse-mode activity of the NCX (Van Emous *et al.*, 2001; Cross *et al.*, 1995; Dizon *et al.*, 1998). Therefore it could be hypothesised that glucose and potentially fructose (as a glycolytic substrate) are maintaining glycolytic ATP levels and thus delaying contractile failure via the same/similar pathways as outlined in Figure 3.17.

In terms of the 10mM pyruvate, there could also be an increase in ATP levels but this would primarily be via oxidative phosphorylation, which in turn would increase the amount PCr available to be transferred from the mitochondria via the phosphocreatine transfer shuttle to the myofibrils and thus increasing ATP pools at the myofibrils and aid maintenance of contraction as described previously (section 4.3.1.2).

In addition to there being a delay in contractile failure, a significant delay in $\text{SarCK}_{\text{ATP}}$ channel activation during metabolic inhibition was achieved following 15 minute preconditioning with elevated glucose. Due to glycolytic ATP having been found to

inhibit SarcKATP channels (Weiss 1987), it could be suggested metabolic preconditioning for 15 minutes is maintaining glycolytic ATP in close proximity to the SarcK_{ATP} channels and is therefore responsible for the delay in activation. It could be hypothesised that time to action potential failure would also have been delayed linking in with the delay in contractile failure.

The discrepancy of 5 minutes preconditioning, not having an effect on SarcK_{ATP} channel activation suggests that 5 minutes was not long enough to delay the depletion of glycolytic ATP close to the SarcK_{ATP} channels. It could be that the duration of the preconditioning time with elevated glucose maintained ATP levels in close proximity to the SarcK_{ATP} channels for a while but was not sufficient to prevent a delay in activation during metabolic inhibition. It could be proposed the ATP generated from the preconditioning time may have been “used” and so the only ATP available during metabolic inhibition is that produced by the 3 minute perfusion with 5mM glucose prior to metabolic inhibition.

Metabolic preconditioning with elevated glucose or pyruvate for 5 minutes significantly delayed the time to rigor, while preconditioning with fructose was close to significance with $P=0.052$ (it is proposed had an additional experiment been done, significance may have been reached). Paradoxically 15 minutes preconditioning with any of the elevated metabolic substrates, had no effect on rigor.

The effects observed with preconditioning with elevated glucose and fructose for 5 minutes could further suggest that an increase in anaerobic glycolysis is occurring, resulting in increased glycolytic ATP production, which is preventing rigor and could suggest a similar pathway as outlined in Figure 3.17 is being stimulated. These delays are in agreement with previous studies that have found perfusion with elevated glucose prior to ischaemia in a whole heart setting delays ischaemic contracture (Owen *et al.*, 1990; Kingsley *et al.*, 1991). The 5 minute preconditioning time could be allowing a steady reserve of ATP to build up and the 5mM glucose perfusion following the preconditioning section is adding to this.

The lack of effect with 15 minute preconditioning is surprising and suggests either not enough glycolytic ATP is being produced to prevent rigor which does not correlate

with previous findings in this study or the literature (Owen *et al.*, 1990; Kingsley *et al.*, 1991) or it could suggest mitochondrial ATP is more involved in preventing rigor. Additional it could be hypothesised that preconditioning for 15 minutes followed by perfusion with 5mM glucose is stimulating larger quantities of by-products (i.e. citrate, ATP or fructose 1,6-bisphosphate) that can inhibit certain enzymes blocking glycolysis (Regen *et al.*, 1964; Stanley *et al.*, 2005; Pogson & Randle, 1966; Oguchi *et al.*, 1973) and therefore reducing the available glycolytic ATP.

For the pyruvate data it is suggested that although there may be a delay in contractile failure, the difference in rigor could be due to pyruvate having different effects on PFK-1 (Fralix *et al.*, 1992). The 5 minutes of preconditioning could be long enough to increase ATP at myofibrils therefore preventing rigor, but not long enough to induce sufficient inhibition of PFK-1, and therefore glycolysis. Whilst 15 minutes could cause greater inhibition of PFK-1, preventing glycolysis and therefore reducing the amount of glycolytic ATP available to prevent rigor, as ischaemic contracture is believed to occur when anaerobic glycolysis ceases (Owen *et al.*, 1990; Cross *et al.*, 1995; Kingsley *et al.*, 1991).

Upon re-energisation, the metabolic preconditioning experiments were perfused with 5mM glucose and 5mM pyruvate, this matches the conditions for those cardiomyocytes within this chapter that were perfused throughout the protocol under normoglycaemic conditions with 5mM pyruvate, therefore any differences seen between the data sets during re-energisation are due to the metabolic preconditioning.

All three, 5 minute metabolic preconditioning protocols significantly increased the percentage of 'non-hypercontracted' cardiomyocytes. These results suggest the benefits of elevated substrates prior to metabolic inhibition are able to continue until the time of re-energisation, so that upon re-energisation the cardiomyocytes maybe "more stable". This is proposed to occur as a result of preconditioning preventing a higher level of ischaemic damage. For instance if glycolytic ATP production was being maintained throughout metabolic inhibition, ionic homeostasis would not be disrupted, as a result increases in $[Ca^{2+}]_i$ would be prevented, which upon re-

energisation are usually associated with causing hypercontracture as discussed in section 3.3.2. In addition it could suggest the metabolic preconditioning is delaying mitochondrial repolarisation upon re-energisation, which would stimulate less ATP production and together with the prevention in $[Ca^{2+}]_i$ would stimulate less hypercontracture (as outlined in Figure 3.20), resulting in the observed increase in 'non-hypercontracture'.

Paradoxically, the 15 minute metabolic preconditioning protocols had no effect although the fructose data had a P value of 0.07 (suggesting had another experiment been performed significance may have been reached). These results suggest there may be no beneficial or detrimental effect initially upon re-energisation of elevating substrates prior to metabolic inhibition for this length of time.

Contractile recovery following metabolic preconditioning was different to the data where the cardiomyocytes had been perfused throughout the protocol under normoglycaemic conditions with 5mM pyruvate, as a significant increase in contractile recovery by the end of 10 minutes of re-energisation was observed for both preconditioning times for all 3 metabolic substrates. This suggests the potential benefits of perfusing with elevated metabolic substrate concentrations prior to metabolic inhibition are maintained all the way through to re-energisation or impact so greatly during metabolic inhibition that they enable improved recovery by the end of re-energisation. The possible mechanisms for this could include slowed mitochondrial repolarisation, which may reduce mPTP opening. As functional mitochondria are essential to recovery of contractile function (Fralix *et al.*, 1992), and traditional IPC has been found to maintain functional mitochondria by preserving the mitochondrial membrane potential throughout the preceding ischaemic/reperfusion period, causing reduced ROS production; maintained mitochondrial ultrastructure, and preserved Cyt C levels within the mitochondria, which together reduces the open probability of mPTP and thus less apoptosis is stimulated (Quarrie *et al.*, 2012). It could be suggested metabolic preconditioning is also enabling preservation of the mitochondrial membrane potential and reducing opening of mPTP resulting in less cell death.

Improved ionic homeostasis prior to and during metabolic inhibition could play a role. This would be achieved by the elevated substrates maintaining activity of ATP-dependent transports and pumps such as the Na⁺/K⁺ ATPase and SERCA for longer during metabolic inhibition. This would prevent the Na⁺ accumulation and the subsequent acidosis and the preceding Ca²⁺ overload as previously mentioned (Section 3.3.2). This hypothesis would coincide with the belief that traditional IPC can improve the rate of glycolytic flux (Yabe *et al.*, 1997) and improve ATP production, therefore maintaining ATP dependent pumps/transporters and stimulate the actions outlined above (Van Emous *et al.*, 1998; Van Emous *et al.*, 2001; Fralix *et al.*, 1992; Xu *et al.*, 1995; Cross *et al.*, 1995). This suggests metabolic preconditioning may be stimulating similar pathways as traditional IPC.

Additionally, it cannot be ruled out that as the time prior to metabolic inhibition was extended in these experiments, glycogen stores may have been elevated in these experiments. This would increase the amount of glycolytic substrate available to the cardiomyocytes during metabolic inhibition, thus improving ionic homeostasis during metabolic inhibition, which could impact on re-energisation. The fructose data may be as a result of fructose activating MitoK_{ATP} as mentioned previously in section 3.3.4 stimulating pathways outlined for IPC in Figure 1.13. In terms of elevated pyruvate there could be an increase in NADH, as a result upon re-energisation oxidative phosphorylation would be stimulated, resulting in increased ATP production aiding improved contractile recovery. Increased stimulation of oxidative phosphorylation may be expected to also result in opening of mPTP, however the acidity related to pyruvate may prevent this and improve contractile recovery. Previous studies have shown traditional IPC is only achieved in pyruvate perfused hearts when the time length of the ischaemic insults is increased, suggesting pyruvate is resistance to a certain level of ischaemic damage (Sargent *et al.*, 1994). This suggests the improved contractile recovery observed with metabolic preconditioning could be due to pyruvate increasing the threshold to which ischaemic damage has to be reached to enable damage, this may be because pyruvate has its own protective effects such as ROS production, stimulating mPTP closure as discussed in section 4.3.2.2.

A previous study that used preconditioned isolated cardiomyocytes (preconditioning was achieved during isolation) that were then subjected to a similar metabolic inhibition/reperfusion protocol as in this study, showed that perfusion with 20mM glucose was detrimental to the cardiomyocytes compared to those perfused with 5mM glucose (in terms of a lower percentage recovery and increased hypercontracture). This effect was attributed to activation of PKC α and PKC β I, as once these were inhibited (with Gö6976 and tat-peptides) the detrimental effects were relieved (Sims *et al.*, 2014). This study suggests an elevated glucose concentration after IPC is detrimental and could have clinical relevance for those who suffer from angina and are more predisposed to an acute AMI. However the effect achieved with metabolic preconditioning within this study was on none preconditioned cardiomyocytes and could suggest a benefit for a short burst of 20mM glucose prior to metabolic inhibition.

5.3.1.2 Metabolic postconditioning appears to be cardioprotective

In the postconditioning experiments, cardiomyocytes were perfused with 20mM glucose and 5mM pyruvate upon re-energisation for either the whole 10 minutes or just the first 5 minutes. The timing was split, to try and identify if cardioprotection can be achieved within the first few critical minutes of re-energisation (Hausenloy *et al.*, 2003). Postconditioning had no effect on the percentage of 'non-hypercontracted' cardiomyocytes. This suggests elevating glucose solely upon re-energisation is not altering or improving $[Ca^{2+}]_i$ or NADH levels to a point where hypercontracture is affected in a negative or positive way, therefore there was no effect on the amount of non-hypercontracture. In order to achieve a higher percentage of 'non-hypercontracture', it could be suggested elevated metabolic substrates may need to be present either prior to metabolic inhibition and/or during re-energisation.

By the end of 10 minutes re-energisation, metabolic postconditioning (for both time durations) increased the percentage of contractile recovery. The postconditioning data suggests perfusing with elevated substrates upon re-energisation could be reducing re-energisation injury by increasing the ATP available to the cardiomyocytes. This would allow ATP-dependent pumps/transporters to re-establish activation rapidly,

restoring ionic homeostasis quickly thus preventing detrimental effects such as Ca^{2+} overload (Figure 3.20). Additionally these results suggest elevated glucose may only be required within the first few minutes of re-energisation to impart cardioprotection.

These results do not fit with the findings by Vanoverschelde *et al* (1994), who suggests there is no benefit upon reperfusion of perfusing with an increased level of glucose and/or insulin (10mM glucose and 140mU/l insulin) (Vanoverschelde *et al.*, 1994). This difference may be due to the reperfusion only being with 10mM glucose, while the post-ischaemic effect seen in this study is achieved via perfusion with 20mM glucose. The results in this study do coincide with the suggestions by Jeremy *et al* (1992 and 1993), that not only is an intact glycolytic pathway necessary upon re-energisation in order to achieve sufficient recovery but it is also essential during the early stages of reperfusion (Jeremy *et al.*, 1992 and Jeremy *et al.*, 1993). Therefore the results in this study suggest re-energisation with elevated glucose (even for just the initial stage) following a period of metabolic inhibition is essential to improving recovery.

Collectively the results in this chapter suggest there may be a role for metabolic pre/post-conditioning. These experiments identify a potential role for elevating metabolic substrates in the context of a simulated ischaemic/reperfusion injury protocol, which may be as effective as traditional IPC and IPostcon.

CHAPTER 6

GENERAL DISCUSSION

6. General Discussion

The overall aim of this project was to investigate the response of isolated ventricular cardiomyocytes to acute changes in metabolic substrates, while being subjected to a simulated ischaemia/reperfusion injury protocol. Due to previous studies focusing primarily on the whole heart, a simulated ischaemic/reperfusion injury was used to investigate the potential cellular effects.

In particular previous studies have postulated that perfusion with elevated glucose limits ischaemic damage, possibly due to anaerobic glycolytic metabolism being able to maintain ATP production during the period of ischaemia. Therefore the potential cellular benefits of increasing the availability of the glycolytic substrates, glucose and fructose (prior to and following a period of metabolic inhibition) were investigated (Chapter 3). From these investigations, it was observed that normoglycaemic and hyperglycaemic conditions provided different outcomes to the cardiomyocytes. Therefore as oxidative phosphorylation plays a key role in generating ATP prior to and after ischaemia, the effect of altering substrates related to oxidative phosphorylation were assessed by altering the concentration of pyruvate and adding octanoate to the perfusate (Chapter 4). Based on these studies and the suggestions that cardioprotection observed with ischaemic conditioning may involve metabolism, hypotheses were made as to whether the cardioprotection elicited by traditional IPC/IPostcon could be replicated as a type of metabolic conditioning in isolated cardiomyocytes by perfusion with certain metabolic substrates/concentrations (that achieved cardioprotection in chapter 3 and 4) either prior to (preconditioning) or after (postconditioning) the period of “ischaemia” (Chapter 5).

6.1 The impact of elevating glycolytic substrates at a cellular level

Numerous whole heart studies have identified the cardioprotective benefits of elevated glucose at the time of ischaemia (Bricknell & Opie, 1978; Vanoverschelde *et al.*, 1994; Wang *et al.*, 2005; Owen *et al.*, 1990; Jeremy *et al.*, 1993), with many of them suggesting the protection observed is in relation to maintained glycolytic metabolism during the period of ischaemia.

The data from this investigation coincides with their suggestions that elevated concentrations of glycolytic substrates are cardioprotective. Cardioprotection was achieved by perfusing isolated cardiomyocytes with an elevated glucose/fructose concentration (in particular 20mM glucose). The advantage of using a simulated “ischaemia/reperfusion” protocol is that the impact of elevating these substrates at a cellular level can be investigated. Elevated glucose concentrations delay several of the parameters which occur during ischaemia (i.e. contractile failure and rigor). These delays are postulated to be due to maintained glycolytic ATP production during metabolic inhibition, with maintenance at a greater level with 20mM glucose.

This study was able to link the delay in contractile failure with a delay in action potential failure and a delay in SarcK_{ATP} channel opening which importantly is showing what effect in particular 20mM glucose is having at a cellular level. The delays in these parameters, as previously discussed in section 3.3.1 are believed to be due to several of the glycolytic enzymes being closely associated with the sarcolemmal membrane and SR (Dhar-Chowdhury *et al.*, 2005; Jovanovic *et al.*, 2005; Hong *et al.*, 2011; Xu *et al.*, 1995; Pierce & Philipson, 1985), which means the continued anaerobic glycolysis ATP production is within close proximity to the specific areas which rely on ATP for function or regulation.

The suggestion that the ATP delaying opening of the SarcK_{ATP} channels is from the maintained glycolytic ATP production is in finding with other studies that show glycolytic ATP maintains their closure. The Mg²⁺-Green fluorescence data further indicates that ATP production is maintained with elevated glucose.

The preferential use of glycolytic ATP at specific locations has given foundation to the belief that glycolytic ATP is crucial to maintaining function and prevents ischaemic injury by maintaining activity of Na⁺/K⁺ ATPase during ischaemia, leading to reduced [Na⁺]_i, which prevents the NCX from working in reverse therefore preventing the accumulation of [Ca²⁺]_i (Van Emous *et al.*, 2001; Cross *et al.*, 1995; Dizon *et al.*, 1998). Increased ATP also maintains SERCA activity and therefore supports maintained Ca²⁺ homeostasis not only during ischaemia but also upon re-energisation (Xu *et al.*, 1995; Kockskamper *et al.*, 2005; Zima *et al.*, 2006). The benefits of this then have implication

upon re-energisation in that the ionic homeostasis is not disrupted and recommended glycolytic ATP production stimulates activity of these ATP-dependent pumps/transporters again aiding recovery. The ability of elevated glucose (20mM glucose) to maintain ATP production and as a result delay ATP depletion at a crucial location within the cardiomyocytes and therefore prevent “ischaemic injury” during metabolic inhibition is indicated in this study by an improvement in contractile recovery and Ca^{2+} transients upon re-energisation. Further work is required to determine if any of the ATP-dependent pumps/transporters (i.e. Na^+/K^+ ATPase) are maintaining activity for longer during ischaemia due to the elevated glucose.

Functional mitochondria are essential to the recovery of contractile function, as inhibiting glucose oxidation with cyanide prevents contractile recovery in glucose perfused hearts (Fralix *et al.*, 1992). At 20mM glucose there is a suggestion that glycolytic ATP recommences before mitochondrial ATP production, giving rise to increased “non-hypercontracture”. As mitochondrial repolarisation may play a role in this upon re-energisation, which can affect the outcome of the cardiomyocytes further studies to investigate the mitochondrial membrane potential could be measured using the dye tetramethyl rhodamine ethyl ester (TMRE). In addition it is proposed the activity of the mPTP is also affected, not only with glycolytic substrates but also by metabolic substrates for oxidative phosphorylation, therefore it would be interesting to investigate mPTP activity (using the fluorescent dye tetramethyl rhodamine methyl ester (TMRM)) with different glycolytic substrate concentration through the simulated “ischaemic/reperfusion” protocol.

There may be a potential role for glycogen within the experiments, as previous studies have suggested a role for glycogen but to establish if glycogen was playing a role in this study, more experiments would be required.

In conclusion these results suggest elevating glucose/ fructose at a cellular level is cardioprotective. However due to there being a strong association with hyperglycaemia having an adverse outcome on AMI, the experiments in chapter 5 could establish if a “burst” of an elevated concentration of a glycolytic substrates would be applicable.

6.2 Does oxidative phosphorylation impact on the glycolytic effect?

In terms of the data presented here, there is an indication that pyruvate (prior to metabolic inhibition) may impact on the effect of glycolytic ATP's ability to delay contractile failure and rigor. As reducing pyruvate to a physiological concentration resulted in these two parameters occurring earlier than when pyruvate was perfused at 5mM. In terms of the contractile failure, it is proposed that this may be due to a decrease in PCr, so less ATP is available to be transferred to the myofibrils, which links in with previous studies that suggest early contractile failure is linked to a decrease in PCr rather than ATP (Allen & Orchard, 1987; Rauch *et al.*, 1994; Cross *et al.*, 1995; Kingsley *et al.*, 1991). This could indicate more research is required in the field as many experiments are carried out at a physiological pyruvate concentration.

The early time to rigor development implies a role for mitochondria ATP in preventing development, which links in with previous findings (Veksler *et al.*, 1997) but disagrees with other suggestions that it relies on glycolytic ATP (Bricknell *et al.*, 1981; Owen *et al.*, 1990; Cross *et al.*, 1995; Kingsley *et al.*, 1999). Therefore it raises questions as to whether this discrepancy is related to this investigation being based on a cellular level rather than a whole heart, or it could suggest both pathways are involved or that at a cellular level rigor development is very much dependent on what substrate is available.

The idea that glycolytic ATP is responsible for maintaining activity of several glycolytic ATP dependent pumps/transporters at the sarcolemmal membrane is not hindered, as the action potential failure time and $\text{Sarck}_{\text{ATP}}$ activation time was unaffected by reducing pyruvate. These observations support the idea that glycolytic ATP dominates at these locations. Evidence from these studies, also suggests contractile recovery relies predominantly on the availability of glycolytic ATP, as no changes in contractile recovery levels were observed.

Previous studies have shown elevating pyruvate is also cardioprotective (Kerr *et al.*, 1999; Flood *et al.*, 2003), the findings in this study suggest that in isolated cardiomyocytes this cardioprotective effect is only additional in the presence of normoglycaemic concentrations. This could indicate that elevating pyruvate alone

under normoglycaemic conditions is enough to provide cardioprotection. At an elevated glucose concentration, the addition of pyruvate had no effect but from these studies it is unclear as to whether it is the elevated glucose concentration or the elevated pyruvate concentration having the effect.

Octanoate had a detrimental effect on the recovery of isolated cardiomyocytes, particular when associated with a hyperglycaemic glucose concentration. This may indicate that upon re-energisation glycolysis and glucose oxidation were uncoupled resulting in reperfusion injury, which coincides with previous fatty acid studies (Longnus *et al.*, 2001; Lopaschuk *et al.*, 1993; Lopaschuk *et al.*, 1990; Johnston & Lewandowski, 1991). The exact mechanisms behind the damage caused by octanoate were not investigated but it is proposed it could involve inhibition of PDH and/or PFK-1 (Longnus *et al.*, 2001; Lopaschuk *et al.*, 1990; Neely *et al.*, 1972; Lopaschuk *et al.*, 1993). In relation to the hypothesis that PDH was involved a known stimulant of PDH, pyruvate was added but this did not improve recovery significantly, suggesting at a cellular level 5mM pyruvate does not stimulate PDH “enough”.

In conclusion this chapter shows that metabolic substrates related to oxidative phosphorylation can alter the response of isolated cardiomyocytes to a simulated “ischaemic/reperfusion” injury protocol.

6.3 Can metabolic pre/postconditioning replicate traditional ischaemic conditioning?

As the mechanisms behind both traditional IPC and Ipostcon are believed to involve metabolism/metabolic substrates and previous findings within this study suggest elevating substrates is cardioprotective, this study aimed to investigate for the first time if metabolic preconditioning and postconditioning could be achieved in isolated cardiomyocytes and identify what may be happening at a cellular level. These experiments were designed to address the gap in the literature, as the literature does not fully investigate metabolic pre/postconditioning in isolated cardiomyocytes.

Interestingly metabolic preconditioning not only improved contractile recovery, but from the data it is suggested preconditioning for 5 minutes can elicit cardioprotection,

suggesting a short period of elevated substrates prior to metabolic inhibition can limit ischaemic injury.

Not only is it suggested metabolic preconditioning may be stimulating similar pathways as traditional IPC (i.e. preserving mitochondrial membrane potential (Quarrie *et al.*, 2012) and improving glycolytic flux (Yabe *et al.*, 1997) and therefore maintaining glycolytic ATP production), but it could also be stimulating pathways as outlined in previous chapters (i.e. improving glycogen stores).

The discrepancy with some of the 15 minute data suggest further studies are required to establish exactly by which mechanisms metabolic preconditioning may be working, to identify whether different duration of preconditioning activates different pathways and could help identify the best/shortest preconditioning time required to achieve cardioprotection.

The postconditioning protocols reveal that re-energisation with an elevated glucose concentration is cardioprotective to isolated cardiomyocytes although no immediate impact upon re-energisation (i.e. no reduction in non-hypercontracture) was observed, which could suggest the benefit needs to come prior to re-energisation (i.e. need more reduction in ischaemic damage) in order to prevent hypercontracture. The postconditioning period does indicate though that the metabolic postconditioning period need only be 5 minutes. This could also indicate that cardioprotection can be achieved by manipulating the first half of re-energisation and that the initial few minutes of re-energisation are critical, therefore being able to manipulate this time with different substrates may preventing injury.

These metabolic preconditioning experiments help to address the gaps in the literature and provide a novel insight as to whether a simple increase in a metabolic substrate concentration at a cellular level, either prior to or after a period of ischemia maybe beneficial by providing a burst of “energy”. In addition these pre/postconditioning could allow improved protocols to combat ischaemic damage, also gives the possibility that re-energisation injury can be prevented simply with a short burst of elevated glucose upon re-energisation. Caution is needed though as the clinical administration of this directly to the heart may be difficult.

6.4 Clinical implications

Following an AMI the most effective way to limit ischaemic injury and improve prognosis is to restore blood flow to the ischaemic myocardium. In a clinical setting this is achieved by revascularisation, either by thrombolytic treatment or primary percutaneous coronary intervention (PCI) (coronary angioplasty), and very rarely in the acute setting by coronary artery bypass (CAB) surgery. Of these PCI (with or without a stent) is preferentially and most commonly used, as outcomes are better than with thrombolysis. However even after successful revascularisation, a no-flow phenomenon can occur, where blood flow to the ischaemic tissue is still impaired due to changes to the microvasculature. This can result in the re-occurrence of an elevation in the ST segment (Iwakura *et al.*, 2001; Rezkalla & Kloner, 2002).

Individuals presenting with hyperglycaemia at the time of AMI have been found to be more at risk of this no-flow phenomenon and as a result have re-elevations in the ST segment (Iwakura *et al.*, 2001). This could relate to changes in the endothelium, as hyperglycaemia can stimulate increases in AGEs, free radicals, oxidative stress, fatty acid oxidation and PKC activity, while inhibiting nitric oxide production, all of which contribute to the formation of endothelial dysfunction (Brownlee, 2005; Highlander & Shaw, 2010). The risk of no reflow possibly as a result of endothelial dysfunction, could relate to findings that individuals who present with hyperglycaemia at the time of AMI, or who have persistent hyperglycaemia following the event, are more likely to have adverse outcomes and a poor prognosis (increased short and long term mortality rates). It has also been found that the association of admission hyperglycaemic, with adverse outcome after AMI is irrespective of the prior diabetes status of the individual patient (Goyal *et al.*, 2006; Squire *et al.*, 2009; Svensson *et al.*, 2005; Kosiborod *et al.*, 2005).

Hypoglycaemia in the first few days after AMI, and episodes of hypoglycaemia in coronary heart disease, have also been seen as markers of possible future ischaemic damage and associated with symptoms of cardiac ischaemia and poor prognosis following an AMI. In a clinical setting it would be advantageous to prevent hypoglycaemic episodes (Svensson *et al.*, 2005; Desouza *et al.*, 2003).

From a clinical perspective both hyperglycaemia and hypoglycaemia are detrimental at the time of AMI and that glycaemic control may improve prognosis. In this study acutely perfusing with a hypoglycaemic glucose concentration resulted in a low percentage recovery following the metabolic inhibition and re-energisation protocol. Whereas acutely perfusing with hyperglycaemic glucose concentrations resulted in a cardioprotective phenotype which contradicts the clinical aspects. This contradiction may be due to this study model involving only isolated cardiomyocytes therefore there is a lack of vasculature structure (i.e. endothelium). The fatty acid experiments showed that upon re-energisation under hyperglycaemic conditions fatty acids are detrimental, which more closely resembles what would happen in a clinical setting, however free fatty acid levels are not measured upon admission with AMI, and the fatty acid level associated with a myocardial infarction or uncontrolled diabetes is elevated compared to the concentration used in this study (Lopaschuk *et al.*, 2010). In addition many of the diabetic human and animal studies related to chronic conditions, while this study only investigated acute conditions. Therefore it is possible that the difference seen between our study and those in a clinical setting and in diabetic animals is a result of a difference in model and conditions.

6.5 Study limitations

6.5.1 Isolated with 10mM glucose

In this study adult rat ventricular cardiomyocytes were isolated and maintained until use in Tyrode solution containing 10mM glucose. As 10mM glucose is within the hyperglycaemic glucose concentration range, it cannot be ruled out that this glucose concentration within the Tyrode solution is possibly impacting on the cardiomyocytes until use, in terms of ATP and or glycogen levels prior to experimental use. One group has suggested that in order to investigate changes in glucose concentrations, cardiomyocytes should be isolated at 5mM glucose (Bell *et al.*, 2011). This is due to the standard glucose concentration used for isolations being within the diabetic range and the concerns that higher glucose concentration may cause pathophysiological conditions. However numerous studies referenced within this thesis, that investigate the effects of metabolic substrates (including glucose) isolate at 10/11mM glucose,

they may use glucose due to a lack of alternative energy supply in the perfusate, in addition the impact of glucose on the heart may not have previously been associated with pathophysiology. In this study to try and minimise the potential effect of 10mM glucose, a control experiment of 5mM glucose was always carried out first each day, to verify cardiomyocyte conditions as the day progressed; another control of 5mM glucose should have been carried out at the end of the day. Following the control, experiments were then carried out in a random order, so that all experiments of one concentration were not carried out on the same day or at the same time of day. There was no evidence to suggest that the cardiomyocyte behaved differently between am and pm. Data presented in this thesis suggests that, as there were differences in a number of the markers of ischaemic and re-energisation injury between the glucose concentrations of 5-30mM, isolation and maintenance of cardiomyocytes 10mM glucose may be having little impact on the results.

6.5.2 Improving the measurement of contractile viability

At the end of the metabolic inhibition and re-energisation protocol in the contractile function experiments, recovery was marked as the percentage of cardiomyocytes regaining contractile function in time with EFS. As a more accurate measurement of contractile viability, a hypotonic solution containing Trypan blue could have been perfused on at the end of each experiment (Turrell *et al.*, 2011). This would induce mechanical stress and as Trypan blue is selectively taken up by cardiomyocytes which have permeable membranes (i.e. those that have undergone necrotic injury) a more reliable conformation of cardiomyocyte viability could be taken at the end of the 10 minutes of re-energisation.

6.5.3 Defining SarcK_{ATP} channel activation

Using patch clamp electrophysiology recording, whole-cell configuration was used to detect activation of the SarcK_{ATP} channels, in this configuration dialysis would occur which could have a significant effect on the results by altering ion channel activity, as the intracellular pipette solution would become continuous with the cytosolic solution. For example EGTA in the intracellular solution would buffer any changes in $[Ca^{2+}]_i$, while the presence of ATP/ADP could change the [ATP]/[ADP] ratio, these nucleotides

could also be lost, which would impact on the SarcK_{ATP} channels. This could explain the difference seen in the time to SarcK_{ATP} channel activation under hyperglycaemic conditions when in the cell-attached configuration verse whole-cell configuration. In addition in the cell-attached configuration, the cardiomyocytes would be using less ATP due to them being fairly quiescent. Cell-attached configuration experiments were performed to further identify if the channel being recorded was SarcK_{ATP}, as the cell-attached configuration allows the conductance of the channel to be measured. By measuring the conductance of the single channels being recorded, these can be compared to previously published values for channels containing the Kir6.2 subunit and could indicate the channel being recorded is SarcK_{ATP}. Cell attached experiments, rather than pharmacological inhibition experiments were carried out due to pharmacological inhibitors of SarcK_{ATP} (such as Glibenclamide (which is also not selective and therefore cannot distinguish between SarcK_{ATP} and MitoK_{ATP} channels), Glimepiride and HMR1098), have been demonstrated to be ineffective during metabolic inhibition due to an increase in intracellular ADP (Findlay, 1993; Lawrence *et al.*, 2002; Rainbow *et al.*, 2005).

6.5.4 Modification of the Mg²⁺-Green experiments

The Mg²⁺-Green experiments in this study were carried out in quiescent (non-contracting) cardiomyocytes (compared to all other full metabolic inhibition and re-energisation experiments), this was to help prevent movement artefacts as this is a non-ratiometric dye, which means it is sensitive to movement and changes in cell shape, particularly during rigor and hypercontracture. This means that in these cardiomyocytes if changes in shape occur, where for instance the cardiomyocyte contracts and shortens in cell length, there would be a concentrated pool of the dye within the focal plane which results in an increase in fluorescence but would not represent changes in Mg²⁺. In quiescent cardiomyocytes ATP is used at a slower rate, resulting in conditions that do not perfectly match previous experiments, i.e. limited ATP hydrolysis which could give an inaccurate depletion of ATP throughout the protocol. Therefore we are aware that the Mg²⁺-Green experiments within this study can only give an accurate interpretation of changes in ATP within the same cardiomyocyte but not between cardiomyocytes. Quiescent cardiomyocytes also

means contractile recovery could not be measured, therefore in future Mg^{2+} -Green experiments, the cardiomyocytes would be stimulated to contract via EFS, during the initial period of perfusion with Tyrode before metabolic inhibition, and the contracting cardiomyocytes marked. Then at the end of the re-energisation, the cardiomyocytes would be stimulated again, and it would be noted which of the original contracting cardiomyocytes had been able to recover contraction. From this a clear observation of the Mg^{2+} -Green fluorescence against those that either did or did not recover contraction could be achieved.

6.5.5 Limited fatty acid concentration

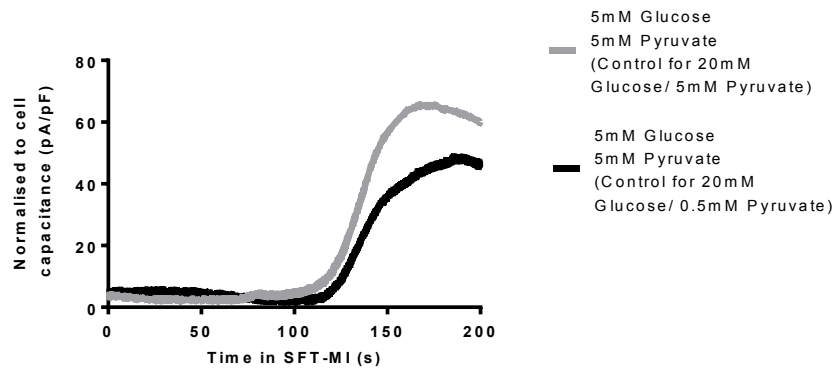
During diabetes and following an AMI, circulating fatty acid levels can be elevated to concentrations $>2\text{mM}$ (Lopaschuk *et al.*, 2010), which can be detrimental to the myocardium during reperfusion. Initially in this study, cardiomyocytes were perfused with an elevated octanoate concentration of 2.4mM , this concentration prevented contraction with EFS therefore we chose to use octanoate in all fatty acid experiments at a physiological concentration of 0.5mM .

6.6 Overall conclusion

The data in this thesis has demonstrated that perfusing with elevated metabolic substrates (glucose, fructose and pyruvate) imparts a metabolic dependent cardioprotection in isolated cardiomyocytes when subjected to a metabolic inhibition and re-energisation protocol. This cardioprotection is altered during metabolic inhibition or re-energisation depending on the concentration of the oxidative phosphorylation metabolic substrate pyruvate and is completely abrogated by the addition of octanoate to the perfusate. This cardioprotection was also replicated by metabolic pre/postconditioning with glucose, fructose or pyruvate at elevated concentrations. As this study considered changes in multiple substrates at once, which gives a more realistic idea of physiological conditions, it does lead to problems in distinguishing the actions of specific metabolic substrates. Therefore further investigations would be needed to identify precise mechanisms which confer this cardioprotection and whether distinct regulation of specific enzymes such as PFK-1 and PDH or ATP dependent pumps/transporters such as Na^+/K^+ ATPase are involved.

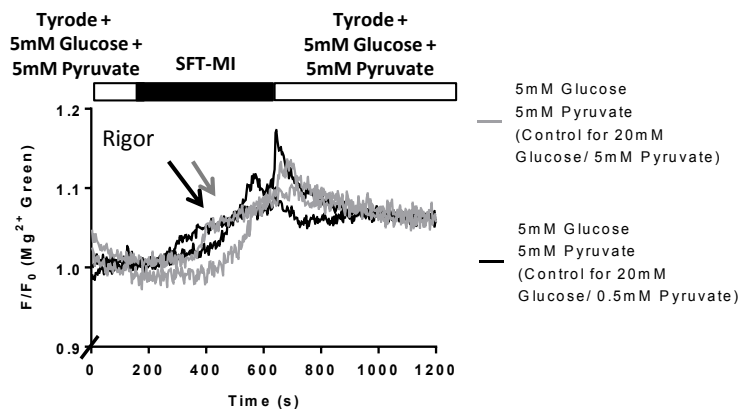
However from the $\text{SarcK}_{\text{ATP}}$ and Mg^{2+} -Green data it is strongly suggested that ATP levels within the cardiomyocytes during metabolic inhibition and re-energisation are principally involved. The ATP is believed to be derived from anaerobic glycolysis, with oxidative phosphorylation contributing to the ATP levels prior to metabolic inhibition and during re-energisation. It could be proposed that increases in glycogen stores may play a role during metabolic inhibition. Depending on the metabolic substrate, difference in mitochondrial depolarisation during metabolic inhibition and repolarisation during re-energisation may also be involved.

Appendix



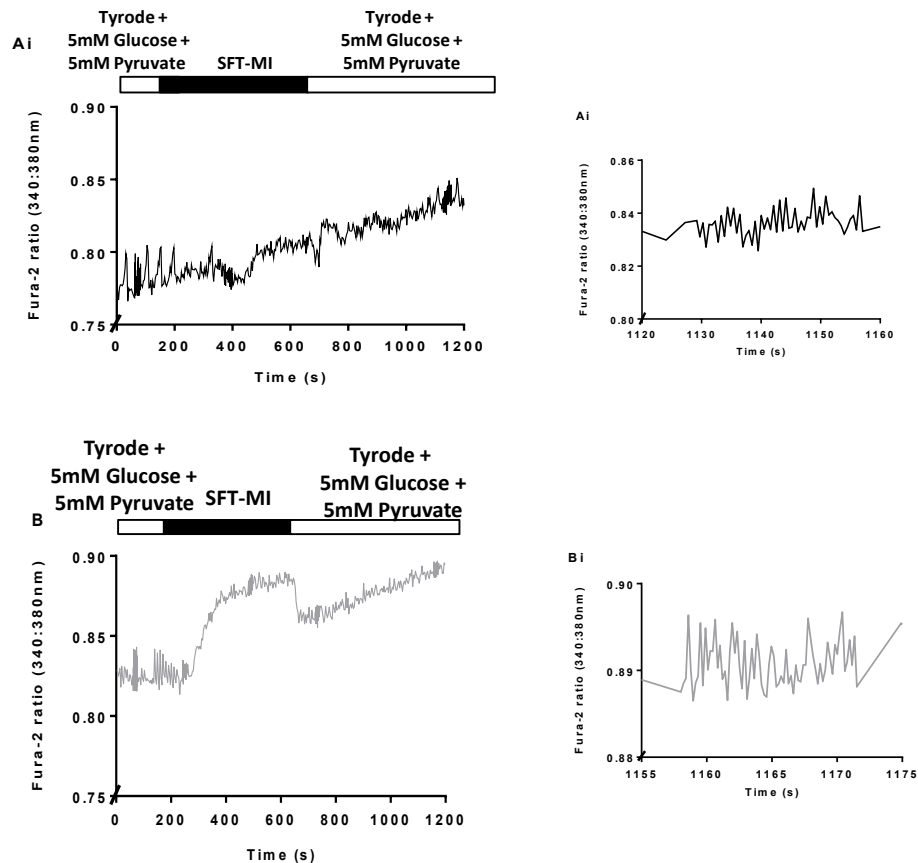
Appendix Figure 1 The control $\text{SarCK}_{\text{ATP}}$ current traces recorded during metabolic inhibition.

Example of control $\text{SarCK}_{\text{ATP}}$ traces recorded from cardiomyocyte pre-incubated in 5mM glucose with 5mM pyruvate, prior to superfusion with metabolic inhibition. One trace represents the control recorded on the same day as perfused with 20mM glucose and 5mM pyruvate (grey trace) and the other represents the control recorded on the same day as perfused with 20mM glucose and 0.5mM pyruvate (black trace). Each trace was normalised to the cell capacitance. Time to the $\text{SarCK}_{\text{ATP}}$ current activation during SFT-MI was measured at the point at which the basal outward current had increased by 20pA.



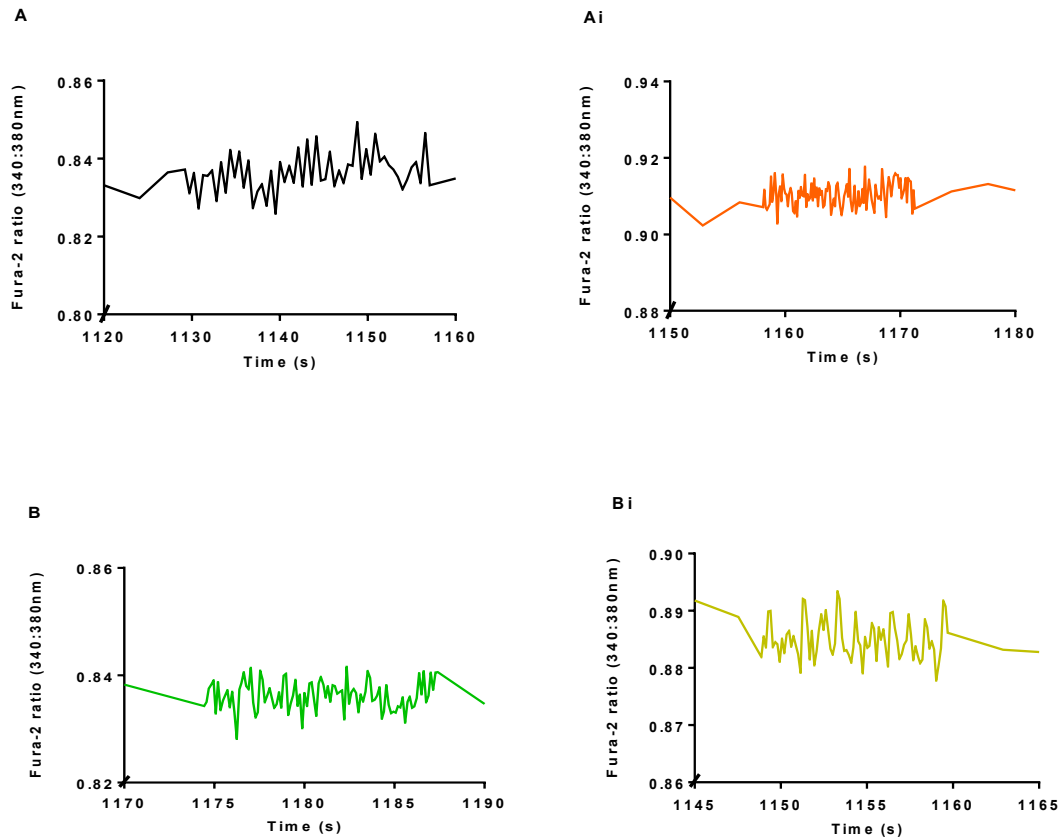
Appendix Figure 2 The control Mg^{2+} -Green fluorescence recordings during metabolic inhibition and re-energisation in response to acute changes in extracellular glucose.

Example traces showing the time course of changes in Mg^{2+} -Green fluorescence for cardiomyocytes perfused with 5mM glucose and 5mM pyruvate, prior to metabolic inhibition and during re-energisation. Two trace represents the control recorded on the same day as perfused with 20mM glucose and 5mM pyruvate (grey trace) and the other two represent the control recorded on the same day as perfused with 20mM glucose and 0.5mM pyruvate (black trace). In the trace the expected times for the development of rigor are indicated by arrows.



Appendix Figure 3 The control Fura-2 ratios recording during metabolic inhibition and re-energisation.

- (A) Example control trace recording of the Fura-2 ratio (340:380nm) for a cardiomyocyte exposed to 5mM and 5mM pyruvate glucose prior to metabolic inhibition and during re-energisation recorded on the same day as perfused with 20mM glucose and 0.5mM pyruvate (black trace)
- (Ai) A zoomed in areas of (A) showing the Fura-2 ratio (340:380nm) near to the end of re-energisation to illustrate the Ca^{2+} transient which would be used to determine recovery.
- (B) Example control trace recording of the Fura-2 ratio (340:380nm) for a cardiomyocyte exposed to 5mM and 5mM pyruvate glucose prior to metabolic inhibition and during re-energisation recorded on the same day as perfused with 20mM glucose and 5mM pyruvate (grey trace).
- (Bi) A zoomed in areas of (B) showing the Fura-2 ratio (340:380nm) near to the end of re-energisation to illustrate the Ca^{2+} transient which would be used to determine recovery.



Appendix Figure 4 The Ca²⁺ transient captured at the end of re-energisation for those cardiomyocytes perfused with either 5mM or 20mM glucose in combination with either 5mM or 0.5mM pyruvate.

- (A) Example trace recording showing the Fura-2 ratio (340:380nm) near to the end of re-energisation to illustrate the Ca²⁺ transient which would be used to determine recovery for a cardiomyocyte exposed to 5mM glucose and 5mM pyruvate prior to metabolic inhibition and during re-energisation.
- (Ai) Example trace recording showing the Fura-2 ratio (340:380nm) near to the end of re-energisation to illustrate the Ca²⁺ transient which would be used to determine recovery for a cardiomyocyte exposed to 5mM glucose and 0.5mM pyruvate prior to metabolic inhibition and during re-energisation.
- (B) Example trace recording showing the Fura-2 ratio (340:380nm) near to the end of re-energisation to illustrate the Ca²⁺ transient which would be used to determine recovery for a cardiomyocyte exposed to 20mM glucose and 5mM pyruvate prior to metabolic inhibition and during re-energisation.
- (Bi) Example trace recording showing the Fura-2 ratio (340:380nm) near to the end of re-energisation to illustrate the Ca²⁺ transient which would be used to determine recovery for a cardiomyocyte exposed to 20mM glucose and 0.5mM pyruvate prior to metabolic inhibition and during re-energisation.

REFERENCES

- Acehan, D., Jiang, X., Morgan, D.G., Heuser, J.E., Wang, X., Akey, C.W., 2002. Three-dimensional structure of the apoptosome: implications for assembly, procaspase-9 binding, and activation. *Molecular Cell*. 9, 423-432.
- Aerni-Flessner, L., Abi-Jaoude, M., Koenig, A., Payne, M., Hruz, P.W., 2012. GLUT4, GLUT1, and GLUT8 are the dominant GLUT transcripts expressed in the murine left ventricle. *Cardiovascular Diabetology*. 11, 63.
- Allen, D.G. & Orchard, C.H., 1987. Myocardial contractile function during ischemia and hypoxia. *Circulation Research*. 60, 153-168.
- Arya, D.S., Bansal, P., Ojha, S.K., Nandave, M., Mohanty, I., Gupta, S.K., 2006. Pyruvate provides cardioprotection in the experimental model of myocardial ischemic reperfusion injury. *Life Sciences*. 79, 38-44.
- Auchampach, J.A., Grover, G.J., Gross, G.J., 1992. Blockade of ischaemic preconditioning in dogs by the novel ATP dependent potassium channel antagonist sodium 5-hydroxydecanoate. *Cardiovascular Research*. 26, 1054-1062.
- Augustus, A.S., Kako, Y., Yagyu, H., Goldberg, I.J., 2003. Routes of FA delivery to cardiac muscle: modulation of lipoprotein lipolysis alters uptake of TG-derived FA. *American Journal of Physiology. Endocrinology and Metabolism*. 284, E331-9.
- Backer, J.M., Myers, M.G., Jr, Shoelson, S.E., Chin, D.J., Sun, X.J., Miralpeix, M., Hu, P., Margolis, B., Skolnik, E.Y., Schlessinger, J., 1992. Phosphatidylinositol 3'-kinase is activated by association with IRS-1 during insulin stimulation. *The EMBO Journal*. 11, 3469-3479.
- Baczko, I., Giles, W.R., Light, P.E., 2004. Pharmacological activation of plasma-membrane KATP channels reduces reoxygenation-induced Ca(2+) overload in cardiac myocytes via modulation of the diastolic membrane potential. *British Journal of Pharmacology*. 141, 1059-1067.
- Bais, R., James, H.M., Roife, A.M. and Conyers, R.A., 1985. 'The purification and properties of human liver ketohexokinase. A role for ketohexokinase and fructose-bisphosphate aldolase in the metabolic production of oxalate from xylitol', *The Biochemical journal*, 230(1), 53-60.
- Banerjee, S.K., McGaffin, K.R., Pastor-Soler, N.M., Ahmad, F., 2009. SGLT1 is a novel cardiac glucose transporter that is perturbed in disease states. *Cardiovascular Research*. 84, 111-118.
- Bell, R.M., Mocanu, M.M., Yellon, D.M., 2011. Retrograde heart perfusion: the Langendorff technique of isolated heart perfusion. *Journal of Molecular and Cellular Cardiology*. 50, 940-950.

Benzi, R.H. & Lerch, R., 1992. Dissociation between contractile function and oxidative metabolism in postischemic myocardium. Attenuation by ruthenium red administered during reperfusion. *Circulation Research*. 71, 567-576.

Berg, J.M., Tymoczko, J.L. and Stryer, L., 2007. *Biochemistry*. Sixth edition ed. United States of America: W.H. Freeman and company.

Bers, D.M., 2002. Cardiac excitation-contraction coupling. *Nature*. 415, 198-205.

Bers, D.M., 2001. *Excitation-contraction coupling and cardiac contractile force*. 2nd edn ed. Dordrecht; The Netherlands: Kluwer Academic.

Binas, B., Danneberg, H., McWhir, J., Mullins, L., Clark, A.J., 1999. Requirement for the heart-type fatty acid binding protein in cardiac fatty acid utilization. *FASEB Journal : Official Publication of the Federation of American Societies for Experimental Biology*. 13, 805-812.

Blanchette-Mackie, E.J., Masuno, H., Dwyer, N.K., Olivecrona, T., Scow, R.O., 1989. Lipoprotein lipase in myocytes and capillary endothelium of heart: immunocytochemical study. *The American Journal of Physiology*. 256, E818-28.

Bolli, R., Li, Q.H., Tang, X.L., Guo, Y., Xuan, Y.T., Rokosh, G., Dawn, B., 2007. The late phase of preconditioning and its natural clinical application--gene therapy. *Heart Failure Reviews*. 12, 189-199.

Bowers, K.C., Allshire, A.P., Cobbold, P.H., 1993. Continuous measurements of cytoplasmic ATP in single cardiomyocytes during simulation of the "oxygen paradox". *Cardiovascular Research*. 27, 1836-1839.

Boyett, M.R., 2009. 'And the beat goes on.' The cardiac conduction system: the wiring system of the heart. *Experimental Physiology*. 94, 1035-1049.

Brennan, S., Jackson, R., Patel, M., Sims, M.W., Hudman, D., Norman, R.I., Lodwick, D. and Rainbow, R.D., 2015. 'Early opening of sarcolemmal ATP-sensitive potassium channels is not a key step in PKC-mediated cardioprotection', *Journal of Molecular and Cellular Cardiology*, 79, 42-53.

Bricknell, O.L., Daries, P.S., Opie, L.H., 1981. A relationship between adenosine triphosphate, glycolysis and ischaemic contracture in the isolated rat heart. *Journal of Molecular and Cellular Cardiology*. 13, 941-945.

Bricknell, O.L. & Opie, L.H., 1978. Effects of substrates on tissue metabolic changes in the isolated rat heart during underperfusion and on release of lactate dehydrogenase and arrhythmias during reperfusion. *Circulation Research*. 43, 102-115.

Brownlee, M., 2005. The pathobiology of diabetic complications: a unifying mechanism. *Diabetes*. 54, 1615-1625.

- Buja, L.M., 2005. Myocardial ischemia and reperfusion injury. *Cardiovascular Pathology : The Official Journal of the Society for Cardiovascular Pathology*. 14, 170-175.
- Burant, C.F., Takeda, J., Brot-Laroche, E., Bell, G.I., Davidson, N.O., 1992. Fructose transporter in human spermatozoa and small intestine is GLUT5. *The Journal of Biological Chemistry*. 267, 14523-14526.
- Camello-Almaraz, C., Gomez-Pinilla, P.J., Pozo, M.J., Camello, P.J., 2006. Mitochondrial reactive oxygen species and Ca²⁺ signaling. *American Journal of Physiology. Cell Physiology*. 291, C1082-8.
- Cannell, M.B. & Kong, C.H., 2012. Local control in cardiac E-C coupling. *Journal of Molecular and Cellular Cardiology*. 52, 298-303.
- Cardone, M.H., Roy, N., Stennicke, H.R., Salvesen, G.S., Franke, T.F., Stanbridge, E., Frisch, S., Reed, J.C., 1998. Regulation of cell death protease caspase-9 by phosphorylation. *Science (New York, N.Y.)*. 282, 1318-1321.
- Cavallini, L., Valente, M., Rigobello, M.P., 1990. The protective action of pyruvate on recovery of ischemic rat heart: comparison with other oxidizable substrates. *Journal of Molecular and Cellular Cardiology*. 22, 143-154.
- Cave, A.C., Ingwall, J.S., Friedrich, J., Liao, R., Saupe, K.W., Apstein, C.S., Eberli, F.R., 2000. ATP synthesis during low-flow ischemia: influence of increased glycolytic substrate. *Circulation*. 101, 2090-2096.
- Cheng, H., Lederer, W.J., Cannell, M.B., 1993. Calcium sparks: elementary events underlying excitation-contraction coupling in heart muscle. *Science (New York, N.Y.)*. 262, 740-744.
- Cheung, M.M., Kharbanda, R.K., Konstantinov, I.E., Shimizu, M., Frndova, H., Li, J., Holtby, H.M., Cox, P.N., Smallhorn, J.F., Van Arsdel, G.S., Redington, A.N., 2006. Randomized controlled trial of the effects of remote ischemic preconditioning on children undergoing cardiac surgery: first clinical application in humans. *Journal of the American College of Cardiology*. 47, 2277-2282.
- Cittadini, A., Galeotti, T., Terranova, T., 1971. The effect of pyruvate on cyanide-inhibited respiration in intact ascites tumor cells. *Experientia*. 27, 633-635.
- Cleveland, J.C., Jr, Meldrum, D.R., Cain, B.S., Banerjee, A., Harken, A.H., 1997. Oral sulfonylurea hypoglycemic agents prevent ischemic preconditioning in human myocardium. Two paradoxes revisited. *Circulation*. 96, 29-32.
- Cole, W.C., McPherson, C.D., Sontag, D., 1991. ATP-regulated K⁺ channels protect the myocardium against ischemia/reperfusion damage. *Circulation Research*. 69, 571-581.

- Cong, L.N., Chen, H., Li, Y., Zhou, L., McGibbon, M.A., Taylor, S.I., Quon, M.J., 1997. Physiological role of Akt in insulin-stimulated translocation of GLUT4 in transfected rat adipose cells. *Molecular Endocrinology (Baltimore, Md.)*. 11, 1881-1890.
- Cook, G.C., 1971. Absorption and metabolism of D(--) fructose in man. *The American Journal of Clinical Nutrition*. 24, 1302-1307.
- Correa, F., Garcia, N., Gallardo-Perez, J., Carreno-Fuentes, L., Rodriguez-Enriquez, S., Marin-Hernandez, A., Zazueta, C., 2008. Post-conditioning preserves glycolytic ATP during early reperfusion: a survival mechanism for the reperfused heart. *Cellular Physiology and Biochemistry : International Journal of Experimental Cellular Physiology, Biochemistry, and Pharmacology*. 22, 635-644.
- Costa, A.D., Jakob, R., Costa, C.L., Andrukhiv, K., West, I.C., Garlid, K.D., 2006. The mechanism by which the mitochondrial ATP-sensitive K⁺ channel opening and H₂O₂ inhibit the mitochondrial permeability transition. *The Journal of Biological Chemistry*. 281, 20801-20808.
- Creager, M.A., Luscher, T.F., Cosentino, F., Beckman, J.A., 2003. Diabetes and vascular disease: pathophysiology, clinical consequences, and medical therapy: Part I. *Circulation*. 108, 1527-1532.
- Crompton, M. & Costi, A., 1988. Kinetic evidence for a heart mitochondrial pore activated by Ca²⁺, inorganic phosphate and oxidative stress. A potential mechanism for mitochondrial dysfunction during cellular Ca²⁺ overload. *European Journal of Biochemistry / FEBS*. 178, 489-501.
- Crompton, M., Costi, A., Hayat, L., 1987. Evidence for the presence of a reversible Ca²⁺-dependent pore activated by oxidative stress in heart mitochondria. *The Biochemical Journal*. 245, 915-918.
- Cross, D.A., Alessi, D.R., Cohen, P., Andjelkovich, M., Hemmings, B.A., 1995. Inhibition of glycogen synthase kinase-3 by insulin mediated by protein kinase B. *Nature*. 378, 785-789.
- Cross, H.R., Opie, L.H., Radda, G.K., Clarke, K., 1996. Is a high glycogen content beneficial or detrimental to the ischemic rat heart? A controversy resolved. *Circulation Research*. 78, 482-491.
- Cross, H.R., Radda, G.K., Clarke, K., 1995. The role of Na⁺/K⁺ ATPase activity during low flow ischemia in preventing myocardial injury: a ³¹P, ²³Na and ⁸⁷Rb NMR spectroscopic study. *Magnetic Resonance in Medicine : Official Journal of the Society of Magnetic Resonance in Medicine / Society of Magnetic Resonance in Medicine*. 34, 673-685.
- Crowley, L.V., 2007. *An Introduction to Human Disease Pathology and Pathophysiology Correlations*. Seventh edition ed. Unites States of America: Jones and Bartlett Publishers Inc.

de Jonge, R. & de Jong, J.W., 1999. Ischemic preconditioning and glucose metabolism during low-flow ischemia: role of the adenosine A1 receptor. *Cardiovascular Research*. 43, 909-918.

Delbosc, S., Paizanis, E., Magous, R., Araiz, C., Dimo, T., Cristol, J.P., Cros, G., Azay, J., 2005. Involvement of oxidative stress and NADPH oxidase activation in the development of cardiovascular complications in a model of insulin resistance, the fructose-fed rat. *Atherosclerosis*. 179, 43-49.

Delhumeau, G., Cruz-Mendoza, A.M., Gomez Lojero, C., 1994. Protection of cytochrome c oxidase against cyanide inhibition by pyruvate and alpha-ketoglutarate: effect of aeration in vitro. *Toxicology and Applied Pharmacology*. 126, 345-351.

Dennis, S.C., Padmas, A., DeBuysere, M.S., Olson, M.S., 1979. Studies on the regulation of pyruvate dehydrogenase in the isolated perfused rat heart. *The Journal of Biological Chemistry*. 254, 1252-1258.

Depre, C. & Taegtmeyer, H., 2000. Metabolic aspects of programmed cell survival and cell death in the heart. *Cardiovascular Research*. 45, 538-548.

Desouza, C., Salazar, H., Cheong, B., Murgo, J., Fonseca, V., 2003. Association of hypoglycemia and cardiac ischemia: a study based on continuous monitoring. *Diabetes Care*. 26, 1485-1489.

D'hahan, N., Moreau, C., Prost, A.L., Jacquet, H., Alekseev, A.E., Terzic, A., Vivaudou, M., 1999. Pharmacological plasticity of cardiac ATP-sensitive potassium channels toward diazoxide revealed by ADP. *Proceedings of the National Academy of Sciences of the United States of America*. 96, 12162-12167.

Dhar-Chowdhury, P., Harrell, M.D., Han, S.Y., Jankowska, D., Parachuru, L., Morrissey, A., Srivastava, S., Liu, W., Malester, B., Yoshida, H., Coetzee, W.A., 2005. The glycolytic enzymes, glyceraldehyde-3-phosphate dehydrogenase, triose-phosphate isomerase, and pyruvate kinase are components of the K(ATP) channel macromolecular complex and regulate its function. *The Journal of Biological Chemistry*. 280, 38464-38470.

Di Lisa, F., Menabo, R., Canton, M., Barile, M., Bernardi, P., 2001. Opening of the mitochondrial permeability transition pore causes depletion of mitochondrial and cytosolic NAD⁺ and is a causative event in the death of myocytes in postischemic reperfusion of the heart. *The Journal of Biological Chemistry*. 276, 2571-2575.

Dickson, E.W., Tubbs, R.J., Porcaro, W.A., Lee, W.J., Blehar, D.J., Carraway, R.E., Darling, C.E., Przyklenk, K., 2002. Myocardial preconditioning factors evoke mesenteric ischemic tolerance via opioid receptors and K(ATP) channels. *American Journal of Physiology. Heart and Circulatory Physiology*. 283, H22-8.

Dizon, J., Burkhoff, D., Tauskela, J., Whang, J., Cannon, P., Katz, J., 1998. Metabolic inhibition in the perfused rat heart: evidence for glycolytic requirement for normal sodium homeostasis. *The American Journal of Physiology*. 274, H1082-9.

- Doblado, M. & Moley, K.H., 2009. Facilitative glucose transporter 9, a unique hexose and urate transporter. *American Journal of Physiology. Endocrinology and Metabolism*. 297, E831-5.
- Doege, H., Bocianski, A., Scheepers, A., Axer, H., Eckel, J., Joost, H.G., Schurmann, A., 2001. Characterization of human glucose transporter (GLUT) 11 (encoded by SLC2A11), a novel sugar-transport facilitator specifically expressed in heart and skeletal muscle. *The Biochemical Journal*. 359, 443-449.
- Doege, H., Schurmann, A., Bahrenberg, G., Brauers, A., Joost, H.G., 2000. GLUT8, a novel member of the sugar transport facilitator family with glucose transport activity. *The Journal of Biological Chemistry*. 275, 16275-16280.
- Douard, V. & Ferraris, R.P., 2008. Regulation of the fructose transporter GLUT5 in health and disease. *American Journal of Physiology. Endocrinology and Metabolism*. 295, E227-37.
- Duehlmeier, R., Sammet, K., Widdel, A., von Engelhardt, W., Wernery, U., Kinne, J., Sallmann, H.P., 2007. Distribution patterns of the glucose transporters GLUT4 and GLUT1 in skeletal muscles of rats (*Rattus norvegicus*), pigs (*Sus scrofa*), cows (*Bos taurus*), adult goats, goat kids (*Capra hircus*), and camels (*Camelus dromedarius*). *Comparative Biochemistry and Physiology. Part A, Molecular & Integrative Physiology*. 146, 274-282.
- Dzeja, P.P., Zeleznikar, R.J., Goldberg, N.D., 1998. Adenylate kinase: kinetic behavior in intact cells indicates it is integral to multiple cellular processes. *Molecular and Cellular Biochemistry*. 184, 169-182.
- Eisner, D.A., Nichols, C.G., O'Neill, S.C., Smith, G.L., Valdeolmillos, M., 1989. The effects of metabolic inhibition on intracellular calcium and pH in isolated rat ventricular cells. *The Journal of Physiology*. 411, 393-418.
- Elliott, A.C., Smith, G.L., Allen, D.G., 1989. Simultaneous measurements of action potential duration and intracellular ATP in isolated ferret hearts exposed to cyanide. *Circulation Research*. 64, 583-591.
- Elrod, J.W., Harrell, M., Flagg, T.P., Gundewar, S., Magnuson, M.A., Nichols, C.G., Coetzee, W.A., Lefer, D.J., 2008. Role of sulfonylurea receptor type 1 subunits of ATP-sensitive potassium channels in myocardial ischemia/reperfusion injury. *Circulation*. 117, 1405-1413.
- England, P.J. & Randle, P.J., 1967. Effectors of rat-heart hexokinases and the control of rates of glucose phosphorylation in the perfused rat heart. *The Biochemical Journal*. 105, 907-920.
- Erhardt, P., Schremser, E.J., Cooper, G.M., 1999. B-Raf inhibits programmed cell death downstream of cytochrome c release from mitochondria by activating the MEK/Erk pathway. *Molecular and Cellular Biology*. 19, 5308-5315.

Fabiato, A. & Fabiato, F., 1978. Effects of pH on the myofilaments and the sarcoplasmic reticulum of skinned cells from cardiac and skeletal muscles. *The Journal of Physiology*. 276, 233-255.

Figueredo, V.M., Dresdner, K.P., Jr, Wolney, A.C., Keller, A.M., 1991. Postischemic reperfusion injury in the isolated rat heart: effect of ruthenium red. *Cardiovascular Research*. 25, 337-342.

Findlay, I., 1993. Effects of glibenclamide upon ATP-sensitive K channels during metabolic inhibition of isolated rat cardiac myocytes. *Cardiovascular Drugs and Therapy / Sponsored by the International Society of Cardiovascular Pharmacotherapy*. 7 Suppl 3, 495-497.

Findlay, I. & Faivre, J.F., 1991. ATP-sensitive K channels in heart muscle. Spare channels. *FEBS Letters*. 279, 95-97.

Fiordaliso, F., Leri, A., Cesselli, D., Limana, F., Safai, B., Nadal-Ginard, B., Anversa, P., Kajstura, J., 2001. Hyperglycemia activates p53 and p53-regulated genes leading to myocyte cell death. *Diabetes*. 50, 2363-2375.

Flood, A., Hack, B.D., Headrick, J.P., 2003. Pyruvate-dependent preconditioning and cardioprotection in murine myocardium. *Clinical and Experimental Pharmacology & Physiology*. 30, 145-152.

Fong, J.C. & Schulz, H., 1977. Purification and properties of pig heart crotonase and the presence of short chain and long chain enoyl coenzyme A hydratases in pig and guinea pig tissues. *The Journal of Biological Chemistry*. 252, 542-547.

Fralix, T.A., Steenbergen, C., London, R.E., Murphy, E., 1992. Metabolic substrates can alter postischemic recovery in preconditioned ischemic heart. *The American Journal of Physiology*. 263, C17-23.

Fukumoto, H., Seino, S., Imura, H., Seino, Y., Eddy, R.L., Fukushima, Y., Byers, M.G., Shows, T.B., Bell, G.I., 1988. Sequence, tissue distribution, and chromosomal localization of mRNA encoding a human glucose transporter-like protein. *Proceedings of the National Academy of Sciences of the United States of America*. 85, 5434-5438.

Galagudza, M., Kurapeev, D., Minasian, S., Valen, G., Vaage, J., 2004. Ischemic postconditioning: brief ischemia during reperfusion converts persistent ventricular fibrillation into regular rhythm. *European Journal of Cardio-Thoracic Surgery : Official Journal of the European Association for Cardio-Thoracic Surgery*. 25, 1006-1010.

Garcia-Dorado, D., Ruiz-Meana, M., Inserte, J., Rodriguez-Sinovas, A., Piper, H.M., 2012. Calcium-mediated cell death during myocardial reperfusion. *Cardiovascular Research*. 94, 168-180.

- Garlid, K.D., Paucek, P., Yarov-Yarovoy, V., Sun, X., Schindler, P.A., 1996. The mitochondrial KATP channel as a receptor for potassium channel openers. *The Journal of Biological Chemistry*. 271, 8796-8799.
- Garrido, C., Galluzzi, L., Brunet, M., Puig, P.E., Didelot, C., Kroemer, G., 2006. Mechanisms of cytochrome c release from mitochondria. *Cell Death and Differentiation*. 13, 1423-1433.
- Gelpi, J.L., Dordal, A., Montserrat, J., Mazo, A., Cortes, A., 1992. Kinetic studies of the regulation of mitochondrial malate dehydrogenase by citrate. *The Biochemical Journal*. 283 (Pt 1), 289-297.
- Gho, B.C., Schoemaker, R.G., van den Doel, M.A., Duncker, D.J., Verdouw, P.D., 1996. Myocardial protection by brief ischemia in noncardiac tissue. *Circulation*. 94, 2193-2200.
- Gimeno, R.E., Ortegon, A.M., Patel, S., Punreddy, S., Ge, P., Sun, Y., Lodish, H.F., Stahl, A., 2003. Characterization of a heart-specific fatty acid transport protein. *The Journal of Biological Chemistry*. 278, 16039-16044.
- Gordin, D., Forsblom, C., Ronnback, M., Groop, P.H., 2008. Acute hyperglycaemia disturbs cardiac repolarization in Type 1 diabetes. *Diabetic Medicine : A Journal of the British Diabetic Association*. 25, 101-105.
- Goresky, C.A., Stremmel, W., Rose, C.P., Guirguis, S., Schwab, A.J., Diede, H.E., Ibrahim, E., 1994. The capillary transport system for free fatty acids in the heart. *Circulation Research*. 74, 1015-1026.
- Goyal, A., Mahaffey, K.W., Garg, J., Nicolau, J.C., Hochman, J.S., Weaver, W.D., Theroux, P., Oliveira, G.B., Todaro, T.G., Mojcik, C.F., Armstrong, P.W., Granger, C.B., 2006. Prognostic significance of the change in glucose level in the first 24 h after acute myocardial infarction: results from the CARDINAL study. *European Heart Journal*. 27, 1289-1297.
- Granfeldt, A., Lefer, D.J., Vinten-Johansen, J., 2009. Protective ischaemia in patients: preconditioning and postconditioning. *Cardiovascular Research*. 83, 234-246.
- Grant, A.O., 2009. Cardiac ion channels. *Circulation. Arrhythmia and Electrophysiology*. 2, 185-194.
- Greenwalt, D.E., Scheck, S.H., Rhinehart-Jones, T., 1995. Heart CD36 expression is increased in murine models of diabetes and in mice fed a high fat diet. *The Journal of Clinical Investigation*. 96, 1382-1388.
- Griffiths, E.J. & Halestrap, A.P., 1995. Mitochondrial non-specific pores remain closed during cardiac ischaemia, but open upon reperfusion. *The Biochemical Journal*. 307 (Pt 1), 93-98.

Griffiths, E.J. & Halestrap, A.P., 1993. Protection by Cyclosporin A of ischemia/reperfusion-induced damage in isolated rat hearts. *Journal of Molecular and Cellular Cardiology*. 25, 1461-1469.

Gross, G.J. & Auchampach, J.A., 1992. Role of ATP dependent potassium channels in myocardial ischaemia. *Cardiovascular Research*. 26, 1011-1016.

Grover, G.J. & Garlid, K.D., 2000. ATP-Sensitive potassium channels: a review of their cardioprotective pharmacology. *Journal of Molecular and Cellular Cardiology*. 32, 677-695.

Gumina, R.J., Pucar, D., Bast, P., Hodgson, D.M., Kurtz, C.E., Dzeja, P.P., Miki, T., Seino, S., Terzic, A., 2003. Knockout of Kir6.2 negates ischemic preconditioning-induced protection of myocardial energetics. *American Journal of Physiology. Heart and Circulatory Physiology*. 284, H2106-13.

Habets, D.D., Coumans, W.A., Voshol, P.J., den Boer, M.A., Febbraio, M., Bonen, A., Glatz, J.F., Luiken, J.J., 2007. AMPK-mediated increase in myocardial long-chain fatty acid uptake critically depends on sarcolemmal CD36. *Biochemical and Biophysical Research Communications*. 355, 204-210.

Haddock, B.A., Yates, D.W., Garland, P.B., 1970. The localization of some coenzyme A-dependent enzymes in rat liver mitochondria. *The Biochemical Journal*. 119, 565-573.

Halestrap, A.P., 2012. The monocarboxylate transporter family--Structure and functional characterization. *IUBMB Life*. 64, 1-9.

Halestrap, A.P., 1991. Calcium-dependent opening of a non-specific pore in the mitochondrial inner membrane is inhibited at pH values below 7. Implications for the protective effect of low pH against chemical and hypoxic cell damage. *The Biochemical Journal*. 278 (Pt 3), 715-719.

Halestrap, A.P., Clarke, S.J., Javadov, S.A., 2004. Mitochondrial permeability transition pore opening during myocardial reperfusion--a target for cardioprotection. *Cardiovascular Research*. 61, 372-385.

Halestrap, A.P. & Denton, R.M., 1974. Specific inhibition of pyruvate transport in rat liver mitochondria and human erythrocytes by alpha-cyano-4-hydroxycinnamate. *The Biochemical Journal*. 138, 313-316.

Halestrap, A.P. & Price, N.T., 1999. The proton-linked monocarboxylate transporter (MCT) family: structure, function and regulation. *The Biochemical Journal*. 343 Pt 2, 281-299.

Halkos, M.E., Kerendi, F., Corvera, J.S., Wang, N.P., Kin, H., Payne, C.S., Sun, H.Y., Guyton, R.A., Vinten-Johansen, J., Zhao, Z.Q., 2004. Myocardial protection with postconditioning is not enhanced by ischemic preconditioning. *The Annals of Thoracic Surgery*. 78, 961-9; discussion 969.

Hanley, P.J., Mickel, M., Loffler, M., Brandt, U., Daut, J., 2002. K(ATP) channel-independent targets of diazoxide and 5-hydroxydecanoate in the heart. *The Journal of Physiology*. 542, 735-741.

Hausenloy, D.J., Duchen, M.R., Yellon, D.M., 2003. Inhibiting mitochondrial permeability transition pore opening at reperfusion protects against ischaemia-reperfusion injury. *Cardiovascular Research*. 60, 617-625.

Hausenloy, D.J., Ong, S.B., Yellon, D.M., 2009. The mitochondrial permeability transition pore as a target for preconditioning and postconditioning. *Basic Research in Cardiology*. 104, 189-202.

Hausenloy, D.J., Tsang, A., Yellon, D.M., 2005. The reperfusion injury salvage kinase pathway: a common target for both ischemic preconditioning and postconditioning. *Trends in Cardiovascular Medicine*. 15, 69-75.

Hausenloy, D.J. & Yellon, D.M., 2010. The second window of preconditioning (SWOP) where are we now? *Cardiovascular Drugs and Therapy / Sponsored by the International Society of Cardiovascular Pharmacotherapy*. 24, 235-254.

Hausenloy, D.J. & Yellon, D.M., 2008. Remote ischaemic preconditioning: underlying mechanisms and clinical application. *Cardiovascular Research*. 79, 377-386.

Hausenloy, D.J. & Yellon, D.M., 2006. Survival kinases in ischemic preconditioning and postconditioning. *Cardiovascular Research*. 70, 240-253.

Hausenloy, D.J. & Yellon, D.M., 2003. The mitochondrial permeability transition pore: its fundamental role in mediating cell death during ischaemia and reperfusion. *Journal of Molecular and Cellular Cardiology*. 35, 339-341.

Hayat, S.A., Patel, B., Khattar, R.S., Malik, R.A., 2004. Diabetic cardiomyopathy: mechanisms, diagnosis and treatment. *Clinical Science (London, England : 1979)*. 107, 539-557.

Heather, L.C. & Clarke, K., 2011. Metabolism, hypoxia and the diabetic heart. *Journal of Molecular and Cellular Cardiology*. 50, 598-605.

Heather, L.C., Cole, M.A., Lygate, C.A., Evans, R.D., Stuckey, D.J., Murray, A.J., Neubauer, S., Clarke, K., 2006. Fatty acid transporter levels and palmitate oxidation rate correlate with ejection fraction in the infarcted rat heart. *Cardiovascular Research*. 72, 430-437.

Heather, L.C., Howell, N.J., Emmanuel, Y., Cole, M.A., Frenneaux, M.P., Pagano, D., Clarke, K., 2011. Changes in cardiac substrate transporters and metabolic proteins mirror the metabolic shift in patients with aortic stenosis. *PloS One*. 6, e26326.

- Hedo, J.A. & Simpson, I.A., 1984. Internalization of insulin receptors in the isolated rat adipose cell. Demonstration of the vectorial disposition of receptor subunits. *The Journal of Biological Chemistry*. 259, 11083-11089.
- Herzig, S., Raemy, E., Montessuit, S., Veuthey, J.L., Zamboni, N., Westermann, B., Kunji, E.R., Martinou, J.C., 2012. Identification and functional expression of the mitochondrial pyruvate carrier. *Science (New York, N.Y.)*. 337, 93-96.
- Highlander, P. & Shaw, G.P., 2010. Current pharmacotherapeutic concepts for the treatment of cardiovascular disease in diabetics. *Therapeutic Advances in Cardiovascular Disease*. 4, 43-54.
- Hill, M.M., Clark, S.F., Tucker, D.F., Birnbaum, M.J., James, D.E., Macaulay, S.L., 1999. A role for protein kinase B β /Akt2 in insulin-stimulated GLUT4 translocation in adipocytes. *Molecular and Cellular Biology*. 19, 7771-7781.
- Holmuhamedov, E.L., Jovanovic, S., Dzeja, P.P., Jovanovic, A., Terzic, A., 1998. Mitochondrial ATP-sensitive K⁺ channels modulate cardiac mitochondrial function. *The American Journal of Physiology*. 275, H1567-76.
- Hong, M., Kefaloyianni, E., Bao, L., Malester, B., Delaroche, D., Neubert, T.A., Coetzee, W.A., 2011. Cardiac ATP-sensitive K⁺ channel associates with the glycolytic enzyme complex. *FASEB Journal : Official Publication of the Federation of American Societies for Experimental Biology*. 25, 2456-2467.
- Houten, S.M. & Wanders, R.J., 2010. A general introduction to the biochemistry of mitochondrial fatty acid β -oxidation. *Journal of Inherited Metabolic Disease*. 33, 469-477.
- Hove-Madsen, L. & Bers, D.M., 1993. Sarcoplasmic reticulum Ca²⁺ uptake and thapsigargin sensitivity in permeabilized rabbit and rat ventricular myocytes. *Circulation Research*. 73, 820-828.
- Huser, J. & Blatter, L.A., 1999. Fluctuations in mitochondrial membrane potential caused by repetitive gating of the permeability transition pore. *The Biochemical Journal*. 343 Pt 2, 311-317.
- Huttemann, M., Lee, I., Pecinova, A., Pecina, P., Przyklenk, K., Doan, J.W., 2008. Regulation of oxidative phosphorylation, the mitochondrial membrane potential, and their role in human disease. *Journal of Bioenergetics and Biomembranes*. 40, 445-456.
- Inagaki, K., Begley, R., Ikeno, F., Mochly-Rosen, D., 2005. Cardioprotection by epsilon-protein kinase C activation from ischemia: continuous delivery and antiarrhythmic effect of an epsilon-protein kinase C-activating peptide. *Circulation*. 111, 44-50.
- Inoue, I., Nagase, H., Kishi, K., Higuti, T., 1991. ATP-sensitive K⁺ channel in the mitochondrial inner membrane. *Nature*. 352, 244-247.

Inserte, J., Garcia-Dorado, D., Ruiz-Meana, M., Padilla, F., Barrabes, J.A., Pina, P., Agullo, L., Piper, H.M., Soler-Soler, J., 2002. Effect of inhibition of Na(+)/Ca(2+) exchanger at the time of myocardial reperfusion on hypercontracture and cell death. *Cardiovascular Research*. 55, 739-748.

Iwakura, K., Ito, H., Kawano, S., Shintani, Y., Yamamoto, K., Kato, A., Ikushima, M., Tanaka, K., Kitakaze, M., Hori, M., Higashino, Y., Fujii, K., 2001. Predictive factors for development of the no-reflow phenomenon in patients with reperfused anterior wall acute myocardial infarction. *Journal of the American College of Cardiology*. 38, 472-477.

James, D.E., Brown, R., Navarro, J., Pilch, P.F., 1988. Insulin-regulatable tissues express a unique insulin-sensitive glucose transport protein. *Nature*. 333, 183-185.

Janier, M.F., Vanoverschelde, J.L., Bergmann, S.R., 1994. Ischemic preconditioning stimulates anaerobic glycolysis in the isolated rabbit heart. *The American Journal of Physiology*. 267, H1353-60.

Januszewicz, W., Sznajderman, M., Ciswicka-Sznajderman, M., Wocial, B., Rymaszewski, Z., 1971. Plasma free fatty acid and catecholamine levels in patients with acute myocardial infarction. *British Heart Journal*. 33, 716-718.

Jennings, R.B., Reimer, K.A., Steenbergen, C., 1991. Effect of inhibition of the mitochondrial ATPase on net myocardial ATP in total ischemia. *Journal of Molecular and Cellular Cardiology*. 23, 1383-1395.

Jeremy, R.W., Ambrosio, G., Pike, M.M., Jacobus, W.E., Becker, L.C., 1993. The functional recovery of post-ischemic myocardium requires glycolysis during early reperfusion. *Journal of Molecular and Cellular Cardiology*. 25, 261-276.

Jeremy, R.W., Koretsune, Y., Marban, E., Becker, L.C., 1992. Relation between glycolysis and calcium homeostasis in postischemic myocardium. *Circulation Research*. 70, 1180-1190.

Ji, L., Zhang, X., Liu, W., Huang, Q., Yang, W., Fu, F., Ma, H., Su, H., Wang, H., Wang, J., Zhang, H., Gao, F., 2013. AMPK-regulated and Akt-dependent enhancement of glucose uptake is essential in ischemic preconditioning-alleviated reperfusion injury. *PloS One*. 8, e69910.

Jiang, G. & Zhang, B.B., 2003. Glucagon and regulation of glucose metabolism. *American Journal of Physiology. Endocrinology and Metabolism*. 284, E671-8.

Johnson-Delaney, C.A., 2008. *Exotic Companion Medicine Handbook for Veterinarians*. Kirkland, Washington: Eastside Avian and Exotic Animal Medical Centre.

Johnston, D.L. & Lewandowski, E.D., 1991. Fatty acid metabolism and contractile function in the reperfused myocardium. Multinuclear NMR studies of isolated rabbit hearts. *Circulation Research*. 68, 714-725.

- Joost, H.G., Bell, G.I., Best, J.D., Birnbaum, M.J., Charron, M.J., Chen, Y.T., Doege, H., James, D.E., Lodish, H.F., Moley, K.H., Moley, J.F., Mueckler, M., Rogers, S., Schurmann, A., Seino, S., Thorens, B., 2002. Nomenclature of the GLUT/SLC2A family of sugar/polyol transport facilitators. *American Journal of Physiology. Endocrinology and Metabolism*. 282, E974-6.
- Jordan, J.E., Simandle, S.A., Tulbert, C.D., Busija, D.W., Miller, A.W., 2003. Fructose-fed rats are protected against ischemia/reperfusion injury. *The Journal of Pharmacology and Experimental Therapeutics*. 307, 1007-1011.
- Jovanovic, S., Du, Q., Crawford, R.M., Budas, G.R., Stagljär, I., Jovanovic, A., 2005. Glyceraldehyde 3-phosphate dehydrogenase serves as an accessory protein of the cardiac sarcolemmal K(ATP) channel. *EMBO Reports*. 6, 848-852.
- Takei, M., Noma, A., Shibasaki, T., 1985. Properties of adenosine-triphosphate-regulated potassium channels in guinea-pig ventricular cells. *The Journal of Physiology*. 363, 441-462.
- Kalra, B.S. & Roy, V., 2011. Efficacy of Metabolic Modulators in Ischemic Heart Disease: An Overview. *Journal of Clinical Pharmacology*. page num?
- Karmazyn, M., 1988. Amiloride enhances postischemic ventricular recovery: possible role of Na⁺-H⁺ exchange. *The American Journal of Physiology*. 255, H608-15.
- Katz, A.M., 1973. Effects of ischemia on the contractile processes of heart muscle. *The American Journal of Cardiology*. 32, 456-460.
- Kayano, T., Fukumoto, H., Eddy, R.L., Fan, Y.S., Byers, M.G., Shows, T.B., Bell, G.I., 1988. Evidence for a family of human glucose transporter-like proteins. Sequence and gene localization of a protein expressed in fetal skeletal muscle and other tissues. *The Journal of Biological Chemistry*. 263, 15245-15248.
- Kennedy, S.G., Kandel, E.S., Cross, T.K., Hay, N., 1999. Akt/Protein kinase B inhibits cell death by preventing the release of cytochrome c from mitochondria. *Molecular and Cellular Biology*. 19, 5800-5810.
- Kentish, J.C., 1986. The effects of inorganic phosphate and creatine phosphate on force production in skinned muscles from rat ventricle. *The Journal of Physiology*. 370, 585-604.
- Kerbey, A.L., Radcliffe, P.M., Randle, P.J., Sugden, P.H., 1979. Regulation of kinase reactions in pig heart pyruvate dehydrogenase complex. *The Biochemical Journal*. 181, 427-433.
- Kerbey, A.L., Randle, P.J., Cooper, R.H., Whitehouse, S., Pask, H.T., Denton, R.M., 1976. Regulation of pyruvate dehydrogenase in rat heart. Mechanism of regulation of proportions of dephosphorylated and phosphorylated enzyme by oxidation of fatty acids and ketone bodies and of effects of diabetes: role of coenzyme A, acetyl-

coenzyme A and reduced and oxidized nicotinamide-adenine dinucleotide. *The Biochemical Journal*. 154, 327-348.

Kerr, P.M., Suleiman, M.S., Halestrap, A.P., 1999. Reversal of permeability transition during recovery of hearts from ischemia and its enhancement by pyruvate. *The American Journal of Physiology*. 276, H496-502.

Kersten, J.R., Montgomery, M.W., Ghassemi, T., Gross, E.R., Toller, W.G., Pagel, P.S., Warltier, D.C., 2001. Diabetes and hyperglycemia impair activation of mitochondrial K(ATP) channels. *American Journal of Physiology. Heart and Circulatory Physiology*. 280, H1744-50.

Kersten, J.R., Schmeling, T.J., Orth, K.G., Pagel, P.S., Warltier, D.C., 1998. Acute hyperglycemia abolishes ischemic preconditioning in vivo. *The American Journal of Physiology*. 275, H721-5.

Kersten, J.R., Toller, W.G., Gross, E.R., Pagel, P.S., Warltier, D.C., 2000. Diabetes abolishes ischemic preconditioning: role of glucose, insulin, and osmolality. *American Journal of Physiology. Heart and Circulatory Physiology*. 278, H1218-24.

Kharbanda, R.K., Li, J., Konstantinov, I.E., Cheung, M.M., White, P.A., Frndova, H., Stokoe, J., Cox, P., Vogel, M., Van Arsdell, G., MacAllister, R., Redington, A.N., 2006. Remote ischaemic preconditioning protects against cardiopulmonary bypass-induced tissue injury: a preclinical study. *Heart (British Cardiac Society)*. 92, 1506-1511.

Kharbanda, R.K., Mortensen, U.M., White, P.A., Kristiansen, S.B., Schmidt, M.R., Hoschtitzky, J.A., Vogel, M., Sorensen, K., Redington, A.N., MacAllister, R., 2002. Transient limb ischemia induces remote ischemic preconditioning in vivo. *Circulation*. 106, 2881-2883.

Kin, H., Zhao, Z.Q., Sun, H.Y., Wang, N.P., Corvera, J.S., Halkos, M.E., Kerendi, F., Guyton, R.A., Vinten-Johansen, J., 2004. Postconditioning attenuates myocardial ischemia-reperfusion injury by inhibiting events in the early minutes of reperfusion. *Cardiovascular Research*. 62, 74-85.

King, L.M. & Opie, L.H., 1998a. Glucose and glycogen utilisation in myocardial ischemia--changes in metabolism and consequences for the myocyte. *Molecular and Cellular Biochemistry*. 180, 3-26.

King, L.M. & Opie, L.H., 1998b. Glucose delivery is a major determinant of glucose utilisation in the ischemic myocardium with a residual coronary flow. *Cardiovascular Research*. 39, 381-392.

Kingsley, P.B., Sako, E.Y., Yang, M.Q., Zimmer, S.D., Ugurbil, K., Foker, J.E., From, A.H., 1991. Ischemic contracture begins when anaerobic glycolysis stops: a ³¹P-NMR study of isolated rat hearts. *The American Journal of Physiology*. 261, H469-78.

Kitakaze, M., 2010. How to mediate cardioprotection in ischemic hearts--accumulated evidence of basic research should translate to clinical medicine. *Cardiovascular Drugs and Therapy / Sponsored by the International Society of Cardiovascular Pharmacotherapy*. 24, 217-223.

Klip, A. & Paquet, M.R., 1990. Glucose transport and glucose transporters in muscle and their metabolic regulation. *Diabetes Care*. 13, 228-243.

Kloner, R.A., Dow, J., Bhandari, A., 2006. Postconditioning markedly attenuates ventricular arrhythmias after ischemia-reperfusion. *Journal of Cardiovascular Pharmacology and Therapeutics*. 11, 55-63.

Knox, B.E. & Tsong, T.Y., 1984. Voltage-driven ATP synthesis by beef heart mitochondrial F₀F₁-ATPase. *The Journal of Biological Chemistry*. 259, 4757-4763.

Kobayashi, K. & Neely, J.R., 1983. Effects of ischemia and reperfusion on pyruvate dehydrogenase activity in isolated rat hearts. *Journal of Molecular and Cellular Cardiology*. 15, 359-367.

Kockskamper, J., Zima, A.V., Blatter, L.A., 2005. Modulation of sarcoplasmic reticulum Ca²⁺ release by glycolysis in cat atrial myocytes. *The Journal of Physiology*. 564, 697-714.

Kohn, M.C., Achs, M.J., Garfinkel, D., 1979. Computer simulation of metabolism in pyruvate-perfused rat heart. II. Krebs cycle. *The American Journal of Physiology*. 237, R159-66.

Kopustinskiene, D.M., Liobikas, J., Skemiene, K., Malinauskas, F., Toleikis, A., 2010. Direct effects of K(ATP) channel openers pinacidil and diazoxide on oxidative phosphorylation of mitochondria in situ. *Cellular Physiology and Biochemistry : International Journal of Experimental Cellular Physiology, Biochemistry, and Pharmacology*. 25, 181-186.

Korge, P., Honda, H.M., Weiss, J.N., 2001. Regulation of the mitochondrial permeability transition by matrix Ca(2+) and voltage during anoxia/reoxygenation. *American Journal of Physiology. Cell Physiology*. 280, C517-26.

Kosiborod, M., Inzucchi, S.E., Krumholz, H.M., Xiao, L., Jones, P.G., Fiske, S., Masoudi, F.A., Marso, S.P., Spertus, J.A., 2008. Glucometrics in patients hospitalized with acute myocardial infarction: defining the optimal outcomes-based measure of risk. *Circulation*. 117, 1018-1027.

Kosiborod, M., Rathore, S.S., Inzucchi, S.E., Masoudi, F.A., Wang, Y., Havranek, E.P., Krumholz, H.M., 2005. Admission glucose and mortality in elderly patients hospitalized with acute myocardial infarction: implications for patients with and without recognized diabetes. *Circulation*. 111, 3078-3086.

Koster, J.C., Permutt, M.A., Nichols, C.G., 2005. Diabetes and insulin secretion: the ATP-sensitive K⁺ channel (K⁺ATP) connection. *Diabetes*. 54, 3065-3072.

Kowaltowski, A.J., Seetharaman, S., Paucek, P., Garlid, K.D., 2001. Bioenergetic consequences of opening the ATP-sensitive K⁺ channel of heart mitochondria. *American Journal of Physiology. Heart and Circulatory Physiology*. 280, H649-57.

Kuzuya, T., Hoshida, S., Yamashita, N., Fuji, H., Oe, H., Hori, M., Kamada, T., Tada, M., 1993. Delayed effects of sublethal ischemia on the acquisition of tolerance to ischemia. *Circulation Research*. 72, 1293-1299.

Laclau, M.N., Boudina, S., Thambo, J.B., Tariosse, L., Gouverneur, G., Bonoron-Adele, S., Saks, V.A., Garlid, K.D., Dos Santos, P., 2001. Cardioprotection by ischemic preconditioning preserves mitochondrial function and functional coupling between adenine nucleotide translocase and creatine kinase. *Journal of Molecular and Cellular Cardiology*. 33, 947-956.

Ladilov, Y.V., Siegmund, B., Piper, H.M., 1995. Protection of reoxygenated cardiomyocytes against hypercontracture by inhibition of Na⁺/H⁺ exchange. *The American Journal of Physiology*. 268, H1531-9.

LaNoue, K.F., Bryla, J., Williamson, J.R., 1972. Feedback interactions in the control of citric acid cycle activity in rat heart mitochondria. *The Journal of Biological Chemistry*. 247, 667-679.

Lawrence, C.L., Billups, B., Rodrigo, G.C., Standen, N.B., 2001. The KATP channel opener diazoxide protects cardiac myocytes during metabolic inhibition without causing mitochondrial depolarization or flavoprotein oxidation. *British Journal of Pharmacology*. 134, 535-542.

Lawrence, C.L., Rainbow, R.D., Davies, N.W., Standen, N.B., 2002. Effect of metabolic inhibition on glimepiride block of native and cloned cardiac sarcolemmal K(ATP) channels. *British Journal of Pharmacology*. 136, 746-752.

Leblanc, N. & Hume, J.R., 1990. Sodium current-induced release of calcium from cardiac sarcoplasmic reticulum. *Science (New York, N.Y.)*. 248, 372-376.

Lederer, W.J., Nichols, C.G., Smith, G.L., 1989. The mechanism of early contractile failure of isolated rat ventricular myocytes subjected to complete metabolic inhibition. *The Journal of Physiology*. 413, 329-349.

Levesque, P.C., Leblanc, N., Hume, J.R., 1994. Release of calcium from guinea pig cardiac sarcoplasmic reticulum induced by sodium-calcium exchange. *Cardiovascular Research*. 28, 370-378.

Levi, A.J., Spitzer, K.W., Kohmoto, O., Bridge, J.H., 1994. Depolarization-induced Ca entry via Na-Ca exchange triggers SR release in guinea pig cardiac myocytes. *The American Journal of Physiology*. 266, H1422-33.

Levick, J.R., 2010. *An Introduction To Cardiovascular Physiology*. Fifth edition ed. London: Hodder Arndd.

Leyssens, A., Nowicky, A.V., Patterson, L., Crompton, M., Duchen, M.R., 1996. The relationship between mitochondrial state, ATP hydrolysis, $[Mg^{2+}]_i$ and $[Ca^{2+}]_i$ studied in isolated rat cardiomyocytes. *The Journal of Physiology*. 496 (Pt 1), 111-128.

Libby, P., Maroko, P.R., Braunwald, E., 1975. The effect of hypoglycemia on myocardial ischemic injury during acute experimental coronary artery occlusion. *Circulation*. 51, 621-626.

Light, P.E., Kanji, H.D., Fox, J.E., French, R.J., 2001. Distinct myoprotective roles of cardiac sarcolemmal and mitochondrial KATP channels during metabolic inhibition and recovery. *FASEB Journal : Official Publication of the Federation of American Societies for Experimental Biology*. 15, 2586-2594.

Linn, T.C., Pettit, F.H., Reed, L.J., 1969. Alpha-keto acid dehydrogenase complexes. X. Regulation of the activity of the pyruvate dehydrogenase complex from beef kidney mitochondria by phosphorylation and dephosphorylation. *Proceedings of the National Academy of Sciences of the United States of America*. 62, 234-241.

Lipp, P., Laine, M., Tovey, S.C., Burrell, K.M., Berridge, M.J., Li, W., Bootman, M.D., 2000. Functional InsP3 receptors that may modulate excitation-contraction coupling in the heart. *Current Biology : CB*. 10, 939-942.

Liu, Y., Ren, G., O'Rourke, B., Marban, E., Seharaseyon, J., 2001. Pharmacological comparison of native mitochondrial K(ATP) channels with molecularly defined surface K(ATP) channels. *Molecular Pharmacology*. 59, 225-230.

Liu, Y., Sato, T., O'Rourke, B., Marban, E., 1998. Mitochondrial ATP-dependent potassium channels: novel effectors of cardioprotection? *Circulation*. 97, 2463-2469.

Longmore, W.J., 1968. The effect of variation of CO₂ concentration on pyruvate metabolism in vitro. *Biochemistry*. 7, 3227-3231.

Longnus, S.L., Wambolt, R.B., Barr, R.L., Lopaschuk, G.D., Allard, M.F., 2001. Regulation of myocardial fatty acid oxidation by substrate supply. *American Journal of Physiology. Heart and Circulatory Physiology*. 281, H1561-7.

Lopaschuk, G.D., Spafford, M.A., Davies, N.J., Wall, S.R., 1990. Glucose and palmitate oxidation in isolated working rat hearts reperfused after a period of transient global ischemia. *Circulation Research*. 66, 546-553.

Lopaschuk, G.D., Ussher, J.R., Folmes, C.D., Jaswal, J.S., Stanley, W.C., 2010. Myocardial fatty acid metabolism in health and disease. *Physiological Reviews*. 90, 207-258.

Lopaschuk, G.D., Wambolt, R.B., Barr, R.L., 1993. An imbalance between glycolysis and glucose oxidation is a possible explanation for the detrimental effects of high levels of fatty acids during aerobic reperfusion of ischemic hearts. *The Journal of Pharmacology and Experimental Therapeutics*. 264, 135-144.

Lopaschuk, G.D., Witters, L.A., Itoi, T., Barr, R., Barr, A., 1994. Acetyl-CoA carboxylase involvement in the rapid maturation of fatty acid oxidation in the newborn rabbit heart. *The Journal of Biological Chemistry*. 269, 25871-25878.

Luiken, J.J., Turcotte, L.P., Bonen, A., 1999. Protein-mediated palmitate uptake and expression of fatty acid transport proteins in heart giant vesicles. *Journal of Lipid Research*. 40, 1007-1016.

Luiken, J.J., van Nieuwenhoven, F.A., America, G., van der Vusse, G.J., Glatz, J.F., 1997. Uptake and metabolism of palmitate by isolated cardiac myocytes from adult rats: involvement of sarcolemmal proteins. *Journal of Lipid Research*. 38, 745-758.

Malfitano, C., Alba Loureiro, T.C., Rodrigues, B., Sirvente, R., Salemi, V.M., Rabechi, N.B., Lacchini, S., Curi, R., Irigoyen, M.C., 2010. Hyperglycaemia protects the heart after myocardial infarction: aspects of programmed cell survival and cell death. *European Journal of Heart Failure*. 12, 659-667.

Mallet, R.T., 2000. Pyruvate: metabolic protector of cardiac performance. *Proceedings of the Society for Experimental Biology and Medicine. Society for Experimental Biology and Medicine (New York, N.Y.)*. 223, 136-148.

Mallet, R.T. & Sun, J., 1999. Mitochondrial metabolism of pyruvate is required for its enhancement of cardiac function and energetics. *Cardiovascular Research*. 42, 149-161.

Manning Fox, J.E., Kanji, H.D., French, R.J., Light, P.E., 2002. Cardiospecificity of the sulphonylurea HMR 1098: studies on native and recombinant cardiac and pancreatic K(ATP) channels. *British Journal of Pharmacology*. 135, 480-488.

Mapanga, R.F., Joseph, D., Symington, B., Garson, K.L., Kimar, C., Kelly-Laubscher, R., Essop, M.F., 2014. Detrimental effects of acute hyperglycaemia on the rat heart. *Acta Physiologica (Oxford, England)*. 210, 546-564.

Marber, M.S., Latchman, D.S., Walker, J.M., Yellon, D.M., 1993. Cardiac stress protein elevation 24 hours after brief ischemia or heat stress is associated with resistance to myocardial infarction. *Circulation*. 88, 1264-1272.

Massoudy, P., Becker, B.F., Seligmann, C., Gerlach, E., 1995. Preischemic as well as postischemic application of a calcium antagonist affords cardioprotection in the isolated guinea pig heart. *Cardiovascular Research*. 29, 577-582.

- McCormack, J.G., Halestrap, A.P., Denton, R.M., 1990. Role of calcium ions in regulation of mammalian intramitochondrial metabolism. *Physiological Reviews*. 70, 391-425.
- McGarry, J.D. & Foster, D.W., 1980. Regulation of hepatic fatty acid oxidation and ketone body production. *Annual Review of Biochemistry*. 49, 395-420.
- McGarry, J.D., Leatherman, G.F., Foster, D.W., 1978. Carnitine palmitoyltransferase I. The site of inhibition of hepatic fatty acid oxidation by malonyl-CoA. *The Journal of Biological Chemistry*. 253, 4128-4136.
- Mellor, K., Ritchie, R.H., Meredith, G., Woodman, O.L., Morris, M.J., Delbridge, L.M., 2010. High-fructose diet elevates myocardial superoxide generation in mice in the absence of cardiac hypertrophy. *Nutrition (Burbank, Los Angeles County, Calif.)*. 26, 842-848.
- Mellor, K.M., Bell, J.R., Wendt, I.R., Davidoff, A.J., Ritchie, R.H., Delbridge, L.M., 2011. Fructose modulates cardiomyocyte excitation-contraction coupling and Ca²(+)-handling in vitro. *PloS One*. 6, e25204.
- Mellor, K.M., Wendt, I.R., Ritchie, R.H., Delbridge, L.M., 2012. Fructose diet treatment in mice induces fundamental disturbance of cardiomyocyte Ca²⁺ handling and myofilament responsiveness. *American Journal of Physiology. Heart and Circulatory Physiology*. 302, H964-72.
- Mellors, L.J., Kotsanas, G., Wendt, I.R., 1999. Effects of pyruvate on intracellular Ca²⁺ regulation in cardiac myocytes from normal and diabetic rats. *Clinical and Experimental Pharmacology & Physiology*. 26, 889-897.
- Moreno, K.X., Sabelhaus, S.M., Merritt, M.E., Sherry, A.D., Malloy, C.R., 2010. Competition of pyruvate with physiological substrates for oxidation by the heart: implications for studies with hyperpolarized [1-¹³C]pyruvate. *American Journal of Physiology. Heart and Circulatory Physiology*. 298, H1556-64.
- Mueckler, M., 1994. Facilitative glucose transporters. *European Journal of Biochemistry / FEBS*. 219, 713-725.
- Mueckler, M., Caruso, C., Baldwin, S.A., Panico, M., Blench, I., Morris, H.R., Allard, W.J., Lienhard, G.E., Lodish, H.F., 1985. Sequence and structure of a human glucose transporter. *Science (New York, N.Y.)*. 229, 941-945.
- Mullinax, T.R., Mock, J.N., McEvily, A.J., Harrison, J.H., 1982. Regulation of mitochondrial malate dehydrogenase. Evidence for an allosteric citrate-binding site. *The Journal of Biological Chemistry*. 257, 13233-13239.
- Murphy, E., Perlman, M., London, R.E., Steenbergen, C., 1991. Amiloride delays the ischemia-induced rise in cytosolic free calcium. *Circulation Research*. 68, 1250-1258.

- Murry, C.E., Jennings, R.B., Reimer, K.A., 1986. Preconditioning with ischemia: a delay of lethal cell injury in ischemic myocardium. *Circulation*. 74, 1124-1136.
- Murthy, M.S. & Pande, S.V., 1987. Malonyl-CoA binding site and the overt carnitine palmitoyltransferase activity reside on the opposite sides of the outer mitochondrial membrane. *Proceedings of the National Academy of Sciences of the United States of America*. 84, 378-382.
- Nakano, A., Cohen, M.V., Downey, J.M., 2000. Ischemic preconditioning: from basic mechanisms to clinical applications. *Pharmacology & Therapeutics*. 86, 263-275.
- Neely, J.R., Denton, R.M., England, P.J., Randle, P.J., 1972. The effects of increased heart work on the tricarboxylate cycle and its interactions with glycolysis in the perfused rat heart. *The Biochemical Journal*. 128, 147-159.
- Nerbonne, J.M. & Kass, R.S., 2005. Molecular physiology of cardiac repolarization. *Physiological Reviews*. 85, 1205-1253.
- Nguyen, T.P., Qu, Z., Weiss, J.N., 2014. Cardiac fibrosis and arrhythmogenesis: the road to repair is paved with perils. *Journal of Molecular and Cellular Cardiology*. 70, 83-91.
- Nichols, C.G. & Lederer, W.J., 1990a. The regulation of ATP-sensitive K⁺ channel activity in intact and permeabilized rat ventricular myocytes. *The Journal of Physiology*. 423, 91-110.
- Nichols, C.G. & Lederer, W.J., 1990b. The role of ATP in energy-deprivation contractures in unloaded rat ventricular myocytes. *Canadian Journal of Physiology and Pharmacology*. 68, 183-194.
- Nishino, Y., Miura, T., Miki, T., Sakamoto, J., Nakamura, Y., Ikeda, Y., Kobayashi, H., Shimamoto, K., 2004. Ischemic preconditioning activates AMPK in a PKC-dependent manner and induces GLUT4 up-regulation in the late phase of cardioprotection. *Cardiovascular Research*. 61, 610-619.
- Noma, A., 1983. ATP-regulated K⁺ channels in cardiac muscle. *Nature*. 305, 147-148.
- Nuskova, H., Vrbacky, M., Drahota, Z., Houstek, J., 2010. Cyanide inhibition and pyruvate-induced recovery of cytochrome c oxidase. *Journal of Bioenergetics and Biomembranes*. 42, 395-403.
- O'Brien, K.D., Ferguson, M., Gordon, D., Deeb, S.S., Chait, A., 1994. Lipoprotein lipase is produced by cardiac myocytes rather than interstitial cells in human myocardium. *Arteriosclerosis and Thrombosis : A Journal of Vascular Biology / American Heart Association*. 14, 1445-1451.
- Oguchi, M., Gerth, E., Fitzgerald, B., Park, J.H., 1973. Regulation of glyceraldehyde 3-phosphate dehydrogenase by phosphocreatine and adenosine triphosphate. IV.

Factors affecting in vivo control of enzymatic activity. *The Journal of Biological Chemistry*. 248, 5571-5576.

Olowe, Y. & Schulz, H., 1980. Regulation of thiolases from pig heart. Control of fatty acid oxidation in heart. *European Journal of Biochemistry / FEBS*. 109, 425-429.

Owen, P., Dennis, S., Opie, L.H., 1990. Glucose flux rate regulates onset of ischemic contracture in globally underperfused rat hearts. *Circulation Research*. 66, 344-354.

Oxman, T., Arad, M., Klein, R., Avazov, N., Rabinowitz, B., 1997. Limb ischemia preconditions the heart against reperfusion tachyarrhythmia. *The American Journal of Physiology*. 273, H1707-12.

Park, O.J., Cesar, D., Faix, D., Wu, K., Shackleton, C.H., Hellerstein, M.K., 1992. Mechanisms of fructose-induced hypertriglyceridaemia in the rat. Activation of hepatic pyruvate dehydrogenase through inhibition of pyruvate dehydrogenase kinase. *The Biochemical Journal*. 282 (Pt 3), 753-757.

Paucek, P., Mironova, G., Mahdi, F., Beavis, A.D., Woldegiorgis, G., Garlid, K.D., 1992. Reconstitution and partial purification of the glibenclamide-sensitive, ATP-dependent K⁺ channel from rat liver and beef heart mitochondria. *The Journal of Biological Chemistry*. 267, 26062-26069.

Paulson, D.J. & Crass, M.F., 3rd, 1982. Endogenous triacylglycerol metabolism in diabetic heart. *The American Journal of Physiology*. 242, H1084-94.

Peart, J.N. & Gross, G.J., 2002. Sarcolemmal and mitochondrial K(ATP) channels and myocardial ischemic preconditioning. *Journal of Cellular and Molecular Medicine*. 6, 453-464.

Peart, J.N. & Headrick, J.P., 2009. Clinical cardioprotection and the value of conditioning responses. *American Journal of Physiology. Heart and Circulatory Physiology*. 296, H1705-20.

Pell, T.J., Baxter, G.F., Yellon, D.M., Drew, G.M., 1998. Renal ischemia preconditions myocardium: role of adenosine receptors and ATP-sensitive potassium channels. *The American Journal of Physiology*. 275, H1542-7.

Pelsters, M.M., Lutgerink, J.T., Nieuwenhoven, F.A., Tandon, N.N., van der Vusse, G.J., Arends, J.W., Hoogenboom, H.R., Glatz, J.F., 1999. A sensitive immunoassay for rat fatty acid translocase (CD36) using phage antibodies selected on cell transfectants: abundant presence of fatty acid translocase/CD36 in cardiac and red skeletal muscle and up-regulation in diabetes. *The Biochemical Journal*. 337 (Pt 3), 407-414.

Perez, P.J., Ramos-Franco, J., Fill, M., Mignery, G.A., 1997. Identification and functional reconstitution of the type 2 inositol 1,4,5-trisphosphate receptor from ventricular cardiac myocytes. *The Journal of Biological Chemistry*. 272, 23961-23969.

- Phay, J.E., Hussain, H.B., Moley, J.F., 2000. Strategy for identification of novel glucose transporter family members by using internet-based genomic databases. *Surgery*. 128, 946-951.
- Pierce, G.N. & Philipson, K.D., 1985. Binding of glycolytic enzymes to cardiac sarcolemmal and sarcoplasmic reticular membranes. *The Journal of Biological Chemistry*. 260, 6862-6870.
- Piper, H.M., Abdallah, Y., Schafer, C., 2004. The first minutes of reperfusion: a window of opportunity for cardioprotection. *Cardiovascular Research*. 61, 365-371.
- Pogson, C.I. & Randle, P.J., 1966. The control of rat-heart phosphofructokinase by citrate and other regulators. *The Biochemical Journal*. 100, 683-693.
- Poole, R.C., Sansom, C.E., Halestrap, A.P., 1996. Studies of the membrane topology of the rat erythrocyte H⁺/lactate cotransporter (MCT1). *The Biochemical Journal*. 320 (Pt 3), 817-824.
- Qian, T., Nieminen, A.L., Herman, B., Lemasters, J.J., 1997. Mitochondrial permeability transition in pH-dependent reperfusion injury to rat hepatocytes. *The American Journal of Physiology*. 273, C1783-92.
- Qin, D., Huang, B., Deng, L., El-Adawi, H., Ganguly, K., Sowers, J.R., El-Sherif, N., 2001. Downregulation of K(+) channel genes expression in type I diabetic cardiomyopathy. *Biochemical and Biophysical Research Communications*. 283, 549-553.
- Quarrie, R., Lee, D.S., Steinbaugh, G., Cramer, B., Erdahl, W., Pfeiffer, D.R., Zweier, J.L., Crestanello, J.A., 2012. Ischemic preconditioning preserves mitochondrial membrane potential and limits reactive oxygen species production. *The Journal of Surgical Research*. 178, 8-17.
- Rainbow, R.D., Lodwick, D., Hudman, D., Davies, N.W., Norman, R.I., Standen, N.B., 2004. SUR2A C-terminal fragments reduce KATP currents and ischaemic tolerance of rat cardiac myocytes. *The Journal of Physiology*. 557, 785-794.
- Rainbow, R.D., Norman, R.I., Hudman, D., Davies, N.W., Standen, N.B., 2005. Reduced effectiveness of HMR 1098 in blocking cardiac sarcolemmal K(ATP) channels during metabolic stress. *Journal of Molecular and Cellular Cardiology*. 39, 637-646.
- Rainbow, R.D., Hardy, M.E., Standen, N.B. and Davies, N.W. 2006. 'Glucose reduces endothelin inhibition of voltage-gated potassium channels in rat arterial smooth muscle cells', *The Journal of physiology*, 575(Pt 3), 833-844.
- Ramasamy, R., Hwang, Y.C., Whang, J., Bergmann, S.R., 2001. Protection of ischemic hearts by high glucose is mediated, in part, by GLUT-4. *American Journal of Physiology. Heart and Circulatory Physiology*. 281, H290-7.

- Randle, P.J., Newsholme, E.A., Garland, P.B., 1964. Regulation of glucose uptake by muscle. 8. Effects of fatty acids, ketone bodies and pyruvate, and of alloxan-diabetes and starvation, on the uptake and metabolic fate of glucose in rat heart and diaphragm muscles. *The Biochemical Journal*. 93, 652-665.
- Rauch, U., Schulze, K., Witzelbichler, B., Schultheiss, H.P., 1994. Alteration of the cytosolic-mitochondrial distribution of high-energy phosphates during global myocardial ischemia may contribute to early contractile failure. *Circulation Research*. 75, 760-769.
- Regen, D.M., Davis, W.W., Morgan, H.E., Park, C.R., 1964. The Regulation of Hexokinase and Phosphofructokinase Activity in Heart Muscle. Effects of Alloxan Diabetes, Growth Hormone, Cortisol, and Anoxia. *The Journal of Biological Chemistry*. 239, 43-49.
- Ren, J. & Ceylan-Isik, A.F., 2004. Diabetic cardiomyopathy: do women differ from men? *Endocrine*. 25, 73-83.
- Rezkalla, S.H. & Kloner, R.A., 2002. No-reflow phenomenon. *Circulation*. 105, 656-662.
- Ricci, J.E., Munoz-Pinedo, C., Fitzgerald, P., Bailly-Maitre, B., Perkins, G.A., Yadava, N., Scheffler, I.E., Ellisman, M.H., Green, D.R., 2004. Disruption of mitochondrial function during apoptosis is mediated by caspase cleavage of the p75 subunit of complex I of the electron transport chain. *Cell*. 117, 773-786.
- Ripoll, C., Lederer, W.J. and Nichols, C.G., 1993. 'On the mechanism of inhibition of KATP channels by glibenclamide in rat ventricular myocytes', *Journal of cardiovascular electrophysiology*, 4(1), 38-47.
- Rodrigo, G.C., Lawrence, C.L., Standen, N.B., 2002. Dinitrophenol pretreatment of rat ventricular myocytes protects against damage by metabolic inhibition and reperfusion. *Journal of Molecular and Cellular Cardiology*. 34, 555-569.
- Rodrigo, G.C. & Samani, N.J., 2008. Ischemic preconditioning of the whole heart confers protection on subsequently isolated ventricular myocytes. *American Journal of Physiology. Heart and Circulatory Physiology*. 294, H524-31.
- Rodrigo, G.C. & Standen, N.B., 2005. Role of mitochondrial re-energization and Ca²⁺ influx in reperfusion injury of metabolically inhibited cardiac myocytes. *Cardiovascular Research*. 67, 291-300.
- Rogers, S., Macheda, M.L., Docherty, S.E., Carty, M.D., Henderson, M.A., Soeller, W.C., Gibbs, E.M., James, D.E., Best, J.D., 2002. Identification of a novel glucose transporter-like protein-GLUT-12. *American Journal of Physiology. Endocrinology and Metabolism*. 282, E733-8.

Saddik, M., Gamble, J., Witters, L.A., Lopaschuk, G.D., 1993. Acetyl-CoA carboxylase regulation of fatty acid oxidation in the heart. *The Journal of Biological Chemistry*. 268, 25836-25845.

Salway, J.G., 2004. *Metabolism at a Glance*. Third edition ed. Oxford: Blackwell.

Sargent, C.A., Dzwonczyk, S., Sleph, P., Wilde, M., Grover, G.J., 1994. Pyruvate increases threshold for preconditioning in globally ischemic rat hearts. *The American Journal of Physiology*. 267, H1403-9.

Sato, T., Sasaki, N., Seharaseyon, J., O'Rourke, B., Marban, E., 2000. Selective pharmacological agents implicate mitochondrial but not sarcolemmal K(ATP) channels in ischemic cardioprotection. *Circulation*. 101, 2418-2423.

Schaap, F.G., Binas, B., Danneberg, H., van der Vusse, G.J., Glatz, J.F., 1999. Impaired long-chain fatty acid utilization by cardiac myocytes isolated from mice lacking the heart-type fatty acid binding protein gene. *Circulation Research*. 85, 329-337.

Schaap, F.G., van der Vusse, G.J., Glatz, J.F., 1998. Fatty acid-binding proteins in the heart. *Molecular and Cellular Biochemistry*. 180, 43-51.

Schafer, C., Ladilov, Y., Inserte, J., Schafer, M., Haffner, S., Garcia-Dorado, D., Piper, H.M., 2001. Role of the reverse mode of the Na⁺/Ca²⁺ exchanger in reoxygenation-induced cardiomyocyte injury. *Cardiovascular Research*. 51, 241-250.

Schifferdecker, J. & Schulz, H., 1974. The inhibition of L-3-hydroxyacyl-CoA dehydrogenase by acetoacetyl-CoA and the possible effect of this inhibitor on fatty acid oxidation. *Life Sciences*. 14, 1487-1492.

Seino, S., 1999. ATP-sensitive potassium channels: a model of heteromultimeric potassium channel/receptor assemblies. *Annual Review of Physiology*. 61, 337-362.

Severs, N.J., Bruce, A.F., Dupont, E., Rothery, S., 2008. Remodelling of gap junctions and connexin expression in diseased myocardium. *Cardiovascular Research*. 80, 9-19.

Shepherd, D. & Garland, P.B., 1969. The kinetic properties of citrate synthase from rat liver mitochondria. *The Biochemical Journal*. 114, 597-610.

Sims, M.W., Winter, J., Brennan, S., Norman, R.I., Ng, G.A., Squire, I.B. and Rainbow, R.D. 2014., 'PKC-mediated toxicity of elevated glucose concentration on cardiomyocyte function', *American journal of physiology. Heart and circulatory physiology*, 307(4), H587-97

Sipido, K.R., Carmeliet, E., Van de Werf, F., 1998. T-type Ca²⁺ current as a trigger for Ca²⁺ release from the sarcoplasmic reticulum in guinea-pig ventricular myocytes. *The Journal of Physiology*. 508 (Pt 2), 439-451.

- Smith, C.M., Bryla, J., Williamson, J.R., 1974. Regulation of mitochondrial alpha-ketoglutarate metabolism by product inhibition at alpha-ketoglutarate dehydrogenase. *The Journal of Biological Chemistry*. 249, 1497-1505.
- Smith, C.M. & Williamson, J.R., 1971. Inhibition of citrate synthase by succinyl-CoA and other metabolites. *FEBS Letters*. 18, 35-38.
- Solow, B.T., Harada, S., Goldstein, B.J., Smith, J.A., White, M.F., Jarett, L., 1999. Differential modulation of the tyrosine phosphorylation state of the insulin receptor by IRS (insulin receptor subunit) proteins. *Molecular Endocrinology (Baltimore, Md.)*. 13, 1784-1798.
- Squire, I.B., Nelson, C.P., Ng, L.L., Jones, D.R., Woods, K.L., Lambert, P.C., 2009. Prognostic value of admission blood glucose concentration and diabetes diagnosis on survival after acute myocardial infarction; Results from 4702 index cases in routine practice. *Clinical Science (London, England : 1979)*.
- St Maurice, M., Reinhardt, L., Surinya, K.H., Attwood, P.V., Wallace, J.C., Cleland, W.W., Rayment, I., 2007. Domain architecture of pyruvate carboxylase, a biotin-dependent multifunctional enzyme. *Science (New York, N.Y.)*. 317, 1076-1079.
- Stanley, W.C., Recchia, F.A., Lopaschuk, G.D., 2005. Myocardial substrate metabolism in the normal and failing heart. *Physiological Reviews*. 85, 1093-1129.
- Steinbusch, L.K., Schwenk, R.W., Ouwens, D.M., Diamant, M., Glatz, J.F., Luiken, J.J., 2011. Subcellular trafficking of the substrate transporters GLUT4 and CD36 in cardiomyocytes. *Cellular and Molecular Life Sciences : CMLS*. 68, 2525-2538.
- Stowe, D.F., 1999. Understanding the temporal relationship of ATP loss, calcium loading, and rigor contracture during anoxia, and hypercontracture after anoxia in cardiac myocytes. *Cardiovascular Research*. 43, 285-287.
- Sugden, P.H., Kerbey, A.L., Randle, P.J., Waller, C.A., Reid, K.B., 1979. Amino acid sequences around the sites of phosphorylation in the pig heart pyruvate dehydrogenase complex. *The Biochemical Journal*. 181, 419-426.
- Sun, H.Y., Wang, N.P., Kerendi, F., Halkos, M., Kin, H., Guyton, R.A., Vinten-Johansen, J., Zhao, Z.Q., 2005. Hypoxic postconditioning reduces cardiomyocyte loss by inhibiting ROS generation and intracellular Ca²⁺ overload. *American Journal of Physiology. Heart and Circulatory Physiology*. 288, H1900-8.
- Spuler, A., Endres, W. and Grafe, P., 1988. 'Glucose depletion hyperpolarizes guinea pig hippocampal neurons by an increase in potassium conductance', *Experimental neurology*, 100(1), 248-252.
- Suzuki, M., Sasaki, N., Miki, T., Sakamoto, N., Ohmoto-Sekine, Y., Tamagawa, M., Seino, S., Marban, E., Nakaya, H., 2002. Role of sarcolemmal K(ATP) channels in

cardioprotection against ischemia/reperfusion injury in mice. *The Journal of Clinical Investigation*. 109, 509-516.

Svensson, A.M., McGuire, D.K., Abrahamsson, P., Dellborg, M., 2005. Association between hyper- and hypoglycaemia and 2 year all-cause mortality risk in diabetic patients with acute coronary events. *European Heart Journal*. 26, 1255-1261.

Swynghedauw, B., 1999. Molecular mechanisms of myocardial remodeling. *Physiological Reviews*. 79, 215-262.

Tamargo, J., Caballero, R., Gomez, R., Valenzuela, C., Delpon, E., 2004. Pharmacology of cardiac potassium channels. *Cardiovascular Research*. 62, 9-33.

Tani, M., 1990. Mechanisms of Ca²⁺ overload in reperfused ischemic myocardium. *Annual Review of Physiology*. 52, 543-559.

Tani, M. & Neely, J.R., 1989. Role of intracellular Na⁺ in Ca²⁺ overload and depressed recovery of ventricular function of reperfused ischemic rat hearts. Possible involvement of H⁺-Na⁺ and Na⁺-Ca²⁺ exchange. *Circulation Research*. 65, 1045-1056.

Tanti, J.F., Grillo, S., Gremeaux, T., Coffey, P.J., Van Obberghen, E., Le Marchand-Brustel, Y., 1997. Potential role of protein kinase B in glucose transporter 4 translocation in adipocytes. *Endocrinology*. 138, 2005-2010.

Thomas, A.P. & Halestrap, A.P., 1981. Identification of the protein responsible for pyruvate transport into rat liver and heart mitochondria by specific labelling with [3H]N-phenylmaleimide. *The Biochemical Journal*. 196, 471-479.

Thorens, B. & Mueckler, M., 2010. Glucose transporters in the 21st Century. *American Journal of Physiology. Endocrinology and Metabolism*. 298, E141-5.

Thornton, J.D., Thornton, C.S., Sterling, D.L., Downey, J.M., 1993. Blockade of ATP-sensitive potassium channels increases infarct size but does not prevent preconditioning in rabbit hearts. *Circulation Research*. 72, 44-49.

Tong, H., Chen, W., London, R.E., Murphy, E., Steenbergen, C., 2000. Preconditioning enhanced glucose uptake is mediated by p38 MAP kinase not by phosphatidylinositol 3-kinase. *The Journal of Biological Chemistry*. 275, 11981-11986.

Townsend, N., Wickramasinghe, K., Bhatnagar, P., Smolina, K., Nichols, M., Leal, J., Luengo-Fernandez, R., Rayner, M., 2012. *Coronary heart disease statistics 2012 edition*. British Heart Foundation: London.

Turrell, H.E., Rodrigo, G.C., Norman, R.I., Dickens, M., Standen, N.B., 2011. Phenylephrine preconditioning involves modulation of cardiac sarcolemmal K(ATP) current by PKC delta, AMPK and p38 MAPK. *Journal of Molecular and Cellular Cardiology*. 51, 370-380.

Uldry, M., Ibberson, M., Horisberger, J.D., Chatton, J.Y., Riederer, B.M., Thorens, B., 2001. Identification of a mammalian H(+)-myo-inositol symporter expressed predominantly in the brain. *The EMBO Journal*. 20, 4467-4477.

Uldry, M. & Thorens, B., 2004. The SLC2 family of facilitated hexose and polyol transporters. *Pflugers Archiv : European Journal of Physiology*. 447, 480-489.

Ussher, J.R., Wang, W., Gandhi, M., Keung, W., Samokhvalov, V., Oka, T., Wagg, C.S., Jaswal, J.S., Harris, R.A., Clanachan, A.S., Dyck, J.R., Lopaschuk, G.D., 2012. Stimulation of glucose oxidation protects against acute myocardial infarction and reperfusion injury. *Cardiovascular Research*. 94, 359-369.

Utter, M.F. & Keech, D.B., 1963. Pyruvate Carboxylase. I. Nature of the Reaction. *The Journal of Biological Chemistry*. 238, 2603-2608.

Utter, M.F. & Keech, D.B., 1960. Formation of oxaloacetate from pyruvate and carbon dioxide. *The Journal of Biological Chemistry*. 235, PC17-8.

Van der Vusse, G.J., Glatz, J.F., Stam, H.C., Reneman, R.S., 1992. Fatty acid homeostasis in the normoxic and ischemic heart. *Physiological Reviews*. 72, 881-940.

Van Echteld, C.J., Kirkels, J.H., Eijgelshoven, M.H., van der Meer, P., Ruigrok, T.J., 1991. Intracellular sodium during ischemia and calcium-free perfusion: a ²³Na NMR study. *Journal of Molecular and Cellular Cardiology*. 23, 297-307.

Van Emous, J.G., Lankamp, C.L., Ruigrok, T.J., van Echteld, C.J., 1998. Glycolytic ATP production is not essential for Na(+)-K⁺ ATPase function and contractile recovery during postischemic reperfusion in isolated rat hearts. *Magma (New York, N.Y.)*. 6, 177-178.

Van Emous, J.G., Schreur, J.H., Ruigrok, T.J., Van Echteld, C.J., 1998. Both Na⁺-K⁺ ATPase and Na⁺-H⁺ exchanger are immediately active upon post-ischemic reperfusion in isolated rat hearts. *Journal of Molecular and Cellular Cardiology*. 30, 337-348.

Van Emous, J.G., Vleggeert-Lankamp, C.L., Nederhoff, M.G., Ruigrok, T.J., Van Echteld, C.J., 2001. Postischemic Na(+)-K(+)-ATPase reactivation is delayed in the absence of glycolytic ATP in isolated rat hearts. *American Journal of Physiology. Heart and Circulatory Physiology*. 280, H2189-95.

Van Schaftingen, E., 1994. Short-term regulation of glucokinase. *Diabetologia*. 37 Suppl 2, S43-7.

Vanden Hoek, T.L., Becker, L.B., Shao, Z., Li, C., Schumacker, P.T., 1998. Reactive oxygen species released from mitochondria during brief hypoxia induce preconditioning in cardiomyocytes. *The Journal of Biological Chemistry*. 273, 18092-18098.

- Vanden Hoek, T.L., Li, C., Shao, Z., Schumacker, P.T., Becker, L.B., 1997. Significant levels of oxidants are generated by isolated cardiomyocytes during ischemia prior to reperfusion. *Journal of Molecular and Cellular Cardiology*. 29, 2571-2583.
- Vandenberg, J.I., Metcalfe, J.C., Grace, A.A., 1993. Mechanisms of pHi recovery after global ischemia in the perfused heart. *Circulation Research*. 72, 993-1003.
- Vander Heide, R.S., Angelo, J.P., Altschuld, R.A., Ganote, C.E., 1986. Energy dependence of contraction band formation in perfused hearts and isolated adult myocytes. *The American Journal of Pathology*. 125, 55-68.
- Vander Heide, R.S., Rim, D., Hohl, C.M., Ganote, C.E., 1990. An in vitro model of myocardial ischemia utilizing isolated adult rat myocytes. *Journal of Molecular and Cellular Cardiology*. 22, 165-181.
- Vannier, C. & Ailhaud, G., 1989. Biosynthesis of lipoprotein lipase in cultured mouse adipocytes. II. Processing, subunit assembly, and intracellular transport. *The Journal of Biological Chemistry*. 264, 13206-13216.
- Vanoverschelde, J.L., Janier, M.F., Bakke, J.E., Marshall, D.R., Bergmann, S.R., 1994. Rate of glycolysis during ischemia determines extent of ischemic injury and functional recovery after reperfusion. *The American Journal of Physiology*. 267, H1785-94.
- Veerkamp, J.H., Van Moerkerk, H.T., Van den Born, J., 1996. No correlation between changes in fatty acid-binding protein content and fatty acid oxidation capacity of rat tissues in experimental diabetes. *The International Journal of Biochemistry & Cell Biology*. 28, 473-478.
- Veksler, V.I., Lechene, P., Matrougui, K., Ventura-Clapier, R., 1997. Rigor tension in single skinned rat cardiac cell: role of myofibrillar creatine kinase. *Cardiovascular Research*. 36, 354-362.
- Verma, S., Fedak, P.W., Weisel, R.D., Butany, J., Rao, V., Maitland, A., Li, R.K., Dhillon, B., Yau, T.M., 2002. Fundamentals of reperfusion injury for the clinical cardiologist. *Circulation*. 105, 2332-2336.
- Vork, M.M., Trigault, N., Snoeckx, L.H., Glatz, J.F., van der Vusse, G.J., 1992. Heterogeneous distribution of fatty acid-binding protein in the hearts of Wistar Kyoto and spontaneously hypertensive rats. *Journal of Molecular and Cellular Cardiology*. 24, 317-321.
- Wang, H.C., Zhang, H.F., Guo, W.Y., Su, H., Zhang, K.R., Li, Q.X., Yan, W., Ma, X.L., Lopez, B.L., Christopher, T.A., Gao, F., 2006. Hypoxic postconditioning enhances the survival and inhibits apoptosis of cardiomyocytes following reoxygenation: role of peroxynitrite formation. *Apoptosis : An International Journal on Programmed Cell Death*. 11, 1453-1460.

- Wang, L., Cherednichenko, G., Hernandez, L., Halow, J., Camacho, S.A., Figueredo, V., Schaefer, S., 2001. Preconditioning limits mitochondrial Ca^{2+} during ischemia in rat hearts: role of K(ATP) channels. *American Journal of Physiology. Heart and Circulatory Physiology*. 280, H2321-8.
- Wang, P., Lloyd, S.G., Chatham, J.C., 2005. Impact of high glucose/high insulin and dichloroacetate treatment on carbohydrate oxidation and functional recovery after low-flow ischemia and reperfusion in the isolated perfused rat heart. *Circulation*. 111, 2066-2072.
- Wang, X., Poole, R.C., Halestrap, A.P., Levi, A.J., 1993. Characterization of the inhibition by stilbene disulphonates and phloretin of lactate and pyruvate transport into rat and guinea-pig cardiac myocytes suggests the presence of two kinetically distinct carriers in heart cells. *The Biochemical Journal*. 290 (Pt 1), 249-258.
- Weinbrenner, C., Nelles, M., Herzog, N., Sarvary, L., Strasser, R.H., 2002. Remote preconditioning by infrarenal occlusion of the aorta protects the heart from infarction: a newly identified non-neuronal but PKC-dependent pathway. *Cardiovascular Research*. 55, 590-601.
- Weiss, J.N. & Lamp, S.T., 1987. Glycolysis preferentially inhibits ATP-sensitive K^{+} channels in isolated guinea pig cardiac myocytes. *Science (New York, N.Y.)*. 238, 67-69.
- Wheeler, T.J. & Chien, S., 2012. Characterization of the high-affinity uptake of fructose-1,6-bisphosphate by cardiac myocytes. *Molecular and Cellular Biochemistry*. 366, 31-39.
- Williams, H., Kerr, P.M., Suleiman, M., Griffiths, E.J., 2000. Differences in the calcium-handling response of isolated rat and guinea-pig cardiomyocytes to metabolic inhibition: implications for cell damage. *Experimental Physiology*. 85, 505-510.
- Wood, I.S. & Trayhurn, P., 2003. Glucose transporters (GLUT and SGLT): expanded families of sugar transport proteins. *The British Journal of Nutrition*. 89, 3-9.
- Wright, E.M., Hirsch, J.R., Loo, D.D., Zampighi, G.A., 1997. Regulation of Na^{+} /glucose cotransporters. *The Journal of Experimental Biology*. 200, 287-293.
- Wu, X., Li, W., Sharma, V., Godzik, A., Freeze, H.H., 2002. Cloning and characterization of glucose transporter 11, a novel sugar transporter that is alternatively spliced in various tissues. *Molecular Genetics and Metabolism*. 76, 37-45.
- Xiao, X.H. & Allen, D.G., 1999. Role of Na^{+} / H^{+} exchanger during ischemia and preconditioning in the isolated rat heart. *Circulation Research*. 85, 723-730.
- Xu, K.Y., Zweier, J.L., Becker, L.C., 1995. Functional coupling between glycolysis and sarcoplasmic reticulum Ca^{2+} transport. *Circulation Research*. 77, 88-97.

- Yabe, K., Nasa, Y., Sato, M., Iijima, R., Takeo, S., 1997. Preconditioning preserves mitochondrial function and glycolytic flux during an early period of reperfusion in perfused rat hearts. *Cardiovascular Research*. 33, 677-685.
- Yang, X., Cohen, M.V., Downey, J.M., 2010. Mechanism of cardioprotection by early ischemic preconditioning. *Cardiovascular Drugs and Therapy / Sponsored by the International Society of Cardiovascular Pharmacotherapy*. 24, 225-234.
- Yang, X.M., Proctor, J.B., Cui, L., Krieg, T., Downey, J.M., Cohen, M.V., 2004. Multiple, brief coronary occlusions during early reperfusion protect rabbit hearts by targeting cell signaling pathways. *Journal of the American College of Cardiology*. 44, 1103-1110.
- Ytrehus, K., Liu, Y., Downey, J.M., 1994. Preconditioning protects ischemic rabbit heart by protein kinase C activation. *The American Journal of Physiology*. 266, H1145-52.
- Zaman, A.G., Helft, G., Worthley, S.G., Badimon, J.J., 2000. The role of plaque rupture and thrombosis in coronary artery disease. *Atherosclerosis*. 149, 251-266.
- Zhang, Y., Han, H., Wang, J., Wang, H., Yang, B., Wang, Z., 2003. Impairment of human ether-a-go-go-related gene (HERG) K⁺ channel function by hypoglycemia and hyperglycemia. Similar phenotypes but different mechanisms. *The Journal of Biological Chemistry*. 278, 10417-10426.
- Zhao, Z.Q., Corvera, J.S., Halkos, M.E., Kerendi, F., Wang, N.P., Guyton, R.A., Vinten-Johansen, J., 2003. Inhibition of myocardial injury by ischemic postconditioning during reperfusion: comparison with ischemic preconditioning. *American Journal of Physiology. Heart and Circulatory Physiology*. 285, H579-88.
- Zima, A.V., Kockskamper, J., Blatter, L.A., 2006. Cytosolic energy reserves determine the effect of glycolytic sugar phosphates on sarcoplasmic reticulum Ca²⁺ release in cat ventricular myocytes. *The Journal of Physiology*. 577, 281-293.
- Zweier, J.L. & Jacobus, W.E., 1987. Substrate-induced alterations of high energy phosphate metabolism and contractile function in the perfused heart. *The Journal of Biological Chemistry*. 262, 8015-8021.